THE INDEPENDENT QUADRATIC OPTIMISATION ALGORITHM FOR THE ACTIVE CONTROL OF NOISE AND VIBRATION

Neil C. Mackenzie

Department of Mechanical Engineering
University of Adelaide
South Australia 5005
Australia

Submitted in fulfilment of the requirements
for the degree of Doctor of Philosophy.

September 1996

To the memory and courage of Stuart Mackenzie
who lost the determination to live
in the confusion of living.

TABLE OF CONTENTS

ABSTRACT

This thesis develops an alternative control strategy, for active noise and vibration control systems, that does not require identification of the cancellation path transfer function (between the control actuator input and error sensor output). It is errors in the identification of the cancellation path transfer function that plague the most commonly used algorithms. The control structure presented in this work uses a lattice filter to generate orthogonal signals for each coefficient of a linear combiner (or control filter). The aim of the Independent Quadratic Optimisation algorithm, developed in this work, is to optimise the coefficients of the control filter independently. For each control filter coefficient, estimates of the cost function are made for different perturbations of the coefficient's value. These cost function estimates, when fitted to a quadratic function, allow the optimum for each coefficient to be determined.

It will be shown by theory, simulation and experiment, that this control strategy is ideal for reducing harmonically related tonal noise. However, the speed of the algorithm is reduced for other types of noise, as the cancellation path transfer function degrades the independence of the control filter coefficients. The parameters that affect the performance of the Independent Quadratic Optimisation algorithm are also assessed using theory, simulation and experiment.

STATEMENT OF ORIGINALITY

This work contains no material which has been accepted for the award of any other degree or diploma in any university or other tertiary institution and, to the best of my knowledge and belief, contains no material previously published or written by any other person, except where due reference has been made in the text.

I give consent to this copy of my thesis, when deposited in the University Library, being available for loan and photocopying.

13/9/96

Neil Christopher Mackenzie Date

ACKNOWLEDGEMENTS

Funding for this research was provided by the Australian Research Council, the Sir Ross and Sir Keith Smith Fund, and the Australian Electrical Research Board.

The work presented in this thesis would not have been possible without the guidance and support from my supervisor, Dr. Colin Hansen, and Dr. Scott Snyder. I am very grateful to Professor Sam Luxton for allowing this work to be conducted within the Department of Mechanical Engineering at the University of Adelaide.

There have been many people that have provided assistance with this work. In particular the technical support from Allan Mittler, Herwig Bode, George Osborne, and George Vokalek was much appreciated, as was the very helpful advice on matters of any kind from Raman Autar. I am grateful to Marshall Day Associates for allowing me to complete this thesis while working in New Zealand. The access to the library at the University of Auckland, as provided by Dr. George Dodd, was also much appreciated.

Most importantly, my parents and my fiancé, Joanne Dickinson deserve special mention; My parents (Heather and Terry Mackenzie) for my upbringing and instilling in me the determination and will to persevere and learn; and, Joanne, without whom this work would never have been completed; Through her never-ending strength and support came the confidence to continue whenever I became disheartened.

1.1 History

Active noise and Vibration Control is considered to have been first proposed by the German Physicist Paul Leug [1933]. His system was based on a feedforward means of control, shown in Figure 1-1, and requires knowledge of the disturbance to be cancelled, to generate a suitably delayed out-of-phase control signal. However, unlike current feedforward systems, Leug's system had no control algorithm or error sensor and thus was not adaptive. In a feedforward system, the control signal is generated using a reference sensor that provides a signal coherent with the noise to be cancelled. For all but periodic noise, this type of system is only possible for waves which propagate slower than the active cancellation system can respond in real-time, and thus exhibit causality. Further advances at this time were prevented by the low level of technology and the political situation of this era.

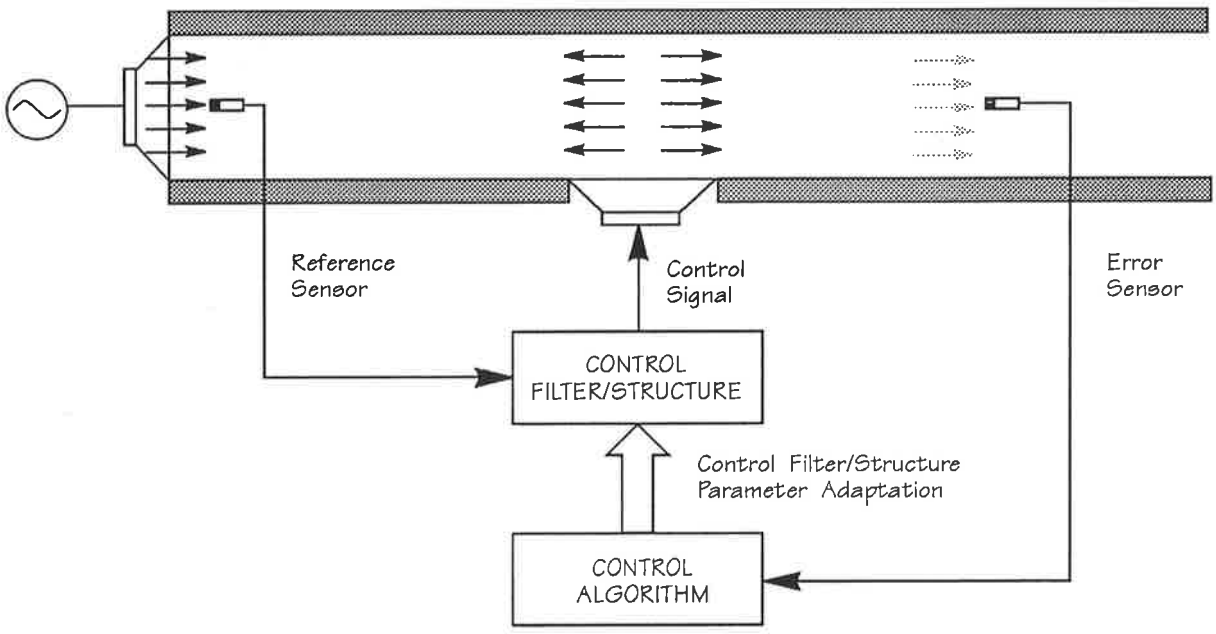

Figure 1-1. Feedforward control configuration.

The performance of the control system is judged by an error sensor or combination of error sensors (in the case of control of evanescent modes or power flow minimisation) placed downstream from the control actuator. Maximum achievable attenuation for systems of this type is limited by reflecting surfaces within the duct. The additional possibility of noise from the control actuator corrupting the signal at the reference sensor contributed to the attempted development of a unidirectional control actuator [Jessel, 1972; Swinbanks, 1973; Leventhall, 1976] through the use of different numbers and configurations of control sources, and a unidirectional error sensor [La Fontaine and Shepherd, 1985] through the use of different numbers and configuration of error sensors. These physical means of avoiding corruption are however limited to narrow-band attenuation, dependent upon the spacing of the transducers. The minimisation of corruption from the reference sensor can also be achieved through a more sophisticated control system as will be discussed in chapter 2.

A later fundamental development by Olson and May [1953] was in the form of feedback control, shown in Figure 1-2. This form of control uses an error sensor to generate an out-of-phase control signal and hence requires no prior knowledge of the primary disturbance. For this reason the method is suited to applications where it is not possible to obtain a coherent reference signal. Such applications include spatially incoherent noise generated by turbulence, noise generated from many sources and paths, and induced resonance where no coherent reference signal is available [Swanson, 1991].

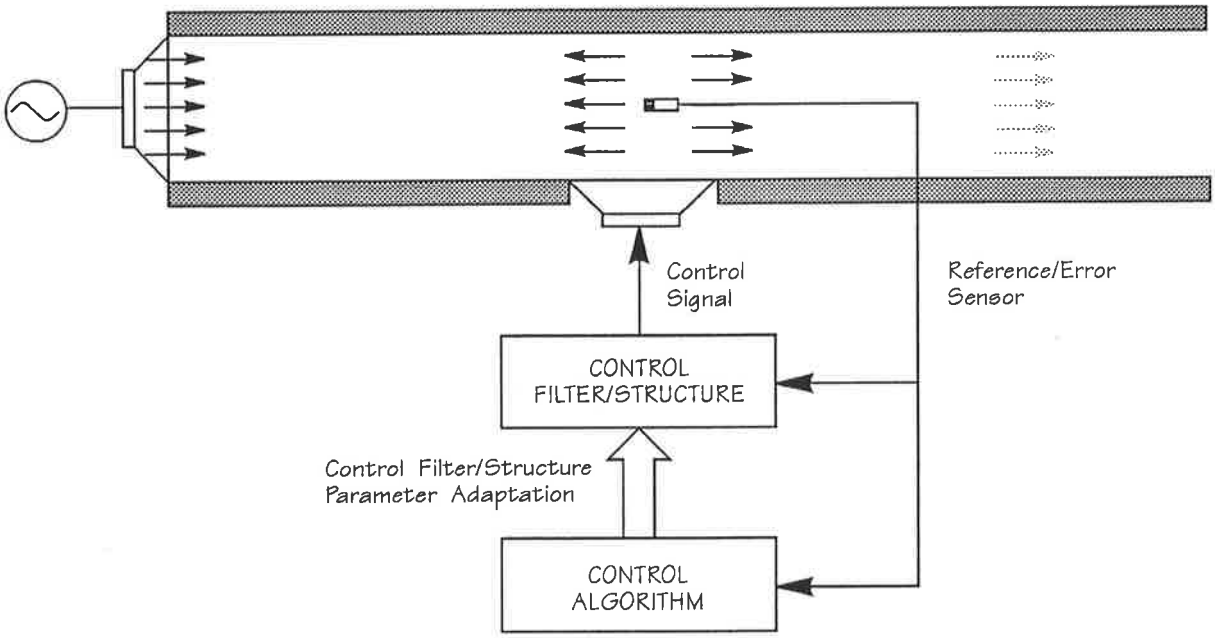

Figure 1-2. Feedback Control Configuration

In a feedback control system, the error sensor signal passes through the controller until it is minimised. This method is prone to instabilities as high gains are required to generate a control signal from the error signal (once this signal itself has been optimally minimised). The time delay from when the control signal is applied to the control actuator and when the response is detected at the error sensor means that only narrow band signals may be cancelled, as will be further discussed in chapter 2. This control arrangement is however particularly successful in headsets [Simshauser, 1955], as the small volume of air behaves as a lumped element therefore reducing restrictions on controller stability and providing broad-band attenuation from an otherwise narrow band control structure.

It is important to note that all of the early developments used fixed filter analogue control systems which were not adaptive to the changing environment within the physical system. To achieve the necessary accuracy in the phase and amplitude of the control signal (for 10-20 dB of attenuation), a complex analogue control system is required. Further to this is the need for the control system to be adaptive in time to the changing characteristics of actuators, sensors and the acoustic media in which they are located. Since the 1980's, there has been a rapidly expanding interest in Active Noise and Vibration Control, principally because of the availability of digital technology, and the dramatic advances in the digital signal processing field initiated for adaptive techniques by Widrow [1960]. The first active noise and vibration control systems implementing digital techniques were developed by Kido [1972] for transformer noise, and by Chaplin [1978] for more general physical systems. The 1980's has seen the development of many different control algorithms and electronic architectures in attempts to overcome the major problems of acoustic feedback between the actuators and sensors, and also the required knowledge of the transfer function between these transducers.

To this point the electronic control element of the overall control system has only been discussed, however the placement, location and type of control actuators and error sensors are also of importance, as are the physical mechanisms that govern the amount of attenuation possible. Jessel [1968] and Malyuzhinets [1969] provided the initial acoustic theory that has since been developed by many different researchers, sporadically in the 1970's for one-dimensional physical systems, and more intensively in the mid 1980's for general physical systems.

Conover [1956] envisaged the use of multiple control sources and error sensors to control free-space radiation, and to some extent developed the first commercial oriented application of active noise and vibration control to control transformer noise. The rewarding commercial prospects together with countless research efforts can only suggest that Active Noise and Vibration Control systems for general physical applications will be available in the near future. Since the 1980's, the widespread application of active noise and vibration control to many commercial problems has led to the formation of companies specialising in this field.

The two major impediments to the progress of a general Active Noise and Vibration Control System are digital signal processing technology and transducer technology. Improvements in signal processing technology has led to advanced control algorithms and electronic architectures. Advances in algorithms have been aimed at improving performance parameters like control system stability, robustness, speed of adaptation and frequency bandwidth of attenuation. Advances in electronic architecture has led to increased speed of operations which, in conjunction with parallel processing, will also inevitably enable the use of more complex control algorithms. The work described here is concerned with developing a more stable control algorithm.

1.2 Problem Definition

The aim of this work is the development of an adaptive algorithm and control architecture, for implementation in active noise and vibration control systems, that avoids the instabilities associated with phase inaccuracies in the cancellation path (or otherwise known as the error path, secondary path, or auxiliary path) transfer function estimation. Current methods of control require knowledge of the cancellation path to reach the optimum of the performance surface in a stable manner. A survey of recently published journal and conference proceedings reveals a body of work directed towards improving transfer function estimates, but no work directed towards developing means of making them unnecessary. Clearly, the latter would be the preferred option in any practical system, and it is towards this option that the work presented in this thesis is directed.

The achievement of this aim requires a significant departure from lines of thought currently being followed in this field, a departure which is necessary if this noise and vibration control technique is to progress to widespread commercial use with the development of a general electronic control system incorporating multiple control actuators and error sensors (and hence multiple error-paths). The specific aims of this work are:

- To study/develop an active control algorithm that eliminates the need to estimate the cancellation path transfer function, by considering an alternative search strategy of the performance surface (defined by error sensors) that

requires no knowledge of the gradient (as most other search strategies do) and relies only on estimates of the performance surface magnitude.

- To develop an efficient means of searching the performance surface, using this strategy, by identifying the principal axes that define the performance surface.

- To demonstrate the effectiveness of this means of control with computer simulations and practical implementation (on suitable digital signal processing hardware) using existing experimental apparatus (for both acoustic control and structural control).

1.3 Thesis Outline

Chapter 2 presents a literature review of the electronic controller development, from a modern control theory perspective. It should be read alongwith the appendix, which presents a background to the control theory concepts discussed in chapter 2. Chapter 2 unifies many of the common heuristically developed algorithms, and offers possible modifications to these that enhance their performance. It assesses both feedforward and feedback control systems (and their combination) using a minimum-variance control scheme and recursive identification methods within the framework of self-tuning regulators. More advanced algorithms are shown to follow from a generalised criterion and robustness conditions related to the accuracy of the identification process. Algorithms that do not require error-path transfer function estimation are introduced, and the Independent Quadratic Optimisation algorithm (that forms the

basis of this work) is conceptualised.

Chapter 3 introduces the lattice filter as a means of obtaining orthogonal signals. The characteristics of the lattice filter are defined, as they relate to the Independent Quadratic Optimisation algorithm, and the effects of a cancellation path transfer function on the independence of control filter coefficients is assessed.

With the means of obtaining orthogonal signals defined, chapter 4 extends the Independent Quadratic Optimisation algorithm concept by analysing its governing equations and parameters. Chapter 4 also presents simulations of the Independent Quadratic Optimisation algorithm for deterministic and random signals in single and multi-channel systems. The simulations highlight the limitations of the Independent Quadratic Optimisation algorithm as pre-empted in chapter 3.

Chapter 5 identifies the requirements of a digital signal processing system, with specific regard to active noise and vibration control. Use is made of these concepts to show the effectiveness of the Independent Quadratic Optimisation algorithm in the real-time control of noise/vibration using various experimental apparatus (ie. a semi-infinite duct and plate).

Finally chapter 6 summarises the findings of this study, and gives suggestions for future research.

1.4 New Work

New work original to this thesis is as follows:

1. Literature review with recommendations for improving commonly used algorithms in active noise and vibration control, as defined from a control theory perspective.

2. Use of the lattice filter to provide orthogonal signals to a linear combiner (or control filter), so that the control filter coefficients can be adapted independently using the Independent Quadratic Optimisation algorithm.

3. The Independent Quadratic Optimisation algorithm, which uses three estimates of the cost function for each independent control filter coefficient, and fits these estimates to a quadratic function to determine the optimum coefficients.

4. Assessment of the effect of parameters of the Independent Quadratic Optimisation algorithm on the performance of this control scheme.

5. Assessment of the limitations of the Independent Quadratic Optimisation algorithm.

6. Experimental verification (both noise and vibration control) of the Independent Quadratic Optimisation algorithm using a transputer network.

2.1 Introduction

In this chapter the electronic controller that generates the control signal, for use in an active noise and vibration control system, will be introduced from a "control theory" perspective. The majority of active noise and vibration control systems developed between 1980 and the early 1990's evolved heuristically from an adaptive signal processing context, largely as a result of the work of Widrow and Stearns [1985]. It is considered that this heuristic approach overlooked many key concepts that are commonly used in control theory, which can simplify and enhance the common algorithms used in active noise and vibration control.

This chapter will examine the standard control systems and their associated algorithms using control theory developed since the 1950's. Classical and modern control will be briefly revised, as will the important clarification between system identification and control. The distinction between control and identification leads to the application of "self-tuning regulators" to active noise and vibration control. The control scheme (that is, control law and parameter adaptation, both of which will be defined shortly), that will be used as a basis for summarising and enhancing common algorithms used in active noise and vibration control, will be defined using a minimum variance approach within the framework of self-tuning regulators. It will be shown that this type of approach leads directly to more complex control schemes for more complex physical systems.

This chapter will also highlight possible new approaches for control scheme

development, and the major problems that need to be addressed in the electronic control system domain of active noise and vibration control.

Alternative methods of control outside the realm of standard control theory will be introduced. As part of this investigation, the Independent Quadratic Optimisation algorithm concept will be introduced as a means of overcoming some of the problems encountered with the standard control algorithms. The Independent Quadratic Optimisation algorithm forms the basis of the remainder of this work.

2.2 Classical versus Modern Control

A control scheme is required when a process output is to be regulated or stabilised within certain desired bounds. Classical control theory was developed by Bode, Nichols and Nyquist in the 1940's, and is based on the graphical representation of the transfer function of a process in "closed-loop" form. Typically a feedback control compensator was used to compensate for poor closed-loop performance (defined by the gain and phase margins of the closed-loop system). This method of control has been applied to active headsets [Carme, 1987; Simshauser, 1955], for which a lumped parameter model of the process is used, and broadband attenuation is achieved. Nelson and Elliott [1992] give an excellent introduction to this method, and appropriate references for a more general study, these being in particular Kuo [1980] and Franklin et al [1990].

More recent control methods ("modern control theory") have used a state-space representation of the physical system. Dohner and Shoureshi [1989], Wu et al [1995] and Hull et al [1991] have given state-space forms with specific regard to active noise and vibration control. Modern control concepts can be used to derive optimal control laws for the system.

Continuous or discrete forms of controllers have been used, with the parameters of discrete forms able to be adapted to account for process changes. Discrete forms of control schemes usually use "adaptive filters", which are discussed in appendix A.1. Adaptive control is an important part of modern control, and it is in this realm that the remainder of this work is focused. Adaptive control is essential as a result of the ever-changing physical environment in which control of noise and vibration is required, and it is this form of control which unless otherwise stated will be discussed throughout this chapter.

It should be noted that the terms "process" and "system" will be used interchangeably, but are to be interpreted as having the same meaning.

2.3 Control versus Identification

In this section the difference between the control of a system and the identification of a system will be highlighted with regard to active noise and vibration control. In particular, two models most commonly used to form a control and identification

scheme, will be introduced.

To achieve control of a system (that is, to achieve a certain output from the system regardless of the input), the expected response of the system (or a similar reference system) to certain inputs is required. That is, to be able to predict the output of the system from an input requires identification of the system. If the system is continually changing then identification must be performed concurrently with control. It is the interaction of these concurrent schemes that can cause the system to behave in an unstable manner.

Unless otherwise stated, the review of control theory will concentrate on single channel systems; that is, systems with a single control source, an error sensor and possibly a reference sensor. The theory for a single-channel system can be extended readily to multi-channel systems.

A simple single channel control system (either feedforward, feedback, or a combination), consisting of a disturbance within a duct that is to be controlled by a single loudspeaker, and measured by a reference sensor and an error sensor is shown in Figure 2-1. The notation used in Figure 2-1 is in keeping with modern control theory. It may be possible to obtain a measure of the disturbance (whether stochastic or deterministic) using the reference signal, $d(n)$. The signal from the error sensor is represented by $y(n)$, and can be considered to be composed of a "reference model" output (that is, the output from the error sensor due to the known and unknown disturbances), $y_m(n)$, and its inverse estimate (that is, the output from the error sensor

due to the control signal), $\hat{y}_m(n)$. Note that $y_m(n)$ and $\hat{y}_m(n)$ are unavailable as they are combined in the vibro-acoustic domain. The control signal is represented as $u(n)$. These signal descriptors will be used to consider the two models commonly used to form a control and identification scheme; that is a "Model Reference" or a "Model Identification" system.

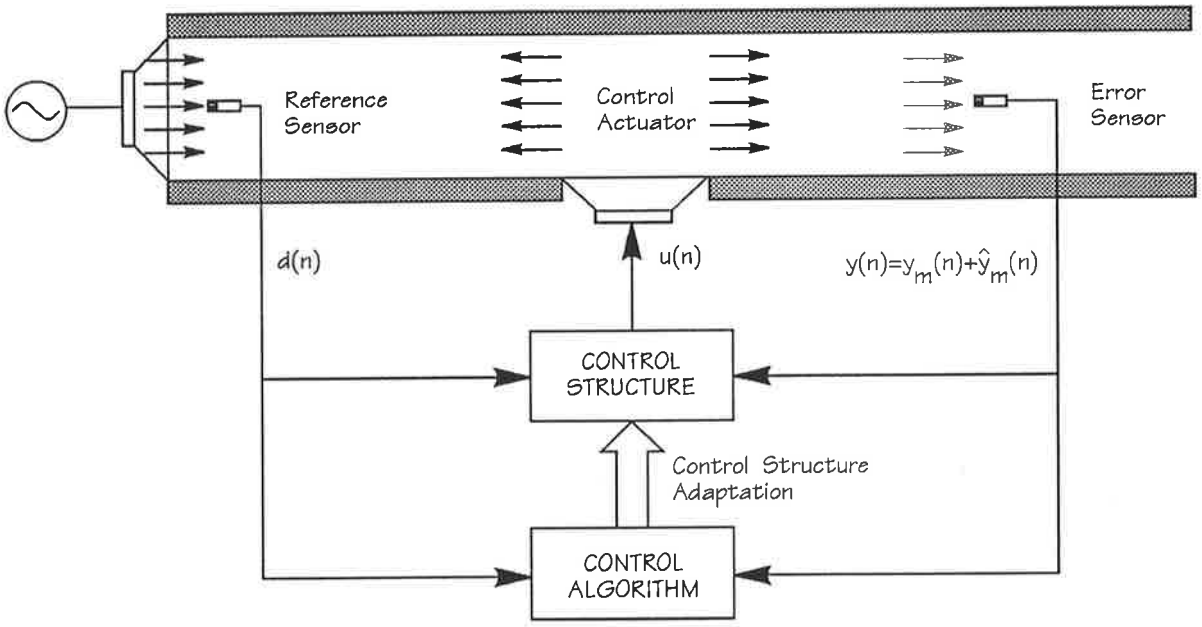

Figure 2-1. One-dimensional single channel (feedforward, feedback or a combination) control system. A measure of the disturbance is given by $d(n)$, the control signal is represented by $u(n)$ and the "process output" is represented by $y(n)$. The process output is composed of the disturbance output (or "reference model output"), $y_m(n)$, and the output from the "control process" is given by $\hat{y}_m(n)$.

A typical Model Reference system is shown in Figure 2-2. The signal descriptors used

in Figure 2-2 are as described above. The "process" is the cancellation path transfer function (also termed the error path, secondary path or auxiliary path transfer function), with the output from the process at the error sensor resulting from the control signal input. The process output must correspond to the inverse estimate of the reference model output.

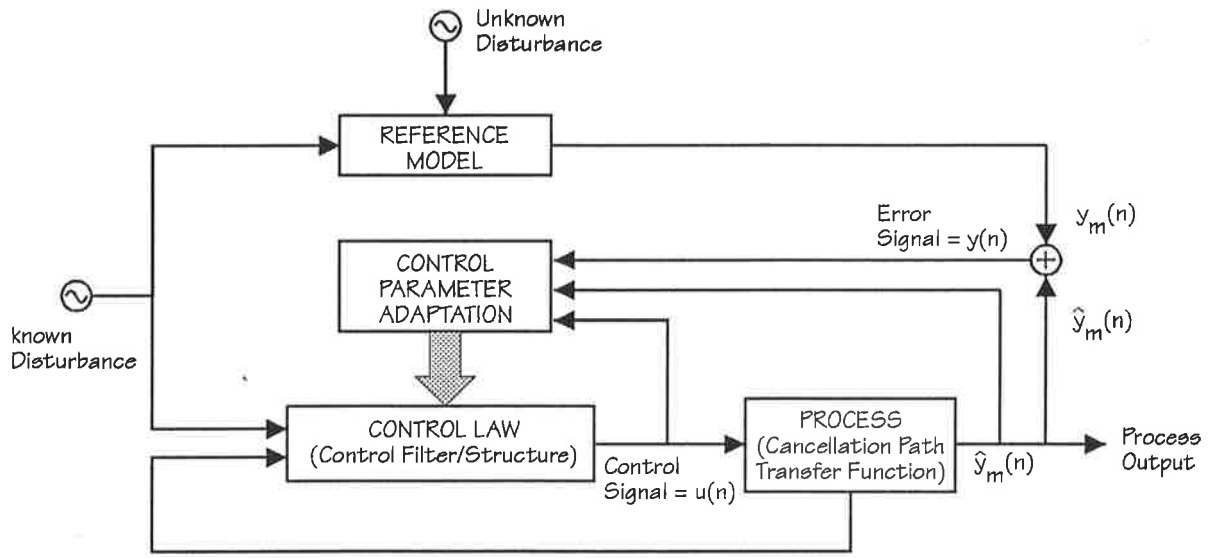

Figure 2-2. Model Reference Adaptive System. The controller generates the control signal that passes through a process (the cancellation path transfer function) and results in a process output at the error sensor which should equal (but be out of phase with) the reference model output at the error sensor, to achieve cancellation.

The reference model is the transfer function from some known disturbance input (eg. duct ventilation fan) to the error sensor. The unknown disturbance could be caused by, for example, flow generated noise within a duct.

The term "control law" is the law from which the control signal is generated by control filters formed in a certain structure (commonly a single filter). The term "control parameter adaptation" relates to the scheme or algorithm used to adapt or optimise the parameters used in the control law.

An alternative interpretation of a Model Reference system uses a theoretical model as the reference model, and the output of the error sensor as the estimate of the reference model output. This interpretation will not be considered further as it is very difficult to accurately construct a theoretical model of complex physical systems. The Model Reference approach represents a typical form of system identification with the prediction error, $y(n)$, also known as the "output-error" in the field of system identification (since the parameters of the control structure are adapted so that the control structure in combination with the process is equivalent to the reference model, as discussed in appendix A.2).

The Model Reference form of control and identification is not suitable for active noise and vibration control because the reference model and its inverse estimate are unavailable to the electronic control system, as they are combined in the vibro-acoustic domain. (However, it will be shown in section 2.4.2 how these signals can be estimated in a form of model reference or output-error control).

It is considered that the "Model Identification" form of control and identification is more appropriate for active noise and vibration control. This system is shown in Figure 2-3, and is more commonly known as a "Self-Tuning Regulator". As for the

Model Reference form, the process is equivalent to the cancellation path transfer function, with however the process output equivalent to the output from the error sensor. Unlike the model reference approach, both the input (ie. control signal) to the process and the output from the process are available for identification. The process has also known (eg. duct ventilation fan) and unknown (eg. flow generated noise within the duct) disturbance inputs.

It should be noted that both the models shown in Figures 2-2 and 2-3, whilst being of either or a combination of feedforward or feedback form, do not explicitly show corruption of the reference signal, which will be made apparent in the next section. This simplification was made so that the difference between the "Model Identification" form and the "Model Reference" form is more readily observable.

The Model Identification scheme first identifies the process (using a model of the process with the parameters of the model termed the identification parameters) and then uses the knowledge of the process determine the control law parameters. In the identification problem, a performance measure based on the prediction error (ie. the difference between the process output and the process output predicted from a model) is used as a means of attaining small identification parameter errors. In the control problem, regulation to a zero process output is desired for active noise and vibration control, with the possibility of substantial control law parameter errors yet still satisfactory control [Cowan and Grant, 1985].

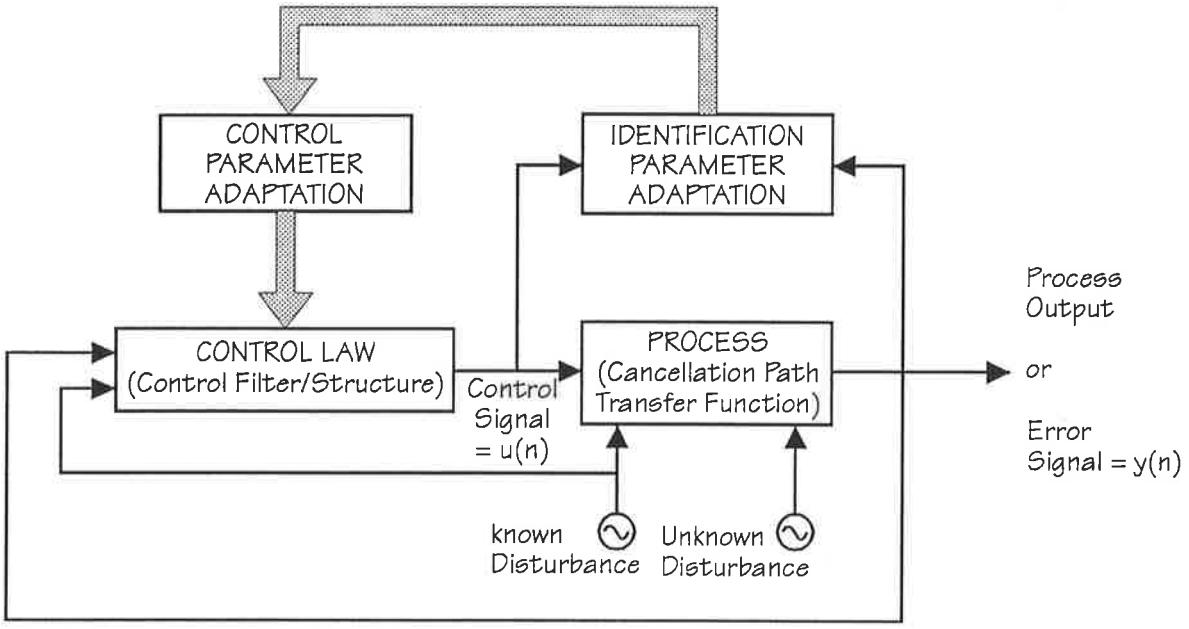

Figure 2-3. Model Identification Adaptive System (Self-Tuning Regulator). The process represents the cancellation path transfer function, with its output the error signal, its input the control signal and the disturbances (which may be measured by the reference sensor or may be unknown).

The control law parameters can be defined directly (or implicitly) if the algorithm used to identify the parameters of the process model is implicitly integrated into the control algorithm, or it can be defined explicitly (or indirectly) if the identification of the process model is treated separately from the control problem. Thus common terms used in the control literature relate to separability (ie. the effect of treating control and identification separately), certainty equivalence (use of the identification parameter estimates as though they have no errors), cautiousness (use of the identification parameters with some degree of identification parameter estimation

error inbuilt into the control algorithm), and dual control (which means that the control scheme must perform both the task of regulation and identification in a cooperative manner; ie. if the optimal control signal is zero then some fluctuation of this signal must be allowed so that identification can take place concurrently) [Goodwin and Sin, 1985; Chalam, 1987; Isermann, 1991].

The key concept throughout this work is that a control law is defined from the identified parameters of the process model. Thus only a single algorithm is required to adapt the process model parameters, and the control law parameters can then be determined (not through adaptation) directly from the identification parameters. In active noise and vibration control, a heuristic development of common algorithms has lead to a combination of both implicit and explicit control parameter determination. The interaction between the identification and control parameter adaptation schemes can lead to instability. The next section will show how these heuristically developed algorithms can be enhanced through definition by the minimum variance approach, discussed generally in appendix A.3.

2.4 Modern Control Theory Applied to Active Noise and Vibration Control

This section will consider self-tuning regulators as applied to active noise and vibration control. As discussed, a self-tuning regulator requires the identification of a system before it can be controlled. The important attributes of an identification and

control scheme have been defined by many researchers [Bitmead et al, 1990; Goodwin and Sin, 1985; Franklin et al, 1990] and relate principally to disturbance rejection (a system that has good regulation in the presence of disturbance signals is said to have good disturbance rejection), sensitivity (a system that has good regulation despite changes in the process parameters, is said to have low sensitivity to these parameters), robustness (a system that has good disturbance rejection and low sensitivity is robust) and stability (bounded system inputs and outputs). These definitions will be used throughout this section.

A self-tuning regulator has three essential components that are discussed in summary form in the appendix. Terms and concepts defined in the appendix will be used throughout this and other chapters, and the appendix is considered an essential accompaniment to this chapter. The appendix is divided into sections as defined below:

- Adaptive digital filters as process models and for control law definition. The different forms and responses of these types of filters are discussed in appendix A.1.

- Identification of process parameters. Appendix A.2 discusses the models used to identify processes, with particular regard to the advantages and disadvantages of non-recursive and recursive forms. Two methodsfor algorithm definition are assessed, with the algorithm type dependent on the process model.

- Control law definition through minimising the variance of the process output. Appendix A.3 describes the minimum variance control approach, with regard to knowledge of identified process parameters.

The common algorithms used in active noise and vibration control will be shown to follow directly from the minimum variance control theory approach. Heuristic improvements of these common algorithms, developed through from 1980 to 1990, will be shown to be standardised by the minimum variance control theory approach. Other means of improving the most common algorithms will be shown as derived from this theory. The use of minimum variance control leads directly to Linear Quadratic Gaussian (LQG) control for non-minimum-phase plants. H_∞ control is a further extension of this and is related to the development of a cautious (as opposed to certainty-equivalence discussed above) controller.

The control theory can be presented using a state-space analysis, but in this chapter it will be presented using transfer functions modelled by polynomials with the delay operator, q^{-1} (a discussion on the use of the delay operator to model transfer functions using polynomials is given in appendix A.1). The term transfer function is used generically; That is, when used in the context of phase and amplitude, the frequency response form is implied, and when used in the context of delays and convolutions, the impulse response form is implied (with further discussion given in appendix A.1).

Results will be presented for a single channel system, but they can be easily extended

to multi-channel systems. This unified view of the most common algorithms is an extension and review of the work by Doelman [1991] and Ren and Kumar [1989].

The most general form of control law incorporating both feedforward and feedback forms of control, as well as allowing for input contamination, will now be considered. Doelman [1991] defined such a system in which the disturbance was partly defined as known or measurable, and partly unknown. The single channel system was excited by these disturbances as well as the control signal. Feedforward control was achieved using a "reference sensor" that unfortunately was also subjected to acoustic feedback (otherwise known as input contamination) from the control source. Feedback control was achieved using an "error sensor". The overall physical system that allows for a feedforward, feedback or a combination of both control schemes is shown in Figure 2-4, with the time delay between the reference sensor and error sensor given by τ_2, between the control actuator and the reference sensor by τ_3, and between the control actuator and the error sensor by τ_1. Note that the location of the algorithm used to adapt the control law parameters is not shown for clarity in Figure 2-4. The signal from the reference sensor is denoted *d(n)*, that from the error sensor by *y(n)* (defined simply to correspond with the control theory literature), and that to the control actuator by *u(n)*.

The corresponding block diagram form is shown in Figure 2-5, incorporating both feedforward and feedback control filters with input contamination of the reference sensor signal. Figure 2-5 shows both the feedforward, G_{FF}, and feedback, G_{FB}, control filters. The other transfer functions are related to the process and the disturbance models. The cancellation path transfer function is represented by G_{PF} and the acoustic feedback transfer function is represented by G_{PB}. The disturbance models are given by G_{DK} representing the transfer function for the measurable disturbance, and G_{DU} representing the transfer function for the unmeasurable disturbance.

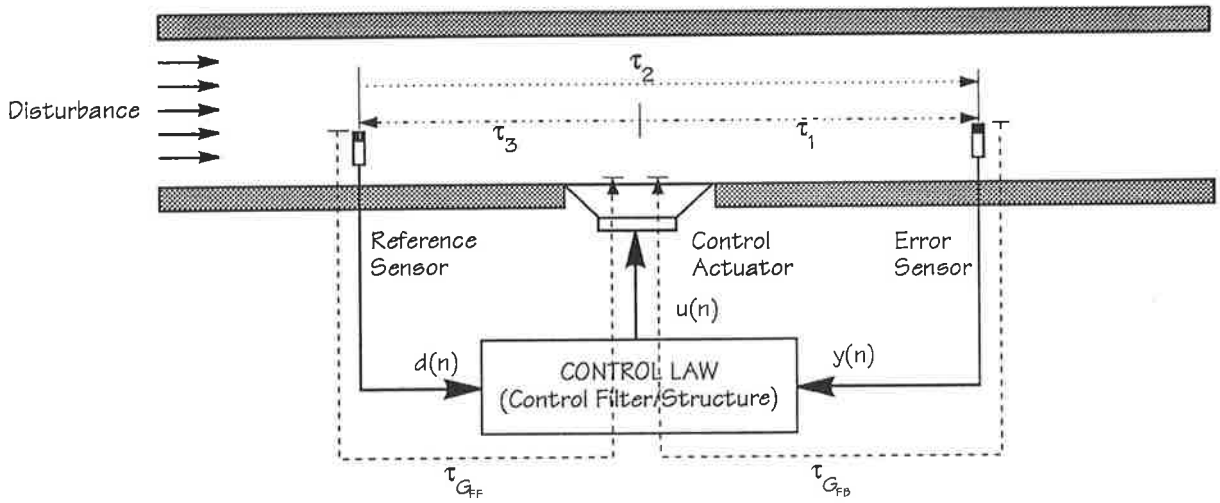

Figure 2-4. Physical layout of a single-channel control system (either feedforward, feedback or a combination of both), with time delays between transducers shown.

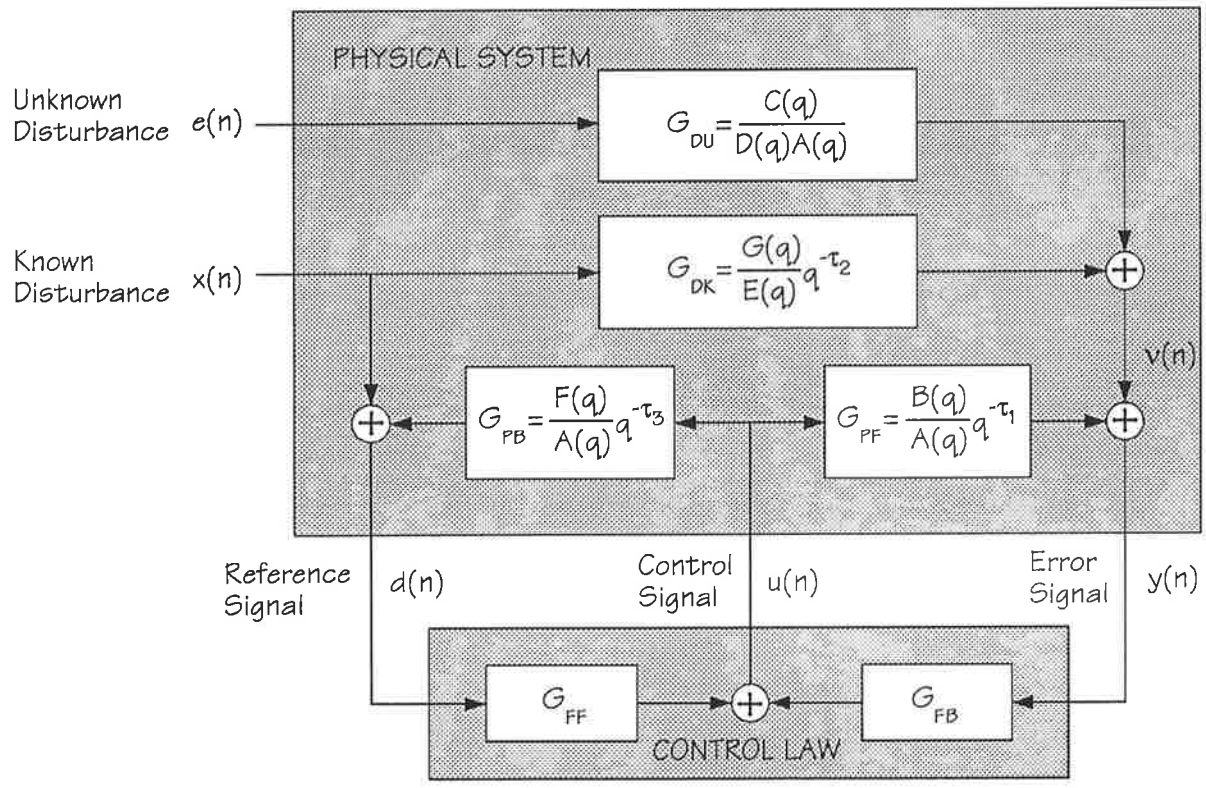

Figure 2-5. Block diagram form of transfer functions comprising the single channel system shown in Figure 2-4.

Before considering the feedforward and feedback components separately, the Diophantine equation will be introduced and the minimum variance control law formulated in its most general form. The Diophantine equation gives an insight into the physical effects and requirements of feedforward and feedback control schemes, which will be discussed in sections 2.4.1.1 and 2.4.1.2. Feedforward and feedback components will be considered separately, using simplifications of the theory to be outlined in this section, and related to the extensive literature on active noise and vibration control to show where commonly used algorithms can be improved. Feedforward control will be considered firstly without and then with input contamination, followed by consideration of feedback control. It will be shown that the control filters can be of infinite (IIR) or finite (FIR) impulse response, dependent upon the type of disturbance to be controlled.

The polynomials shown in Figure 2-5 should strictly be written as for example $A(q)$, but instead will be simplified to A, for ease of presentation. It can be shown using Doelman's [1991] system representation, that the system output (error signal) is given by

$$y(n) = \frac{B}{A}q^{-\tau_1}u(n) + \frac{G}{E}q^{-\tau_2}x(n) + \frac{C}{DA}e(n) \qquad [2\text{-}1]$$

This can alternatively be written as

$$y(n+\tau_1) = \frac{B}{A}u(n) + \frac{G}{E}x(n+\tau_1-\tau_2) + Me(n+\tau_1) + \frac{N}{DA}e(n) \qquad [2\text{-}2]$$

where the Diophantine equation is

$$\frac{C}{DA} = M + q^{-\tau_1}\frac{N}{DA} \qquad [2\text{-}3]$$

with M of order $(\tau_1 - 1)$ and N of order $(n_D + n_A - 1)$. The unpredictable part of the disturbance is $Me(n+\tau_1)$. The predictable part of the disturbance, $\frac{N}{DA}e(n)$, can be rewritten in terms of the known signals, and incorporated into the system output (error signal) to give

$$\hat{y}(n+\tau_1) = \frac{N}{C}y(n) + \frac{BMD}{C}u(n) + \frac{G}{E}q^{\tau_1-\tau_2}\frac{MDA}{C}x(n) \qquad [2\text{-}4]$$

This equation could be used to define the control law (that is, the equation defining how the control signal is to be generated), however the known disturbance is measured by the corrupted reference sensor and is therefore not directly obtainable. Therefore the reference signal should be used instead of the known disturbance when forming the control law. The reference signal is given by

$$d(n) = x(n) + \frac{F}{A}u(n-\tau_3) \qquad [2\text{-}5]$$

Hence the minimum variance predictor can now be written as

$$\hat{y}(n+\tau_1) = \frac{N}{C}y(n) + \left(\frac{BMD}{C} - \frac{FGMD}{EC}q^{\tau_1-\tau_2-\tau_3}\right)u(n) + \frac{G}{E}q^{\tau_1-\tau_2}\frac{MDA}{C}d(n) \qquad [2\text{-}6]$$

The minimum variance control law can therefore be formed as (refer to appendix A.3 for the formulation of the minimum-variance control law)

$$u(n) = -\frac{L}{H}d(n) - \frac{K}{H}y(n) \qquad [2\text{-}7]$$

where

$$K = NE$$
$$L = GMDAq^{\tau_1-\tau_2} \qquad [2\text{-}8a,b,c]$$
$$H = MD(BE - FGq^{\tau_1-\tau_2-\tau_3})$$

Hence to control the system output (that is, regulate the error signal to zero) requires a feedforward (represented by $G_{FF} = -L/H$) and a feedback (represented by

$G_{FB} = -K/H$) control filter, each of infinite impulse response type (as their transfer function requires both a numerator and denominator polynomial for accurate representation). It is also apparent that the polynomials B,C,G and F must be minimum-phase otherwise they would not be invertible (refer to appendix A.1 for stability of inverse based on minimum-phase characteristic). Doelman [1991] presented his work using a generalised criterion (as defined by equation (A-45) in appendix A.3), first proposed by Elliott et al [1987]. This generalised criterion enables the "Generalised Minimum Variance" control law to include pole placement (through use of the polynomials P and Q of the criterion given by equation (A-45) of the appendix), and thus reduce the effect of non-minimum phase zeroes.

2.4.1 Feedforward versus Feedback Control

Equations (2-7) and (2-8) give the requirements for feedforward and feedback control laws. Feedback control is required if $N \neq 0$, which implies that feedback control is only responsible for the reduction of the resonant response caused by stochastic disturbances (ie. the predictable component of the unknown disturbance, as defined by the Diophantine equation (2-3)). Feedforward control will have no impact on the unknown disturbance, and will only reduce the known disturbance by an amount dependent upon the coherence of the reference signal with the known disturbance (as defined by equation (A-24) in appendix A.2.2). The following sections discuss the causality constraints for feedforward and feedback control schemes, and give a brief insight into physical control mechanisms.

2.4.1.1 Causality Constraints

A system is causal if it has a response only after being excited. Causality is not a concern for periodic (deterministic) disturbances (Burgess [1981], as noted by Swanson [1991]), but greatly affects the achievable attenuation of stochastic disturbances. A stochastic disturbance is one in which white Gaussian noise is passed through an Autoregressive Moving Average (ARMA) filter (note that the AR part results in resonance peaks in the spectrum, while the MA part results in anti-resonances or dips/troughs). The causal constraint limits the frequency domain analysis of systems, and requires a separate analysis in the time-domain. The following comments relate specifically to causality constraints for the feedforward and feedback implementations.

- Feedback System.

  The resonances (peaks) of the disturbance can always be cancelled (ie. they are always a component of the predictable part of the disturbance as per the Diophantine equation (2-3)), however the degree to which broadband or coloured noise can be cancelled will depend on the time delay of the cancellation path transfer function, τ_1 (ie. the remaining coloured noise will be the unpredictable component of the Diophantine equation (2-3)). If the delay is minimised, good broadband attenuation can be achieved, and has been observed by Elliott et al [1995].

- Feedforward System.

  Perfect cancellation of a stochastic disturbance is possible provided the time taken for the disturbance to travel from the reference sensor to the control source, τ_2, exceeds the time taken for a measure of the disturbance to pass from the reference sensor through the controller and finally re-enter the "physical system" via the control actuator (this "electronic" time delay is known as the "group delay"), τ_G, and is shown in Figure 2-4 for both feedforward and feedback control schemes. The solution of the Diophantine equation also requires $\tau_2 \geq \tau_1$, which means that the distance from the control actuator to the error sensor must be less than the distance from the reference sensor to the error sensor.

2.4.1.2 Physical Control Mechanisms

A control source can act to reflect energy (and in so doing possibly change the impedance seen by the disturbance, provided it is placed near enough to it and the disturbance is periodic) or absorb energy (although this can result in greater power output by the disturbance and is therefore not an efficient form of control). A control source generally acts to both absorb and reflect energy [Snyder and Hansen, 1989]. The physical control mechanism depends on the type of disturbance (eg. periodic or stochastic), the directionality of the control actuator, the type of control scheme (ie. feedforward or feedback), and the type of physical system (ie. reverberant or non-

reverberant).

The impedance seen by a random noise source in a non-reverberant system cannot be changed, as enforced by the causality principle. Therefore the physical control mechanism for this type of source/system arrangement must be the absorption of energy. However for a reverberant system with a random noise source, the control mechanisms can be either absorption or impedance change.

Consider a periodic source in a duct. An omni-directional control source placed in a duct acts to primarily reflect energy, unloading the disturbance source, and storing the transient energy in a standing wave. This type of control source also acts to absorb energy in a minor way to avoid any resonance between the control and disturbance sources. However, a directional control source placed in a duct, cannot change the impedance seen by the disturbance source, therefore it can only absorb energy.

If it is possible to change the impedance seen by the disturbance, global attenuation can be achieved. As feedforward systems require a measure of the disturbance, they can be placed near the source of the disturbance and can therefore lead to global attenuation. On the other hand, feedback systems require no *a priori* measure of the disturbance and therefore result in zonal attenuation. Therefore, when feedback control systems are placed in the free-field at remote distances from the disturbance source, they must absorb energy to be effective. If the disturbance excites modes/resonances of the physical system, then these resonances can be damped, resulting in global attenuation by a feedback controller.

2.4.2 Feedforward Control Algorithms

It is apparent from the minimum variance control law defined by equation (2-7) that only a feedforward controller will be required if the predictable part of the unknown disturbance is zero. This requires that the polynomial N is zero, which is possible provided that DA is a factor of C, so that the Diophantine equation becomes $C/DA=M$. This means that there is no correlation between the plant output (or error signal) $y(n)$, and any part of the unknown disturbance, implying that this disturbance cannot be minimised at all. Thus only the known (or measurable) disturbance can be minimised with feedforward control. As noted by Swanson [1991], and discussed above, the principles of causality and coherence between the reference sensor and the error sensor are essential to feedforward control.

Snyder [1991a] used a state-space representation of a system to show that feedforward control alters the zeroes of a system, or the frequencies where a non-zero input will have a zero output. Snyder [1991a] also notes that feedforward control, by altering the zeroes of a system, in effect alters the impedance of a system to an incoming disturbance. This has also been made apparent by Elliott and Darlington [1985], who show that a feedforward system using a synchronously sampled reference signal is effectively an adaptive notch filter with the notch centred at the frequency of the disturbance.

2.4.2.1 Without Corruption

The simplest case of active noise and vibration control involves the use of a reference sensor that is not corrupted by acoustic feedback from the control actuator.

The first active noise control system implemented by Conover [1956] managed to avoid acoustic feedback. This system involved the control of noise from transformers, radiating harmonic frequency components with a fundamental of twice the frequency of the electrical supply. With full-wave rectification and band-pass filtering, the harmonic reference signals were produced, the phase and amplitude of which could be adapted in a feedforward sense to minimise the sound pressure level at discrete locations. This is a typical example of wave-form synthesis of the reference signal from synchronous sampling (eg. use of a tachometer on rotating/reciprocating machinery). Chaplin et al [1978,1980,1983] used synchronous sampling to provide a periodic pulse, from which the control signal could be generated (by "waveform synthesis") with frequency components corresponding to the fundamental and first few harmonics of the periodic pulse. Elliott and Darlington [1985] have assessed synchronous sampled signals as a special case of stability analysis, but also have shown how waveform synthesis can be implemented digitally. Dines [1984] used the light emission from unsteady burning in a turbulent flame, as the independent reference and achieved broadband attenuation of the generated noise field.

Attempts to avoid acoustic feedback were made using unidirectional control sources and reference sensors. Eghtesadi and Leventhal [1981] developed the "Chelsea

Dipole" in which corruption of the reference sensor was eliminated by placing it equi-distance between two control actuators driven out of phase and placed a half-wavelength apart. Nelson and Elliott [1992] showed that acoustic feedback can be reduced using two monopole sources driven out-of-phase with an appropriate delay dependent upon their spacing. This type of "dipole" system was implemented by Swinbanks [1973]. Nelson and Elliott [1992] also showed that unidirectional radiation can be achieved using a combination of a dipole and a monopole, as was first suggested in the theory developed by Jessel [1968] and Malyuzhinets [1969]. This approach was used by Jessel and Mangiante [1972] and is known as a "tripole system", with similar studies performed later by Canevet [1978] and Berengier and Roure [1980]. Attempts were also made by La Fontaine [1983] and Shepherd [1985] to make the reference sensor directional. Warnaka [1982] gives a good summary of these physical techniques, based on fixed-filter compensation.

The most commonly used adaptive feedforward algorithm in active noise and vibration control will now be derived from the minimum variance control theory. The model for this system is shown in Figure 2-6, where again it should be noted that the location of the algorithm used to adapt the control law parameters is not shown for clarity.

The minimum variance controller can be written using equation (2-6) with $N=0$ and $C/DA=M$, such that the predictor becomes

$$\hat{y}(n) = \frac{B}{A} q^{-\tau_1} \left[u(n) + \frac{GA}{EB} q^{\tau_1-\tau_2} x(n) \right] \qquad [2\text{-}9]$$

It is apparent (by comparison with appendix A.2.1) that the predictor is in output-

error form, and the minimum variance control law is given by

$$u(n) = Wx(n) \qquad [2\text{-}10]$$

with the control filter given by

$$W = -\left(\frac{G}{E}q^{-\tau_2}\right)\Big/\left(\frac{B}{A}q^{-\tau_1}\right) \qquad [2\text{-}11]$$

It is apparent from this equation that an IIR filter is required to estimate $\hat{W}$, however it is common to estimate $\hat{W}$ using a only a FIR filter. This simplification is often used in ducts, for which $E=A=1$ can be assumed as the system is non-reverberant, and for periodic noise it can be shown that B is a factor of G.

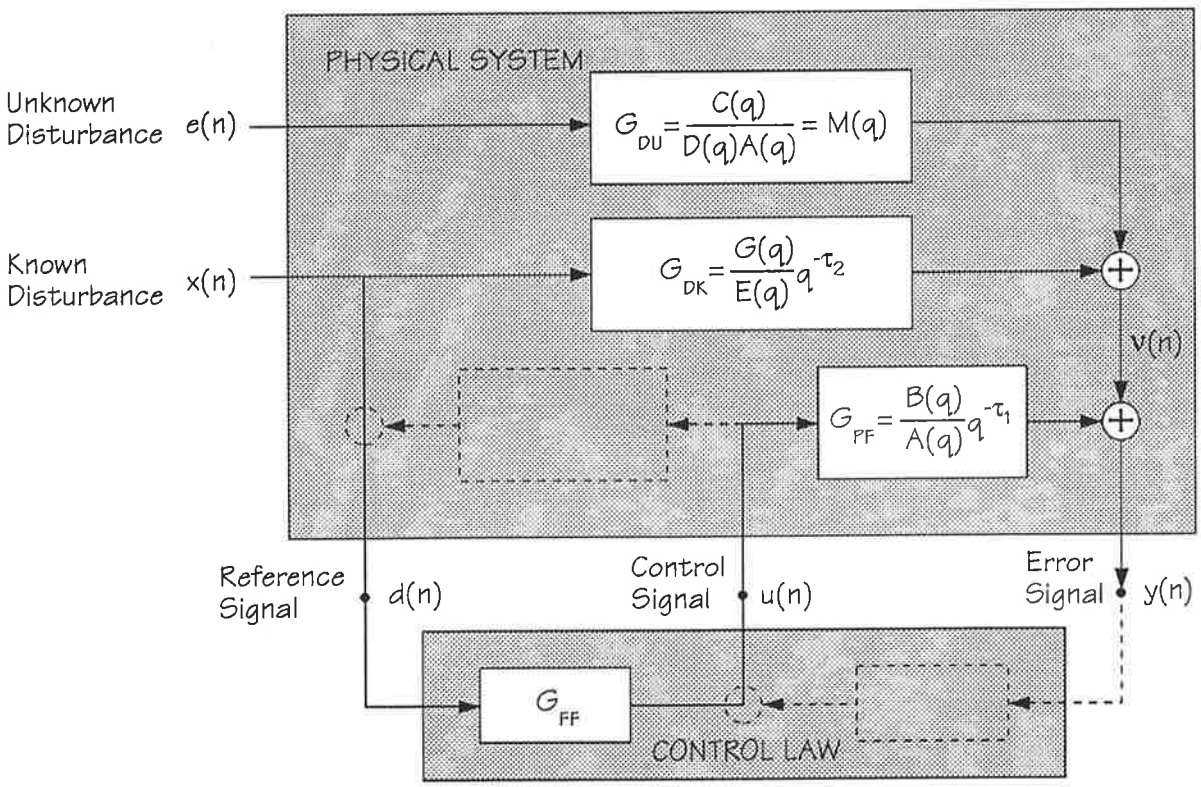

Figure 2-6. Feedforward Control without corruption of the reference signal.

The most common implementation (in active noise and vibration control) of this control scheme is the filtered-X algorithm (note that the most general form of the least mean squares or stochastic gradient algorithm is defined in appendix A.2.3), for which the cancellation path transfer function is firstly identified. The means of identifying this transfer function will be discussed shortly, but it is important to note the assumed knowledge of this transfer function. In accordance with appendix A.2.1.1, the regressor (or set of delayed filtered reference signal samples), $\phi(n)$, is defined using the reference signal filtered by the cancellation path transfer function, and the parameter vector (or set of control filter coefficients), $\hat{\theta}(n)$, consists of only the control filter coefficients, such that

$$\begin{aligned} \phi(n) &= [x^F(n),\ldots,x^F(n-n_W)]^T \\ \hat{\theta}(n) &= [\hat{w}_0(n),\ldots,\hat{w}_{n_W}(n)]^T \end{aligned} \qquad [2\text{-}12a,b]$$

where $x^F(n)$ represents the reference signal filtered by the cancellation path transfer function. The prediction error, $\varepsilon(n)$, can be written strictly using the predictor, $\hat{y}(n)$, in the form of equation (2-9), such that

$$\varepsilon(n) = y(n) - [\, u^F(n) - \hat{\theta}^T(n)\phi(n) \,] \qquad [2\text{-}14]$$

This form of prediction error has been termed the "augmented error", however it is commonly assumed that since control filter adaptation takes place slowly (if the Least Mean Squares or equivalently Stochastic Gradient algorithm is used), then the law of commutation holds (for the control filter and cancellation path transfer function convolution operations on the reference signal) and $u^F(n) = \hat{\theta}^T(n)\phi(n)$. The effects of this simplification will be discussed shortly, however with this simplification the prediction error becomes $\varepsilon(n) = y(n)$, and the parameter vector (of control filter coefficients) can be updated using the Least Mean Squares algorithm (or stochastic

gradient algorithm) which in this form has become known as the filtered-X algorithm.

$$\hat{\theta}(n+1) = \hat{\theta}(n) - 2\mu\phi(n)y(n) \qquad [2\text{-}14]$$

This algorithm was originally derived heuristically from the work of Widrow et al [1975] and first used in active noise control by Burgess [1981]. It is important to realise that the definition of the filtered-X algorithm relies on the assumption of slow updating of the control filter coefficients and the approximations discussed in appendix A.2.3 for the general least mean squares (or stochastic gradient) algorithm.

It is not easy to determine the required number of coefficients for the control filter. If there are too many coefficients, the excitation will not be persistent. The persistent excitation condition is discussed in appendix A.2.2, and requires that there be no more coefficients in the control filter than twice the number of spectral components in the reference excitation. However in reality there will always be some noise in the input at all frequencies (eg. from turbulence), therefore providing a uniquely determined set of optimal coefficients. If this noise at some frequencies is very much lower than other spectral components, the disparity will cause very slow convergence for some coefficients. Thus control filter coefficient saturation and instability can occur. To avoid this problem leakage of the coefficients is necessary [Honig and Messerschmitt, 1984]. The use of a leakage term also aids incomplete cancellation of DC offsets, quantisation noise and round-off errors. Isermann [1991] notes that the DC offsets can also be modelled.

The ability to commutate the cancellation path transfer function estimate and the control filter assumes that the control filter is only slowly time varying and therefore

can be considered to be time invariant. The use of the recursive least squares algorithm (discussed in appendix A.2.3) can however increase the convergence rate considerably, thereby invalidating this commutation process. Flockton [1991] has shown by experiment that increased convergence speed, using the standard filtered-X control algorithm, results in an initial instability in convergence that is dependent on phase and delay characteristics of the cancellation path transfer function. Flockton [1991] proposed eliminating the effect of the cancellation path transfer function on the weight adaptation, in a similar way to that of Johnson [1990], by augmenting the error signal to directly obtain the disturbance to be minimised. It appears that a similar approach has also been taken by Doelman [1991] and Kim [1994].

The use of the augmented-error approach eliminates the interplay between system identification and control that is present with the filtered-X algorithm. The degree to which the augmented-error approach is useful, is dependent upon the accuracy in the estimate of the cancellation path transfer function. Flockton's results are similar to Johnson's, finding that the convergence rate of the filtered-X algorithm using the augmented-error was improved only for accurately estimated delays in the cancellation path that are substantially greater than the convergence time of the least mean squares algorithm in the equivalent system with no cancellation path delay. Thus the augmented-error approach is only useful for efficiently implemented fast adaptation algorithms such as the recursive least squares algorithm implemented on a joint process lattice filter [Park and Sommerfeldt, 1994].

Johnson [1990] notes that the augmented-error approach was first proposed by

Ionescu and Monopoli [1977] for "Model Reference Adaptive Control (MRAC)" systems. Astrom and Wittenmark [1989] use the augmented-error concepts to show how the Self Tuning Regulator form is equivalent to the Model Reference Adaptive Control form.

As discussed, the filtered-X algorithm requires the separate identification of the cancellation path transfer function. The required knowledge of the cancellation path transfer function complicates the adaptive control algorithm, unless an algorithm that doesn't require knowledge of this transfer function is used (eg. Smith and Chaplin's [1983] "power sensing" algorithm). A general discussion of these types of algorithms will be presented in section 2.5.

Modelling of the cancellation path transfer function was performed by Eriksson [1989] using a Galois sequence (or Pseudo Random Binary Sequence (PRBS)) as defined by Schroeder [1984]. As discussed in appendix A.2, this is a variant of the instrumental variables technique. It can be shown that the bound (known as the Cramer Rao bound [Ljung and Soderstrom, 1983]) on the covariance of the parameter vector (which now is the vector of parameter estimates for the cancellation path transfer function) is given by [Johnson, 1992]

$$E\{[\hat{\theta} - \theta_0]^T[\hat{\theta} - \theta_0]\} \geq \frac{1}{t(\sigma_w^2/\sigma_\varepsilon^2)} \qquad [2\text{-}15]$$

Here the power of the injected PRBS signal is σ_w^2 and σ_ε^2 is the uncorrelated part of the disturbance (ie. the input to the error sensor other than that resulting from the PRBS). The ratio $\sigma_w^2/\sigma_\varepsilon^2$ can be interpreted as the signal to noise ratio (SNR). It

therefore follows that for low SNR's ($<<1$) essential for limited intrusion, the convergence rate must be very low in order to maintain minimum variance of the cancellation path transfer function estimate. This means that for accurate estimation of the cancellation path transfer function, convergence will only be achieved after an extended period, thus limiting this on-line method of system identification. Use of the PRBS does however ensure the persistent excitation condition is met.

Johnson [1990] used perturbations of the control filter coefficients to obtain substantially improved performance (accuracy and speed) of the estimate for the cancellation path transfer function. Johnson [1990] notes that this novel method is performed only when necessary, with its main disadvantage being its high computational load.

Bao et al [1993] increased the SNR by reducing the power of the noise σ_ε^2 using adaptive noise (electrical or "in-wire") cancellation. They note that a substantially improved speed of convergence results with this method.

The effect of errors in the cancellation path transfer function will now be discussed. For the most general disturbance, the polynomial B (in equations (2-9) and (2-11)) must be minimum phase since it is inverted. It can be shown, using the hyperstability principles developed by Popov or Ljung's Ordinary Differential Equation (ODE) method [Cowan and Grant, 1985; Ljung, 1983], that a necessary condition for convergence of the parameter estimates (which is apparent given the minimum-phase condition on B and the Strictly Positive Real (SPR) condition on A, for algorithm

simplification as discussed in appendix A.2.3) is given by

$$Re\left\{\frac{\hat{G}_{PF}(e^{j\omega})}{G_{PF}(e^{j\omega})}\right\} > 0 \quad \forall\omega \qquad [2\text{-}16]$$

where $G_{PF} = \frac{B}{A}q^{-\tau_1}$ is the cancellation path transfer function and $\hat{G}_{PF}$ is the estimate of this transfer function. This equation suggests that the error in phase between the predicted and the actual cancellation path transfer function must be within $\pm 90°$ for stability, which as will be discussed, has been found by many other researchers. It can be shown that the controller will achieve optimal convergence despite an error in the cancellation path transfer function estimate, provided near complete cancellation of the correlation between *d(n)* (the reference signal) and *y(n)* (the error signal) can be achieved [Ren and Kumar, 1989].

Feintuch et al [1993] analysed the filtered-X algorithm in the frequency-domain, and defined the bounds of stability for the convergence coefficient, μ, as

$$\mu < \frac{1}{P_X \mid G_{PF}(e^{j\omega}) \mid^2} = \frac{1}{P_R} \qquad [2\text{-}17]$$

where P_X represents the maximum power of a spectral term in the reference signal (it can also be defined as the maximum eigenvalue of the autocorrelation matrix for the reference signal), and $\mid G_{PF}(e^{j\omega}) \mid$ represents the amplitude of the discrete frequency response of the cancellation path. Alternatively, P_R, can be used to represent the maximum power of a spectral term in the filtered reference signal . Sommerfeldt and Tichy [1990] also show that the stability bound for the convergence coefficient is given by

$$\mu < \frac{2}{P_X g_{PF_{max}} I J^2} \qquad [2\text{-}18]$$

with I the number of control filter coefficients, J the number of cancellation path transfer function coefficients, and $g_{PF_{max}}$ the maximum coefficient of the cancellation path transfer function.

The effect of errors in the cancellation path transfer function estimate have been well researched. The earliest account of the effect of such errors is made by Morgan [1980]. Errors in the estimates of the cancellation path reduce the bounds of stability for the convergence coefficient, such that

$$\mu < \frac{\cos \phi_{err}(e^{j\omega})}{G_{PF_{err}}(e^{j\omega}) P_R} \qquad [2\text{-}19]$$

where $\phi_{err}(e^{j\omega})$ represents the error in the phase, and $G_{PF_{err}}(e^{j\omega})$ represents the error in magnitude of the cancellation path transfer function estimate, and P_R is defined as above. If $\phi_{err}(e^{j\omega})$ is not within the range $\pm 90°$ for all values of ω, there will be no stability region for the algorithm. It can further be shown that the time constant of adaptation is given by

$$\tau(\omega) = \frac{1}{2 \; P_R G_{PF_{err}}(e^{j\omega})} \qquad [2\text{-}20]$$

Hence if $G_{PF_{err}}(e^{j\omega})$ is sufficiently small, with a small convergence coefficient, the time taken for the algorithm to reach instability will be large.

Phase compensation filters and band limited inputs have been suggested as a means of avoiding this unstable region. Feintuch [1993] suggested applying a simple delay to the reference signal to maintain the error in phase estimation for the cancellation

path transfer function to within $\pm 90°$. This system will not work however if there are resonances within the actuator or sensor response, so that the total phase response cannot be predicted with a linear phase filter of this nature. Widrow and Stearns [1985], as noted by Elliott and Nelson [1994], suggest that if the impulse response of the estimated cancellation path transfer function has *"at least as great a transport delay"* as the actual response, stability can be assured.

Instead of filtering the reference signal with the cancellation path transfer function, the inverse estimate of the cancellation path transfer function can be used to filter the error signal (or process output). It is however possible that the inverse of the cancellation path transfer function is not causal and therefore not physically realisable. Extracting the time delay, $q^{-\tau_1}$, from the cancellation path transfer function, G_{PF}, leaves only the inverse of the ARMA process with no dead-time, B/A, to be determined. This can be viewed as a compensation filter. With this approach however, the delay needs to be estimated and errors in this estimation can also reduce the stability bounds for the convergence coefficient. The effect of a delay on the standard LMS algorithm has been investigated by Kabal [1983]. The ability to model the inverse of the cancellation path transfer function is also corrupted by the primary disturbance, thereby causing the optimal filter to converge to a transfer function other than the required inverse of the cancellation path transfer function, dependent upon the level of the disturbance (ie. a biassed transfer function will result [Eriksson, 1991]). Further discussion of the effect of estimation inaccuracies in delay and cancellation path transfer functions is given by Snyder and Hansen [1990].

Elliott et al [1987] have considered equivalent transfer functions of adaptive systems, fed with harmonic excitation, to assess the stability of the adaptive algorithm. This analysis has been based upon the previous work of Glover [1977], and has also been used for multichannel stability analysis by Boucher et al [1991] and Elliott et al [1992]. Elliott has shown, using a z-transform of the weight adaptation process (in a similar way that Kabal did, although Kabal's [1983] method is more general) that for a synchronously sampled sinusoidal reference input, the adaptive feedforward system can be written as an equivalent linear feedback system. The frequency response of this transfer function represents a notch filter (and for harmonics a comb filter results [Glover, 1977]) centred at the frequency of the reference signal. Recently Morgan and Thi [1993] have proposed using this type of adaptive notch filter [Elliott and Nelson, 1992] to extend the bandwidth of attenuation from narrowband to multi-narrowband (or an adaptive "comb" filter) and even broadband, by cascading a number of these filters.

Analysis of the equivalent linear feedback transfer function using standard root-locus theory can describe the pole movements from within the unit circle, $|z| = 1$, to their bounds of stability on the unit circle. This then can provide the stability bounds of the convergence coefficient, used in the LMS adaptive algorithm. The pole positions can also show the effects of inaccurate delay and error-path estimates for the special case of synchronous sampling. Characteristics (eg. system damping) of the learning curve (mean square error versus sample number) are also elucidated by pole positions.

Darlington [1991] has shown that inaccuracies in delay estimates increases the passband disturbance on both sides of the notch filter, thereby also reducing the effective bandwidth. He has also shown that errors in the estimate of the cancellation path phase increases the passband disturbance on one-side only, dependent upon whether the phase error is positive or negative. The passband disturbance is a result of time variance of the adaptive filter that causes modulation of the frequency component (for a tone) of the filters input. The bandwidth is thus defined by the degree of variance in the adaptive filter, or the rate of adaptation (or coefficient modulation) defined by the convergence coefficient.

The filtered-x algorithm has also been implemented in the frequency domain by Shen and Spanias [1992] based on the work of Widrow et al [1975]. This approach allows independent modal control, with the elimination of the effect of spectral disparity that plagues the equivalent time-domain algorithm. This type of approach also allows control of intensity signals which would otherwise be difficult to control in the time-domain. Another frequency domain approach using transmultiplexers [Cowan and Grant, 1985] has recently been proposed by Thi and Morgan [1993]. Their technique reduces the high computational burden of long FIR filters, with possibly increased convergence speed due to reduced spectral dynamic range within each transmultiplexer band.

The effects of transducer non-linearities [Beltran, 1995] necessitates the use of a controller with a non-linear control characteristic. Neural networks have been presented as a solution [Brown, 1993; Bozich, 1991], yet their speed of convergence is

slow, and they require large amounts of computations [Klippel, 1995]. Recently Klippel [1995] has proposed a non-linear ladder filter (based on a Volterra series) in simplified form, with less complexity and more efficient implementation.

An improvement in the standard feedforward algorithm will now be broached. The interplay between system identification and control can be minimised by rewriting equation (2-9) as

$$\hat{V}\hat{y}(n) = \hat{H}u(n) + \hat{L}x(n) \qquad [2\text{-}21]$$

where

$$\begin{aligned} \hat{V} &= AE \\ \hat{H} &= BEq^{-\tau_1} \\ \hat{L} &= GAq^{-\tau_2} \end{aligned} \qquad [2\text{-}22a,b,c]$$

The control filter coefficients can be found by an implicit system identification and an implicit solution to the Diophantine equation, using the parameter vector and regressor defined as

$$\begin{aligned} \hat{\theta}(n) &= [\hat{h}_0,\ldots,\hat{h}_{n_H},\hat{l}_0,\ldots,\hat{l}_{n_L},\hat{v}_1,\ldots,\hat{v}_{n_V}]^T \\ \phi(n) &= [u(n),\ldots,u(n-n_H),x(n),\ldots,x(n-n_L),\hat{y}(n-1),\ldots,\hat{y}(n-n_V)]^T \end{aligned} \qquad [2\text{-}23a,b]$$

From equation (2-21) the control law can be written as

$$u(n) = -\frac{\hat{L}}{\hat{H}}x(n) \qquad [2\text{-}24]$$

or equivalently as

$$u(n) = -\frac{1}{\hat{h}_0}[\,\hat{l}_0x(n) + \ldots + \hat{l}_{n_L}x(n-n_L) + \hat{h}_1u(n-1) + \ldots + \hat{h}_{n_H}u(n-n_H)\,] \qquad [2\text{-}25]$$

This represents an IIR filter, with the coefficients determined directly from the implicit system identification. Stability depends upon the accuracy of the estimate for V. That is the Strictly Positive Real (SPR) condition is

$$Re\left\{\frac{\hat{V}(e^{j\omega})}{V(e^{j\omega})}\right\} > 0 \quad \forall\omega \qquad [2\text{-}26]$$

This condition determines how accurately the poles of the disturbance model and cancellation path transfer function are estimated. This approach requires only a system identification process, not a combination of "control" and "system identification" adaptations, that is commonly used and can readily result in instability.

The minimum variance predictor, defined by equation (2-21), is in output-error form, and so adaptation can be performed using either the algorithm defined by Hsia [1981] corresponding to the recursive prediction error method in simplified form, or the algorithm defined by Feintuch [1976] corresponding to the recursive pseudo-linear regression approach in simplified form. These algorithms are discussed in more detail in appendix A.2. Hsia's [1981] algorithm is more accurate and requires little more computation. Ren and Kumar [1989] have defined a similar algorithm (to the algorithm defined by Hsia) in SHARF form, and further note that $\hat{h}_0 \neq 0$ for causality. It should also be noted that the output-error approach can be improved with the use of a residual term included in the regressor, to better approximate $\hat{y}(n)$, as discussed in appendix A.2.

Sommerfeldt and Tichy [1990,1991], Eriksson [1991], Kuo [1992] and van Overbeek [1991] have developed similar techniques, and most recently, Reichard et al [1993] and Leung [1993] have proposed similar on-line system identification techniques for the frequency domain. These authors predict the process output in a similar manner to that of equation (2-21), such that (note that they assume $\hat{V} \simeq 1$ as per the Recursive

Pseudo-Linear Regression algorithms discussed in appendix A.2)

$$\hat{y}(n) = \hat{H}u(n) + \hat{L}x(n) \qquad [2\text{-}27]$$

With the regressor and parameter vector defined as

$$\hat{\theta}(n) = [\hat{h}_0,\ldots,\hat{h}_{n_H},\hat{l}_0,\ldots,\hat{l}_{n_L}]^T$$
$$\phi(n) = [u(n),\ldots,u(n-n_H),x(n),\ldots,x(n-n_L)]^T \qquad [2\text{-}28a,b]$$

The parameter vector is adapted recursively using

$$\varepsilon(n) = y(n) - \hat{y}(n) = y(n) - \phi^T(n)\hat{\theta}(n)$$
$$\hat{\theta}(n+1) = \hat{\theta}(n) + \frac{\alpha}{ß + \phi^T(n)\phi(n)}\phi(n)\varepsilon(n) \qquad [2\text{-}29a,b]$$

where the autocorrelation matrix and gain factor are approximated by

$$\gamma(n)R_{\phi\phi}^{-1}(n) = \frac{\alpha}{ß + \phi^T(n)\phi(n)}I \qquad [2\text{-}30]$$

This algorithm is known as the projection algorithm or normalised LMS algorithm, and is an extension of the stochastic gradient method for the recursive pseudo-linear regression approach. At this point the control law could have been obtained as per equation (2-25), however these authors used only $\hat{H}$ as the estimated cancellation path transfer function, and the filtered-X algorithm defined by equation (2-15). The use of the filtered-X algorithm causes biassed system identification terms $\hat{H}$ and $\hat{L}$, if the process output reaches zero before convergence of $\hat{H}$ and $\hat{L}$ (ie. the control filter coefficient adaptation scheme converges before the system identification adaptation scheme) [Wangler and Heiland, 1992]. This is because, if *y(n)* (ie. the error signal) is held at zero by the "control" adaptation of the filtered-X algorithm (as it ideally will be), then the "system identification" adaptation which attempts to minimise $\varepsilon(n)$, will be forced to minimise $\hat{y}(n)$ instead. This means that $\hat{H}$ and $\hat{L}$ will converge to incorrect values (possibly outside their stability range). If the physical system then

changes and $y(n)$ becomes non-zero, the control filter coefficients will be adapted again using the last converged system identification term $\hat{H}$. Thus if $\hat{H}$ is outside the stability range, then instability will result. Similar results have also been found by Bao et al [1993], who suggest that the rate of convergence of the filtered-X algorithm be set less than the "on-line" system identification algorithm.

It is to be noted that if the filtered-X algorithm is not used in conjunction with the on-line system identification algorithm, and instead the control coefficients are derived from the implicit system identification as per equation (2-25), then the system will be stable. The interplay between the control law scheme and the system identification algorithm in this approach, is well explained by Bitmead et al [1990]. Their results lead to a discussion on robust control in section 2.4.5.

To achieve global control of noise or vibration in three-dimensional physical systems, will require multiple actuators and sensors. Elliott et al [1987] first developed a multi-channel form of the filtered-X algorithm. The cost function for minimisation is the sum of the squares of all the error sensors. Elliott et al [1987] suggested an alternative cost function criterion known as the "minimax" criterion, which instead of minimising the sum of all errors, minimises the largest error. Kuo [1993] presented a method for efficiently measuring on-line the cancellation path transfer functions using random noise, with each channel decoupled using an appropriate delay. As discussed, the cancellation path transfer function can also be measured on-line using available signals, without the addition of random noise, but this method is unreliable unless certain precautions are taken (as discussed above). A reliable method of control

using only a single adaptation scheme has also been described here.

A number of authors [Snyder et al, 1992a,b; Elliott et al, 1987, 1992; Boucher et al, 1991] have assessed the asymptotic properties of the multi-channel filtered-X algorithm. Elliott et al [1987, 1992] and Boucher et al [1991] suggest that the inclusion of an effort weighting (thus forming a Generalised Minimum Variance (GMV) approach discussed in appendix A.3) results in increased robustness to errors in the cancellation path transfer function estimates. Elliott and Nelson [1994] note that this term is equivalent to having a "leak" in the algorithm (as used for DC-offset compensation [Gitlin et al, 1982]). Widrow and Stearns [1985], as noted by Elliott and Nelson [1994], show that the presence of low level uncorrelated noise (eg. caused by turbulence or the like) is also equivalent to having a "leak" in the algorithm. It is considered here that this enhances compliance with the persistent excitation condition, with more accurate parameter estimates determined. A weighting term also limits high levels of control signals that could generate non-linearities from the control actuators, therefore improving robustness.

Elliott and Nelson [1994] note that the convergence time of the different modes of the system are dependent on the eigenvalues of the autocorrelation matrix, as has been discussed for the single channel case. For a multi-channel system, the eigenvalues of the autocorrelation matrix are not only dependent upon the spectral properties of the reference signal, but also on the spatial distribution of transducers.

Elliott et al [1991] examined the effect of inter-channel coupling, by considering

instead of a single multi-channel controller, a number of single-channel controllers. They show that stability can be achieved provided the error sensor of a single channel system is closer to the control actuator of that system than of another, which is similar to the causality constraints defined for a one-dimensional feedforward system in section 2.4.1.1.

Swanson [1993] analysed the on-line system identification method, originally proposed by Sommerfeldt and Tichy [1990], with the filtered-X algorithm in a multi-channel system. He used a "polynomial matrix method" to allow individual or combinations of error sensors to define the criterion for optimisation by particular control actuators. He notes that the placement of the error sensors and control sources affects convergence of the algorithm, with their optimal locations dependent on the spatial modal structure of the disturbance. He also shows that if two or more of the control source/error sensor paths are linearly dependent, then instability can occur.

Snyder and Hansen [1992a] have also examined the convergence characteristics of the multi-channel filtered-X algorithm, finding similar results to Swanson [1993]. They note that when the number of error sensors exceeds the number of control sources, with some degree of redundancy (or linear dependence between control source/error sensor paths) the minimum achievable mean square error will be non-zero. They note that the convergence coefficient bound, discussed earlier in this section, is further reduced as the number of error sensors is increased. They also note that the cross-coupling between transducers defined by the eigen properties of the system, leads to optimum control filters that are not unique, but depend on the adaptation strategy (ie.

adapt all coefficients of each channel in turn, or adapt all coefficients of all channels simultaneously). Their results suggest the inclusion of a control effort term in the criterion, thus leading to Generalised Minimum Variance (GMV) control and ultimately Linear Quadratic Gaussian (LQG) control to be discussed in section 2.4.5.

Snyder et al [1992b] also note the importance of observability and controllability (state-space terminology) of offending modes, as defined by the placement of transducers (a similar discussion can also be found in Swanson [1986]).

2.4.2.2 With Corruption

Figure 2-7 shows the inclusion of an acoustic feedback transfer function that results in contamination of the reference sensor. From equation (2-6), with $M=C/DA$ and $N=0$, it is apparent that the minimum variance predictor can be written as:

$$\hat{y}(n) = \frac{B}{A}q^{-\tau_1}\left[\left(1 - \frac{FG}{BE}q^{\tau_1-\tau_2-\tau_3}\right)u(n) + \frac{AG}{BE}q^{\tau_1-\tau_2}d(n)\right] \qquad [2\text{-}31]$$

or by direct comparison of terms, it can be equivalently written as

$$\hat{y}(n) = \hat{G}_{PF}[\hat{H}u(n) + \hat{W}d(n)] \qquad [2\text{-}32]$$

where

$$\hat{G}_{PF} = \frac{\hat{B}}{\hat{A}} q^{-\tau_1}$$

$$\hat{H} = 1 - \frac{\hat{F}\hat{G}}{\hat{B}\hat{E}} q^{\tau_1-\tau_2-\tau_3} \qquad [2\text{-}33a,b,c]$$

$$\hat{W} = \frac{\hat{G}\hat{A}}{\hat{B}\hat{E}} q^{\tau_1-\tau_2}$$

The control law is then given by

$$u(n) = -\frac{\hat{W}}{\hat{H}} d(n) \qquad [2\text{-}34]$$

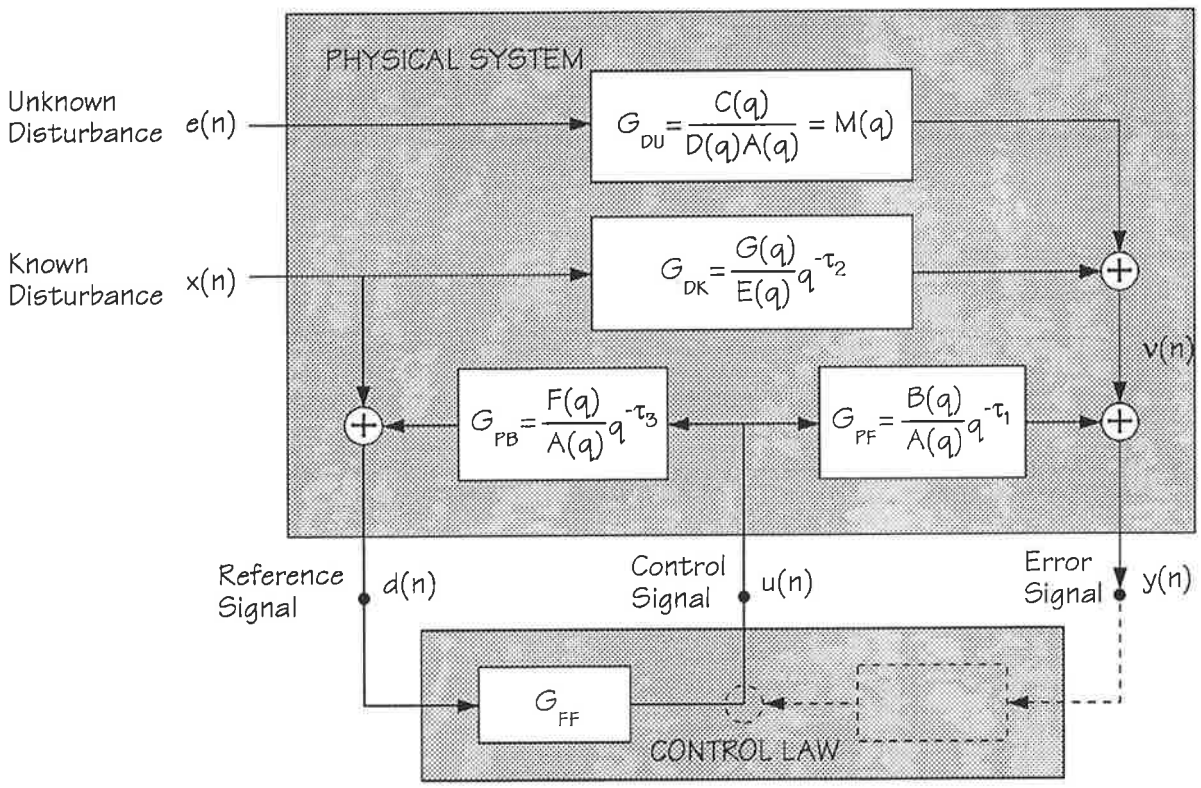

Figure 2-7. Feedforward control with corruption of the reference signal by acoustic feedback from the control actuator.

Since $\hat{H}$ involves a transfer function difference, then it is unlikely that $\hat{H}$ is a factor of $\hat{W}$ and therefore the use of an FIR filter is not possible and an IIR filter must be used. It is interesting to note that $\hat{W}$ corresponds to the controller without corruption, as defined in the last section. Eriksson [1987, 1991a, 1991b] used a modified form of the RLMS algorithm (developed by Feintuch [1976]), known as the filtered-U algorithm, to adapt the coefficients of $\hat{H}$ and $\hat{W}$ based on an estimate of the cancellation path transfer function $\hat{G}_{PF}$. The cancellation path transfer function was estimated on-line using a pseudo random binary sequence (PRBS) [Eriksson, 1989] as previously discussed. The filtered-U algorithm is defined using the parameter vector and regressor, such that

$$\begin{aligned} \hat{\theta}(n) &= [\hat{h}_0,\ldots,\hat{h}_{n_H},\hat{w}_0,\ldots,\hat{w}_{n_W}] \\ \phi(n) &= [u^F(n),\ldots,u^F(n-n_H),d^F(n),\ldots,d^F(n-n_W)] \end{aligned} \qquad [2\text{-}35a,b]$$

where the superscript, F, refers to filtering by the cancellation path transfer function. The prediction error and parameter vector update equation can be written as

$$\begin{aligned} \varepsilon(n) &= y(n) - \phi^T(n)\hat{\theta}(n) \\ \hat{\theta}(n+1) &= \hat{\theta}(n) - 2\mu\phi(n)\varepsilon(n) \end{aligned} \qquad [2\text{-}36a,b]$$

Note however that the prediction error was estimated as $\varepsilon(n) \approx y(n)$, which as discussed is only true for slow variations of the process (cancellation path transfer function) and control filters. The interplay between control and system identification can be eliminated using the "augmented-error".

The control law defined by equation (2-34) can be written as

$$u(n) = -\frac{1}{\hat{h}_0}[\hat{w}_0 d(n) + \ldots + \hat{w}_{n_W} d(n-n_W) + \hat{h}_1 u(n-1) + \ldots + \hat{h}_{n_H} u(n-n_H)] \qquad [2\text{-}37]$$

Eriksson [1991a,b] first suggested the application of a fixed "SHARF filter" in active

noise and vibration control, with the prefilter equivalent to the polynomial AE. The use of such a filter is discussed in appendix A.2. Eriksson [1987b] gives many methods to obtain an estimate for the cancellation path transfer function.

It will be shown later that Eriksson [1991a,b] uses a combination of feedforward and feedback control to obtain what he terms an "equation-error IIR filter", however the IIR filter used in this section can be considered to be of output-error type. A FIR control filter can be used by rewriting equation (2-32) as

$$\hat{y}(n) = \hat{G}_{PF}[(1 - \hat{G}_{PB}\hat{W})u(n) + \hat{W}d(n)] \qquad [2\text{-}38]$$

with the control law thus becoming

$$u(n) = \frac{\hat{W}}{1-\hat{G}_{PB}\hat{W}}d(n) \qquad [2\text{-}39]$$

This equation can alternatively be written as

$$u(n) = \hat{W}\tilde{x}(n) \qquad [2\text{-}40]$$

where

$$\tilde{x}(n) = -\hat{G}_{PB}u(n) + d(n) \qquad [2\text{-}41]$$

This form of control compensates for the acoustic feedback corruption of the reference sensor, but requires the estimation of the acoustic feedback transfer function, $\hat{G}_{PB}$. With good compensation $\tilde{x}(n) \approx x(n)$, and the controller is equivalent to the feedforward controller without corruption, as defined by equation (2-10).

As discussed in the previous section, initial attempts to compensate for acoustic feedback used fixed-filters to create uni-directional transducers. As noted by Eriksson [1992], Ross [1982] developed techniques using fixed filters, together with adaptive

filters, to reduce the effect of acoustic feedback. Warnaka et al [1984] used similar fixed filters (with adaptive filters) to compensate for acoustic feedback as well as the cancellation path transfer function.

Besides the moving average parts of the plant transfer functions (ie. B, F and G) complying with the minimum-phase condition, other stability conditions that ensure convergence must be satisfied. Analysis of the stability of this system is given by Swanson [1991], who notes, as does Eriksson [1991a,b], that the solution for $\hat{H}$ and $\hat{W}$ is not unique. This has also been noted in appendix A.3, in a general discussion on minimum variance control.

An alternative updating method that requires no injection of a random sequence, and requires only a single adaptation algorithm can be developed by rewriting equation (2-31) as

$$AE\hat{y}(n) = (BEq^{-\tau_1} - FGq^{-\tau_2-\tau_3})u(n) + AGq^{-\tau_2}d(n) \qquad [2\text{-}42]$$

or equivalently

$$\hat{V}\hat{y}(n) = \hat{H}'u(n) + \hat{L}d(n) \qquad [2\text{-}43]$$

where

$$\begin{aligned} \hat{V} &= \hat{A}\hat{E} \\ \hat{H}' &= \hat{B}\hat{E}q^{-\tau_1} - \hat{F}\hat{G}q^{-\tau_2-\tau_3} \\ \hat{L} &= \hat{G}\hat{A}q^{-\tau_2} \end{aligned} \qquad [2\text{-}44a,b,c]$$

Again this is an output-error form of control since there is no feedback of the process output included in the predictor. Hence the algorithms of White [1975] or Landau [1976] or simplifications thereof, can be used to adapt the parameter vector, with the

minimum variance control law given by

$$u(n) = -\frac{\hat{L}}{\hat{H}'} d(n) \qquad [2\text{-}45]$$

This type of approach has been suggested by Doelman [1991] and Ren and Kumar [1989]. The minimum-variance criterion has been generalised by Doelman [1991] to include a form of pole-placement Self Tuning Regulator (STR) that accounts for non-minimum-phase transfer functions. This approach was first suggested by Wellstead [1979] in an explicit form. Astrom and Wittenmark [1980] have proposed a pole-zero placement approach. Non-minimum-phase transfer functions can be treated using a Linear Quadratic Gaussian (LQG) approach, which will be summarised in section 2.4.5.

2.4.3 Feedback Control

Feedback control is required where no measurement of the disturbance is available. This type of control scheme was first proposed by Olson [1953, 1956]. Swanson [1991] notes that such applications include spatially incoherent noise generated from turbulence, noise generated from many sources and paths, and induced resonance.

Using a state-space system representation, Snyder [1991] notes that feedback control modifies the poles or resonant frequencies of the system. That is, feedback control alters the duration of the system transient response to an input. Snyder [1991] further states that feedback control is not well suited to the attenuation of periodic

disturbances since complete cancellation is possible [Swanson, 1991], therefore resulting in infinitely high negative gains producing a potentially unstable system response for transients in the error signal. In this section it will be shown that feedback control can always attenuate (or damp) the spectral peaks of a disturbance, but that the broadband attenuation is limited by the time delay between the control actuator and error sensor transducers. Similarly, Swanson [1991] notes that the time delay between the control actuator and the error sensor limits complete cancellation to only periodic disturbances (though good cancellation can be achieved for the spectral peaks of white Gaussian noise passed through an ARMA filter).

An excellent comprehensive study of the fixed filter design of feedback controllers can be found in Nelson and Elliott [1992], with a good summary in Elliott and Nelson [1994]. The design of compensation filters to allow for the instabilities associated with the linear phase response of a delay between the transducers, has been particularly successful for active headsets [Simshauser and Hawley, 1955; Wheeler, 1986; Carme, 1987]. Feedback control has been implemented with some success in ducts by Eghtesadi et al [1983] and Trinder and Nelson [1983].

A purely feedback system is shown in Figure 2-8, where the location of the algorithm or parameter adaptation scheme has not been shown for clarity. There is no measure of a disturbance, hence the only transfer functions shown are the cancellation path transfer function, G_{PF}, the disturbance transfer function, G_{DU}, and the feedback control filter, G_{FB}.

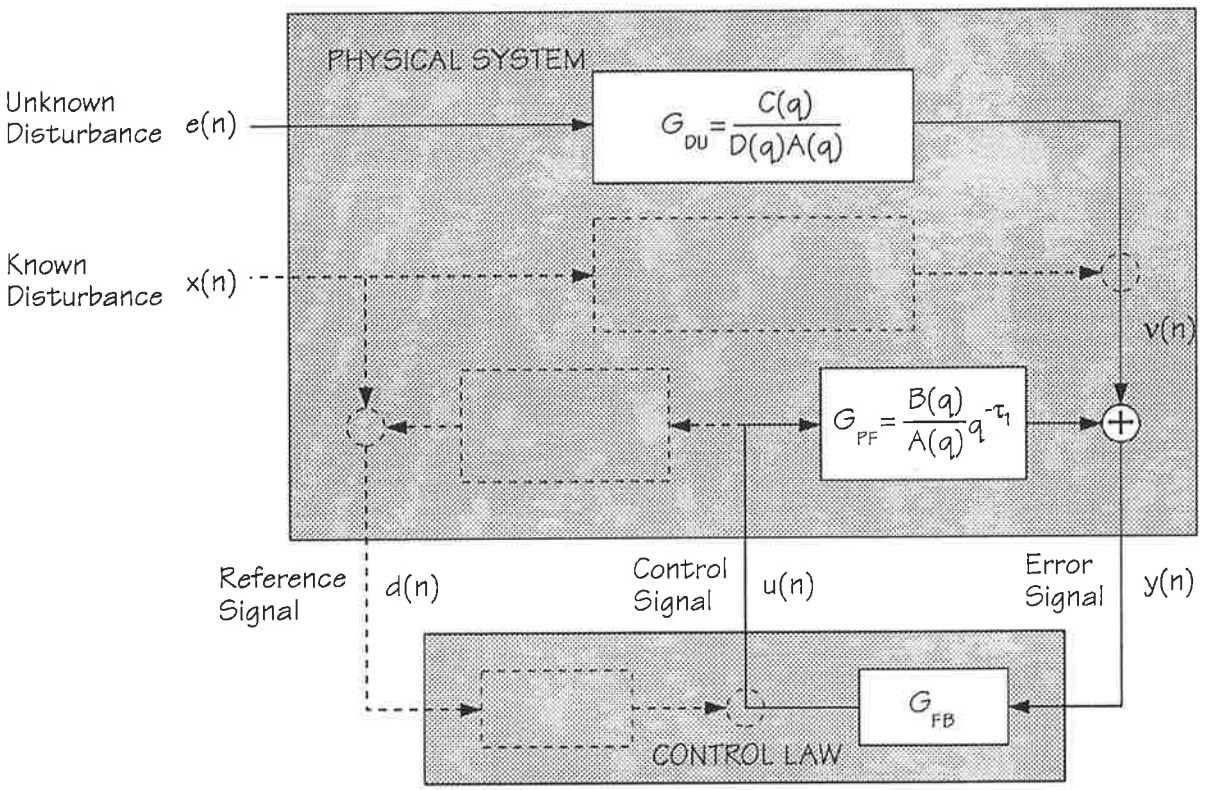

Figure 2-8. Feedback control block diagram.

Using equation (2-4) with $G=0$ and $F=0$, gives the predictor as

$$\hat{y}(n) = \frac{N}{C}q^{-\tau_1}y(n) + \frac{B}{A}q^{-\tau_1}\left(1 - \frac{N}{C}q^{-\tau_1}\right)u(n) \qquad [2\text{-}46]$$

Swanson [1991] notes that this is an ARMAX controller. It can be alternatively written as

$$\hat{y}(n) = \hat{G}_{PF}[\hat{W}y(n) + (1 - \hat{G}_{PF}\hat{W})u(n)] \qquad [2\text{-}47]$$

where

$$\hat{G}_{PF} = \frac{B}{A}q^{-\tau_1}$$
$$\hat{W} = \left(\frac{N}{C}q^{-\tau_1}\right)\Big/\left(\frac{B}{A}q^{-\tau_1}\right) \qquad [2\text{-}48]$$

The control law becomes

$$u(n) = -\frac{\hat{W}}{(1 - \hat{G}_{PF}\hat{W})}y(n) \qquad [2\text{-}49]$$

The controller is able to cancel part of the stochastic disturbance (white Gaussian noise passed through an ARMA filter) as defined by the Diophantine equation (2-3). As discussed, the Diophantine equation separates the disturbance into predictable and unpredictable components dependent upon the delay between the transducers. The parameter estimates can be determined using the recursive least squares algorithm, or simplifications thereof. Swanson [1986] used this type of approach, with a lattice filter efficiently implementing the recursive identification algorithm.

The polynomials B and C must be minimum phase for stability. Swanson [1991] notes that if the disturbance is modelled as an AR process (instead of ARMA), then no attempt will be made to identify the zeroes of C, therefore avoiding estimating non-minimum-phase zeroes. This means that the predictable zeroes (defined by C, or more specifically N) will not be whitened but that the poles (defined by DA) will be damped, therefore limiting the amount of achievable broadband attenuation.

Eriksson [1991a,b] has used the control law of equation (2-49) in what he calls the "purely recursive form of equation-error IIR", as shown in Figure 2-9. A similar approach has also been taken by Elliott [1993], who also interestingly notes [Elliott and Nelson, 1994] that in general B will not be minimum phase. Both Elliott [1993] and Eriksson [1990,1991] approximate $\hat{W}$ by a FIR filter. Elliott and Nelson [1994] suggest that if $\hat{G}_{PF}$ is identical to G_{PF}, the control system effectively becomes a

feedforward type. This transformation is realised using equation (2-49), such that with

$$\tilde{v}(n) = y(n) - u(n)\hat{G}_{PF} \qquad [2\text{-}50]$$

then the equivalent feedforward control law becomes

$$u(n) = \hat{W}\tilde{v}(n) \qquad [2\text{-}51]$$

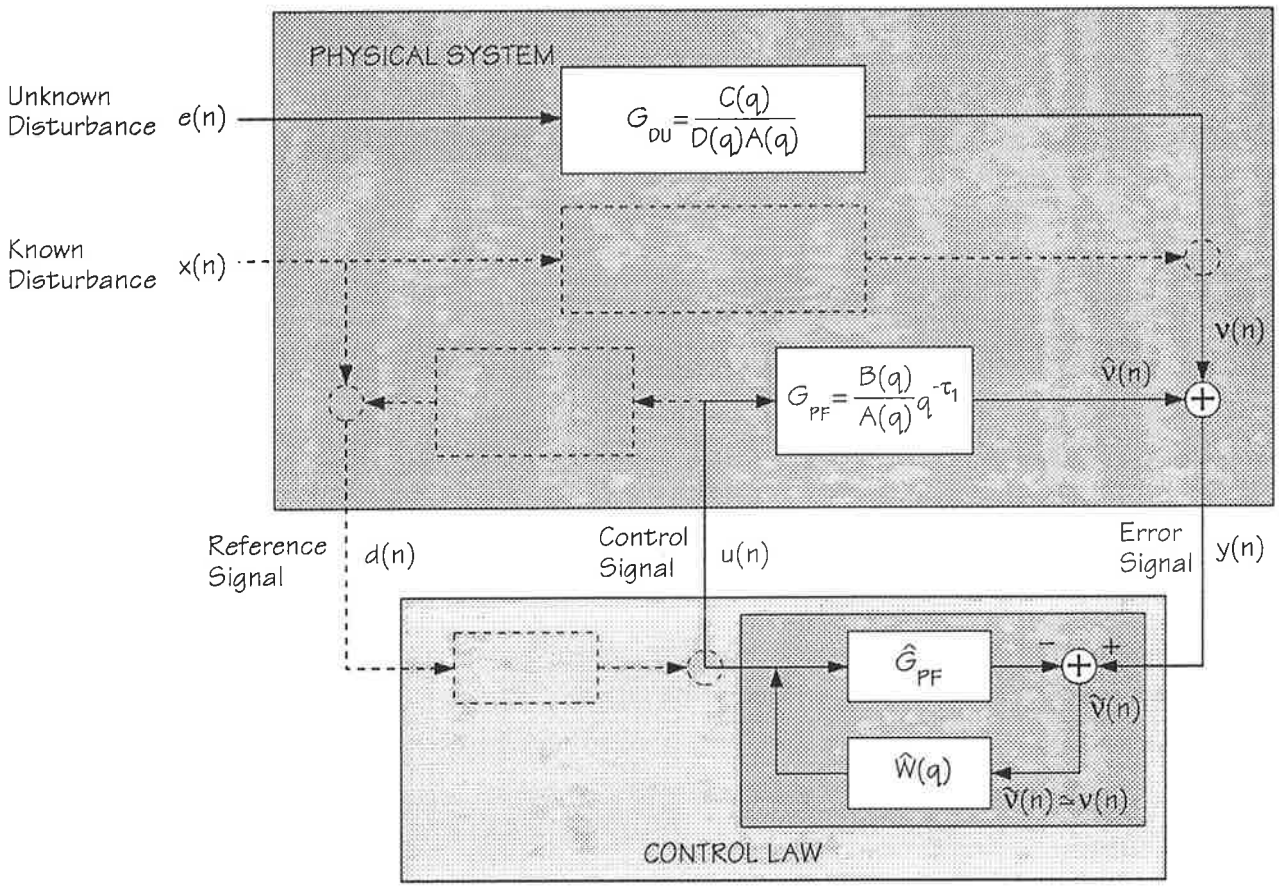

Figure 2-9. "Equation-Error IIR" defined by Eriksson [1991a,b].

If G_{PF} represents a pure delay, then the control problem becomes one of linear prediction, in which the process output (ie. error signal) will be whitened by an amount dependent upon the delay (ie. the disturbance cannot be completely whitened

as per the discussion of the Diophantine equation). The performance of the controller depends upon the statistics of the disturbance, or in other words, how predictable it is. This has distinct parallels with a lattice filter, as discussed in chapter 3.

Elliott et al [1995] describe the transformation of the control system from feedback to feedforward as Internal Model Control (IMC). Elliott et al [1995] note that this structure was first introduced by Newton et al [1956]. This technique has also been described by Chalam [1987] and by Morari and Zofirou [1989] (as noted by Elliott et al [1995]).

Finally, consider rewriting the estimate of the process output (error signal), such that

$$\hat{V}\hat{y}(n) = \hat{K}y(n) + \hat{H}u(n) \qquad [2\text{-}52]$$

where

$$\begin{aligned} \hat{V} &= AC \\ \hat{K} &= ANq^{-\tau_1} \\ \hat{H} &= Bq^{-\tau_1}\left(C - Nq^{-\tau_1}\right) \end{aligned} \qquad [2\text{-}53]$$

This results in the control law

$$u(n) = \frac{-\hat{K}}{\hat{H}}y(n) \qquad [2\text{-}54]$$

It is possible to determine the control filter coefficients implicitly using a single adaptation process, and the ELS or RML algorithms (or simplifications thereof) as appropriate (see Appendix A.2 for the definition of these algorithms). This approach will be stable provided B and C are minimum-phase.

2.4.4 Combined Feedforward/Feedback Control Algorithms

This type of control system and its stability constraints can be derived from the preceding work. Ren and Kumar [1989] and Doelman [1991] have considered this system. Eriksson [1991a,b] has called this general form an "equation-error IIR filter". Saunders et al [1993] have similarly implemented a "hybrid" controller incorporating the feedback part using Linear Quadratic Gaussian control and H_∞ robustness conditions, and the feedforward part using the filtered-X algorithm.

2.4.5 Linear Quadratic Gaussian Control and H_∞ Control

Generalised minimum variance (GMV) controllers are subsets of Linear Quadratic Gaussian (LQG) controllers [Peterka, 1984; Grimble, 1984]. Minimum variance controllers require specific polynomials in the plant to be minimum-phase, thus restricting the application of this control law scheme. Doelman [1993] cites Tohoyama [1991] as evidence of non-minimum-phase polynomials in acoustic systems, and Elliott and Nelson [1994] provide further evidence.

LQG controllers are able to treat non-minimum-phase polynomials. The criterion is given generally by equation (A-45) in appendix A.3, repeated here for ease of reference.

$$J = E[\{P(q)y(n+k) + Q(q)u(n)\}^2 | n] \qquad [2\text{-}55]$$

As discussed by Isermann [1991], the use of $P=1$ and $Q=r$ (a scalar constant) results

in only the zeroes of the moving-average part of the disturbance model, C, affecting stability.

The LQG control scheme is determined firstly by using spectral factorisation [Grimble and Johnson, 1988] of the non-minimum-phase polynomial, into a polynomial with non-minimum-phase zeroes and another with minimum-phase zeroes (termed a Hurwitz polynomial). The minimum-phase zeroes can be cancelled; however, if non-minimum-phase zeroes are used in the denominator of the regulator transfer function (ie. control law scheme), then instability will result. If the reciprocal of the non-minimum-phase polynomial is included in the regulator denominator, then the spectral properties of the non-minimum-phase zeroes can be neutralised [Doelman, 1993]. This method of control has been applied to active noise and vibration control problems in discrete time by Thomas [1995] and Bennett [1991]. It has been applied to continuous time systems represented in state-space form by Bai [1995], who also uses its capacity to effectively cancel spectral peaks (as discussed in section 2.4.5), in conjunction with a technique known as Independent Modal Space Control [Oz and Meirovitch, 1983; Meirovitch, 1990] (which eliminates inter-modal coupling).

Elliott et al [1995] examined performance and robustness issues using H_∞ control theory. This type of controller incorporates a degree of cautiousness defined by a model for the uncertainty in plant estimates [Doyle et al, 1992]. A similar approach has also been developed by Imai et al [1995], also based on the work of Doyle et al [1992].

An excellent study of the interplay between the control law design schema (specifically LQG) and parameter estimation (specifically RLS) in closed-loop is presented using the general framework of Adaptive Predictive Control by Bitmead et al [1990]. In particular, Bitmead et al [1990] note the following points on the interplay:

- Optimum parameter estimation requires persistently exciting inputs; Elliott et al [1995] note that the injection of uncorrelated white Gaussian noise into a closed-loop system can ensure sufficient persistent excitation.

- A feedback controller affects the spectral properties of the plant inputs, therefore affecting the parameter estimates.

Bitmead et al [1990] discuss the potential of H_∞ optimal adaptive control, since it has a design criterion deliberately specified to ensure closed-loop stability, and has many similarities with LQG control. They note that H_∞ control is yet to be fully developed for discrete-time systems.

2.5 Alternative Approach

It has been shown that the stochastic gradient algorithms (LMS or RLMS) commonly used in active noise and vibration control, adapt the coefficients of the control filter, and in so doing require knowledge of part of the physical system, known as the cancellation path transfer function. Gradient approximation in this way is "noisy"

[Widrow and Stearns, 1985], and inaccurate estimates of the cancellation path transfer function can result in instability, as has been discussed in chapter 2. Reliable methods for on-line estimation of the system parameters (not simply the cancellation path transfer function in an explicit form), and formulation of a control scheme have been presented in chapter 2, alongwith original proposals for common algorithm enhancement.

This section is concerned primarily with algorithms that avoid the need to estimate system parameters. These algorithms require time averaged cost function estimates, to avoid estimating the system parameters. Such algorithms can be divided into the following categories:

- "Derivative Measurement"

  The derivatives of the cost function are estimated using finite difference techniques applied to time averaged cost function estimates, and from the derivative estimates the control filter coefficients are adapted to their optima using the steepest-descent algorithm or Newton's Method.

- "Curve-Fitting"

  Time averaged cost function estimates can be fitted to the known shape of the cost function (eg. parabolic) to determine the optimal control filter coefficients corresponding to the minima of the fitted function.

- Random Search

  The optimum of the cost function is found by adapting the control filter coefficients in random directions, thus forming the random search algorithm. Alternatively they can be updated from time averaged cost function estimates at random locations, thus forming the genetic optimisation algorithm.

- Artificial Intelligence

  Rule-based intelligent learning systems, in which the control filter coefficients are adapted to find their optimum values based upon minimisation of the time averaged cost function. Allows global convergence for cost functions with multiple local optima, as the cost function is divided into a number of "hyperspaces". Such algorithms are known as "stochastic learning automata", or "fuzzy logic".

Each type of algorithm described briefly above will now be discussed in more detail. It is important to note that from this point, time averaging is implied by the "cost function estimate" description.

2.5.1 Derivative Estimation and Curve-Fitting

In this approach the derivatives of the cost function can be estimated using finite difference techniques applied to cost function estimates. Such techniques have been

developed and assessed in comparison to least-squares or stochastic approximation algorithms, by Widrow and Stearns [1985] using "central differences". These authors have thoroughly investigated the performance aspects of such algorithms, and specifically compared the steepest-descent algorithm (in which only an estimate of the gradient is used to adapt the coefficients) and Newton's Method (in which both an estimate of the cost function gradient and second derivative are used to adapt the coefficients).

In active noise and vibration control, this type of approach was first taken by Jones [1987] and Silcox [1987]. Finite difference methods applied to cost function estimates were used to estimate the gradient of the cost function in the direction of each control filter coefficient. From this, the cost function was estimated (through time averaging) at four points in the direction of the steepest gradient, and the cost function minimum was found in this direction by fitting these points to a quadratic function. This procedure was then repeated (ie. The direction of steepest gradient was found, a curve-fit was performed in this direction, and the minimum of this curve was found etc.). Jones [1987] and Silcox [1987] claim that this type of algorithm reaches the cost function minimum in about three to four iterations.

This algorithm is shown in Figure 2-10 for adaptation of two control filter coefficients. In Figure 2-10 the gradient is estimated (using finite differences applied to cost function estimates) at the starting point (represented by ⊠). The gradient gives the direction of steepest descent, along which the control coefficients are adapted, and cost function estimates are made (represented by ×). The cost function estimates are

fitted to a quadratic to determine the optimum control coefficients (represented by ⊗). This procedure is reiterated (ie. starting with a gradient estimate at the optimum control filter coefficients, determined for the last direction of steepest descent) using cost function estimates (represented by ○), until the cost function minimum (represented by •) is found.

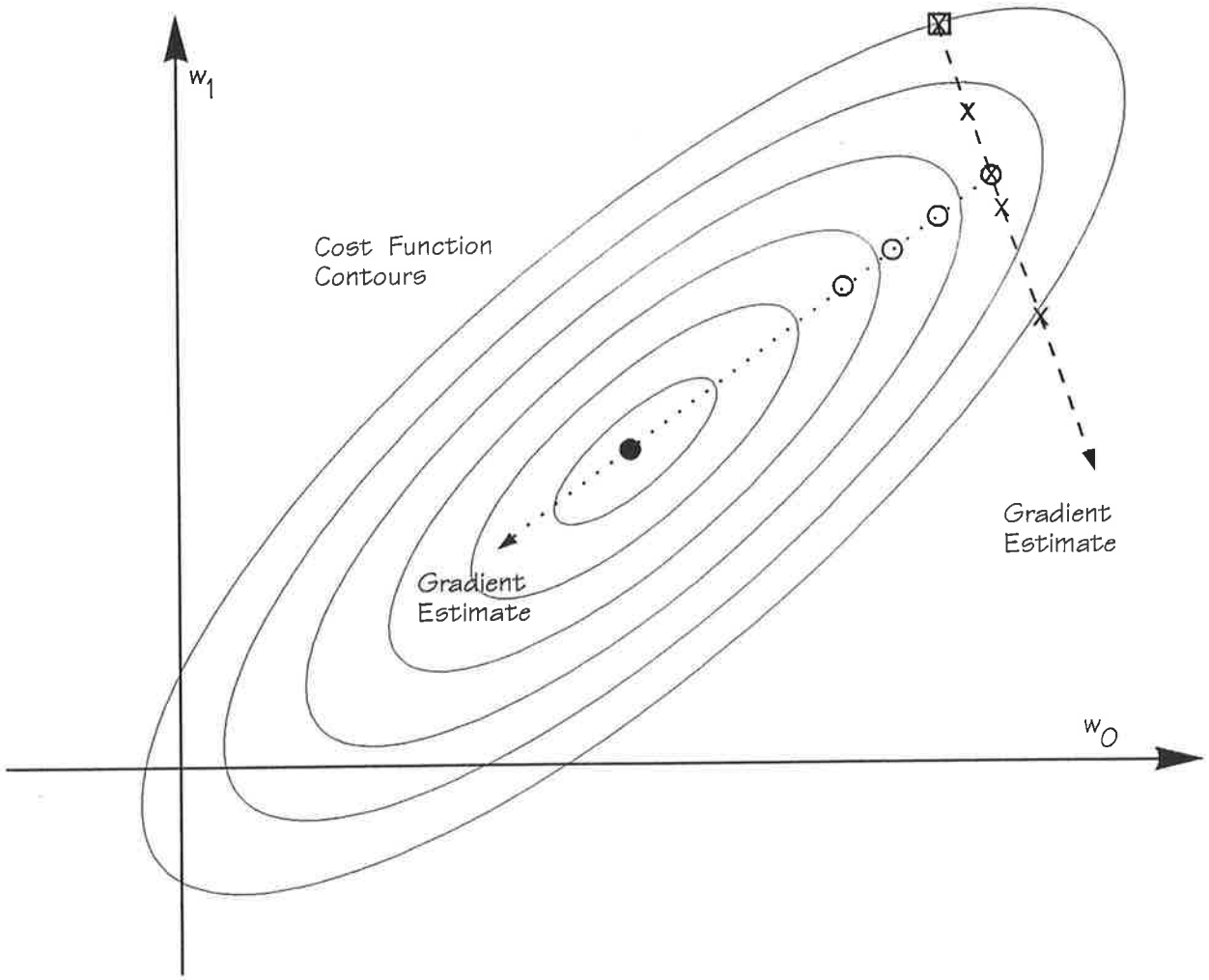

Figure 2-10. Adaptation of control coefficients based on steepest descent gradient estimate and quadratic fitting. The solid lines represent the contours of the cost function, ⊠ represents the starting point, × and ○ represent the cost function estimates in the directions of steepest descent (· · · and – –), ⊗ and • represent the cost function minima in the directions of steepest descent (· · · and – –).

However if the cost function incorporating the cancellation path transfer function can be transformed such that each control filter coefficient represents a principal axis of the cost function, then each control filter coefficient can be adapted independently. A quadratic function needs only three points for complete definition, therefore cost function estimates at three points in each independent control filter coefficient direction leads directly to the optimum of each control filter coefficient, as shown in Figure 2-11. This represents the Independent Quadratic Optimisation algorithm concept. In Figure 2-11 the cost function contours are shown by the solid lines. The cost function is estimated (through time averaging) initially at the location represented by ⊠. Two further estimates of the cost function (represented by $\times$) are made in the direction of the independent control coefficient, k_{w0}. The optimum of the control filter coefficient k_{w0} (represented by ⊗), is found by fitting a quadratic to these estimates. An estimate of the cost function is made at the optimum of the first control filter coefficient, and two further estimates of the cost function are made (represented by ○), before determining the optimum of the second control filter coefficient and therefore the global cost function minimum (represented by •).

The Independent Quadratic Optimisation algorithm's development, simulation and practical implementation are original to this thesis, and were first published in 1991 [Mackenzie and Hansen, 1991a; 1991b; Snyder et al, 1991c]. Without a transfer function in the cancellation path, the control filter coefficients can be made independent using orthogonal reference signals (as opposed to delayed samples of a single reference signal) for each coefficient (refer to appendix A.2.2, in particular equation (A-26) and associated discussion on independent coefficients and principal

axes). This concept will be further discussed in chapter 3, as will the use of a lattice filter to generate orthogonal signals. The effect of the cancellation path transfer function on control filter coefficient independence will also be examined in chapter 3. The effects of the cancellation path transfer function on the Independent Quadratic Optimisation algorithm will be further elucidated after the formulation and simulation of this algorithm in chapter 4. Chapter 5 presents the results of experiments using physical systems. Other work confirming this approach has been presented by Botteldooren [1993].

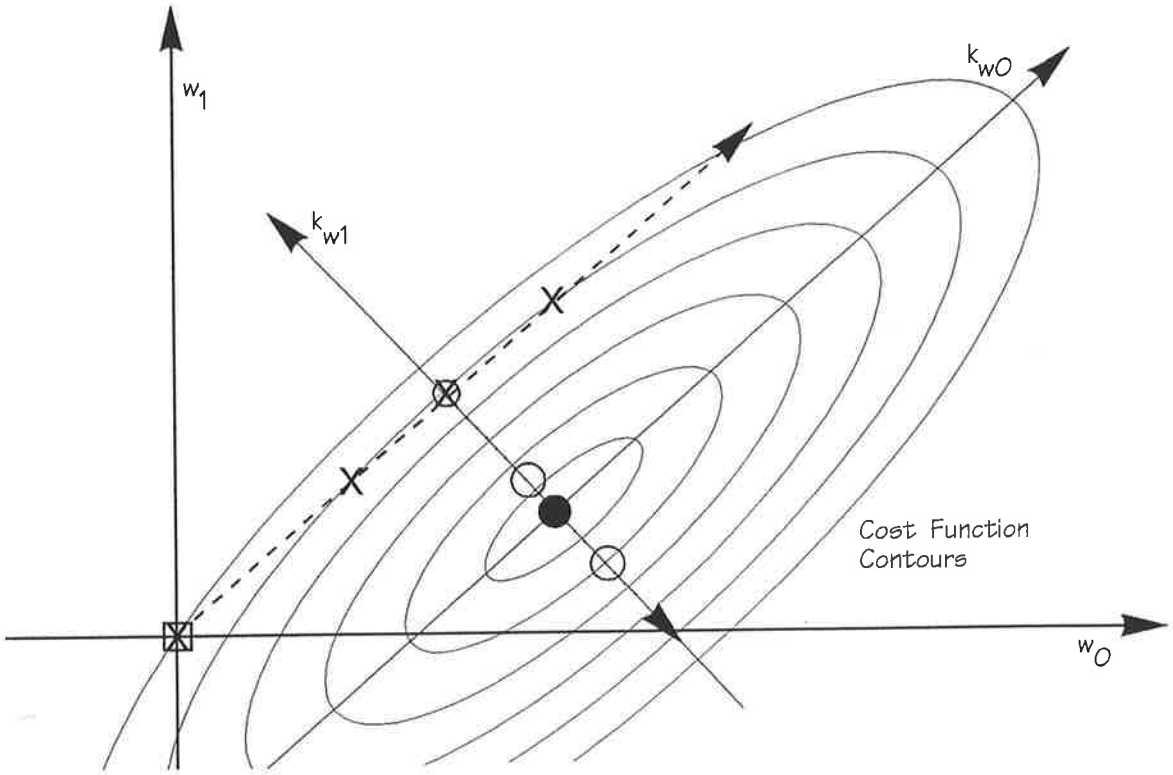

Figure 2-11. Independent Quadratic Optimisation algorithm. Solid lines represent contours of the cost function, ⊠ represents starting point, × represents estimates along first control filter coefficient principal axis, ⊗ represents the optimum for first control filter coefficient, ○ represents estimates along the second control filter coefficient principal axis, and • represents the global cost function minimum.

Recently Clark and Gibbs [1992], Gibbs and Clark [1993] and Kewley et al [1995] discussed a similar algorithm to that presented here, for controlling individual harmonics. The technique presented by these authors uses each individual harmonic and its orthogonal component independently (since harmonics are in effect independent as will be shown in chapter 3). The algorithm used by these authors is based on Newton's Method, and it will be shown in chapter 4 that it is identical to the Independent Quadratic Optimisation algorithm developed here.

2.5.2 Random Search

Widrow and McCool [1976] have assessed a method of searching the cost function using a random search direction. The control filter coefficients are updated in a random direction based on estimates of the cost function, such that

$$W(n+1) = W(n) + \mu [\hat{J}(W(n)) - \hat{J}(W(n)+U(n))] U(n) \qquad [2\text{-}56]$$

where $W(n)$ is a vector of control filter coefficients, μ is the convergence coefficient, $\hat{J}()$ is the estimate of the cost function dependent upon the values of the control filter coefficients, and $U(n)$ is a random control filter coefficient update direction. Widrow and McCool [1976] have shown that the performance of this algorithm is equivalent to the steepest-descent algorithm. The random search algorithm has the advantage of ease of implementation.

Etter and Masukawa [1981], as cited by Widrow and Stearns [1985], have developed an algorithm that examines random "locations" (instead of directions) to determine the

optima of the cost function. This type of algorithm is known as a genetic optimisation algorithm, and has been implemented for use in active noise and vibration control by Curtis [1991] and Wangler [1994, 1995]. The genetic optimisation algorithm uses an "estimation universe" of sets, α_i (of which there are a total of N), of control filter coefficients. The cost function is estimated, through time averaging, for each set of control filter coefficients within the "estimation universe", and then a second "adaptation universe" of control filter coefficient sets is derived, with each original set replicated inversely proportional to the cost function estimate. From this derived "adaptation universe", two sets of control filter coefficients are chosen at random (known as "parents"), and "mutation" is performed to give a new set (known as the "offspring") within a new "estimation universe". The cycle then continues with the cost function again estimated for each set of control filter coefficients within the "estimation universe". "Mutation" is performed by randomly selecting a control filter coefficient from each "parent" to use for the corresponding control filter coefficient of the "offspring". It is apparent that those control filter coefficients that perform better (ie. have a lower cost function estimate) will have less probability of "mutation", ultimately resulting in the "offspring" becoming more and more alike, leading to optimum control filter coefficients. Wangler [1994] gives various modifications that can be made to this algorithm to improve its performance, including a means of restricting the range of values control filter coefficients may take, therefore ensuring stability.

2.5.3 Artificial Intelligence

The methods outlined to this point are capable of locating local minima of a cost function, but not necessarily global minima. Intelligent learning algorithms (ie. Fuzzy Logic [Lebow et al, 1991] or Stochastic Learning Automata [Tang and Mars, 1991]) search the cost function in a probabilistic manner, without reliance on system linearity.

Recently the use of stochastic learning automata has been applied to system identification using the output-error form of IIR filter (specifically chosen to avoid biassing of parameters by incorrectly modelled disturbances as per the equation-error method). The use of the output-error form of system identification is particularly suitable for testing the stochastic learning algorithm in comparison to gradient descent algorithms, since it has a multi-modal cost function (ie. multiple local minima). The block diagram of a learning automaton/environment model is shown in Figure 2-12, as applied to a control problem.

The simplest scheme for finding the optimal set of control filter coefficients uses only a single automaton. This automaton is used to update each component, p_i, of an output probability vector, p, that determines the best performing actions, α_i, within the output set, α. Each action corresponds to a set of control filter coefficients. Hence it can be said that the cost function parameter space is partitioned into a number of hyperspaces, equal to the number of output actions [Tang and Mars, 1991]. The greater the number of output actions, the finer is the quantisation of the parameter space, and therefore the greater is the level of optimisation. Since the

parameter space is partitioned in this manner, the randomness is removed from the search mechanism, and the parameter space is defined only by the stable ranges of the control filter coefficients. The search mechanism can be performed in a hierarchical manner, with a small degree of quantisation of the parameter space initially used, until the region of the global minimum is found, and then the parameter space could be further quantised only in this region, or alternatively a hybrid search technique (eg. gradient descent type etc.) could be used in this region.

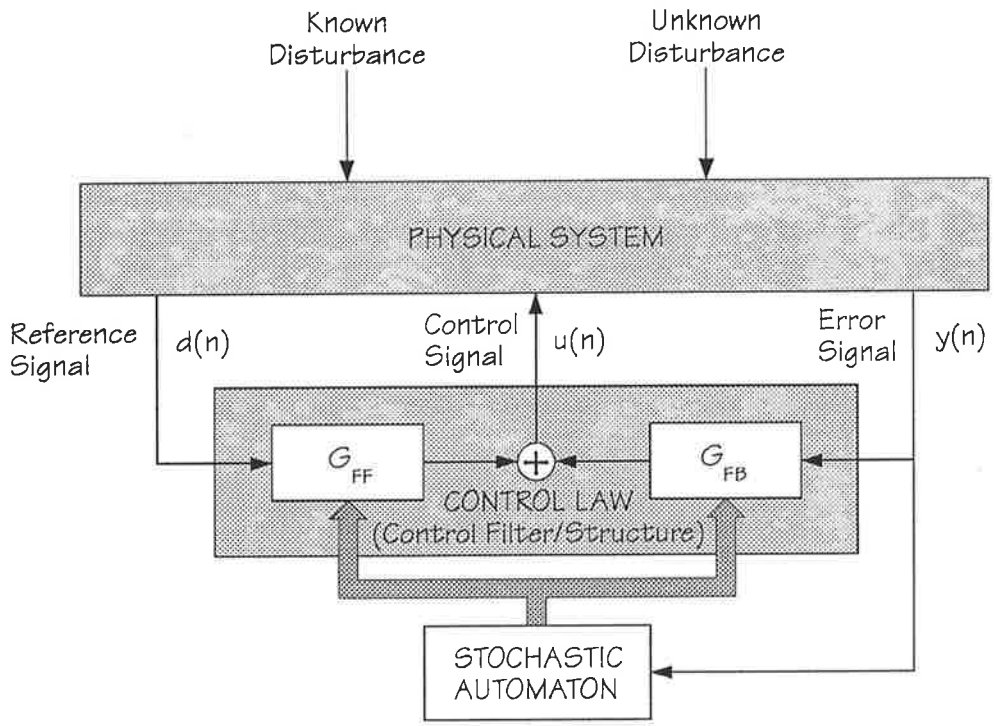

Figure 2-12. Stochastic Learning Automaton applied to active noise and vibration control.

Fuzzy logic was introduced by Zadeh [1973]. It was extended to adaptive control by Procyk and Mamdani [1979] and termed "self-organising controller". It has been applied to active noise and vibration control by Lebow et al [1991] and Subramaniam

et al [1993]. A discussion of fuzzy logic adaptive control is given in Chalam [1987], with its principles very similar to the discussion on stochastic learning automata.

2.5.4 Summary

In all of these time averaged cost function minimisation methods, the speed of convergence to the optimum is severely restricted by the need to estimate the cost function over a number of samples. The lower the number of samples used to estimate the cost function, the less accurate will be the cost function estimates, and the larger will be the convergence time (since inaccurate control filter coefficient optima will be found from the inaccurate cost function estimates). However the greater the number of samples used to estimate the cost function, the more accurate will be the cost function estimates and the greater will be the convergence time. Therefore there is an optimum number of samples for cost function estimation, that corresponds to a minimum convergence time, which can only be found empirically and depends on the statistics of the disturbance. To reduce the order of the parameter space and hence increase convergence time, IIR filters can be used with less coefficients than FIR filters.

The other disadvantages with these types of algorithms are that they can result in high levels of the cost function (and thus poor on-line performance) if the entire parameter space is searched, and they can require a large memory depending on the type of algorithm and the amount of information it needs to store.

The advantages of these types of approach are:

- They are amenable to non-linear systems, and systems in which stationarity cannot be ensured;

- In avoiding biassed parameter estimates, the cost function has multiple local optima, to which most other algorithms would converge. However, some of the algorithms discussed in this section can achieve convergence to a global minimum.

- They have simple hardware implementations (although some types may require considerable memory), and can be applied to non-standard filters.

2.6 Summary

In this chapter the application of modern control theory to active noise and vibration control has been introduced. This theory involves the use of a model of the system, an algorithm to estimate the parameters of the system model, and a control scheme to achieve the desired process output. The differences in the models, and algorithms used to estimate the model parameters have been stressed, and are discussed in the appendix. The common control algorithms were shown to conform to the modern control theory approach. These common algorithms were heuristically developed, and the approach presented in this chapter has highlighted the following improvements that can be made to these algorithms.

- Use of the "augmented-error" approach that avoids the interplay between system identification and control schemes.

- Use of a single adaptive scheme to estimate the parameters of the system model on-line (ie. It is not necessary to identify the cancellation path transfer function parameters and control filter coefficients in parallel; This can result in instability, with the convergence conditions for the control algorithm affected by the accuracy of the cancellation path transfer function estimates).

- Use of the simplified forms (stochastic gradient) of the more accurate recursive prediction error methods for both output-error and equation-error models.

- Use of a Generalised Minimum Variance (GMV) criterion, instead of a minimum variance criterion, to reduce the effect of non minimum-phase processes.

- In many of the models considered in this chapter, numerator polynomials have been assumed to be close to unity so that algorithms for output-error and equation-error forms (eg. ARMAX) can be simplified. This can result in a reduction of broadband attenuation since the prediction of the zeroes of the disturbance model are ignored, however it does avoid the destabilising effects of non-minimum-phase zeroes.

- Use of the Linear Quadratic Gaussian control scheme with spectral factorisation can allow control systems with non-minimum-phase transfer functions to be controlled.

A comparison of adaptive feedforward and feedback control (both individually and in combination) has highlighted many differences. It is apparent that feedforward schemes are equivalent to output-error control models, and feedback schemes are equivalent to equation-error type (such as ARMAX) control models.

The persistent excitation condition was shown to be critical in defining unbiased parameter estimates, as was the choice of an output-error model or an equation-error model. The persistent excitation condition of a system in closed-loop was shown to be affected by the control input to the system, and the use of H_∞ control was discussed as a means of ensuring closed-loop stability.

Finally alternative methods were considered to avoid the need to identify the parameters of the system model. The Independent Quadratic Optimisation algorithm was conceptualised in this chapter and forms the basis of this thesis.

3.1 Introduction

Chapter 2 briefly described the concept of the Independent Quadratic Optimisation algorithm, as a means of generating an optimal control signal without requiring knowledge of the cancellation path transfer function. As discussed in chapter 2, this algorithm adapts coefficients linked to orthogonal (or independent) signals obtained from a lattice filter. The control structure is shown below for ease of reference.

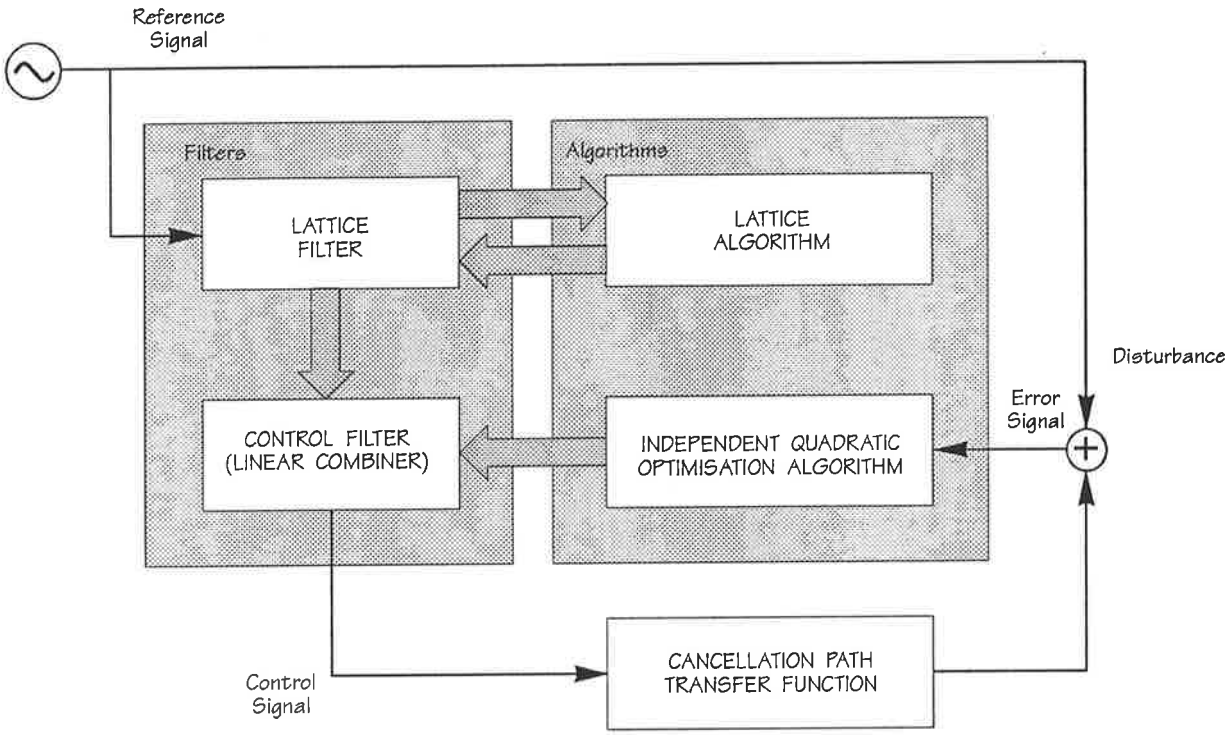

Figure 3-1. Active Noise and Vibration Control Structure.

As shown, there are two algorithms that operate concurrently; The lattice algorithm adapts the coefficients of the lattice filter to generate orthogonal signals, and the Independent Quadratic Optimisation algorithm adapts the coefficients (of the control filter/linear combiner) associated with each orthogonal signal. The internal structure

of the lattice filter (feedforward type) combined with the control filter (linear combiner) is shown in Figure 3-2. The stages within the lattice filter will be examined later in more detail.

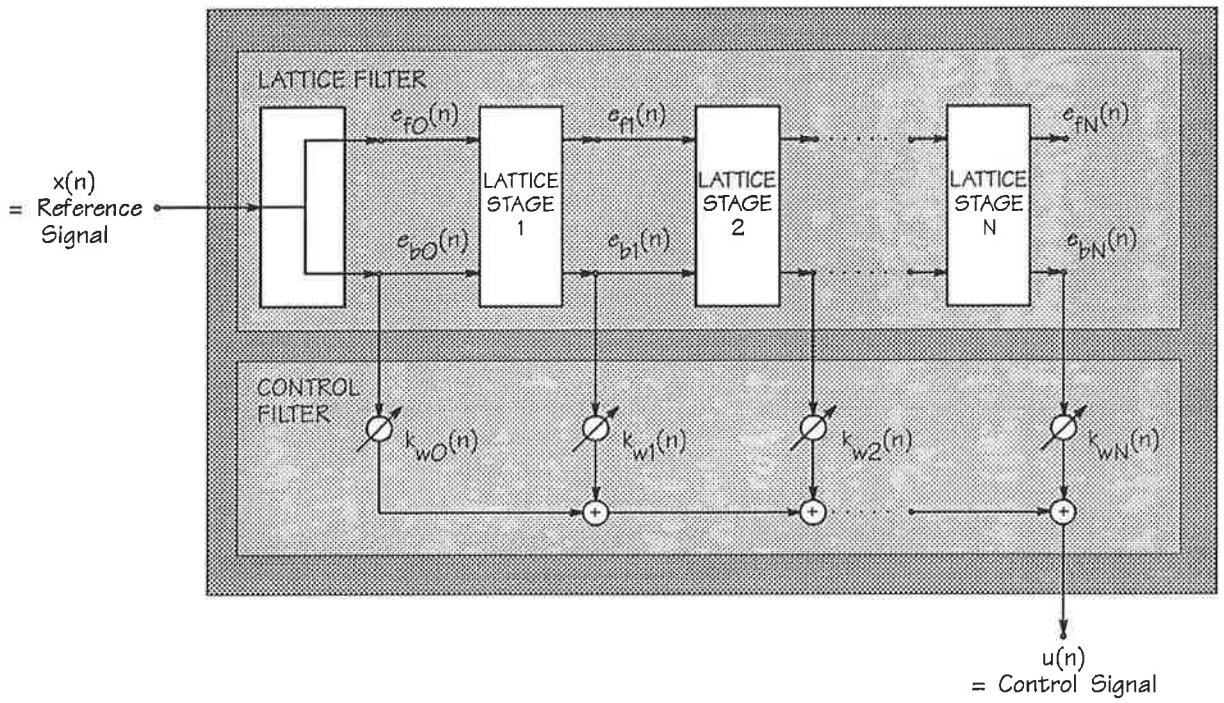

Figure 3-2. Joint-Process or Tapped-Lattice Filter. The input/reference signal is given by $x(n)$, the backward and forward prediction errors by $e_{bi}(n)$ and $e_{fi}(n)$ respectively, the control filter coefficients by $k_{wi}(n)$ and the control signal by $u(n)$.

The combination of a linear combiner with the lattice filter is formally known as a Joint Process Lattice Filter, or a Tapped-Lattice Filter. This type of filter has been used in active noise and vibration control previously [Swanson, 1986; 1991b] and more recently [Park and Sommerfeldt, 1994; Char and Kuo, 1994], however, the algorithms used by these researchers to adapt the coefficients of the filter, requires knowledge of the cancellation path transfer function, as discussed in chapter 2.

This chapter will examine the generation of orthogonal signals by the lattice filter, the use of these orthogonal signals to generate a control signal, and the effect of the cancellation path transfer function on the independence of the control filter coefficients individually associated with each orthogonal signal.

To examine the generation of orthogonal signals by the lattice filter, a brief overview will be given of the signals and coefficients used to define the lattice filter. This lattice filter will then be extended, by combination with a linear combiner (control filter), to show how a control signal can be generated from orthogonal signals. It will be shown that without a transfer function in the cancellation path, the control filter coefficients used to generate the control signal are independent. The effect of the cancellation path transfer function on the independence of the control filter coefficients results in an independence condition that affects the Independent Quadratic Optimisation algorithms speed of convergence to the optimum of the cost function. This will be shown by way of computer simulations in chapter 4.

3.2 Lattice Filter Overview

In this section it will be shown briefly how the structure of the lattice filter is obtained. These results will then be used to show how the lattice filter can generate orthogonal signals. The characteristics of the lattice filter, that affect the Independent Quadratic Optimisation algorithm, will then be identified (with further discussion in chapter 4).

3.2.1 Definition of the Lattice Filter

The lattice filter stems from forward and backward prediction errors of a set of consecutive input signal samples, as shown in Figure 3-3. Given a set of consecutive samples of the input signal, the forward prediction error is the error in predicting the input signal for the next sample following this set, and the backward prediction error is the error in predicting the input signal for the previous sample before this set.

In Figure 3-3, the consecutive input signal samples (total of N) are $x(n)$, ... , $x(n-N+1)$. The input signal to be predicted forward in time is $x(n+1)$, while the input signal to be predicted backward in time is given by $x(n-N)$. To predict the signal forward in time requires forward prediction coefficients f_1, ... , f_N, while to predict the signal backward in time requires backward prediction coefficients b_1, ... , b_N. Thus the errors in predicting the input signal forward and backward in time are $e_{fN}(n+1)$ and $e_{bN}(n)$, respectively.

The forward coefficients are optimised to minimise the forward prediction error. The optimisation criterion is given by (note that j as opposed to J is used as a descriptor for the optimisation criterion as there will be many stages of the lattice filter whereas J will be reserved for the optimisation criterion for the error signal(s) taken from the acoustic domain)

$$j_{fN} = E[e_{fN}^2(n)] \qquad [3\text{-}1]$$

with the forward prediction error written as

$$e_{fN}(n) = x(n) - F_N^T(n)X_N(n-1) \qquad [3\text{-}2]$$

where

$$F_N^T(n) = [\, f_1(n), \ldots, f_N(n) \,] \qquad [3\text{-}3]$$

represents the forward prediction coefficients, and

$$X_N^T(n) = [\, x(n), x(n-1), \ldots, x(n-N+1) \,] \qquad [3\text{-}4]$$

represents the consecutive sequence of input signals.

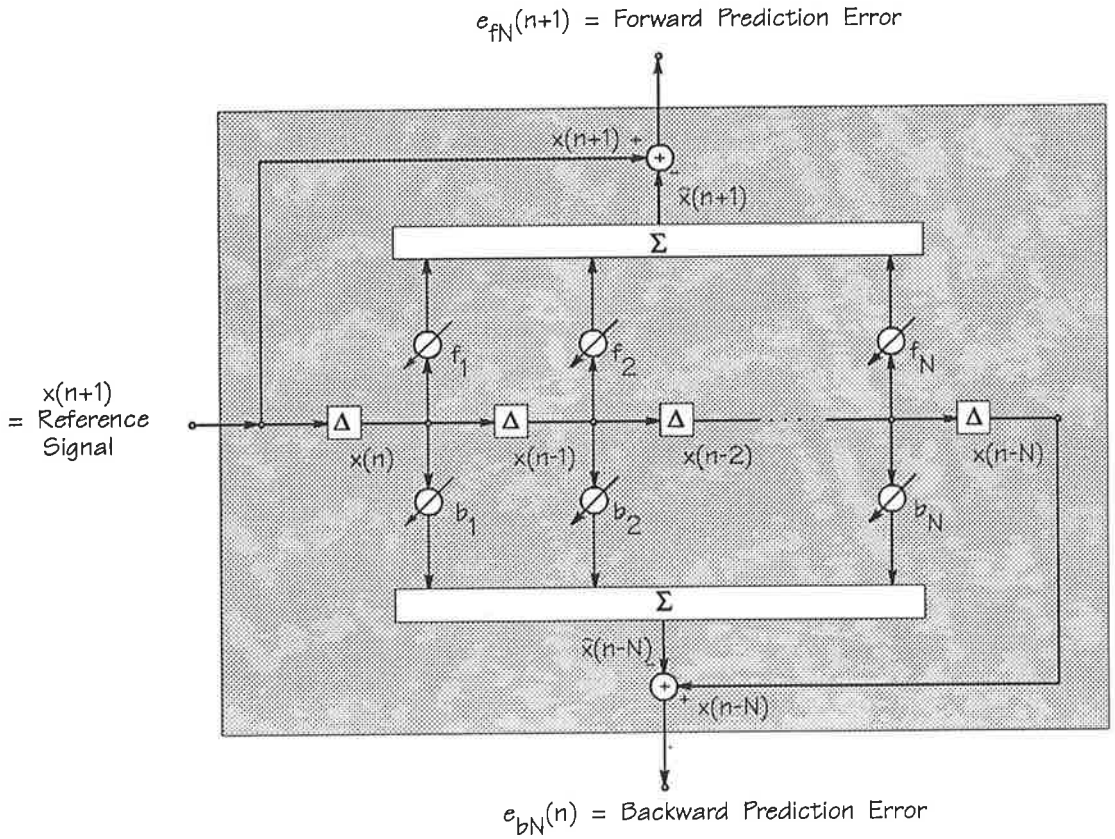

Figure 3-3 Flow Diagram of Linear Prediction Errors. The reference/input signal is $x(n)$ and its estimate is $\hat{x}(n)$, the forward and backward prediction coefficients are f_i and b_i respectively, and the forward and backward prediction errors are $e_{fN}(n)$ and $e_{bN}(n)$ respectively. A continuous set of N reference/input samples is given by $x(n),\ldots,x(n-N+1)$, with $x(n-N)$ the sample before this set and $x(n+1)$ the sample after this set. Δ represents a single sample delay.

Since time dependence has been introduced (to account for the forward prediction coefficient adaptation required to minimise the cost function) into the linear prediction coefficient in equation (3-2), it should also be introduced into the cost function, which is therefore written as $j_{fN}(n)$. The minimum of this cost function occurs when its partial derivative with respect to the forward prediction coefficients, equals zero. That is:

$$\left.\frac{\partial j_{fN}(n)}{\partial F_N(n)}\right|_{F_{Nopt}} = -2E[e_{fN}(n)X_N(n-1)]\Big|_{F_{Nopt}} = 0 \qquad [3\text{-}5]$$

This means that at the optimum, the forward prediction errors are orthogonal to the previous N input signal samples, which can be written as

$$E[e_{fN}(n)x(n-i)] = 0 \text{ for } 1 \le i \le N \qquad [3\text{-}6]$$

This orthogonality condition is critical to the lattice filter structure.

A similar orthogonality condition can be obtained for the backward prediction error. The backward prediction error is orthogonal to the current and previous *(N-1)* input signal samples, which can be written as

$$E[e_{bN}(n)x(n-i)] = 0 \text{ for } 0 \le i \le N-1 \qquad [3\text{-}7]$$

where

$$e_{bN}(n) = x(n-N) - B_N^T(n)X_N(n) \qquad [3\text{-}8]$$

represents the backward prediction errors, with the backward prediction coefficients represented by

$$B_N^T(n) = [\ b_1(n),\ ..,\ b_N(n)\ ] \qquad [3\text{-}9]$$

and the consecutive sequence of input signal samples is represented by equation (3-4).

It is apparent from equation (3-8) that $e_{bN}(n-1)$ is the error in predicting $x(n-N-1)$ from $x(n-1)$, ... ,$x(n-N)$, while from equation (3-2) it is apparent that $e_{fN}(n)$ is the error in predicting $x(n)$ from $x(n-1)$, ... ,$x(n-N)$. Thus the same set of consecutive data samples can be used to predict the input signal both forward and backward in time. This suggests that these prediction errors should be linked in some way.

To understand how the forward and backward prediction errors are linked, consider the next order forward prediction error, such that

$$e_{f(N+1)}(n) = x(n) - F_{N+1}^T(n)X_{N+1}(n-1) \qquad [3\text{-}10]$$

This requires prediction of $x(n)$ from $x(n-1)$, ... , $x(n-N)$, $x(n-N-1)$ (where it should be noted that $x(n-N-1)$ is now also available, as the order has been increased). As discussed above, it is known that $x(n)$ and $x(n-N-1)$ can be predicted from $x(n-1)$, ... ,$x(n-N)$. Further, since $e_{fN}(n)$ contains all of the information regarding the prediction of $x(n)$ from $x(n-1),...,x(n-N)$, and $e_{bN}(n-1)$ contains all of the information regarding the prediction of $x(n-N-1)$ from $x(n-1),...,x(n-N)$, then it can be postulated that:

$$e_{f(N+1)}(n) = e_{fN}(n) - k_{b(N+1)}e_{bN}(n-1) \qquad [3\text{-}11]$$

where, using the orthogonality conditions given by (3-6) and (3-7), the coefficient $k_{b(N+1)}$ can be written as

$$k_{b(N+1)} = \frac{E[e_{fN}(n)e_{bN}(n-1)]}{j_{bN}(n-1)} \qquad [3\text{-}12]$$

A similar result can be formulated for the backward prediction error:

$$e_{b(N+1)}(n) = e_{bN}(n-1) - k_{f(N+1)}e_{fN}(n) \qquad [3\text{-}13]$$

with the orthogonality conditions again allowing the definition for the coefficient $k_{f(N+1)}$ as

$$k_{f(N+1)} = \frac{E[e_{fN}(n)e_{bN}(n-1)]}{j_{fN}(n)} \qquad [3\text{-}14]$$

The coefficients k_{bN} and k_{fN} as described by the above equations, represent the optimal PARCOR coefficients linking the forward and backward prediction errors of the previous stage to the prediction of those errors for the current stage. It is equations (3-11) and (3-13) that define the recursive stages of the lattice structure, as they show that the forward and backward prediction errors are "linked" since they relate to the same set of input signal samples. The structure of each stage of the lattice filter is shown in Figure 3-4. This is known as a feedforward lattice structure. It can be shown that it represents a transfer function with only zeroes.

Alternatively equations (3-11) and (3-13) can be rearranged so that a lattice structure can be formed to represent a transfer function that includes poles (known as a feedback structure), as shown in Figure 3-5. The relevance of this structure to Active Noise and Vibration Control will be discussed in chapter 6. It is the feedforward type of stage that is repeated in the lattice filter, and used throughout this work. Figure 3-4 represents a stage of the lattice filter shown in Figure 3-2.

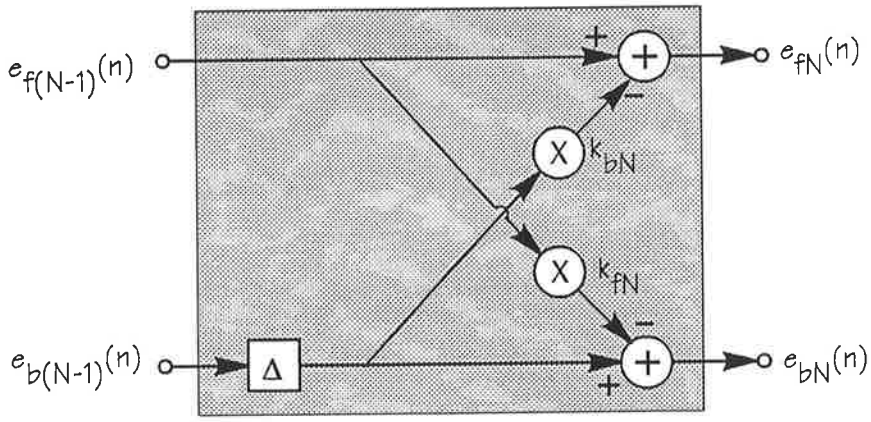

Figure 3-4. Feedforward Lattice Stage. Where $e_{fi}(n)$ and $e_{bi}(n)$ represent the forward and backward prediction errors respectively, and $k_{fi}(n)$ and $k_{bi}(n)$ represent the forward and backward PARCOR coefficients respectively.

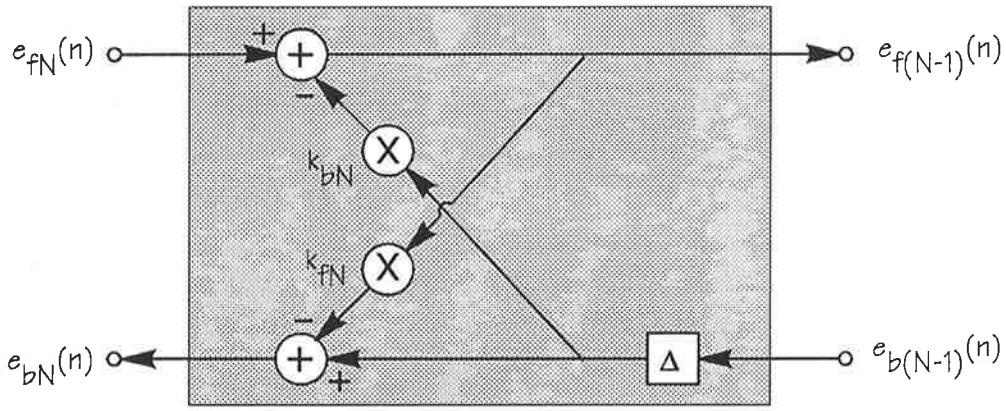

Figure 3-5. Feedback Lattice Stage. Where $e_{fi}(n)$ and $e_{bi}(n)$ represent the forward and backward prediction errors respectively, and $k_{fi}(n)$ and $k_{bi}(n)$ represent the forward and backward PARCOR coefficients respectively.

When the lattice filter is used for estimation, prediction and control, its PARCOR coefficients are optimised to minimise a particular cost function. When used for representing a direct-form transfer function, the PARCOR coefficients are defined without regard to this optimisation. It is the adaptive form that is used throughout this work.

3.2.2 Properties of the Lattice Filter

The assessment of the lattice filter properties is not unique to this thesis, however the relation of these properties to the Independent Quadratic Optimisation algorithm is essential.

As shown in Figure 3-2, the lattice filter consists of stages of identical structure (but varying parameters), the number of which relate to the order (or number of input signal samples) used to predict the input signal. The order required to achieve minimum prediction errors depends upon the statistics of the input signal (since it generates prediction errors or errors relating to the ease and accuracy of predicting a particular signal from a finite set of consecutive samples). For a pure tone, only two stages would be required for optimal prediction, but for a statistically complex autoregressive-moving average (ARMA) signal (as discussed in chapter 2), the order required for optimal prediction could be in the hundreds.

The prediction errors at each stage of the lattice structure, are generated using coefficients defined by the correlation between the forward and backward prediction errors of the previous stage, as shown by equations (3-12) and (3-14). These coefficients replace the linear prediction coefficients in the separate forward and backward linear prediction error equations (ie. those coefficients shown in Figure 3-3). The coefficients (termed PARCOR coefficients for partial correlation, or reflection coefficients as they can model reflections in a vocal tract) of each stage of the lattice filter are adapted independently (of later stages) to minimise the prediction errors at

the output of each stage. This adaptation is essential to obtain orthogonal backward prediction errors.

After the lattice structure has been adapted to produce the orthogonal backward prediction errors, each backward prediction error is weighted by a control filter coefficient, and summed to produce an estimate of the disturbance signal, as shown in Figure 3-2. The Independent Quadratic Optimisation algorithm used to adapt the control filter coefficients will be derived in the next chapter. The aim of the Independent Quadratic Optimisation algorithm is to independently adjust the control filter coefficients without requiring knowledge of the cancellation path transfer function. The independence of the control filter coefficients will be shown in section 3.3.

Assuming the backward prediction coefficients have been optimised so that they no longer vary with time, it can be shown (using the orthogonality conditions given by equations (3-6) and (3-7) that

$$E[e_{bN}(n)e_{bj}(n)] = 0 \quad for \quad 0 \le j \le N-1 \qquad [3\text{-}15]$$

This shows that the backward prediction errors are orthogonal. This is a critical property that is essential to the Independent Quadratic Optimisation algorithm performing efficiently. As discussed in chapter 2, without orthogonal signals, the control filter coefficients would not be independent. It will be shown later however that despite the availability of orthogonal signals, the control filter coefficients' independence is still dependent on the type of input/reference signal, when a transfer function exists in the cancellation path (as for an active noise and vibration control

system).

If the zeroes of an all-zero transfer function lie within the unit circle in the z-domain (ie. the transfer function is minimum phase), then the inverse transfer function must also be stable. It can be shown that this condition corresponds to forward and backward PARCOR coefficients, $|k_{bN}|$ and $|k_{fN}|$, being less than unity. Thus the form of the lattice filter is such that stability is easily ascertained. This is a useful on-line check of stability that further enhances the stable nature of the Independent Quadratic Optimisation algorithm.

For a stationary input signal, the forward and backward prediction error powers are equal, as are the forward and backward PARCOR coefficients, and therefore $k_{fN}(n) = k_{bN}(n) \triangleq k_{f/bN}(n)$ (with $\triangleq$ meaning defined as, and the subscript *f/b* indicating that the PARCOR coefficient is used for both the forward and backward PARCOR coefficients as these are equal). It is possible to show that the mean square prediction errors can be estimated by the following order recursive equations:

$$j_{fN}(n) = j_{f(N-1)}(n)\,[1 - k^2_{f/bN}(n)] \qquad [3\text{-}16]$$

and

$$j_{bN}(n) = j_{b(N-1)}(n-1)\,[1 - k^2_{f/bN}(n)] \qquad [3\text{-}17]$$

Thus it is apparent from the above equations, that with increasing order, the power (or mean square) of the prediction errors decreases (since $|k_{f/bN}|$ must be less than unity for stability). It can be shown [Honig and Messerschmitt, 1984] that the orthogonality conditions indicate that increasing numbers of linear prediction coefficients reduce the prediction error to increasingly white sequences, with reduced

powers. Thus low order stages of the lattice filter will have PARCOR coefficients close to unity (due to good correlation between forward and backward prediction errors at these low order stages) and prediction error powers relatively similar to the input signal power, while high order stages will have low prediction error powers and PARCOR coefficients close to zero. Periodic signals require only two stages of a lattice filter for accurate prediction (the remaining stages have very low powers and are increasingly white). This is an important concept for the Independent Quadratic Optimisation algorithm, since if the powers of the backward prediction errors are reduced with increasing order, then the control filter coefficients will need to be very large, possibly causing overflow. This will be considered further in chapter 5.

The prediction errors at the output of each stage of the lattice filter can be minimised by adapting the PARCOR coefficients using either of the following algorithms.

- **Stochastic Gradient method** (ie. Least Mean Squares (LMS) algorithm); The forward and backward PARCOR coefficients are adapted to minimise each forward ($E[e_{fi}^2(n)]$) and backward ($E[e_{bi}^2(n)]$) prediction error cost function separately, or to minimise their combination ($E[e_{fi}^2(n)] + E[e_{bi}^2(n)]$). The PARCOR coefficients are adapted in the direction of, and in proportion to the steepest descent gradient, determined from an estimate of the gradient of the cost function. This algorithm is summarised in Table 3-1. In Table 3-1, μ represents the convergence coefficient, and the prediction errors and their estimated powers are used to form a normalised stochastic gradient algorithm.

- **Recursive Method** (ie. Recursive Least Squares (RLS) algorithm); The lattice filter consists of decoupled stages at each of which local minimisation of the forward and backward prediction error cost functions occurs. It is the independent adaptation of the PARCOR coefficients to locally minimise each cost function, that makes a lattice filter ideally suited to the recursive least squares algorithm. The recursive least squares algorithm for the lattice structure requires variables to be updated in time and order, since for every new data sample the forward and backward prediction errors must be generated, and the coefficients used to generate them must be adapted. This algorithm adapts the PARCOR coefficients in the direction of the optimum of the forward and backward prediction error cost functions (not necessarily the steepest direction of the cost function). This algorithm is summarised in Table 3-2. In Table 3-2, the factor $\gamma_i(n)$ is known as the "gain constant" or "error ratio", and it can be rewritten as

$$\gamma_i(n) = 1 - \alpha_i(n) \qquad [3\text{-}18]$$

where

$$\alpha_i(n) = X_i^T(n)\bar{R}_{ii}^{X^{-1}}(n)X_i(n) \qquad [3\text{-}19]$$

In these equations, i represents a stage of the lattice filter, $X_i(n)$ represents the vector of delayed reference signal samples, and the inverse of the sample auto-correlation matrix represented by $\bar{R}_{ii}^{X^{-1}}(n)$. It is known [Cowan, C.F.N and Grant, P.N., 1985] that $\alpha_i(n)$ is a measure of the likelihood that the N most recent input data samples come from a Gaussian process with sample auto-correlation $\bar{R}_{ii}^{X}(n)$ determined from all available past samples. A value of $\alpha_i(n)$ close to unity indicates that the recent data samples are likely to have

been generated by the Gaussian process described above, however a value of $\alpha_i(n)$ close to zero indicates that the recent data samples are unexpected. Therefore when $\gamma_i(n)$ is close to unity, it indicates that sudden changes in the process generating the samples has occurred and the magnitude of the step change in the coefficient update algorithm increases. As from the analysis of appendix A.2.3, it is this ability to track changing signals that makes the recursive algorithm very appealing. In appendix A.2.3, the recursive algorithm was shown to be unaffected by the eigenvalue disparity in the autocorrelation matrix, further resulting in increased speed. It is because of all of these advantages that in this work the recursive least squares algorithm will be used to adapt the lattice filter PARCOR coefficients, and thus generate the orthogonal signals.

In the equations in Tables 3-1 and 3-2, ß represents a "forgetting factor" that defines the "memory" or expected stationarity of the input sequence. The optimal PARCOR coefficients are independent of the order of the filter, that is the coefficients are dependent only upon the previous stages and not subsequent stages. Thus the order of a filter can be increased without affecting previously defined coefficients of lower stages of the filter. Hence when the order of a predictor is unknown, the number of stages of the lattice filter can be increased until the prediction error is sufficiently white, and/or reduced in magnitude (as discussed previously). This aids the Independent Quadratic Optimisation algorithm, as it means the coefficients in the control filter can be easily increased.

Table 3-1. Stochastic Approximation Algorithm.
[LATTICE FILTER OF ORDER $N - 1$]

begin

$n = 0$

Time Initialisation

for $i = 0$ to $N - 1$ do

$$e_{fi}(0) = e_{bi}(0) = 0$$

$$k_{fi}(1) = k_{bi}(1) = 0$$

$$j_{fi}(0) = \beta^{N-1} j_0 \ , \quad j_{bi}(0) = \beta^{(N-1)-i} j_0$$

alternatively $j_{f/bi}(0) = (1 + \beta^{-i-1})\beta^N j_0$

continue

Time Recurrence

start : $n = n + 1$

Order Initialisation

$$e_{f0}(n) = e_{b0}(n) = x(n)$$

$$j_{f0}(n) = \beta\, j_{f0}(n-1) + e_{f0}^2(n) \ , \ j_{b0}(n) = \beta\, j_{b0}(n-1) + e_{b0}^2(n)$$

alternatively $j_{f/b0}(n) = \beta\, j_{f/b0}(n-1) + [e_{f0}^2(n) + e_{b0}^2(n-1)]$

Order Recurrence

for $i = 0$ to $N - 2$ do

$$e_{f(i+1)}(n) = e_{fi}(n) - k_{b(i+1)}(n) e_{bi}(n-1)$$

$$e_{b(i+1)}(n) = e_{bi}(n-1) - k_{f(i+1)}(n) e_{fi}(n)$$

$$k_{f(i+1)}(n+1) = k_{f(i+1)}(n) + \frac{e_{fi}(n) e_{b(i+1)}(n)}{j_{fi}(n)}$$

or $k_{f(i+1)}(n+1) = k_{f(i+1)}(n) + 2\mu_i\, e_{fi}(n) e_{b(i-1)}(n-1)$

$$k_{b(i+1)}(n+1) = k_{b(i+1)}(n) + \frac{e_{bi}(n-1) e_{f(i+1)}(n)}{j_{bi}(n-1)}$$

or $k_{b(i+1)}(n+1) = k_{b(i+1)}(n) + 2\mu_i\, e_{bi}(n) e_{f(i-1)}(n)$

alternatively $k_{f/b(i+1)}(n+1) = k_{f/b(i+1)}(n) + \dfrac{e_{bi}(n-1) e_{f(i+1)}(n) + e_{fi}(n) e_{b(i+1)}(n)}{j_{f/bi}(n)}$

or $k_{f/b(i+1)}(n+1) = k_{f/b(i+1)}(n) + 2\mu_i\, [e_{bi}(n) e_{f(i-1)}(n) + e_{fi}(n) e_{b(i-1)}(n-1)]$

$$j_{f(i+1)}(n) = \beta\, j_{f(i+1)}(n-1) + e_{f(i+1)}^2(n)$$

$$j_{b(i+1)}(n) = \beta\, j_{b(i+1)}(n-1) + e_{b(i+1)}^2(n)$$

alternatively $j_{f/bi}(n) = \beta\, j_{f/bi}(n-1) + [e_{fi}^2(n) + e_{bi}^2(n-1)]$

continue

goto start

end

Table 3-2. Recursive Algorithm.
[LATTICE FILTER OF ORDER $N - 1$]

begin

$n = 0$

Time Initialisation

for $i = 0$ to $N - 1$ do

$e_{fi}(0) = e_{bi}(0) = 0$

$k_{fi}(1) = k_{bi}(1) = 0$

$j_{fi}(1) = \beta^{N-1} j_0$, $j_{bi}(1) = \beta^{(N-1)-i} j_0$

$\gamma_i(0) = 1$

continue

Time Recurrence

start : $n = n + 1$

Order Initialisation

$e_{f0}(n) = e_{b0}(n) = x(n)$

$j_{f0}(n+1) = \beta j_{f0}(n) + \gamma_0(n-1) e_{f0}^2(n) = \beta j_{f0}(n) + x^2(n)$

$\gamma_0(n) = 1$

$j_{b0}(n+1) = \beta j_{b0}(n) + \gamma_0(n) e_{b0}^2(n) = \beta j_{b0}(n) + x^2(n)$

Order Recurrence

for $i = 0$ to $N - 2$ do

$e_{f(i+1)}(n) = e_{fi}(n) - k_{b(i+1)}(n) e_{bi}(n-1)$

$e_{b(i+1)}(n) = e_{bi}(n-1) - k_{f(i+1)}(n) e_{fi}(n)$

$$k_{f(i+1)}(n+1) = k_{f(i+1)}(n) + \frac{\gamma_i(n-1) e_{fi}(n) e_{b(i+1)}(n)}{j_{fi}(n+1)}$$

$$k_{b(i+1)}(n+1) = k_{b(i+1)}(n) + \frac{\gamma_i(n-1) e_{bi}(n-1) e_{f(i+1)}(n)}{j_{bi}(n)}$$

$$j_{f(i+1)}(n+1) = \beta j_{f(i+1)}(n) + \gamma_{i+1}(n-1) e_{f(i+1)}^2(n)$$

$$\gamma_{i+1}(n) = \gamma_i(n) - \frac{\gamma_i^2(n) e_{bi}^2(n)}{j_{bi}(n+1)}$$

$$j_{b(i+1)}(n+1) = \beta j_{b(i+1)}(n) + \gamma_{i+1}(n) e_{b(i+1)}^2(n)$$

continue

goto start

end

3.3 Control Filter Coefficient Independence

In this section it will be shown that the control filter coefficients are independent because they are fed by orthogonal signals (ie. the backward prediction errors). The lattice structure can be modified to generate estimation and control signals (as opposed to purely prediction) with the addition of a control filter (linear combiner). The control filter extracts each orthogonal signal generated by the lattice filter and multiplies each signal by a coefficient. The control filter then sums each product to generate the control signal.

Consider firstly the use of this control signal in a system without a cancellation path transfer function, as shown in Figure 3-6 (the location were the cancellation path transfer function would ordinarily be located is shown dotted). In the same manner as the order recursive update equations for the forward and backward prediction errors, it can be shown that the disturbance can be estimated from a linear combination of orthogonal backward prediction errors, such that

$$y(n) = p(n) + K_{wN}^{T}(n)E_{bN}(n) \qquad [3\text{-}20]$$

where N represents the number of control filter coefficients or backward prediction error signals,

$$K_{wN}(n) = [\, k_{w0}(n), \ldots, k_{w(N-1)}(n) \,] \qquad [3\text{-}21]$$

represents the vector of control filter coefficients,

$$E_{bN}(n) = [\, e_{b0}(n), \ldots, e_{b(N-1)}(n) \,] \qquad [3\text{-}22]$$

represents a set of orthogonal backward prediction errors, and

$$R_{11}^{p} = E[p^{2}(n)] \qquad [3\text{-}42]$$

represents the power of the disturbance signal.

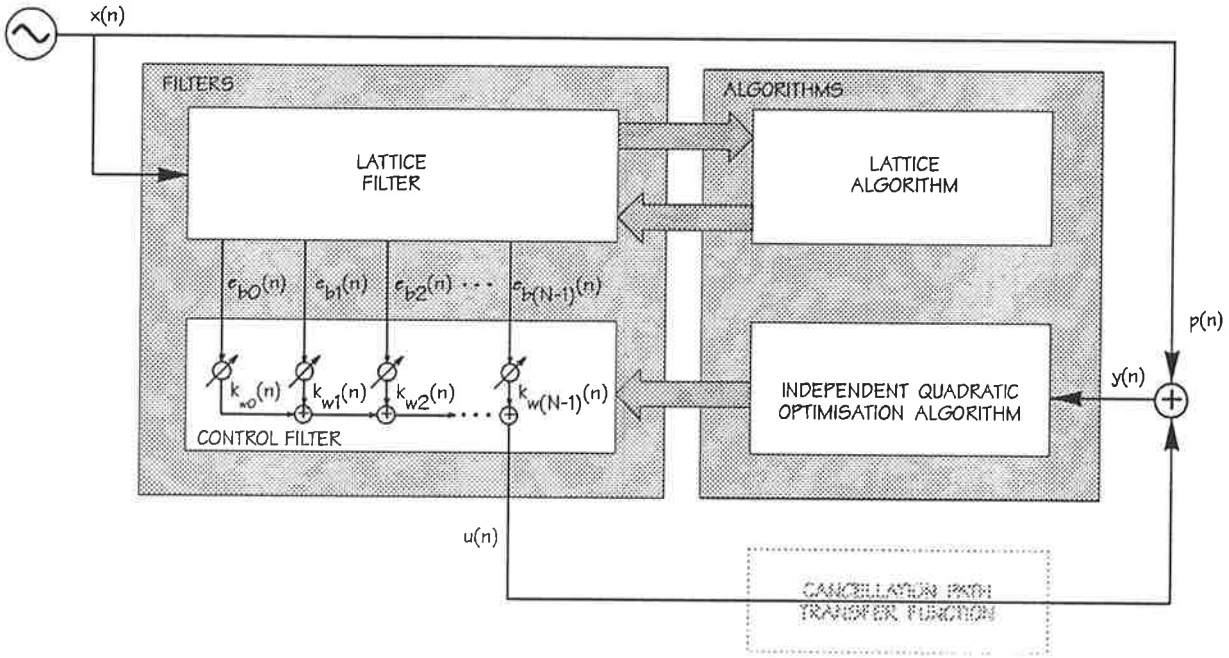

Figure 3-6. Control Structure without Cancellation Path Transfer Function. Where $x(n)$ is the input/reference signal, $p(n)$ is the disturbance, $y(n)$ the error signal, $u(n)$ the control signal, $e_{bi}(n)$ the backward prediction errors and $k_{wi}(n)$ the control filter coefficients.

It will now be shown that the cost function, $J(n) = E[y^2(n)]$, is independently defined by the control filter coefficients. Using the error defined by equation (3-20) the cost function becomes

$$J(n) = R_{11}^{p} + K_{wN}^{T}(n)R_{NN}^{e_b}K_{wN}(n) + 2K_{wN}^{T}(n)C_{N}^{pe_b} \qquad [3\text{-}23]$$

where

$$R_{NN}^{e_b} = E[\,E_{bN}(n)E_{bN}^{T}(n)\,] \qquad [3\text{-}24]$$

represents the correlation matrix of the backward prediction error signals (where the use of the superscript e_b is to make this matrix distinct from that normally used for the delayed reference signal), and

$$C_N^{pe_b} = E[\, p(n)E_{bN}(n)\,] \qquad [3\text{-}25]$$

represents the cross-correlation of the backward prediction error signals with the disturbance signal (where the use of the superscript pe_b is to make this vector distinct from that normally used for the correlation of the reference signal with the disturbance signal) .

Differentiating equation (3-23) with respect to the control filter coefficients yields

$$\left.\frac{\partial j_N(n)}{\partial K_{wN}(n)}\right|_{K_{wN}(n)=K_{w_{opt}}} = 2R_{NN}^{e_b}K_{w_{opt}} + 2C_N^{pe_b} = 0 \qquad [3\text{-}26]$$

which gives the optimal control filter coefficients as

$$K_{w_{opt}} = -R_{NN}^{e_b\,-1}C_N^{pe_b} \qquad [3\text{-}27]$$

Substituting (3-27) into (3-23) yields the optimal cost function as

$$J_{opt} = R_{11}^{p} + K_{w\,opt}^{T}C_N^{pe_b} \qquad [3\text{-}28]$$

Using the above equation with (3-23) gives

$$J(n) = J_{opt} + [K_{wN}(n) - K_{w_{opt}}]^T R_{NN}^{e_b}[K_{wN}(n) - K_{w_{opt}}] \qquad [3\text{-}29]$$

However, due to the orthogonality of the backward prediction errors, equation (3-24) becomes (with j_{bi} representing the power of the backward prediction errors)

$$R_{NN}^{e_b} = diag[\, j_{bi}\,] \qquad [3\text{-}30]$$

and hence equation (3-29) may be rewritten as

$$J(n) = J_{opt} + \sum_{i=0}^{N-1} j_{bi}\,(k_{wi}(n) - k_{wi_{opt}})^2 \qquad [3\text{-}31]$$

This equation shows that each coefficient of the control filter, $k_{wi}(n)$, can be adapted independently, as required for the Independent Quadratic Optimisation algorithm to perform efficiently. That is, the control filter coefficients form principal axes of the cost function, and the optimum value of each therefore doesn't depend on the values of the other coefficients. The optimum control filter coefficients can be determined from equation (3-27), which can be rewritten as

$$k_{wi_{opt}} = \frac{E[\,p(n)e_{bi}(n)\,]}{j_{bi}} \qquad [3\text{-}32]$$

Thus it is also apparent that the optimal control filter coefficients are dependent upon the correlation of the orthogonal backward prediction errors with the disturbance.

3.4 Cancellation Path Transfer Function Effect on Control Filter Coefficient Independence

The previous section showed that the control filter coefficients were independent, without a transfer function in the cancellation path. In this section consideration will be given to the effect on the independence of the control filter coefficients, with the inclusion of a time delay and then a more general transfer function in the cancellation path. With a transfer function or specifically a time delay placed in the cancellation path the structure can be modified to that shown in Figure 3-7. Note the reversal of the order (commutation) of the control filter and the cancellation path transfer function or time delay can be performed as shown, provided both filters are time invariant (see discussion in chapter 2 and Flockton [1993]).

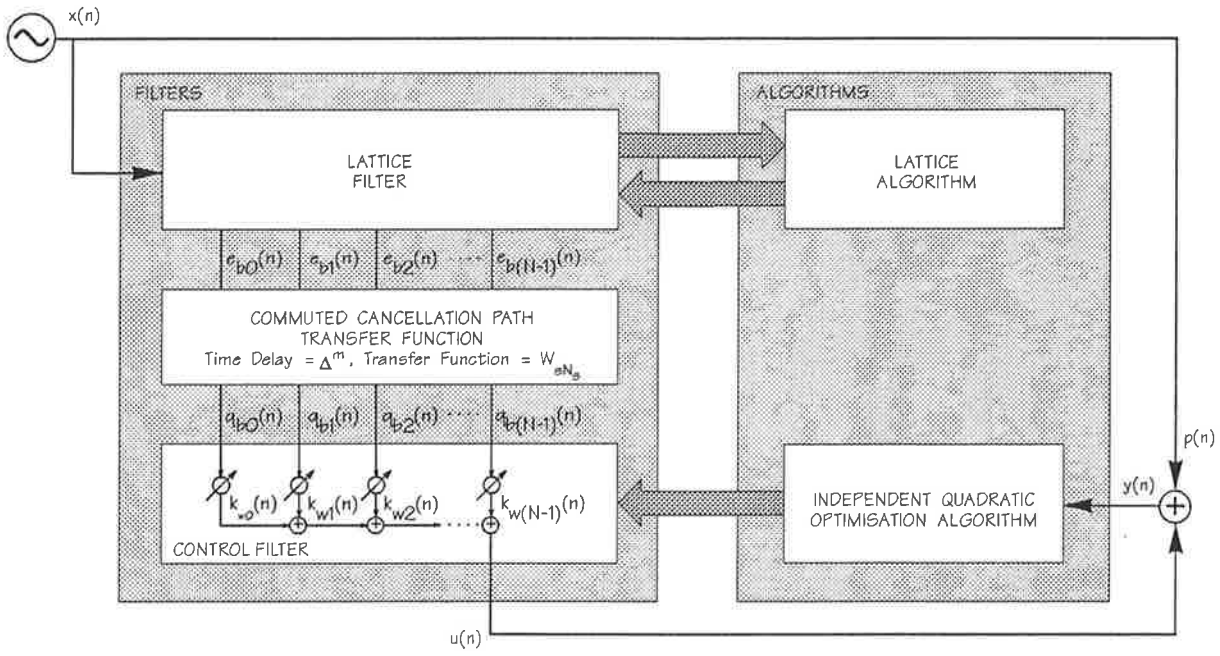

Figure 3-7. Active Noise and Vibration Control Structure. Where $x(n)$ is the input/reference signal, $p(n)$ is the disturbance, $y(n)$ the error signal, $u(n)$ the control signal, $e_{bi}(n)$ the backward prediction errors, $q_{bi}(n)$ the filtered backward prediction error signals and $k_{wi}(n)$ the control filter coefficients. Δ represents a single sample delay and Δ^m represents m samples delay.

The efficiency, or speed of convergence of the Independent Quadratic Optimisation algorithm relies upon the independence of the control filter coefficients. That is, if each coefficient of the control filter forms a principal axis of the cost function, then the optimum of the cost function will be obtained efficiently. However if the control filter coefficients are not principal axes, and cannot therefore be adapted independently, then the speed of the Independent Quadratic Optimisation algorithm will be impaired. This effect on the Independent Quadratic Optimisation algorithm is discussed in chapter 4.

3.4.1 Time Delay Effect

The effect of the time delay on the independence of the control filter coefficients will firstly be considered, using the commuted control structure shown in Figure 3-7. The inclusion of the time delay term, m, in equation (3-20) (ignoring the adaptation of the control filter coefficients to ensure valid commutation), leads to

$$y(n) = p(n) + K_{wN}^{T} E_{bN}(n-m) \qquad [3\text{-}33]$$

with the parameters defined as per equation (3-20). Substituting this into the cost function yields (superscripts have been used to distinguish the use of the backward prediction error signal as opposed to the more familiar delayed reference signal)

$$J = R_{11}^{p} + 2K_{wN}^{T} C_{N}^{pe_b} + K_{wN}^{T} R_{NN}^{e_b} K_{wN}^{T} \qquad [3\text{-}34]$$

where

$$R_{11}^{p} = E[p^{2}(n)] \qquad [3\text{-}35]$$

represents the power of the disturbance signal, and

$$C_{N}^{pe_b} = E[E_{bN}(n-m)p(n)] \qquad [3\text{-}36]$$

represents the cross-correlation of the delayed backward prediction error signals with the disturbance signal, and

$$R_{NN}^{e_b} = E[E_{bN}(n-m)\ E_{bN}^{T}(n-m)] \qquad [3\text{-}37]$$

represents the correlation of the delayed backward prediction error signals.

It can be shown that the non-diagonal terms of the auto-correlation matrix may be written as:

$$E[e_{bu}(n-m)\ e_{bv}(n-m)] = 0 \qquad [3\text{-}38]$$

where $u \neq v$, $u,v = 0...(N-1)$. Hence the control filter coefficients will be

independent, regardless of the time delay. That is, a time delay in the cancellation path does not affect the independence of the control filter coefficients, and therefore the Independent Quadratic Optimisation algorithm operates at peak efficiency.

3.4.2 Transfer Function Effect

The effect of a general transfer function (modelled by a finite impulse response filter) in the cancellation path, on the independence of control filter coefficients will now be considered using the commuted control structure shown in Figure 3-7. Consider the inclusion of the transfer function in equation (3-20) (again ignoring the adaptation of the control filter coefficients), such that

$$y(n) = p(n) + K_{wN}^{T}\{E_{bN}(n) \otimes W_{sN_s}(n)\} \qquad [3\text{-}39]$$

where N represents the number of control filter coefficients (and hence backward prediction error signals), N_s represents the number of cancellation path transfer function coefficients, and

$$E_{bN}(n) \otimes W_{sN}(n) = [\ e_{b0}(n) \otimes W_{sN_s}(n),\ ...,\ e_{b(N-1)}(n) \otimes W_{sN_s}(n)\ ]^{T} \qquad [3\text{-}40]$$

with $\otimes$ representing the convolution operator, $W_{sN_s}(n)$ the cancellation path transfer function, and all other parameters defined as per equation (3-20).

Substituting equation (3-39) into the cost function yields

$$J = R_{11}^{p} + 2K_{wN}^{T} C_{N}^{pe_b \otimes w_s} + K_{wN}^{T} R_{NN}^{e_b \otimes w_s} K_{wN} \qquad [3\text{-}41]$$

where superscripts have again been used to make the use of the filtered (by the

cancellation path transfer function) backward prediction errors distinct from the delayed reference signal normally used, with

$$R_{11}^{p} = E[p^2(n)] \qquad [3\text{-}42]$$

representing the power of the disturbance signal,

$$C_N^{pe_b \otimes w_s} = E[E_{bN}(n) \otimes W_{sN_s} \cdot p(n)] \qquad [3\text{-}43]$$

representing the cross-correlation of the filtered (by the cancellation path transfer function) backward prediction error signals with the disturbance signal, and

$$R_{NN}^{e_b \otimes w_s} = E[(E_{bN}(n) \otimes W_{sN_s})(E_{bN}(n) \otimes W_{sN_s})^T] \qquad [3\text{-}44]$$

representing the correlation of the filtered (by the cancellation path transfer function) backward prediction error signals. Equation (3-41) can be written in the form of (3-29), with the independence of the control filter coefficients dependent on the off-diagonal terms of the autocorrelation matrix defined by equation (3-44). It can be shown that the off-diagonal terms of the auto-correlation matrix may be written as

$$E[e_{bu}(n) \otimes W_{sN_s} \cdot e_{bv}(n) \otimes W_{sN_s}] = \sum_{i=0}^{N_s-1} \sum_{j=i+1}^{N_s-1} w_{si} w_{sj} \left\{ \begin{array}{l} E[e_{bu}(n-i)e_{bv}(n-j)] \\ + E[e_{bu}(n-j)e_{bv}(n-i)] \end{array} \right\} \qquad [3\text{-}45]$$

where $u \neq v$ $u,v = 0,\ldots,N-1$. Therefore the condition for control filter coefficient independence is

$$E[\, e_{bu}(n)e_{bv}(n-m) + e_{bu}(n-m)e_{bv}(n)\,] = 0 \qquad [3\text{-}46]$$

where $m = 0,\ldots,N_s-1$. The significance of this condition, will be considered for a pure tone, a periodic signal and a white noise signal. If this condition is not met, it means that the Independent Quadratic Optimisation algorithm will not operate at peak efficiency, but will converge in a stable manner to the cost function optimum.

3.4.2.1 Pure Tone

To determine whether the independence condition is met for a pure tone, consider a sinusoidal signal, defined with amplitude X_0, phase θ_0, frequency ω, sampling frequency ω_s, and therefore $\omega_0 = 2\pi\omega/\omega_s$ (with ω_s/ω the "sampling ratio"), such that

$$x(n) = X_0 \sin(n\omega_0 + \theta_0) = e_{b0}(n) = e_{f0}(n) \qquad [3\text{-}47]$$

Using equations (3-12) and (3-13), it can be shown that

$$k_{f1}^{opt} = k_{b1}^{opt} = \cos\omega_0 \qquad [3\text{-}48]$$

and therefore that the backward prediction error generated by the first stage of the lattice is given by

$$e_{b1}(n) = X_0 \sin\omega_0 \sin(n\omega_0 - \pi/2) \qquad [3\text{-}49]$$

Further analysis shows that $k_{b2}^{opt} = -1$ and hence that $e_{bi}(n) = 0$ *for* $i \geq 2$. This is intuitive since a pure tone can have only a single orthogonal component. It is apparent that a pure tone satisfies the independence condition since each term of the independence condition can be written as :

$$E[\, e_{b0}(n) e_{b1}(n-m) \,] = -\frac{1}{2} X_0^2 \sin\omega_0 \sin(m\omega_0) \qquad [3\text{-}50]$$

and

$$E[\, e_{b0}(n-m) e_{b1}(n) \,] = \frac{1}{2} X_0^2 \sin\omega_0 \sin(m\omega_0) \qquad [3\text{-}51]$$

and therefore their combination is zero.

3.4.2.2 Periodic Signal

It will now be examined whether periodic signals satisfy the independence condition. It could be expected that the harmonic components of a periodic signal would each be phase shifted by 90°, indicating that the lattice filter would generate only a single orthogonal signal for any periodic signal, and hence that the condition for coefficient independence would also hold, as for a pure tone. A periodic disturbance with a fundamental and a harmonic component will now be considered, with the reference signal given by

$$x(n) = X_0 \sin(n\omega_0) + X_1 \sin(n\omega_1) = e_{b0}(n) = e_{f0}(n) \qquad [3\text{-}52]$$

with $\omega_1 = k\omega_0$. The following knowledge of expectations for periodic signals ω_0 and $\omega_1 = k\omega_0$ where $k \epsilon \mathbb{I}^+$ will be used :

$$E[\sin(n\omega_0 + \theta_a)\sin(n\omega_0 + \theta_b)] = \frac{1}{2}\cos(\theta_a - \theta_b) \qquad [3\text{-}53]$$

and

$$E[\sin(n\omega_0 + \theta_0)\sin(n\omega_1 + \theta_1)] = 0 \qquad [3\text{-}54]$$

Using equations (3-12) and (3-13), and the above knowledge, it can be shown that the optimal PARCOR coefficients are given by

$$k_{b1}^{opt} = k_{f1}^{opt} = \frac{X_0^2 \cos\omega_0 + X_1^2 \cos\omega_1}{X_0^2 + X_1^2} \qquad [3\text{-}55]$$

The backward prediction errors can be calculated using the PARCOR coefficients, to give

$$e_{b1}(n) = \begin{aligned} & X_0 \sin\omega_0 \sin(n\omega_0 - \pi/2) + X_1 \sin\omega_1 \sin(n\omega_1 - \pi/2) \\ & + \frac{X_1^2}{X_0^2 + X_1^2}(\cos\omega_0 - \cos\omega_1) X_0 \sin(n\omega_0) \\ & + \frac{X_0^2}{X_0^2 + X_1^2}(\cos\omega_1 - \cos\omega_0) X_1 \sin(n\omega_1) \end{aligned} \qquad [3\text{-}56]$$

It is apparent that the first stage orthogonal component generated by the lattice filter does not consist of only the fundamental and harmonic terms shifted in phase by 90°, as intuitively expected. Therefore the independence condition is not necessarily satisfied. It can readily be shown that $e_{b0}(n)$ and $e_{b1}(n)$ are orthogonal, and the independence condition can be examined by considering each term of the independence condition, such that

$$E[\, e_{b0}(n-m) e_{b1}(n) \,] = \frac{1}{2} \left\{ \begin{aligned} & X_0 A_0 \sin(m\omega_0) + X_1 A_1 \sin(m\omega_1) \\ & + X_0^2 B_1 \cos(m\omega_0) + X_1^2 B_0 \cos(m\omega_1) \end{aligned} \right\} \qquad [3\text{-}57]$$

and

$$E[\, e_{b0}(n) e_{b1}(n-m) \,] = \frac{1}{2} \left\{ \begin{aligned} & - X_0 A_0 \sin(m\omega_0) - X_1 A_1 \sin(m\omega_1) \\ & + X_0^2 B_1 \cos(m\omega_0) + X_1^2 B_0 \cos(m\omega_1) \end{aligned} \right\} \qquad [3\text{-}58]$$

where

$$A_0 = X_0 \sin\omega_0 \;,\; A_1 = X_1 \sin\omega_1 \qquad [3\text{-}59a,b]$$

and

$$B_1 = \frac{X_1^2}{X_0^2 + X_1^2}(\cos\omega_0 - \cos\omega_1) \;,\; B_0 = \frac{X_0^2}{X_0^2 + X_1^2}(\cos\omega_1 - \cos\omega_0) \qquad [3\text{-}60a,b]$$

The independence condition is therefore not satisfied as

$$E[e_{b0}(n)e_{b1}(n-m)] + E[e_{b0}(n-m)e_{b1}(n)] = \frac{X_0^2 X_1^2}{X_0^2 + X_1^2}[(\cos\omega_0 - \cos\omega_1)(\cos(m\omega_0) - \cos(m\omega_1))] \quad [3\text{-}61]$$

Hence with a periodic input, the control filter coefficients will not be independent for a cancellation path transfer function, due to the extraneous components generated by the lattice. These extraneous components can be removed by orthogonalising each harmonic in isolation. This has recently been proposed by Gibbs et al [1993] and Kewley et al [1995].

An intuitive interpretation is that if extraneous components were not present, and the lattice filter generated a single backward prediction error signal (or orthogonal signal, with each harmonic component orthogonal by a 90° phase shift), then there would only be two signals available to be fed into the control filter coefficients. This would result in incomplete cancellation of a disturbance with the same two tones, as two separate coefficients would be required for each tone (ie. four coefficients in total), to achieve complete cancellation for each tonal component. That is, the optimal control filter coefficients would be the average of those for each harmonic component in isolation. Hence to obtain optimal control, or complete cancellation, it would be expected that more than one orthogonal signal would be required to be generated by the lattice filter, as is shown by the results above.

It can be shown that for each tone, components with and without a phase shift of 90°

remain in each backward prediction error generated from increasing stages of a lattice. However, the power of the prediction errors of orders greater than two, rapidly decreases in magnitude as the number of stages in the filter increases. This effect will be considered further in chapter 4, with regard to the Independent Quadratic Optimisation algorithm.

3.4.2.3 White Noise

Consider white noise passed through the lattice filter, with again the input signal defined such that ($r_x(n)$ represents white noise)

$$x(n) = r_x(n) = e_{b0}(n) = e_{f0}(n) \qquad [3\text{-}62]$$

with

$$k_{fi}^{opt} = k_{bi}^{opt} = 0 \qquad [3\text{-}63]$$

and therefore

$$e_{bi}(n) = r_x(n-i) \quad and \quad e_{fi}(n) = r_x(n) \qquad [3\text{-}64]$$

Hence the independence condition becomes

$$\begin{aligned} &E[\, e_{bu}(n-i)e_{b\nu}(n-j) + e_{bu}(n-j)e_{b\nu}(n-i)\,] \\ &= E[\, r_x(n-u-i)r_x(n-\nu-j) + r_x(n-u-j)r_x(n-\nu-i)\,] \end{aligned} \qquad [3\text{-}65]$$

which is zero unless $(u+i) = (\nu+j)$ or $(u+j) = (\nu+i)$. The independence condition will however be non-zero for most non-diagonal terms. The same result holds for an autoregressive moving average signal (ie. a signal generated by passing white noise through an IIR filter). Therefore the independence condition is not satisfied for white or broadband noise.

3.4.2.4 Summary

The results discussed in the preceding section show that control filter coefficient independence can be guaranteed for pure tones or periodic signals in which the harmonics can be isolated and individually orthogonalised by a single stage lattice filter, before use in a linear combiner. This concept is shown in Figure 3-8. This satisfies the independence condition given by equation (3-46), since each individual harmonic has been shown to satisfy it (according to section 3.4.2.1), and harmonics are themselves independent as shown by equation (3-54). The Independent Quadratic Optimisation algorithm has been extended in this way by Botteldooren [1993] and also by Clark et al [1992], Gibbs et al [1993] and Kewley et al [1995].

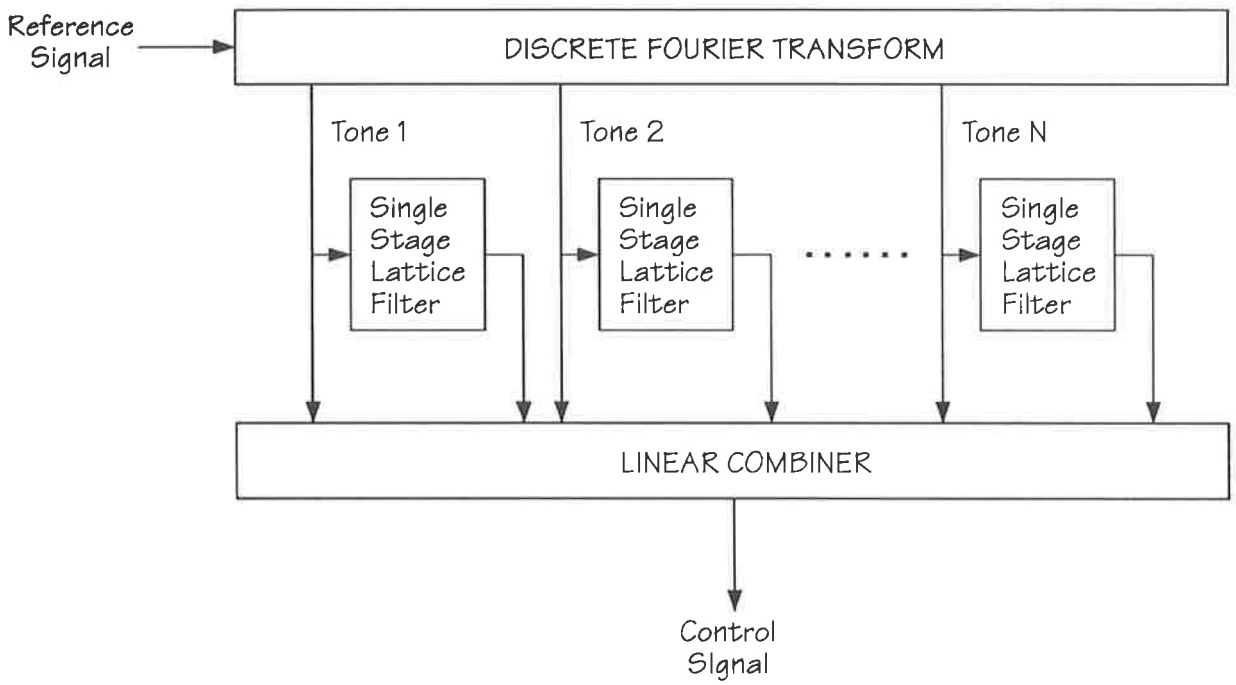

Figure 3-8. Individual orthogonalisation of harmonic components of a periodic signal, before combination in a linear combiner.

For other signals, control filter coefficient independence cannot be guaranteed. If the independence condition is not satisfied, the Independent Quadratic Optimisation algorithm (to be developed in the next chapter) will be less efficient; That is, slower to converge, but it will still have inherent stability.

3.5 Summary

In this chapter the lattice filter was introduced as a means of providing orthogonal signals for use by the Independent Quadratic Optimisation algorithm. The lattice filter was shown to be particularly suited to the extremely fast recursive least squares algorithm, enabling the orthogonal backward prediction errors to be quickly available. The lattice filter was found to have many desirable properties that were specifically suited to the Independent Quadratic Optimisation algorithm, namely:

- The lattice filter is a form of linear prediction with the prediction accuracy determined by the magnitude of the backward prediction error signals. That is, the more complex the input/reference signal (in terms of signal statistics), the more stages will be required for prediction. Hence the lattice filter, through the generated backward prediction error signals, gives an indication of the number of control filter coefficients required for control.

- PARCOR coefficients of each stage of the lattice are adapted independently to later stages, therefore the lattice can be extended to the required number of

stages to achieve optimum control, without affecting previously converged PARCOR coefficients.

- The lattice filter is defined such that, provided the absolute magnitude of the PARCOR coefficients is less than unity, stability is assured; This links well with the established stability concept of the Independent Quadratic Optimisation algorithm.

Although the backward prediction error signal generated by the lattice are orthogonal, it should be emphasised that they represent **prediction errors**, and as such will decrease in power with increasing stages of the lattice (ie. with increasing numbers of samples used in prediction) eventually becoming white noise sequences with low signal powers. As the power of the backward prediction error signals decrease, this means that the control filter coefficients magnitude must increase to generate the control signal, possibly leading to an overflow. This represents the only disadvantage of the lattice filter when used to generate orthogonal signals.

When the backward prediction errors used with the individual coefficients of the control filter (linear combiner), the control filter coefficients were found to be independent provided no transfer function existed in the cancellation path. It was shown that a delay in the cancellation path did not affect the independence of the control filter coefficients; However, any other type of transfer function in the cancellation path reduced the independence of the control filter coefficients for all signals other than pure tones. Orthogonalising each harmonic individually has been

shown to provide a means of overcoming this limitation. It was noted that loss of independence of the control filter coefficients only reduced the speed of convergence and not the stability of the Independent Quadratic Optimisation algorithm (as will be shown in chapter 4).

4.1 Introduction

Chapter 2 examined the standard algorithms used in Active Noise and Vibration Control, to achieve optimal control (ie. minimum mean square error) in the presence of destabilising system identification inaccuracies. Chapter 2 described an outline of the Independent Quadratic Optimisation (IQO) algorithm, which uses orthogonal signals to enable independent adaptation of control filter coefficients to reach the optimum of a cost function based on a quadratic criterion. In so doing it eliminates the need to estimate the cancellation path transfer function, and therefore avoids the instabilities that plague the current standard algorithms, due to inaccuracies in this estimate. Chapter 3 described the lattice filter as a means of generating orthogonal signals to be used in the Independent Quadratic Optimisation algorithm. The characteristics of the lattice filter were examined with regard to the Independent Quadratic Optimisation algorithm. The structure of a typical single channel active noise and vibration control system, with regard to the Independent Quadratic Optimisation algorithm, is shown in Figure 4-1, for ease of reference.

The concept behind the Independent Quadratic Optimisation algorithm is revisited before this novel algorithm is formally derived and analysed, with regard to the parameters that affect its performance. Simulations of this algorithm will be performed for a pure tone, white noise and their combination to confirm the theory derived in this chapter. The algorithm will be extended for multi-channel control, with further simulations highlighting effects that are similar to standard algorithms for multi-channel control.

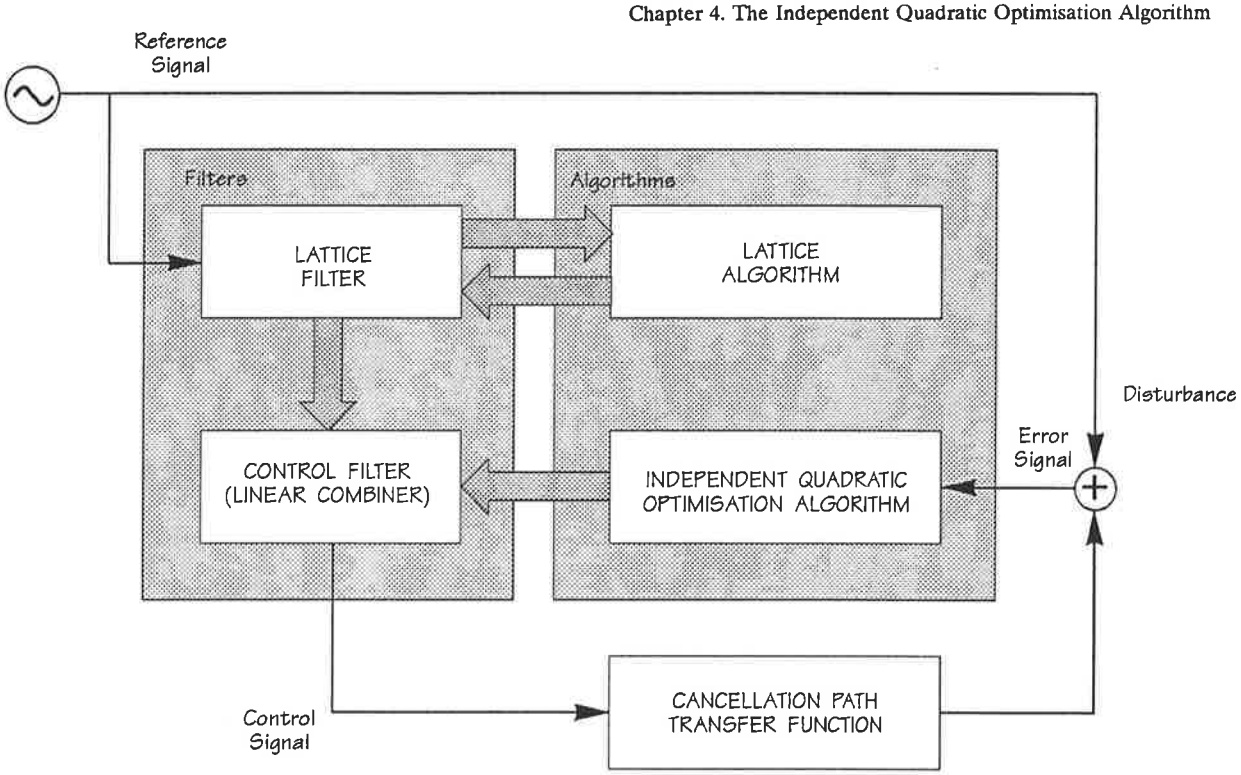

Figure 4-1. Single channel active noise and vibration control structure.

4.2 Concept

In this section the concept of the Independent Quadratic Optimisation algorithm will be revisited using the work presented thus far. The Independent Quadratic Optimisation algorithm will be applied to a feedforward control scheme, without acoustic feedback corrupting the reference signal.

In chapter 2, it was shown (see equation (2-10)) that the control signal, $u(n)$, could be obtained using a linear combination of coefficients $w_i(n)$, with delayed reference signal samples $x(n-i)$, such that (with N the number of control filter coefficients or reference signal samples)

$$u(n) = W_N^T(n)X_N(n) \quad [4\text{-}1]$$

where the vector of control filter coefficients (ie. the parameter vector, θ) is given by

$$W_N(n) = [\ w_0(n),\ldots,w_{N-1}(n)\ ]^T \quad [4\text{-}2]$$

and the vector of delayed reference signal samples is given by

$$X_N(n) = [\ x(n),\ldots,x(n-N+1)\ ]^T \quad [4\text{-}3]$$

It was also shown that the regressor, $\phi(n)$, is given by a vector of delayed filtered reference signal samples (see equation (2-12)), such that using the theory outlined in appendix A.2.2 (in particular equation (A-25)), the cost function $J(n)$ can be written as

$$J(n) = J_{opt} + (W_N(n) - W_{N_{opt}})^T R_{\phi\phi}(W_N(n) - W_{N_{opt}}) \quad [4\text{-}4]$$

with J_{opt}, the optimum of the cost function with corresponding optimal control filter coefficients W_{opt}, and $R_{\phi\phi}$ the autocorrelation matrix of the delayed filtered reference signal samples. It was further shown in appendix A.2.2, that this equation could be simplified by diagonalising the autocorrelation matrix using its eigenvalues and associated eigenvectors, such that (see equation (A-26))

$$J(n) = J_{opt} + V_N^{*T}(n)\Lambda V_N^*(n) \quad [4\text{-}5]$$

where

$$V_N^*(n) = Q^T(W_N(n) - W_{N_{opt}}) \quad [4\text{-}6]$$

represents a set of principal axes of the cost function, with Λ the eigenvalue matrix (in which the off diagonal terms are zero and the diagonal terms correspond to the eigenvalues), and Q is the corresponding modal matrix of eigenvectors.

The Independent Quadratic Optimisation algorithm concept uses the principal axes of the cost function to avoid the need to estimate the cancellation path transfer function.

The Independent Quadratic Optimisation algorithm concept is shown in Figure 4-2. In Figure 4-2, $w_o(n)$ and $w_1(n)$ are components of the vector $W_N(n)$, and $k_{w0}(n)$ and $k_{w1}(n)$ are coefficients of the vector $V_N^*(n)$. As shown in Figure 4-2, w_0 and w_1 represent arbitrary axes of the cost function, and k_{w0} and $k_{w1}(n)$ represent principal axes of the cost function. For each coefficient in turn, the Independent Quadratic Optimisation algorithm determines its optimum by estimating the cost function at three points in the direction of each coefficients axis, and fitting a quadratic to these estimates to find the optimum coefficient corresponding to the minimum of the quadratic. Figure 4-2 shows that with coefficients that are principal axes of the cost function (such coefficients will be termed independent), the minimum of the cost function is reached in two steps (with three estimates per step), while for coefficients that are arbitrary axes of the cost function (such coefficients are termed dependent), the optimum of the cost function is reached after a considerably greater number of steps.

The principal axes cannot be found in practice since diagonalising a matrix would take too long and expectations would be required. An alternative means of obtaining independent coefficients was shown in chapter 3. In chapter 3, it was shown that the cost function could be written as (see equation (3-31) of section 3-3)

$$J(n) = J_{opt} + \sum_{i=0}^{N-1} j_{bi}(k_{wi}(n) - k_{wi_{opt}}) \qquad [4\text{-}7]$$

where, on comparison with equation (4-5), j_{bi} corresponds to the eigenvalues of the autocorrelation matrix, and $(k_{wi}(n) - k_{wi_{opt}})$ represent the principal axes of the cost function. The effect of the cancellation path transfer function on the control filter

coefficient independence was also examined in chapter 3. It was apparent in that examination, that if the independence of the coefficients is degraded, the speed of convergence of this algorithm is reduced. This limitation will be discussed later in this chapter.

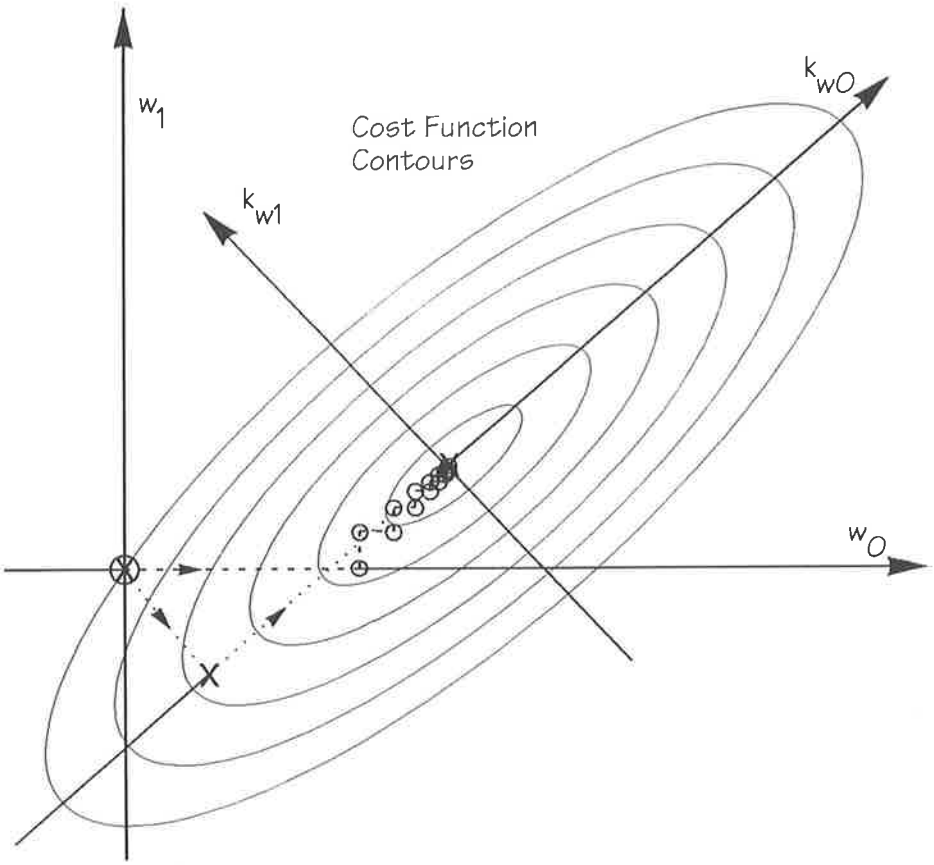

Figure 4-2. The paths to the cost function optimum are shown by - -o- - for optimisation along the axes w_0, w_1, and by · · ·X· · · for optimisation along the principal axes, k_{w0}, k_{w1}. Cost function contours are also shown.

4.3 Formulation

In this section the equations used to define the Independent Quadratic Optimisation algorithm will be derived. A heuristic assessment of the effects of parameters, used to

define the algorithm, on the stability and minimum obtainable value of the cost function will be made and proved in a later section of this chapter.

The Independent Quadratic Optimisation algorithm can be developed to ensure efficient adaptation as follows:

(a) Delay estimating the mean square error (after changing any part of the control filter) by a number of samples equivalent to a time greater than the time taken for the control signal to reach the error sensor.

(b) Perform a sufficient average of the mean square error dependent upon the required variance of the mean square error estimate from the actual mean square error value This will affect the minimum mean square error obtained and the level of stability.

(c) Change the particular value of the control filter coefficient (based upon the level of the mean square error last predicted) and perform (a) to (b) twice more. If the second mean square error estimate is greater than the first, change the control filter coefficient to be used for the third estimate in the opposite "direction" to that of the first change.

(d) Determine the optimum value for the particular control filter coefficient by fitting the estimated points to a quadratic function.

(e) Change to a new control filter coefficient and repeat (a) to (e).

As discussed in chapter 3, the lattice structure generates orthogonal signals using the Recursive Least Squares algorithm discussed in chapters 2 and 3. It is only the coefficients of the control filter (linear combiner) that are adapted by the Independent Quadratic Optimisation algorithm.

Consider a quadratic defined by three estimates of the mean square error at three values of an independent control coefficient of the control filter (linear combiner), as shown in Figure 4-3. Such a quadratic function can be written, using the theory outlined for equation (4-7), as (with j_{bi} representing the power of the backward prediction error fed from the lattice filter, into the *ith* control filter coefficient)

$$\hat{J}_{i_m} = \hat{J}_{i_{opt}} + j_{bi}(k_{wi_m} - k_{wi_{opt}})^2 \qquad [4\text{-}8]$$

where $0 \le i \le N-1$, and i corresponds to the control filter coefficient number, and $0 \le m \le 2$, with m corresponding to the estimate number. Note that $\hat{J}_i$ has been used as a descriptor for the cost function, with the cost function dependent on all control filter coefficients, with however the others remaining fixed while k_{wi} is changed.

Equation (4-8) can be rewritten as

$$k_{wi_{opt}} = k_{wi_m} \pm \sqrt{\frac{\hat{J}_{i_m} - \hat{J}_{i_{opt}}}{\hat{j}_{bi}}} \qquad [4\text{-}9]$$

To eliminate the need to know or estimate j_{bi} (which is affected by the cancellation path transfer function since commutation of the cancellation path transfer function

leads to filtered backward prediction error signals, as per equation (3-44) and Figure 3-7), in determining the optimal control filter coefficient value (corresponding to minimum mean square error), three control filter coefficient sample points are required, as shown in Figure 4-3.

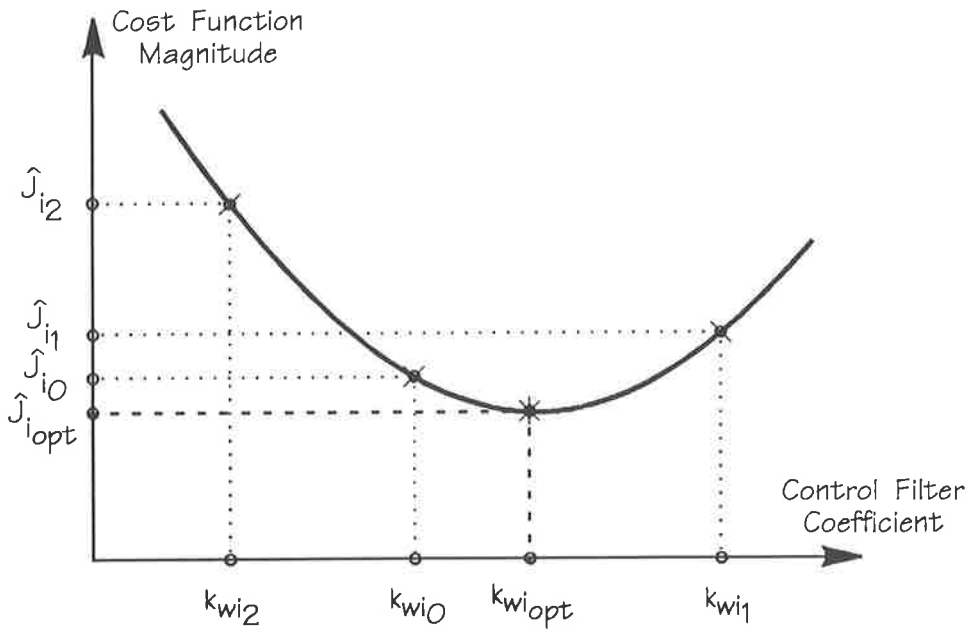

Figure 4-3. Quadratic defined by three values of a control filter coefficient k_{wi_0}, k_{wi_1}, *and* k_{wi_2}, with respective cost function estimates $\hat{J}_{i_0}$, $\hat{J}_{i_1}$, *and* $\hat{J}_{i_2}$. The optimum of the quadratic is given by $\hat{J}_{i_{opt}}$ at $k_{wi_{opt}}$.

The control filter coefficient step size should ideally be made proportional to the inverse of j_{bi}, since it relates to the gradient of the cost function (ie. the steeper the gradient, the smaller the step size should be and vice-versa), however this term is not available as it is affected by the cancellation path transfer function. Therefore the control filter coefficient step size is made proportional to the cost function magnitude at the last estimation point, such that

$$k_{wi_m} \triangleq k_{wi_{m-1}} \pm \alpha_i \sqrt{\hat{J}_{i_{m-1}}} \qquad [4\text{-}10]$$

where α_i represents the control filter coefficient step-size factor.

Solving for $k_{wi_{opt}}$ using equation (4-8) for estimates $m = 0$ and 1 yields

$$\frac{1}{j_{bi}} = \frac{(k_{wi_0}^2 - k_{wi_1}^2) - 2k_{wi_{opt}}(k_{wi_0} - k_{wi_1})}{\hat{J}_{i_0} - \hat{J}_{i_1}} \qquad [4\text{-}11]$$

Similarly, solving for $k_{wi_{opt}}$ using equation (4-8) for estimates $m = 0$ and 2 yields

$$\frac{1}{j_{bi}} = \frac{(k_{wi_0}^2 - k_{wi_2}^2) - 2k_{wi_{opt}}(k_{wi_0} - k_{wi_2})}{\hat{J}_{i_0} - \hat{J}_{i_2}} \qquad [4\text{-}12]$$

Equating (4-11) and (4-12) gives the optimal control filter coefficient (corresponding to minimum mean square error) as

$$k_{wi_{opt}} = \frac{1}{2} \frac{\hat{J}_{i_0}(k_{wi_1}^2 - k_{wi_2}^2) + \hat{J}_{i_1}(k_{wi_2}^2 - k_{wi_0}^2) + \hat{J}_{i_2}(k_{wi_0}^2 - k_{wi_1}^2)}{\hat{J}_{i_0}(k_{wi_1} - k_{wi_2}) + \hat{J}_{i_1}(k_{wi_2} - k_{wi_0}) + \hat{J}_{i_2}(k_{wi_0} - k_{wi_1})} \qquad [4\text{-}13]$$

Thus it has been shown that the optimal control filter coefficients can be obtained from three estimates of the cost function corresponding to each adjusted control filter coefficient value.

The parameters affecting the accuracy of the estimated optimal control filter coefficients (corresponding to minimum mean square error), are considered heuristically :

(a) The number of samples taken to estimate the cost function.

The number of samples taken to estimate the cost function results in a more accurate estimate of the cost function minimum [Mackenzie, N.C., 1991a, 1991b]. The accuracy of the cost function estimate relative to the actual value (ie. the standard deviation) is dependent upon the signal statistics of the sampled disturbance, relative to the level of extraneous noise present. For periodic signals, the standard deviation will be dependent upon the number of samples taken during any period, and the number of periods over which samples are taken. For ARMA signals however, a very large number of averages are required to obtain a "reasonable" estimate of the cost function.

(b) The control coefficient step size is based upon the control coefficient step size factor α_i.

As shown in Figure 4-4, the control filter coefficient step size influences the number of averages required to obtain accurate estimates of the control coefficients corresponding to the cost function minimum [Mackenzie, N.C., 1991b]. The control filter coefficient step size also dictates the required accuracy of the cost function estimates to achieve a certain excess mean square error [Mackenzie, N.C., 1991b]. The excess mean square error is the mean square error above the minimum achievable, once adaptation of control filter coefficients has reached steady-state. In Figure 4-4 two different control filter coefficient step size factors, α, are shown for cost function estimates $\square$ and $\triangle$.

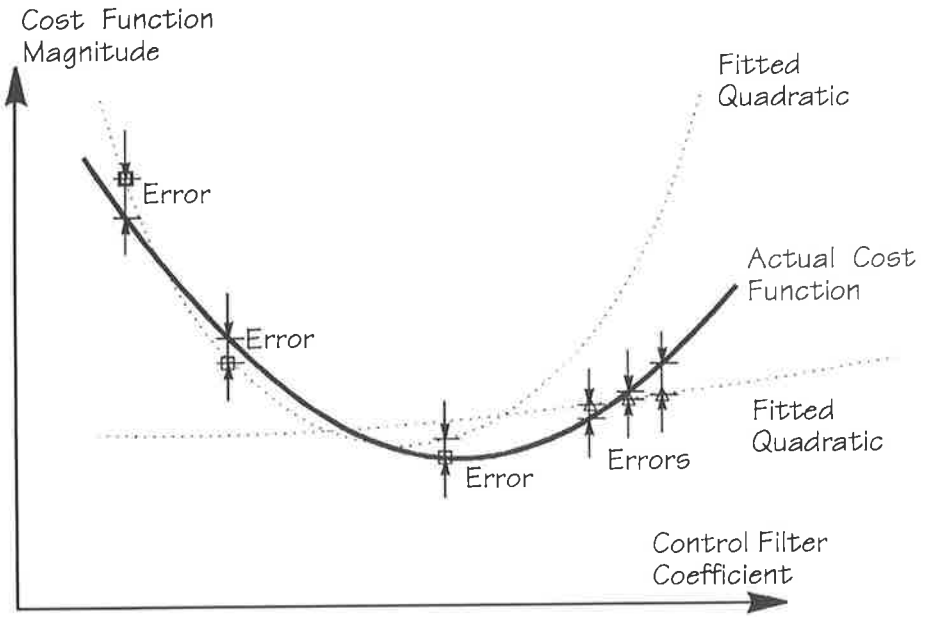

Figure 4-4. Effect of control filter coefficient step size and number of averages on determination of optimal control coefficients (corresponding to the minimum cost function). □ represents a sufficiently large step size and ▵ represents a step size that is too small.

Consider the estimates of the cost function represented by a □ in Figure 4-4. The control filter coefficients corresponding to these estimates are at large enough steps to allow some inaccuracy in the cost function estimates. The optimum control filter coefficient will not be too far removed from the ideal, upon fitting a quadratic to these estimates. However the same cannot be said for the estimates of the cost function represented by a ▵ in Figure 4-4. Here any inaccuracies in the cost function estimates will lead to algorithm instability, as optimum control filter coefficients determined from a quadratic fitted to the cost function estimates, will have large random deviations from the ideal

because the control filter coefficient step size is not large enough. Hence the smaller the control filter coefficient step size factor, the larger the number of averages required to reduce the inaccuracy in the cost function estimate.

As shown by equation (4-10), the control filter coefficient step size was chosen to be proportional to the current mean square error estimate or its square root [Mackenzie, N.C., 1991a]. This was deliberately imposed so that upon reaching the minimum mean square error, the variance of the mean square error about the optimum (known as the excess mean square error) would be minimal. However, it is apparent from the above discussion, that there is a minimum control filter coefficient step size factor for a given number of averages, above which stability of the algorithm will be ensured. This is given by the degree of curvature of the cost function for any particular control filter coefficient. As shown by equation (4-8), the degree of curvature is given by the second derivative of the cost function which equals j_{bi}. Hence an estimate of j_{bi} is also required and can be found from equations (4-11) and (4-12), such that

$$\hat{j}_{bi} = \frac{\hat{J}_{i_0}(k_{wi_2} - k_{wi_1}) + \hat{J}_{i_1}(k_{wi_0} - k_{wi_2}) + \hat{J}_{i_2}(k_{wi_1} - k_{wi_0})}{(k_{wi_0} - k_{wi_1})(k_{wi_0} - k_{wi_2})(k_{wi_2} - k_{wi_1})} \qquad [4\text{-}14]$$

where the control filter coefficient values are k_{wi_0}, k_{wi_1}, *and* k_{wi_2}, with respective cost function estimates $\hat{J}_{i_0}$, $\hat{J}_{i_1}$, *and* $\hat{J}_{i_2}$. Hence for "highly curved" quadratic cost functions, the control filter coefficient step size can be relatively small, while for relatively "flat" quadratic cost functions, the control filter coefficient step size needs to be relatively large [Mackenzie, N.C., 1991b]. The degree of curvature is not however available until the first estimates have been

made. Thus the initial value of the control filter coefficient step size factor needs to be set based on the allowed maximum output voltage from the controller, the magnitude of the backward prediction error signals, and a limited understanding of the gain imparted by the control source(s). Its value will depend upon the levels of deviation from the initial mean square error that it allows. A limit on the control signal output voltage can be set so that if it is exceeded as a result of the magnitude of the step size factor, the step size factor can be reduced as required, and tested again. This iterative approach will only occur at the start of control, with initially a conservative low value of the step size factor set. Once steady state has been reached, the control filter coefficient step size factor for each control filter coefficient is proportional to the degree of curvature, as discussed.

Consider now estimates of the cost function at distances remote from the minimum. Here the cost function estimates will have a large step size, which could result in overload of the actuators and algorithm instability. The maximum step size is thus also defined as inversely proportional to the degree of curvature. Thus for highly curved cost functions, the maximum step size must be strictly enforced. Again, initially a measure of the curvature will be unknown, and so a limit must be based on the control signal output voltage.

(c) The extraneous noise (uncorrelated to the disturbance as measured by the reference or error signal) content of the disturbance (or signal to noise ratio).

As discussed at remark (a), the signal to noise ratio will affect the number of averages required to obtain reasonably accurate cost function estimates.

(d) The independence condition discussed in chapter 3, section 3.4.2.

It was shown in chapter 3 that the independence condition was satisfied for pure tones, but for ARMA signals (ie. broadband noise) or periodic signals, the condition was not satisfied. With the control filter coefficients not completely independent, the Independent Quadratic Optimisation algorithm will converge at a slower speed. Thus the statistics of the disturbance not only affect the required number of averages but also the independence condition. It should be noted that the periodic or harmonic content of the disturbance relative to the ARMA (broadband) content is a separate consideration to the signal to noise (ie. extraneous) parameter discussed above.

The following section will simulate the Independent Quadratic Optimisation algorithm for control of a pure tone, white noise and their combination. This will be performed to confirm the Independent Quadratic Optimisation algorithm concept.

4.4 Simulations

The following set of simulations highlight the limitations of the Independent Quadratic Optimisation algorithm. The simulations consider reference signals

consisting of a pure tone and/or white noise. The Independent Quadratic Optimisation algorithm will be considered with fixed parameters (ie. control filter coefficient step size factor, and number of averages).

Knowledge of the cancellation path transfer function is not required for the Independent Quadratic Optimisation algorithm. The cancellation path transfer function has been chosen with a phase change of 90°. This was specifically chosen because if the standard algorithms (discussed in chapter 2) were to operate with this magnitude of error in the cancellation path transfer function phase, they would become unstable (ie. If standard algorithms were to assume there was no transfer function in the cancellation path, then the cancellation path transfer function used here, can be viewed as an error in estimating the cancellation path transfer function by the standard algorithms, causing instability). Hence it would seem that the use of this cancellation path transfer function is a good test of the Independent Quadratic Optimisation algorithm's stability.

Figure 4-5 shows the disturbance and cancellation path transfer functions to be used in the simulations. For all types of signals considered in the simulations to follow, the disturbance and cancellation path transfer functions have two FIR type coefficients. The disturbance transfer function (arbitrarily chosen) had the coefficients 5.767 and -4.576, corresponding to an amplitude change of 2.0 and a phase change of 45°. The number of samples delay used was 5 for a delay in the cancellation path. The cancellation path transfer function had the coefficients 3.078 and -3.236, corresponding to an amplitude change of 1.0 and a phase change of 90°.

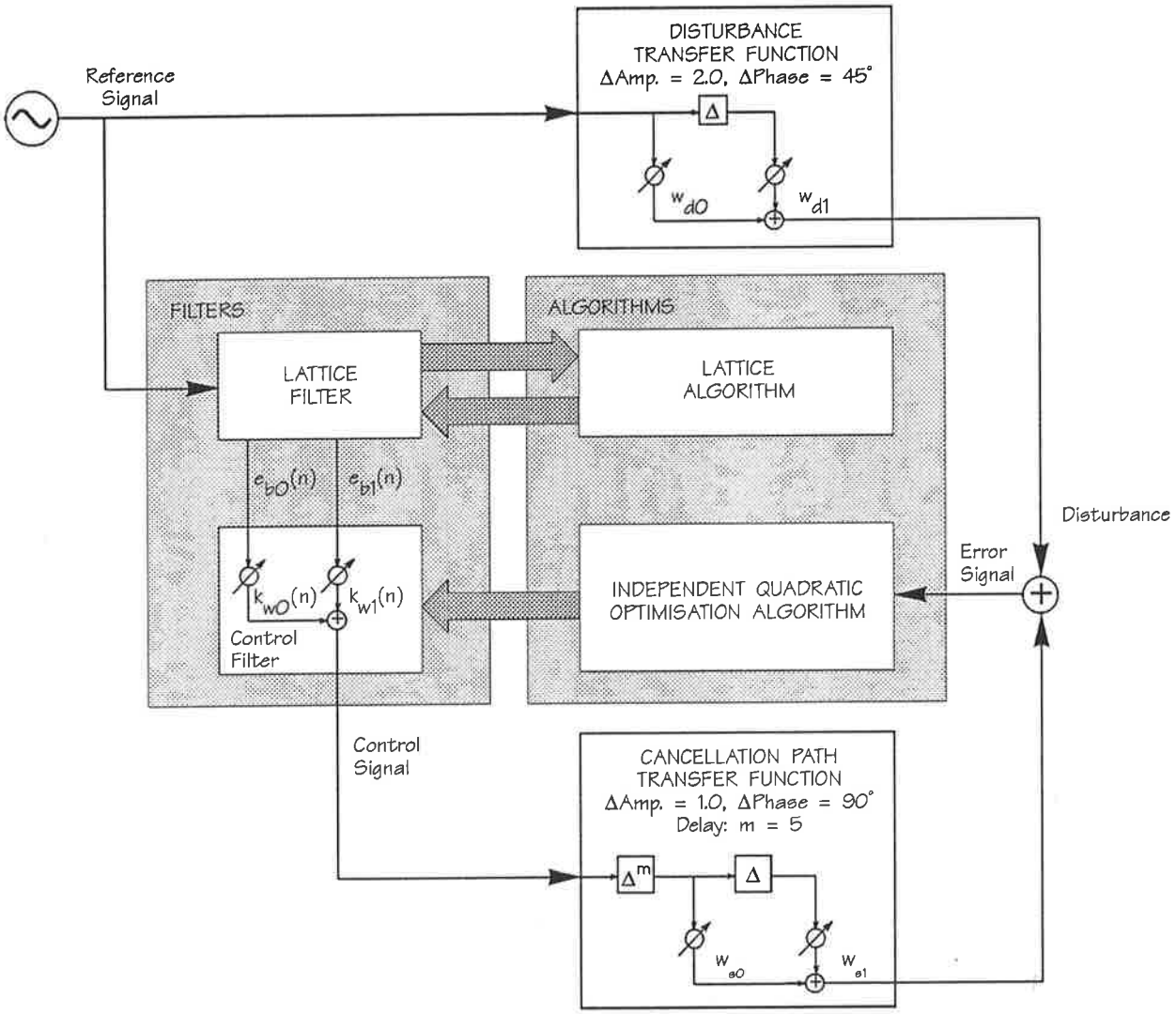

Figure 4-5. Transfer functions used to simulate an Active Noise and Vibration Control System. The disturbance transfer function represented by FIR filter coefficients, w_{d0}, w_{d1}, and the cancellation path transfer function is represented by FIR filter coefficients w_{s0}, w_{s1}. The lattice Filter generates orthogonal signals $e_{b0}(n)$, $e_{b1}(n)$, which are used in the control filter (linear combiner) with control coefficients $k_{w0}(n)$, $k_{w1}(n)$. Δ represents a single sample delay and Δ^m represents a delay of m samples.

The other parameters used for the simulation were arbitrarily chosen. The sampling ratio used was 20, the number of samples delay before averaging was 10, and the number of averages taken for the pure tone reference signal was 200, while for the white noise reference signal, with or without the pure tone component, the number of averages taken was 2000. There was no uncorrelated white noise in the error signal. The coefficients of the control filter (linear combiner), fed with orthogonal signals from the lattice filter, were initialised to zero.

4.4.1 Pure Tone Reference Signal

The power of the pure tone reference signal used was arbitrarily chosen as 0.5 (to give a unit amplitude sinusoidal wave). The control filter coefficient step size factor was arbitrarily chosen as 0.5 for control filter coefficient k_{w0}, and for control filter coefficient k_{w1} it was 1.5 since the magnitude of the backward prediction error signal corresponding to this coefficient was lower than the reference signal.

Figures 4-6 (a) to (c) show the path of the control filter coefficients to the minimum mean square error, projected onto the mean square error contour map, for various types of cancellation path transfer functions (ie. none, time delay, and phase change). As shown in the figures as well as theoretically in chapter 3, the control filter coefficients are independent for a pure tone despite the addition of a cancellation path transfer function (phase change or delay; Note that reference to a delay means a certain number of sampling period delays, whereas a phase change is a variable time

delay, as considered in chapter 3, sections 3.4.1 and 3.4.2 respectively). The Independent Quadratic Optimisation algorithm converges to the optimum without knowledge of the cancellation path transfer function. Upon reaching the optimum control filter coefficients, adaptation continues with the control filter coefficients adapted proportional to the mean square error at the optimum, to ensure minimum excess mean square error.

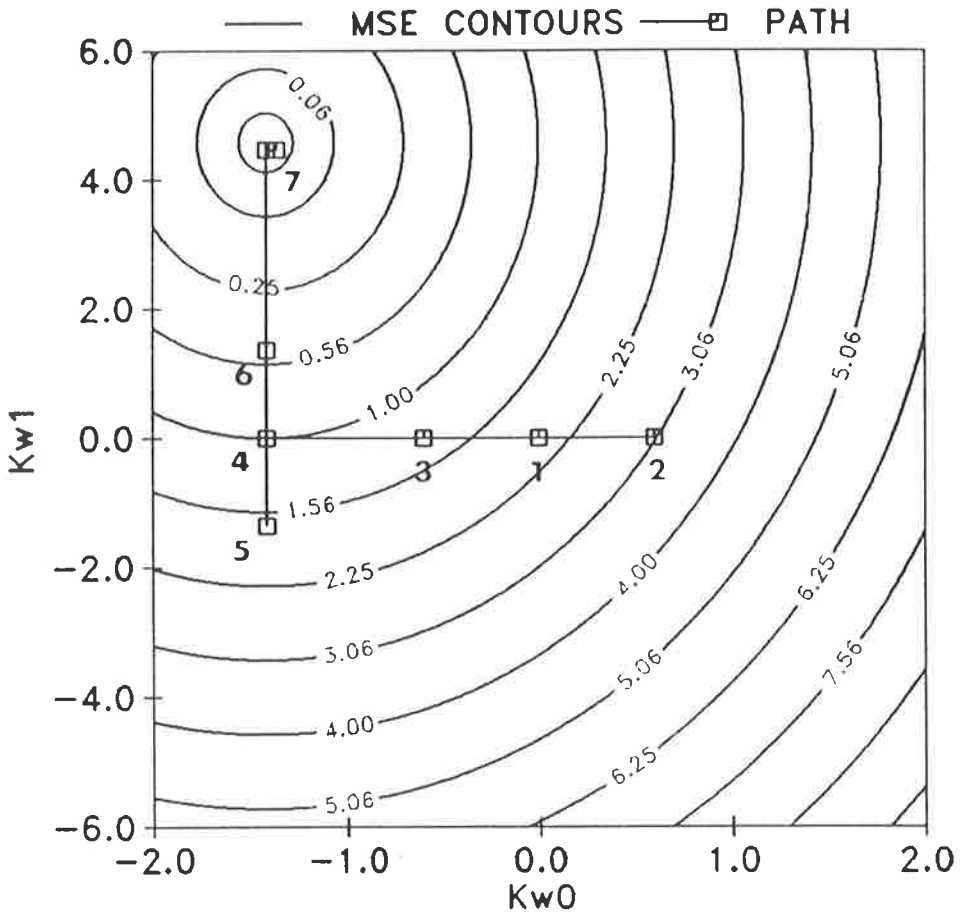

Figure 4-6(a). The paths of the control filter coefficients are shown numbered (with estimated cost function locations given by □) leading to the optimum of the cost function. The cost function contours are also shown as solid curved lines. The results in this figure are representative of no transfer function in the cancellation path.

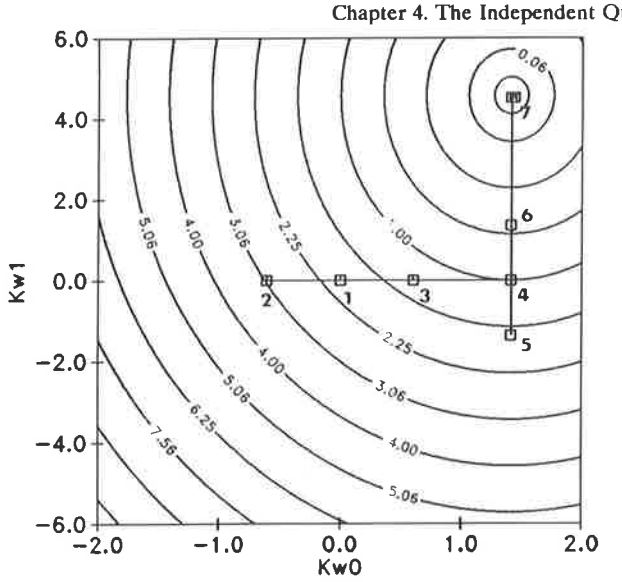

Figure 4-6(b). The paths of the control filter coefficients are shown numbered (with estimated cost function locations given by □) leading to the optimum of the cost function. The cost function contours are also shown as solid curved lines. The results in this figure are representative of a time delay in the cancellation path.

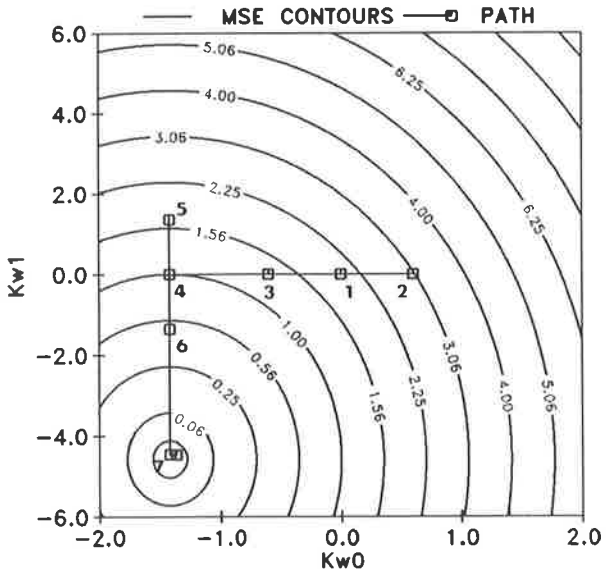

Figure 4-6(c). The paths of the control filter coefficients are shown numbered (with estimated cost function locations given by □) leading to the optimum of the cost function. The cost function contours are also shown as solid curved lines. The results in this figure are representative of a transfer function (phase change) in the cancellation path.

Figure 4-7 shows the convergence of the error signal magnitude for no transfer function in the cancellation path. As discussed, the excess mean square error at the optimum is dependent upon the number of averages taken and the control filter coefficient step size factor. Figure 4-8 shows the control filter coefficient adaptation for no transfer function in the cancellation path. Figures 4-7 and 4-8 illustrate the Independent Quadratic Optimisation algorithm, showing the step in each control filter coefficient (proportional to the mean square error) and corresponding change in the magnitude of the error signal. The error signal and control filter coefficient for the cases in which a transfer function (phase change or delay) exists in the cancellation path are very similar, and will therefore not be shown.

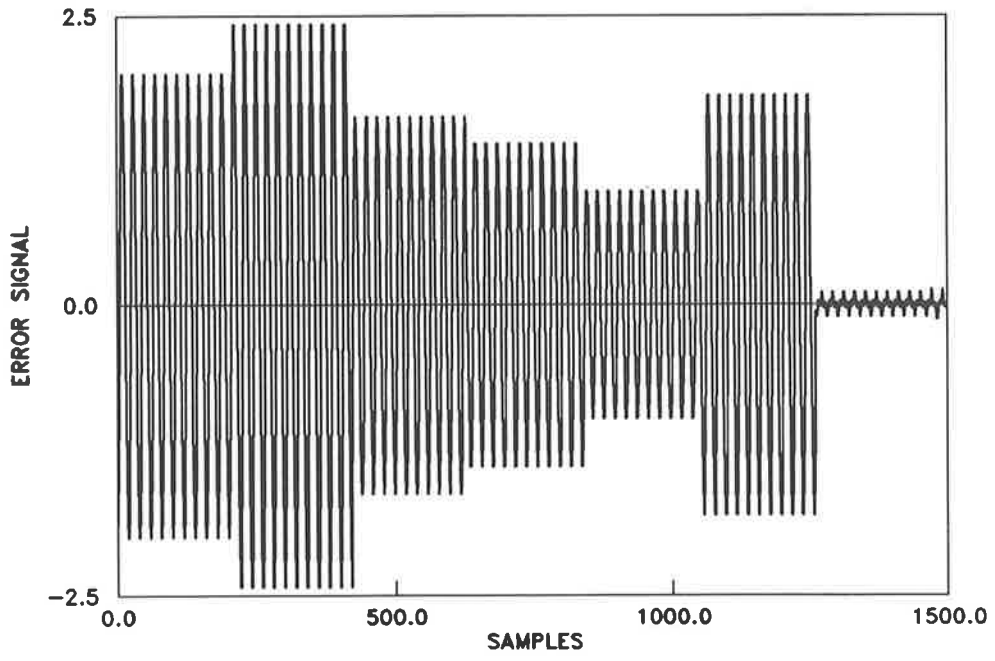

Figure 4-7. Error signal magnitude versus sample number, for no transfer function (phase change or delay) in the cancellation path.

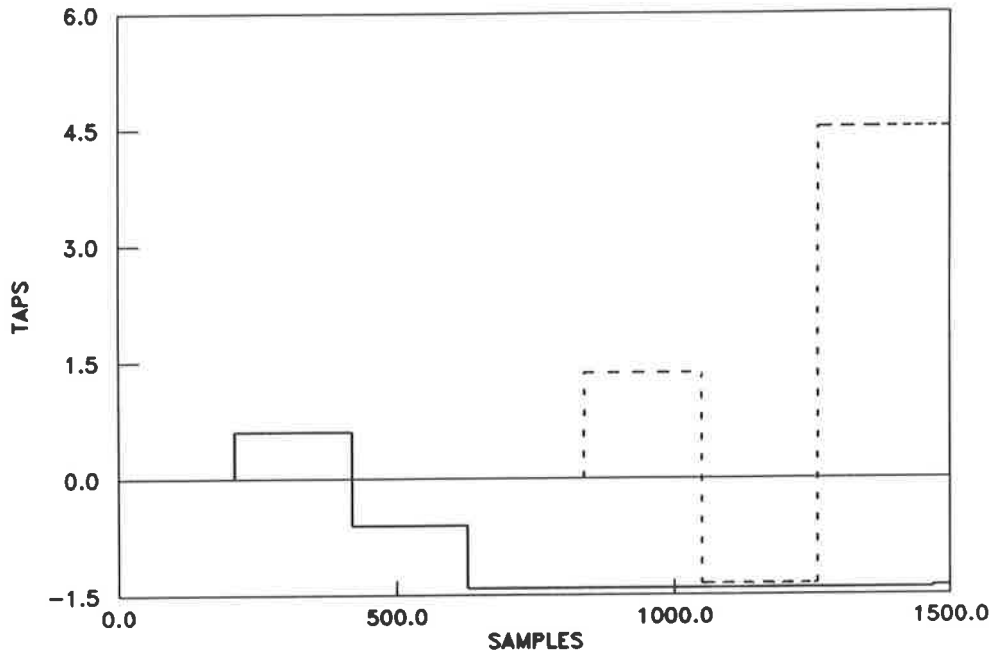

Figure 4-8. Control filter coefficient values versus sample number, for no transfer function (phase change or delay) in the cancellation path. The first control filter coefficient, $k_{w0}(n)$, is represented by —— while the second control filter coefficient, $k_{w1}(n)$, is represented by - - - .

4.4.2 White Noise Reference Signal

The power of the white noise reference signal used was chosen to be the same as was used for the sinusoidal signal 0.5. The control filter coefficient step size factor was arbitrarily chosen as 0.7 for both control filter coefficients k_{w0}, and k_{w1}, as both were of the same magnitude.

Figures 4-9 (a) to (c) show the path of the control filter coefficients to the optimum

mean square error, projected onto the mean square error contour map, for various types of cancellation path transfer functions (ie. none, time delay, and phase change). It should be noted that when white noise is passed through a lattice filter, no adaptation of the lattice filter's PARCOR coefficients are required as the white noise signal samples are already orthogonal, and therefore the lattice filter acts as a tapped-delay-line (or transversal filter); Refer to section 3.4.2.3 for further discussion.

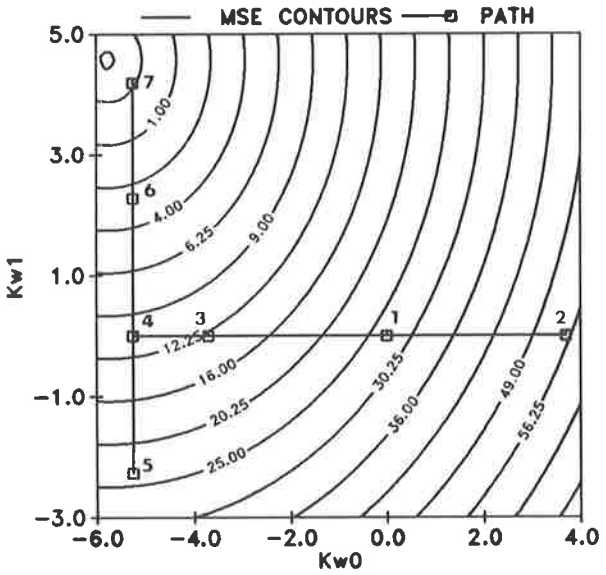

Figure 4-9(a). The paths of the control filter coefficients are shown numbered (with estimated cost function locations given by □) leading to the optimum of the cost function. The cost function contours are also shown as solid curved lines. The results in this figure are representative of no transfer function in the cancellation path.

Figure 4-9(a) corresponds to no transfer function in the cancellation path, and shows that the control filter coefficients are independent, and therefore the Independent Quadratic Optimisation algorithm adapts the control coefficients to reach the

optimum of the cost function in an efficient manner (as discussed in section 4.2). It is apparent that the absolute optimum is not immediately achieved; The attenuation achieved, or proximity to the optimum, will depend on the accuracy of the cost function estimates (ie. number of averages) and the step size factor.

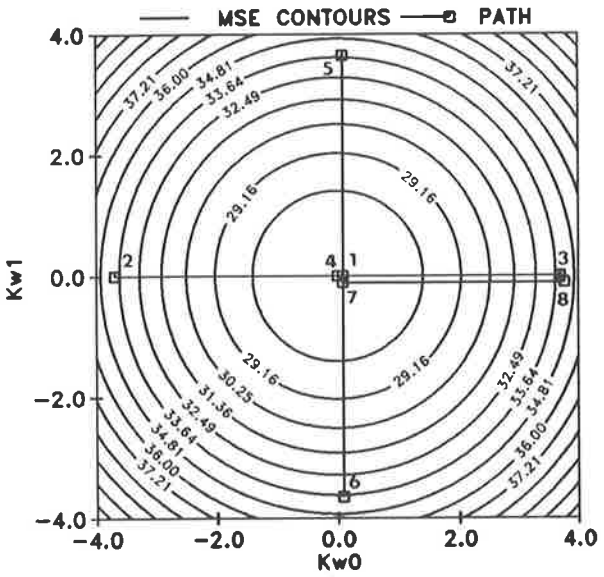

Figure 4-9(b). The paths of the control filter coefficients are shown numbered (with estimated cost function locations given by □) leading to the optimum of the cost function. The cost function contours are also shown as solid curved lines. The results in this figure are representative of a time delay in the cancellation path.

Figure 4-9(b) corresponds to a delay in the cancellation path. Since the delay of 5 in the cancellation path is greater than the number of coefficients within the control filter (linear combiner), the minimum mean square error is non-zero; That is, with only two control filter coefficients corresponding to a time delayed white noise reference signal (since the backward prediction error signals are delayed samples of

the white noise signal, which are orthogonal by definition), it is impossible to generate a control signal delayed by more than two samples, therefore resulting in a non-zero minimum mean square error. As the optimum mean square error is non-zero, the control filter coefficients have large deviations about their optimum values (since the step size factor is proportional to the last cost function estimate), as shown in Figure 4-9(b). Further, the optimal control filter coefficients for a delay of this magnitude are zero (since any cancellation is impossible), and since the control filter coefficients are initialised to zero, they are already at the optimum. Evidence of the independence of control filter coefficients can be seen from Figure 4-9(b), despite the delay in the cancellation path.

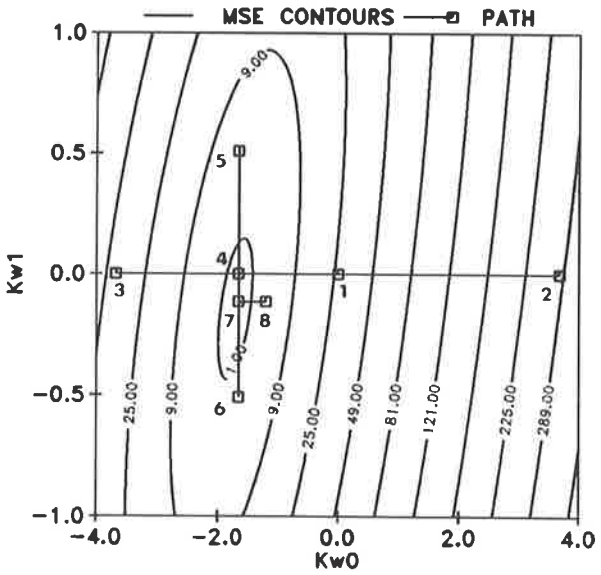

Figure 4-9(c). The paths of the control filter coefficients are shown numbered (with estimated cost function locations given by □) leading to the optimum of the cost function. The cost function contours are also shown as solid curved lines. The results in this figure are representative of a transfer function (phase change) in the cancellation path.

As shown in chapter 3, and evident in Figure 4-9(c) which corresponds to a transfer function in the cancellation path, the control filter coefficients lose their independence upon the inclusion of a cancellation path transfer function. However, the Independent Quadratic Optimisation algorithm converges to the optimum without knowledge of the cancellation path transfer function, and only it's speed (or efficiency) are impaired; This effect will be discussed further in section 4.5.

Figures 4-10 (a) and (b) show the convergence of the error signal magnitude. A near zero minimum mean square error is clearly found for the case for which there is no transfer function in the cancellation path, Figure 4-10(a), with a similar signal variance characteristic also found for the case of a transfer function in the cancellation path. As discussed, the minimum mean square error obtained for these cases is dependent upon the number of averages of the cost function, and the control filter coefficient step size factor. However results shown in Figure 4-10(b), for the case with a delay in the cancellation path, show that a near zero optimum cannot be reached, as discussed. In both figures, steps are apparent in the error signals corresponding to changes in the control filter coefficients.

Figure 4-11 (a) and (b) show the control filter coefficient variation for the case of no transfer function, and the case of a time delay in the cancellation path, respectively. From Figure 4-11(b) it is apparent that the control filter coefficients return to their original, optimal values as discussed, while those shown in Figure 4-11(a) are altered to their optimal values (results are similar for a transfer function in the cancellation path).

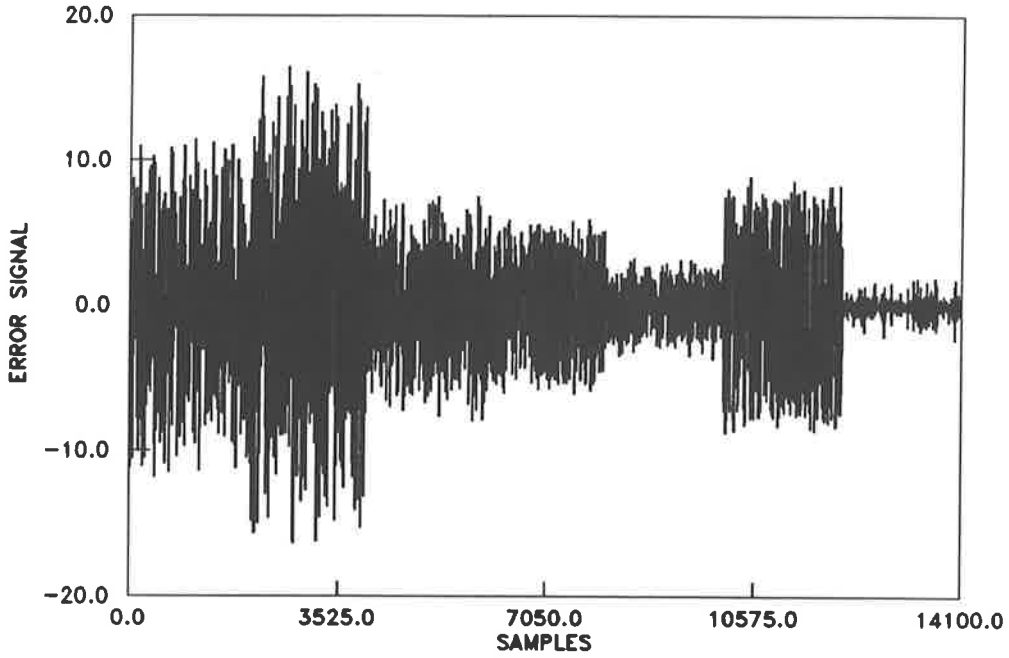

Figure 4-10(a). Error signal magnitude versus sample number, for no transfer function (phase change or delay) in the cancellation path.

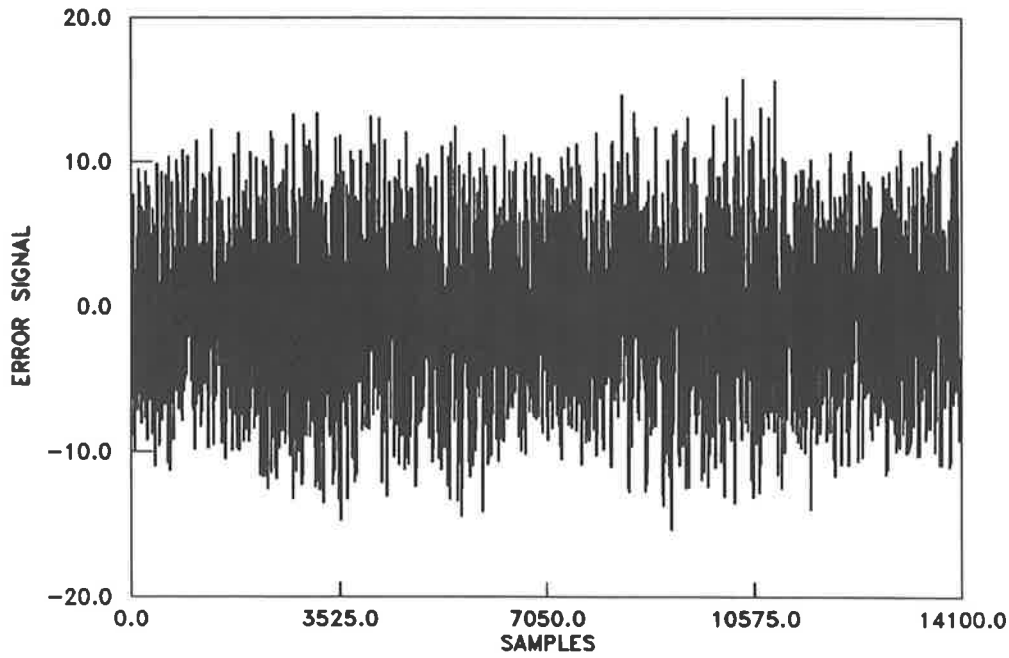

Figure 4-10(b). Error signal magnitude versus sample number, for a delay in the cancellation path.

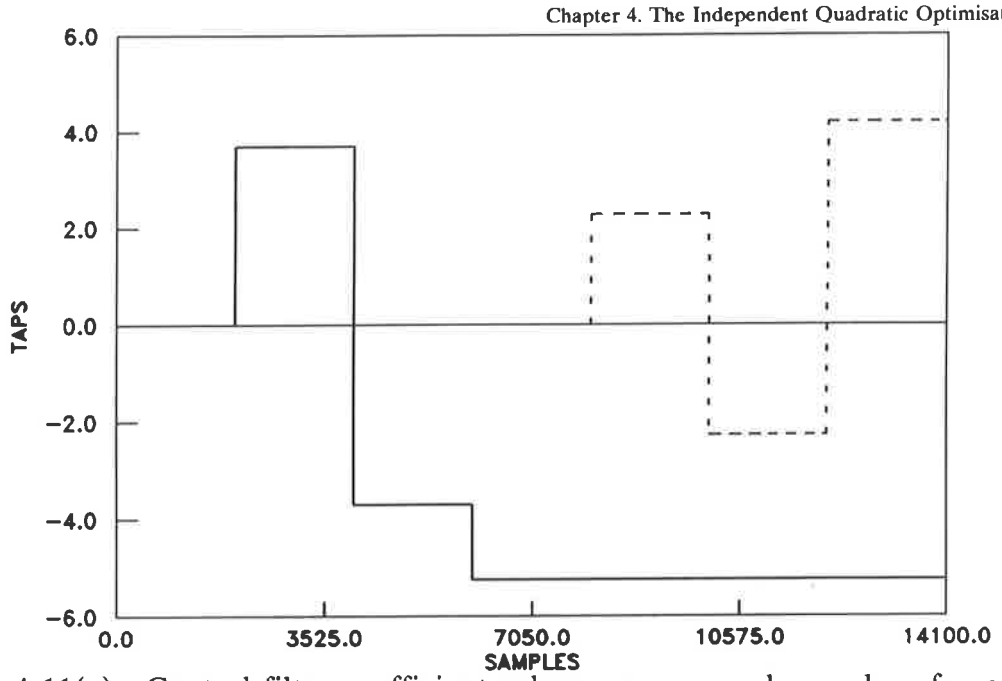

Figure 4-11(a). Control filter coefficient values versus sample number, for no transfer function (phase change or delay) in the cancellation path. The first control filter coefficient, $k_{w0}(n)$, is represented by —— while the second control filter coefficient, $k_{w1}(n)$, is represented by - - -.

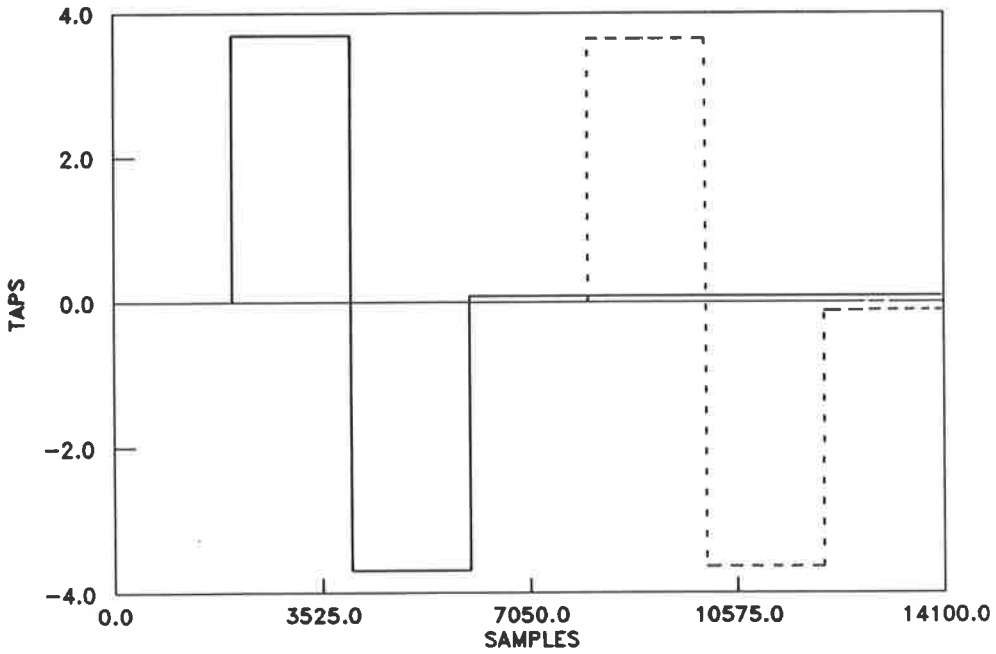

Figure 4-11(b). Control filter coefficient values versus sample number, for a delay in the cancellation path. The first control filter coefficient, $k_{w0}(n)$, is represented by —— while the second control filter coefficient, $k_{w1}(n)$, is represented by - - -.

4.4.3 Pure Tone with White Noise Reference Signal

The power of the pure tone used was 0.5 (as this has been used previously), while that for the white noise signal was arbitrarily chosen as 0.1, giving a form of "signal to noise ratio" of 7 dB. The control filter coefficient step size factor for the first control filter coefficient, k_{w0}, was arbitrarily chosen as 0.7 while for the second control coefficient, k_{w1}, it was 1.0 as the magnitude of the backward prediction error corresponding to this coefficient was lower.

Figures 4-12 (a) to (c) show the path of the control filter coefficients to the optimum mean square error, projected onto the mean square error contour map, for the various types of cancellation path transfer functions (ie. none, time delay, and phase change). As shown theoretically in chapter 3, the control filter coefficients lose their independence at the inclusion of a transfer function in the cancellation path, as apparent in Figure 4-12(c), but remain independent without a transfer function and despite the inclusion of a delay in the cancellation path, as apparent in Figures 4-12 (a) and (b). In all cases the Independent Quadratic Optimisation algorithm converges to the optimum of the cost function without knowledge of the delay or the transfer function. Upon reaching the optimal control coefficient values, the excess mean square error is minimised by adjusting the control filter coefficients proportional to the optimum mean square error. As already discussed, the effects of a transfer function in the cancellation path impair only the speed (or efficiency) of the Independent Quadratic Optimisation algorithm, as the control filter coefficients are not exactly independent; This will be discussed further in section 4.5.

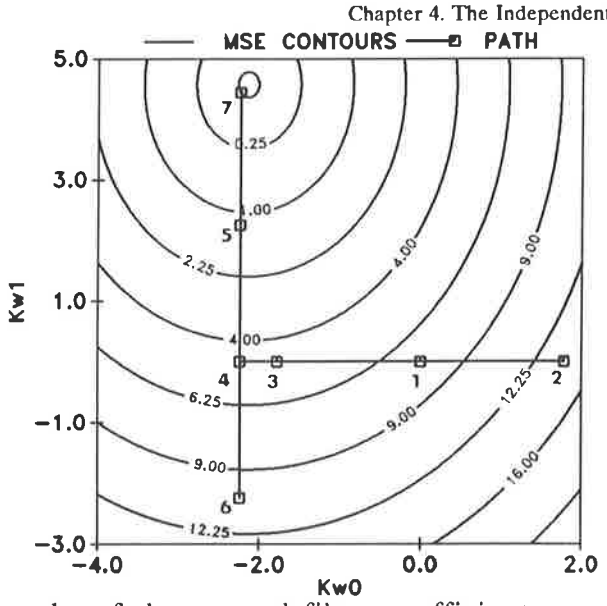

Figure 4-12(a). The paths of the control filter coefficients are shown numbered (with estimated cost function locations given by □) leading to the optimum of the cost function. The cost function contours are also shown as solid curved lines. The results in this figure are representative of no transfer function in the cancellation path.

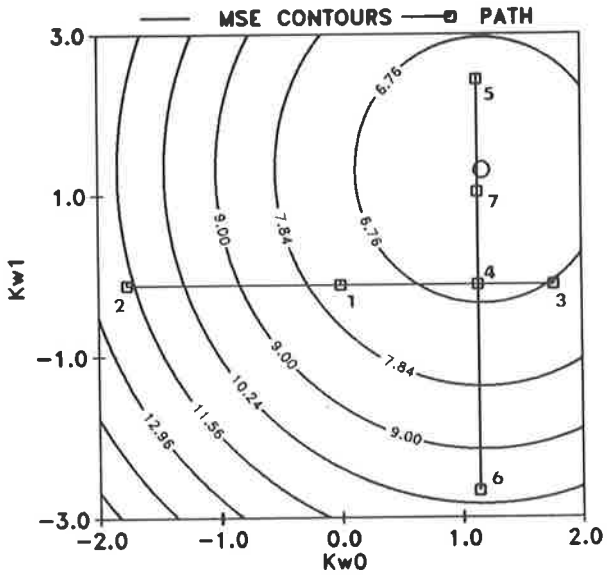

Figure 4-12(b). The paths of the control filter coefficients are shown numbered (with estimated cost function locations given by □) leading to the optimum of the cost function. The cost function contours are also shown as solid curved lines. The results in this figure are representative of a time delay in the cancellation path.

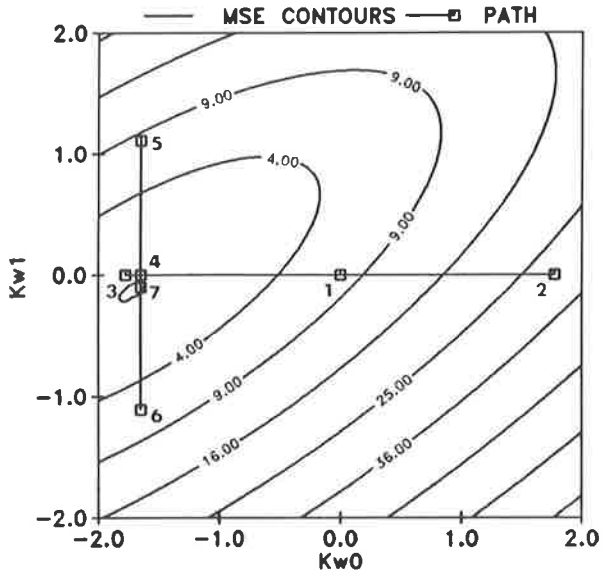

Figure 4-12(c). The paths of the control filter coefficients are shown numbered (with estimated cost function locations given by □) leading to the optimum of the cost function. The cost function contours are also shown as solid curved lines. The results in this figure are representative of a transfer function (phase change) in the cancellation path.

Figures 4-13 (a) to (c) show the convergence of the error signal for the various types of cancellation path transfer functions. As discussed, the minimum mean square error is dependent upon the number of averages taken and the control filter coefficient step size factor. The minimum mean square error is non-zero with a transfer function (delay or phase change) in the cancellation path, as evident by Figures 4-13(b) and (c), and Figures 4-12(b) and (c). The mean square error is non-zero for a delay of 5 in the cancellation path, since this delay means that the white noise cannot be cancelled by the two coefficient control filter (linear combiner), as discussed in the last section. The mean square error is non-zero for an arbitrary phase change in the

cancellation path, since whilst there will be optimal control coefficients for the white noise component, these optimal control coefficients will be different for the tonal component (since the tone is orthogonalised by the lattice filter), with the resulting coefficients an average of the optimal coefficients for the signals considered in isolation.

Figure 4-14 shows the typical convergence characteristics of the control filter coefficients to the optimum for the case of no transfer function in the cancellation path; Step changes in the control filter coefficients are evident, as is a period in which all coefficients remain fixed while the cost function is estimated. The characteristics with a transfer function (whether a pure delay or phase change) in the cancellation path are very similar to those shown in Figure 4-14.

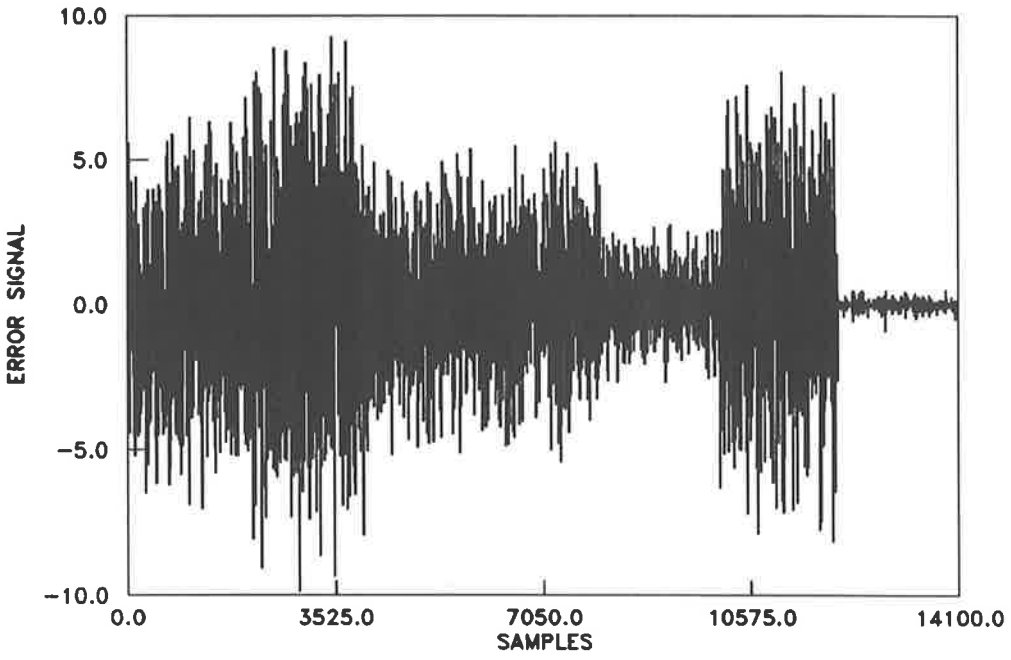

Figure 4-13(a). Error signal magnitude versus sample number, for no transfer function (phase change or delay) in the cancellation path.

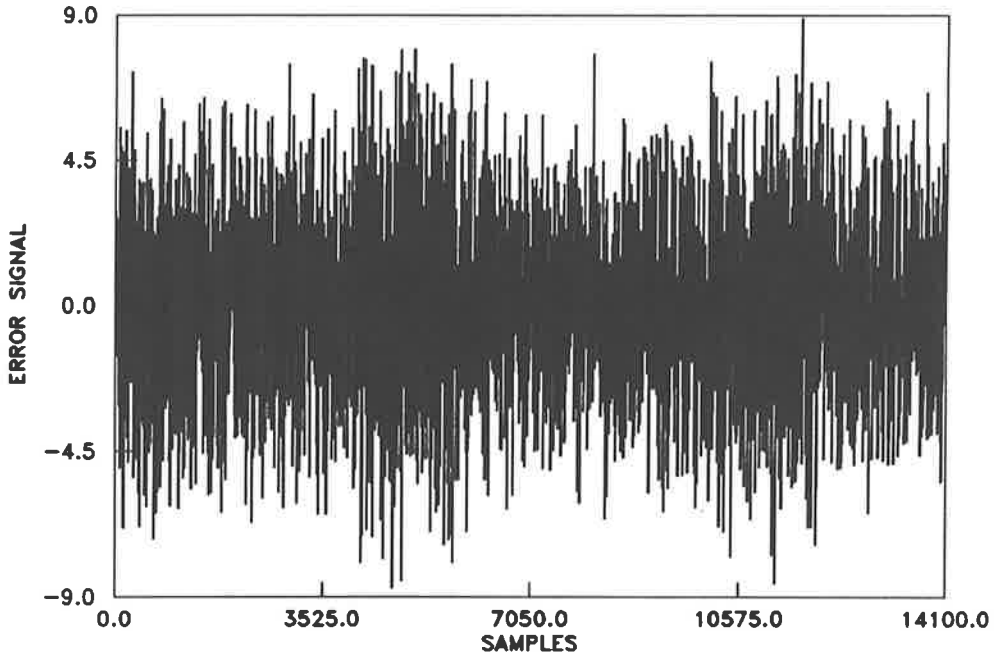

Figure 4-13(b). Error signal magnitude versus sample number, for a delay in the cancellation path.

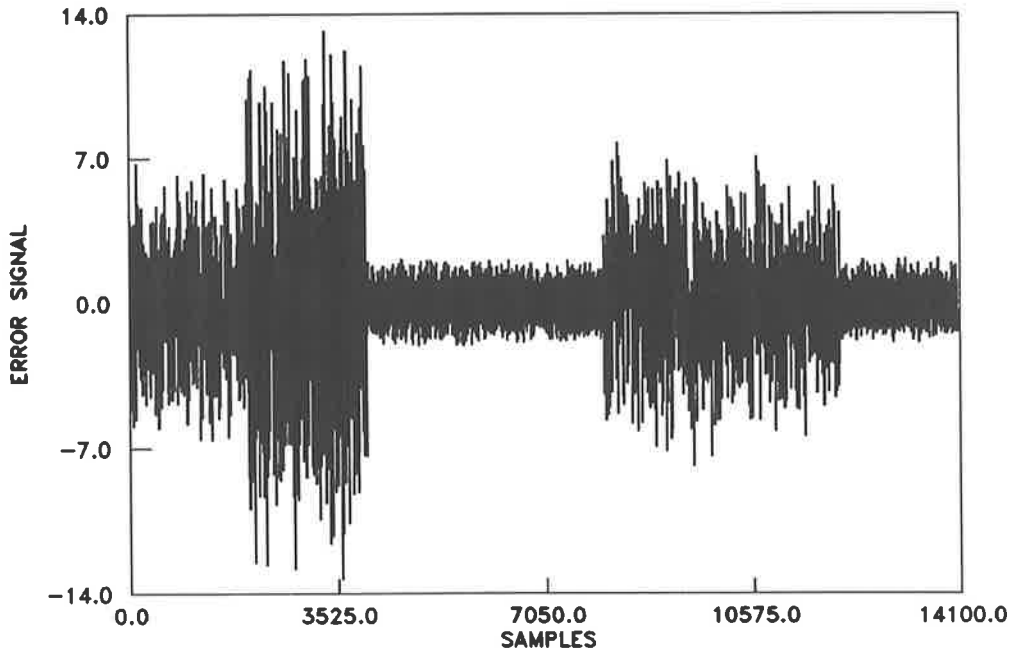

Figure 4-13(c). Error signal magnitude versus sample number, for a transfer function (phase change) in the cancellation path.

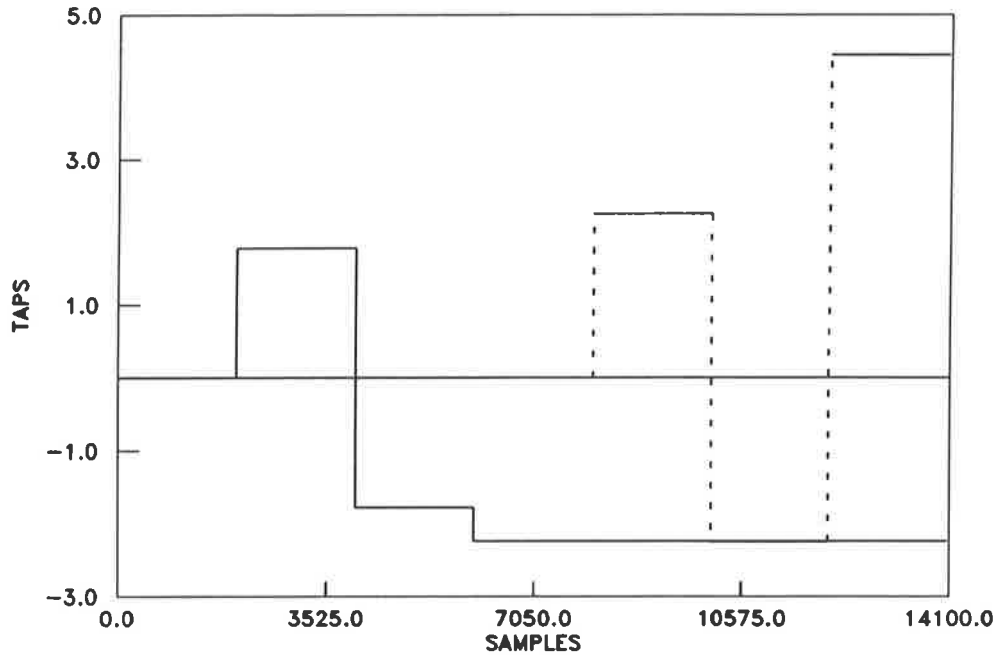

Figure 4-14. Control filter coefficient values versus sample number, for no transfer function (phase change or delay) in the cancellation path. The first control filter coefficient, $k_{w0}(n)$, is represented by —— while the second control filter coefficient, $k_{w1}(n)$, is represented by - - -.

4.4.4 Summary

It has been shown by simulation that the Independent Quadratic Optimisation algorithm enables stable minimisation of the mean square error cost function as it does not require knowledge of the cancellation path transfer function. It has however been shown that with a general transfer function (ie. not a pure time delay but an arbitrary phase change) in the cancellation path the control coefficients lose their independence for all but pure tones. The effects of the number of averages used to estimate the cost function, and the step size factor, on the achievable minimum mean

square error were discussed. When the disturbance consists of white noise in addition to a pure tone, the white noise reduces the efficiency of the Independent Quadratic optimisation algorithm, as the control filter coefficients lose their independence thereby reducing the speed at which the minimum achievable mean square error is achieved. It was also observed that when the delay in the cancellation path transfer function exceeds the number of control filter coefficients, attenuation is impossible for a white noise disturbance. Finally it should be noted that as the step size factor is combined with the cost function estimate to update the control filter coefficients, the excess mean square error will depend on both the minimum achievable mean square error and the magnitude of the step size factor (which ultimately is adjusted depending on the degree of curvature in the direction of each control filter coefficient).

It must be emphasised that the simulations that the cancellation path transfer function reduces the speed (or efficiency), but not stability, of the Independent Quadratic Optimisation algorithm obtaining the optimum control coefficients, but does not affect the stability of the algorithm. This limitation of the Independent Quadratic Optimisation algorithm will be discussed in the next section.

4.5 Limitation

Chapter 3 discussed the generation of orthogonal signals and their combination with a control filter to enable each control filter coefficient to be adapted independently of

one another. Chapter 3 also showed theoretically, the effect of a transfer function (either a pure delay or a more general form of finite impulse response) on the independence of the control filter coefficients. The Independent Quadratic Optimisation algorithm was conceptualised in chapter 2 and formally defined in the beginning of this chapter. The simulation results from the previous section confirm the results from the theory of chapter 3. This section will summarise the key limitation to the Independent Quadratic Optimisation algorithm and suggests means of overcoming it. In doing so, an alternative formulation of the Independent Quadratic Optimisation algorithm was discovered (discussed in section 4.6), being very similar to Newton's Method for finding the zeroes of a function. The alternative formulation leads to a theoretical definition (discussed in section 4.7) of the heuristic interpretation, made in section 4.3, for the manner in which the parameters of the Independent Quadratic Optimisation algorithm affect its performance (ie. minimum achievable mean square error, excess mean square error and convergence time and stability).

It was shown in section 4.2 that if the cost function could be written as (equation (4-7) repeated here for clarity)

$$J(n) = J_{opt} + \sum_{i=0}^{N-1} j_{bi}(k_{wi}(n) - k_{wi_{opt}})^2 \qquad [4\text{-}15]$$

then the control filter coefficients could be adapted independently using the Independent Quadratic Optimisation algorithm. It was shown in chapter 3 (section 3.4.2) that when a transfer function is included in the cancellation path, the cost function for a control signal generated from orthogonal signals becomes (equation (3-

41) repeated here for clarity, with section 3.4.2 defining all terms in the equation):

$$J(n) = R_{11}^{p} + 2K_{wN}^{T}(n)C_{N}^{pe_b \otimes w_s} + K_{wN}^{T}(n)R_{NN}^{e_b \otimes w_s}K_{wN}(n) \qquad [4\text{-}16]$$

The conversion to the form of equation (4-15) dependent on the condition for independence of the control filter coefficients, K_{wN}, given by (as discussed in chapter 3, section 3.4.2, with equation (3-46) repeated here for clarity)

$$E[\, e_{bu}(n)e_{bv}(n-m) + e_{bu}(n-m)e_{bv}(n) \,] = 0 \qquad [4\text{-}17]$$

where $u \neq v$ $u,v = 0,\ldots,N-1$, and $m = 0,\ldots,N_s-1$ with N_s the number of coefficients defining the cancellation path transfer function. It was shown in chapter 3, that the independence condition will only hold for a pure tone. This has also been shown from the simulation results of the section 4.4. If the independence condition is not satisfied, the path that the control filter coefficients take to the optimum of the cost function (through adaptation by the Independent Quadratic Optimisation algorithm) will be slower, as more estimates and quadratic fits are required for each control filter coefficient. However, regardless of whether the independence condition is satisfied, the Independent Quadratic Optimisation algorithm will still converge in a stable manner, to the optimum of the cost function without knowledge of the cancellation path transfer function. The speed of convergence will depend upon the non-zero value of the expectation given by equation (4-17), that is, the degree of independence of the control filter coefficients.

As the Independent Quadratic Optimisation algorithm converges ideally for pure tones only, it leads to the notion of considering in isolation each individual harmonic with and without a 90° change of phase (ie. The orthogonal components of each harmonic). This is a natural extension of the Independent Quadratic Optimisation

concept, that has been published originally by Gibbs et al [1993] and Kewley et al [1995]. The algorithm for independent control filter coefficient optimisation used by these authors was derived from Newton's Method, but it is however similar to that developed in this thesis, as will be shown in the next section.

4.6 Alternative Formulation

In this section the Independent Quadratic Optimisation algorithm will be shown to be similar to Newton's Method. Newton's Method is a method used for finding the zeroes of a function ie. $f(w) = 0$ [Widrow and Stearns, 1985]. A zero is found by recursively adjusting the coefficient w_i, to w_{i+1}, that is the point on the abscissa that intersects the line defined by the gradient of $f(w)$ at w_i, and the point $f(w_i)$. This type of adaptation when used to find the zero of a function is shown in Figure 4-15, where it can seen that

$$\frac{df(w)}{dw} = f'(w_m) = \frac{f(w_m)}{w_m - w_{m+1}} \qquad [4\text{-}18]$$

and hence the updated coefficient, w_{m+1}, can be written as

$$w_{m+1} = w_m - \frac{f(w_m)}{f'(w_m)} \qquad [4\text{-}19]$$

In estimating the minimum of a cost function such as the mean square error, the requirement is for $f(w) = J' = 0$. Thus each coefficient, w_m, is updated based on the substitution of $f(w_m) = J'|_{w_m}$ and $f'(w_m) = J''|_{w_m}$ into equation (4-19), such that

$$w_{m+1} = w_m - \frac{J'|_{w_m}}{J''|_{w_m}} \qquad [4\text{-}20]$$

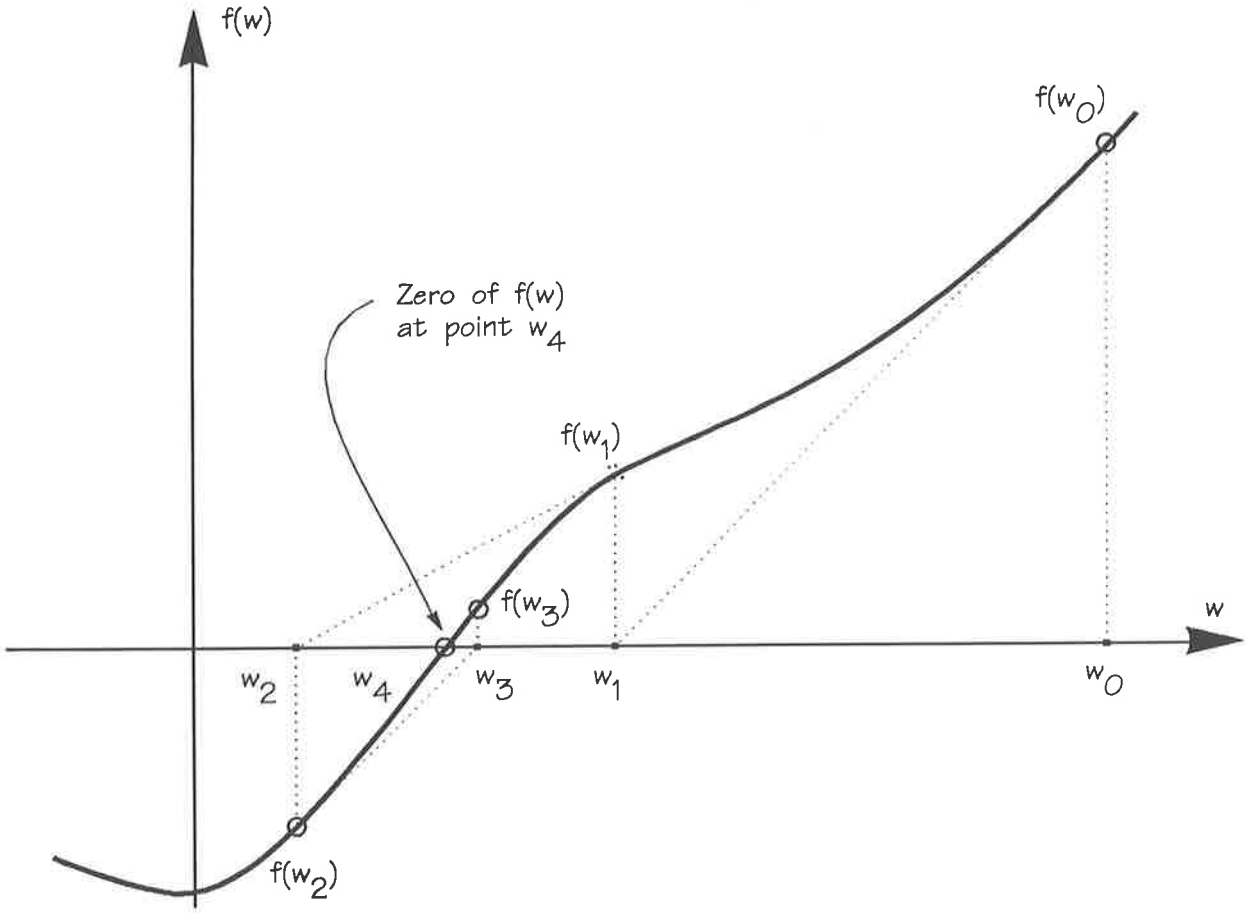

Figure 4-15. Newton's Method of optimisation used to find the zero of a function, $f(w)$. The zero of $f(w)$ is found by starting at w_0, and updating the coefficient w (points w_1, w_2, w_3 and w_w) until the zero of $f(w)$ is found at point w_4.

The gradient and the second derivative of the cost function can be estimated by the central difference theorem [Widrow, B. and Stearns, S.D., 1985; Kewley, D.L. et al, 1995], using estimates of the cost function, such that

$$\hat{J}'\big|_{w_m} = \frac{\hat{J}\big|_{(w_m + \Delta w_m)} - \hat{J}\big|_{(w_m - \Delta w_m)}}{2\Delta w_m} \qquad [4\text{-}21]$$

and

$$\hat{J}''\big|_{w_m} = \frac{\hat{J}\big|_{(w_m - \Delta w_m)} - 2\hat{J}\big|_{w_m} + \hat{j}\big|_{(w_m + \Delta w_m)}}{(\Delta w_m)^2} \qquad [4\text{-}22]$$

Hence, after substituting (4-21) and (4-22) into (4-20), and for clarity using

$$\begin{aligned} \hat{J}_{pos} &= \hat{J}\big|_{(w_m + \Delta w_m)} \\ \hat{J}_{neg} &= \hat{J}\big|_{(w_m - \Delta w_m)} \\ \hat{J}_{cen} &= \hat{J}\big|_{w_m} \end{aligned} \qquad [4\text{-}23a,b,c]$$

results in the control coefficient update equation (4-20) becoming

$$w_{m+1} = \frac{(2w_m - \Delta w_m)\hat{J}_{pos} - (4w_m)\hat{J}_{cen} + (2w_m + \Delta w_m)\hat{J}_{neg}}{2[\hat{J}_{pos} - 2\hat{J}_{cen} + \hat{J}_{neg}]} \qquad [4\text{-}24]$$

This can be compared with the optimal control filter coefficient defined by equation (4-13) in section 4.3 for the Independent Quadratic Optimisation algorithm, where the optimal control filter coefficients are determined by fitting three estimates of the cost function to a quadratic function. On the other hand , Newton's Method is based on a gradient search of the cost function, in which the control coefficients are adapted until a gradient of zero is found. It will now be shown that equation (4-24) is equivalent to equation (4-13). Equation (4-13) is shown below for ease of reference.

$$k_{wi_{opt}} = \frac{1}{2}\frac{\hat{J}_{i_0}(k_{wi_1}^2 - k_{wi_2}^2) + \hat{J}_{i_1}(k_{wi_2}^2 - k_{wi_0}^2) + \hat{J}_{i_2}(k_{wi_0}^2 - k_{wi_1}^2)}{\hat{J}_{i_0}(k_{wi_1} - k_{wi_2}) + \hat{J}_{i_1}(k_{wi_2} - k_{wi_0}) + \hat{J}_{i_2}(k_{wi_0} - k_{wi_1})} \qquad [4\text{-}25]$$

Consider the following substitutions for the variables used in equation (4-13,25)

$$\begin{aligned} k_{wi_2} &= w_m + \Delta w_m \quad with \quad \hat{J}_{i2} = \hat{J}_{pos} = \hat{J}\big|_{(w_m + \Delta w_m)} \\ k_{wi_0} &= w_m - \Delta w_m \quad with \quad \hat{J}_{i0} = \hat{J}_{neg} = \hat{J}\big|_{(w_m - \Delta w_m)} \\ k_{wi_1} &= w_m \quad with \quad \hat{J}_{i1} = \hat{J}_{cen} = \hat{J}\big|_{w_m} \end{aligned} \qquad [4\text{-}26a,b,c]$$

with

$$k_{wi_{opt}} = w_{m+1} \qquad [4\text{-}27]$$

gives

$$w_{m+1} = \frac{1}{2}\left[\frac{(2w_m - \Delta w_m)\hat{j}_{pos} - (4w_m)\hat{j}_{cen} + (2w_m + \Delta w_m)\hat{j}_{neg}}{\hat{j}_{pos} - 2\hat{j}_{cen} + \hat{j}_{neg}}\right] \qquad [4\text{-}28]$$

which is equal to equation (4-24), thus showing that Newton's Method, when used to find the minimum of a quadratic function, is equivalent to using three estimates of the cost function to find the minimum of a parabola formed by these points. If the cost function is not parabolic (ie. if the optimum cannot be found in one cycle) then the cycle continues, until the shape of the cost function approximates that of a parabola. This is shown in Figure 4-16.

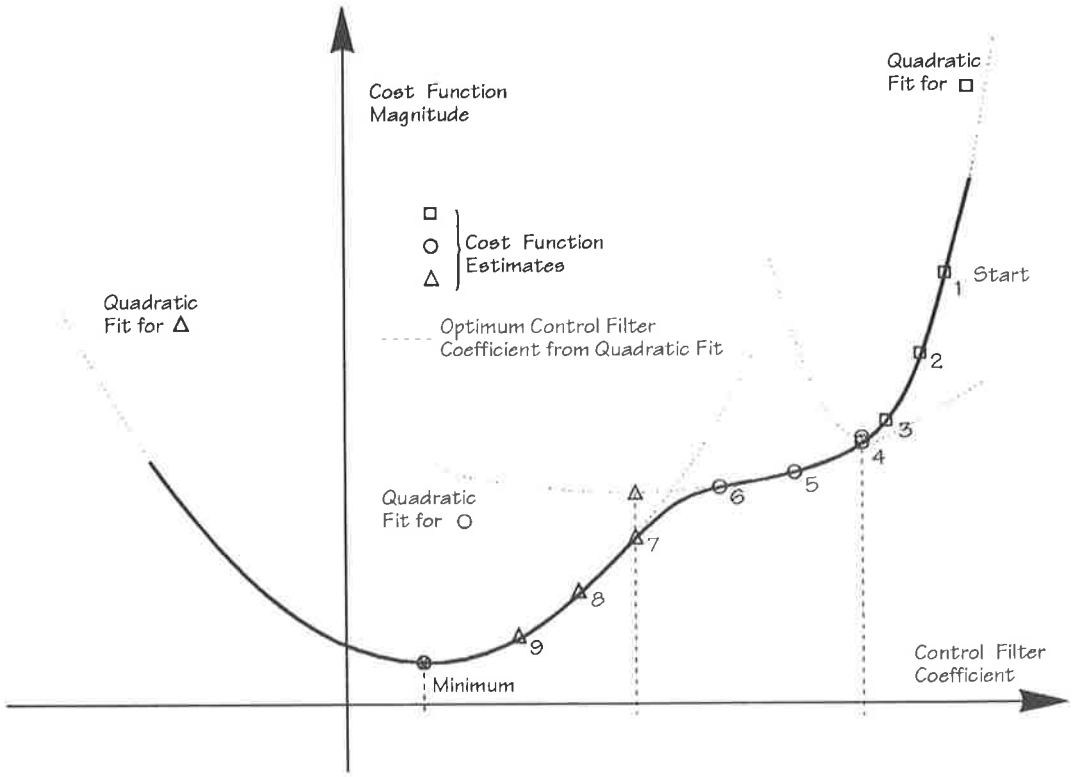

Figure 4-16. Newton's Method as a form of Quadratic Curve Fitting. Quadratic fits to estimates (numbered from start) made as per the Independent Quadratic Optimisation algorithm are shown, leading to the minimum of the cost function.

This is a very interesting result, and suggests that the performance of the Independent Quadratic Optimisation algorithm derived in section 4.3 on a quadratic curve-fit basis using independent control filter coefficients, can be described by considering the discrete estimate form of Newton's Method already analysed by Widrow and Stearns [1985]. The discrete estimate form of Newton's Method will be considered in the next section, to confirm the heuristic comments made in section 4.3, regarding the parameters affecting the Independent Quadratic Optimisation algorithm's performance.

4.7 Performance Analysis

In this section, the analysis by Widrow and Stearns [1985] will be used to confirm the heuristic interpretation (made in section 4.3) of the Independent Quadratic Optimisation algorithm. To simplify this analysis, a constant control filter coefficient step size factor will be used, such that a constant step size in the control filter coefficients can be defined as

$$\delta = (k_{wi_1} - k_{wi_0}) = (k_{wi_2} - k_{wi_1}) \qquad [4\text{-}29]$$

Widrow and Stearns [1985] define the "performance penalty", γ, as the error in estimating J_{cen} from J_{pos} and J_{neg} such that

$$\gamma = \frac{1}{2}(j_{neg} + j_{pos}) - j_{cen} \qquad [4\text{-}30]$$

The "performance penalty" gives the average increase in the cost function from perturbations (or constant deviations) in the control filter coefficients; That is, the

greater the "performance penalty" the better the lesser the achievable mean square error, however the improved performance (in terms of minimum achievable mean square error) comes with a penalty as at the optimum the excess mean square error or variance about the optimum will be greater. An intuitive interpretation of the "performance penalty" comes after substituting the cost function for a single control filter coefficient k_{wi} (defined by equation (4-7)), with equation (4-30) now written as

$$\gamma = j_{bi}\delta^2 \qquad [4\text{-}31]$$

Hence the "performance penalty" incorporates the effects discussed in section 4.3, namely the degree of curvature (described by j_{bi}) and the step size (described by δ), and is not dependent upon the particular value of the control filter coefficient. As discussed in section 4-3 (and shown in Figure 4-4), the higher the curvature, the lower the step size needs to be to obtain an accurate curve fit and therefore optimum control coefficient estimate. This will be shown in theory shortly. The "performance penalty" can be normalised using the minimum of the cost function such that the "perturbation" can defined as [Widrow and Stearns, 1985]

$$P = \frac{\gamma}{J_{opt}} = \frac{j_{bi}\delta^2}{J_{opt}} \qquad [4\text{-}32]$$

and when multiple coefficients (total N) are considered this becomes

$$P = \frac{\bar{j}_{bi}\delta^2}{J_{opt}} \qquad [4\text{-}33]$$

with $\bar{j}_{bi} = \frac{1}{N}\sum_{i=0}^{N-1} j_{bi}$. The physical significance of the "perturbation" will become more apparent later in this section. It will be shown to affect the excess mean square error.

Widrow and Stearns [1985] show that the variance of the estimates of the cost function can be given by

$$var[\hat{J}_m] = \frac{KJ_m}{M} = \sigma_{J_m} \qquad [4\text{-}34]$$

where K is a constant dependent upon the probability distribution of samples of the cost function, M is the number of averages and J_m (with m the estimate number) is the mean of the probability distribution (ie. the actual value of the cost function). For an acoustic error signal $J = E[e^2(n)]$, and since $e(n)$ has a zero mean (providing DC offsets are cancelled in ADC's, amplifiers etc.) and a likely Gaussian (or normal) distribution, K will equal 2.0. Thus from equation (4-34), for the same number of averages, M, the variance in the cost function estimate, σ_{J_m}, is likely to be greater for higher values of the cost function, J_m. It is also apparent from equation (4-34) that for a large number of averages, M, the variance in the cost function estimate is reduced and hence it would be expected that the variance of the cost function about the optimum would also be reduced (since a more accurate curve-fit results); This will become more apparent with the definition of the misadjustment.

Widrow and Stearns [1985] show that the misadjustment (a dimensionless measure of the performance of an adaptive process in terms of the variance of the cost function, or mean square error about the optimum once adaptation has reached steady state) is given by (with $\triangleq$ meaning defined as)

$$misadjustment \triangleq \frac{N\,\bar{j}_{bi}\,\overline{(1/j_{bi})}}{8MP} = \frac{N\,J_{opt}\,\overline{(1/j_{bi})}}{8M\,\delta^2} \qquad [4\text{-}35]$$

This equation could also have been derived by considering the effect of the cost function variance on the optimum control filter coefficient value given by equation (4-13).

From equation (4-35) it is apparent that:

- Larger values of the perturbation, P, (associated with step size and degree of curvature) result in reduced misadjustment (and therefore a more accurate curve-fit) and increased performance. However a large perturbation can result from a large step size, and therefore an increased possibility of creating an overflow of the control filter coefficients and thereby control actuators. A large perturbation can also be a result of a high degree of curvature (as defined by $\bar{j}_{bi}$) or a low value of the optimum cost function (as defined by J_{opt}). That is, a low value of the cost function at its minimum results in reduced variance in the cost function estimates, as defined by equation (4-34). The cost function minimum depends upon the amount of extraneous noise present in the physical system, as well as the statistics of the disturbance and the number of control filter coefficients used to estimate the disturbance. These parameters have also been discussed in section 4.3.

- Larger number of averages M, result in reduced misadjustment (and therefore more accurate curve-fit) and increased performance. However a large number of averages increases the time taken to reach steady state or convergence.

- Larger number of control filter coefficients, N, increases misadjustment and reduces performance. This is because there is an increased variance about the cost function minimum, as a result of the variance of additional control filter coefficients. However a large number of taps increases the bandwidth of attenuation (Note that for a pure tone only two coefficients are required in the control filter (linear combiner)).

- The factor $\bar{j}_{bi}\,\overline{(1/j_{bi})}$ will depend upon the disparity in the frequency components of the filtered orthogonal signals. If the frequency components are highly disparate the misadjustment will increase, however if they are relatively equivalent this factor will not affect the misadjustment.

Hence it is apparent that the signal statistics will affect the required number of averages, and the control filter coefficient step size factor (ie. the control filter coefficients are changed proportional to the cost function estimate) will be determined by the required attenuation and number of averages.

The Independent Quadratic Optimisation algorithm has the added feature of a variable control filter coefficient step size through the use of the control filter coefficient step size factor, and the ability to step only in the direction of decreasing mean square error (ie. it doesn't have to sample about a point as do the discrete gradient estimation methods).

It is also apparent that a minimum perturbation must exist to ensure stability, as

discussed in section 4.3 (ie. If the perturbation were zero, the misadjustment would be infinite, indicating instability).

The Independent Quadratic Optimisation algorithm can also be quite slow during convergence since for each control filter coefficient, the cost function must be estimated three times before the value of the control filter coefficient corresponding to the cost function minimum can be found. Each coefficient of the control filter is also adapted separately, further slowing convergence. Therefore although the algorithm is very stable, it is also quite slow at converging. This will be shown in chapter 5, when a comparison is made between the filtered-X LMS algorithm and the Independent Quadratic Optimisation algorithm.

4.8 Multi-Channel Systems

A multi-channel control system utilising a lattice filter for the active control of noise or vibration of a complex system is shown schematically in Figure 4-17.

A multi-channel system which made use of transversal filters and a multi-channel version of the filtered-X LMS algorithm was first analysed by Elliott, Stothers and Nelson [1987]. As discussed in chapter 2, the bounds of stability for the convergence coefficient of the filtered-X LMS algorithm are limited by the accuracy of the cancellation path transfer function estimate; However, it may also be shown that the bounds are reduced further as the number of error sensors is increased [Snyder, Hansen and Clarke, 1993].

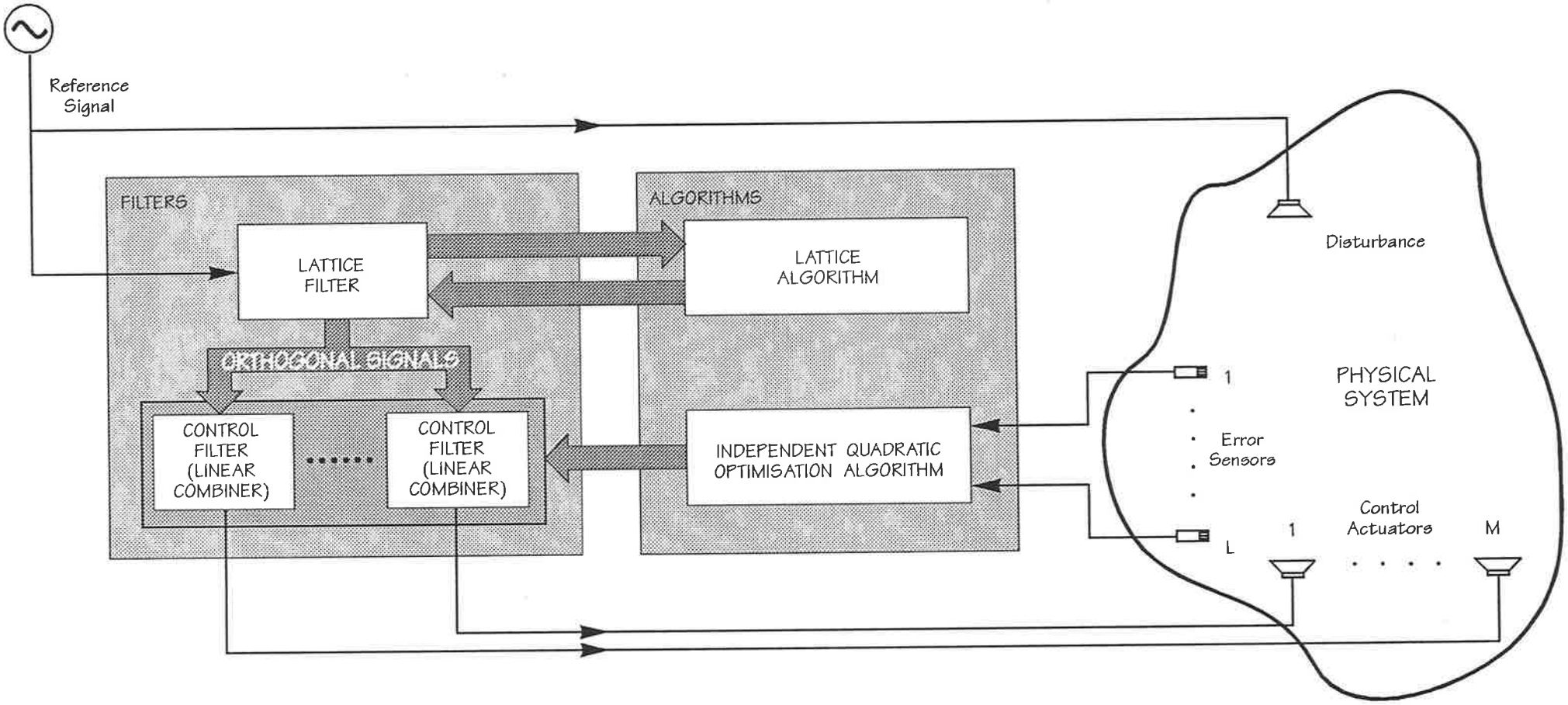

Figure 4-17. Multi-channel control system. Total of L error sensors and M control actuators.

For the system considered here and shown in Figure 4-17, instead of passing the reference signal to a set of transversal filters, the lattice filter generates a set of orthogonal signals which are passed to each control filter (linear combiner). For this system, the cost function given by the mean sum of the square of the signals from each error sensor, can be shown to be a quadratic function of each of the control filter coefficients thus enabling the parabola corresponding to each control filter coefficient to be estimated and the optimum control filter coefficients determined using the Independent Quadratic Optimisation algorithm. If the coefficients are not independent within each control filter (linear combiner) or between the control filters (linear combiners), only the speed of convergence of the control filter coefficients to the values corresponding to the cost function minimum, will be impaired.

4.8.1 Independence Conditions

The independent condition derived in chapter 3 (for the single channel case) will now be examined for the multi-channel system. An attempt will be made in this section to reduce the cost function for a multi-channel system to a form similar to equation (3-31). Consider the cost function of the multi-channel system shown in Figure 4-17.

$$J = E\left[\sum_{l=1}^{L} y_l^2(n)\right] \qquad [4\text{-}36]$$

where l is the error sensor number, with L the total number of error sensors, n the sample number and $y_l(n)$ the error signals given by:

$$y_l(n) = p_l(n) + \sum_{m=1}^{M} \sum_{g=0}^{G-1} h_{lm_g}(n) u_m(n-g) \qquad [4\text{-}37]$$

where m is the control source number with M the total number of control actuators, $p_l(n)$ is the disturbance signal at the particular error sensor, $h_{lm_g}(n)$ represents a coefficient of the cancellation path transfer function with g the coefficient number and G the total number of coefficients, and $u_m(n)$ are the control signals given by:

$$u_m(n) = \sum_{i=0}^{I-1} k_{wm_l}(n) e_{bi}(n) \qquad [4\text{-}38]$$

where $k_{wm_l}(n)$ are the control filter coefficients and $e_{bi}(n)$ are the orthogonal backward prediction error signals, with i the lattice stage number and I the total number of stages in the lattice filter.

Ignoring the adaptation of the control filter coefficients (to ensure that commutation of the cancellation path transfer function is valid, as per the discussion in chapter 2), equation (4-37) can be rewritten as (with the superscript e_b shown to highlight the use of backward prediction error signals as opposed to delayed reference signal samples):

$$y_l(n) = p_l(n) + K_w^T Q_l^{e_b}(n) \qquad [4\text{-}39]$$

where the control filter coefficient vector is defined as:

$$K_w = [\, k_{w1_0}, \ldots, k_{w1_{(I-1)}} \mid \ldots \mid k_{wM_0}, \ldots, k_{wM_{(I-1)}} \,]^T \qquad [4\text{-}40]$$

and the vector of filtered orthogonal backward prediction error signals is defined as:

$$Q_l^{e_b}(n) = [\, q_{l1_0}^{e_b}(n), \ldots, q_{l1_{(I-1)}}^{e_b}(n) \mid \ldots \mid q_{lM_0}^{e_b}(n), \ldots, q_{lM_{(I-1)}}^{e_b}(n) \,]^T \qquad [4\text{-}41]$$

where

$$q_{lm_l}^{e_b}(n) = \sum_{g=0}^{G-1} h_{lm_g}(n) e_{bi}(n-g) \qquad [4\text{-}42]$$

Substituting equation (4-39) into equation (4-36) leads to:

$$J = \sum_{l=1}^{L} \left\{ E[p_l^2(n)] + K_w^T E[Q_l^{e_b}(n) Q_l^{e_b T}(n)] K_w + 2K_w^T E[Q_l^{e_b}(n) p_l(n)] \right\} \qquad [4\text{-}43]$$

From which the optimal control filter coefficients may be found by setting to zero the partial derivative of the cost function, given by equation (4-43), with respect to the control filter coefficients. This leads to the following definition for the control filter coefficients:

$$K_{w_{opt}} = -E\left[\sum_{l=1}^{L} Q_l^{e_b}(n) Q_l^{e_b T}(n)\right]^{-1} E\left[\sum_{l=1}^{L} Q_l^{e_b}(n) p_l(n)\right] \qquad [4\text{-}44]$$

and the optimum value of the cost function may be found by substituting the optimum control filter coefficients into the cost function (equation (4-43)) such that

$$J_{opt} = \sum_{l=1}^{L} \left\{ E[p_l^2(n)] + K_{w_{opt}}^T E[Q_l^{e_b}(n) p_l(n)] \right\} \qquad [4\text{-}45]$$

Using equations (4-44) and (4-45), the cost function defined by equation (4-43) may be written as

$$J = J_{opt} + [K_w - K_{w_{opt}}]^T E\left[\sum_{l=1}^{L} Q_l^{e_b}(n) Q_l^{e_b T}(n)\right] [K_w - K_{w_{opt}}] \qquad [4\text{-}46]$$

To understand the physical significance of this equation, the expectation term will be considered for the following cases:

- two error sensors and one control actuator;
- one error sensor and two control actuators.

The single channel system was examined in chapter 3 and resulted in the definition of the independence condition for control filter coefficient independence, given again here for ease of reference:

$$E[\, e_{bu}(n)e_{bv}(n-m) + e_{bu}(n-m)e_{bv}(n)\,] = 0 \qquad [4\text{-}47]$$

where $u,v = 0,...,N-1$ and $m = 0,...,N_s-1$, with N_s the number of cancellation path transfer function coefficients, and N the number of control filter coefficients. It was shown in chapter 3 that this condition was satisfied only for pure tones.

4.8.1.1 Two Error Sensors and One Control Actuator

Figure 4-18 shows the cancellation path transfer functions, disturbance transfer functions, control actuators and error sensors. For this system the expectation in equation (4-46) (ie. the expectation of the product of the matrix, containing backward prediction errors filtered by the cancellation path transfer functions, with its transform) becomes:

$$E\begin{bmatrix} (e_{b0}(n)\otimes h_{11})^2 + (e_{b0}(n)\otimes h_{21})^2 & (e_{b0}(n)\otimes h_{11})(e_{b1}(n)\otimes h_{11}) \\ & + (e_{b0}(n)\otimes h_{21})(e_{b1}(n)\otimes h_{21}) \\ (e_{b1}(n)\otimes h_{11})(e_{b0}(n)\otimes h_{11}) & \\ + (e_{b1}(n)\otimes h_{21})(e_{b0}(n)\otimes h_{21}) & (e_{b1}(n)\otimes h_{11})^2 + (e_{b1}(n)\otimes h_{21})^2 \end{bmatrix} \qquad [4\text{-}48]$$

where $\otimes$, represents the convolution operator used between the backward prediction error signals, $e_{b0}(n)$ *or* $e_{b1}(n)$, and the cancellation path transfer functions, h_{11} *or* h_{21}. From this equation, it can be shown that the following condition must hold, for the control filter coefficients to be adapted independently :

$$\sum_{l=1}^{2} h_{ll_i} h_{ll_j} E[\, e_{bu}(n-i)e_{bv}(n-j) + e_{bu}(n-j)e_{bv}(n-i)\,] = 0 \qquad [4\text{-}49]$$

where $u \neq v$, $u,v = 0,\ldots,N-1$, and $i, j = 0,\ldots,N_s-1$, with N_s the number of cancellation path transfer function coefficients, and N the number of control filter coefficients.

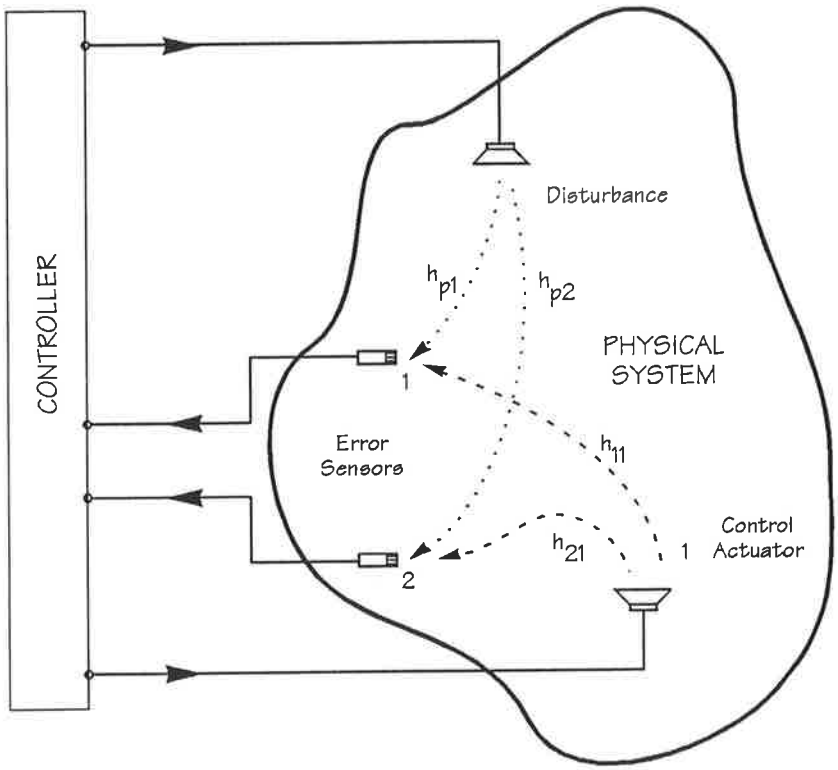

Figure 4-18. Transfer functions for physical system consisting of two error sensors and one control actuator. Transfer functions h_{p1} and h_{p2} are between the disturbance actuator and error sensors 1 and 2, and transfer functions h_{11} and h_{21} are between the control actuator and error sensors 1 and 2.

This condition will hold for pure tones since the expectation in this equation is equivalent to that given by equation (4-47) for the single channel case. However, equation (4-49) also introduces the additional term relating to the transfer functions

between the control actuators and the error sensors. If this additional term is zero, the control filter coefficients will be independent regardless of the type of reference signal. For the two error sensor, one control actuator example, it can be shown that orthogonal cancellation path transfer functions with only two coefficients (ie. FIR type) will ensure the independence condition (equation (4-49)) will be met regardless of the type of reference signal; This effect will be shown from simulations in the next section.

It is also worthwhile considering the minimum mean square error of this particular system. From equation (4-45) the minimum mean square error is given by:

$$J_{opt} = E\left[\begin{array}{l} x(n)\otimes h_{p1}\,[x(n)\otimes h_{p1} + (K_{w\,opt}^{T} E_{bN}(n))\otimes h_{11}] \\ + x(n)\otimes h_{p2}\,[x(n)\otimes h_{p2} + (K_{w\,opt}^{T} E_{bN}(n))\otimes h_{21}] \end{array}\right] \qquad [4\text{-}50]$$

where h_{p1} and h_{p2}, have been introduced as the transfer functions between the disturbance actuator and the error sensor. Converting this representation from the time domain (where the transfer functions are modelled as impulse responses) to the frequency domain (where the transfer functions are modelled as frequency responses), and solving for the relation between the transfer functions for a zero optimum condition gives:

$$\frac{H_{11}(e^{j\omega})}{H_{21}(e^{j\omega})} = -\frac{H_{p2}(e^{j\omega})}{H_{p1}(e^{j\omega})} = \frac{H_{p1}(e^{j\omega})}{H_{p2}(e^{j\omega})} \qquad [4\text{-}51]$$

Thus it is apparent that the optimum cost function can be reduced to near zero if the relative phase and amplitude between h_{p1} and h_{p2} is the same as that betweenh_{11} and h_{21}, but also that the relative phase is 90° and the relative amplitude is unity. If this condition is not met, the optimum cost function will be non-zero, as will be shown

by simulation. Snyder et al [1993] suggest that if equation (4-50) is non-zero, an error sensor is redundant, and therefore that there should be at least as many error sensors as control actuators to ensure there are no redundant transducers, and that a minimum mean square error close to zero can be achieved. The minimum mean square error will however depend on the coupling between each control actuator and the error sensors, as will be considered next.

4.8.1.2 Two Control Actuators and One Error Sensor

Figure 4-19 shows the cancellation path transfer functions, disturbance transfer functions, control actuators and error sensors.

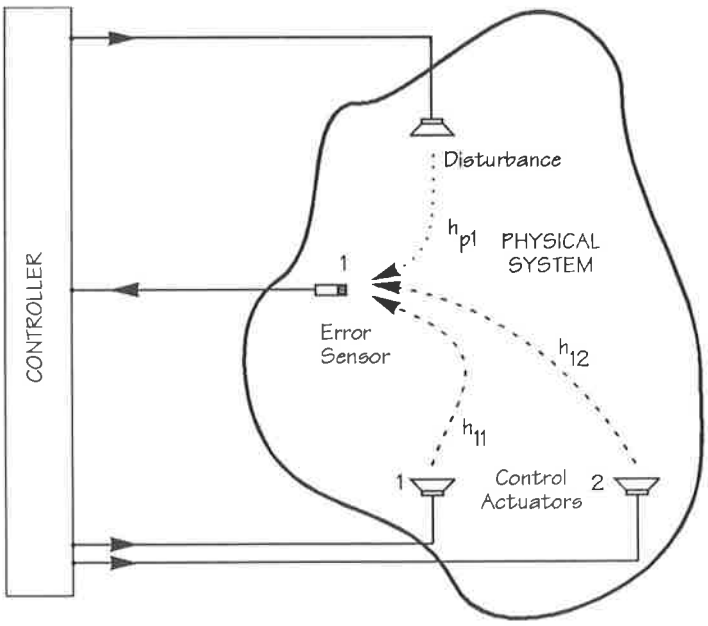

Figure 4-19. Transfer functions for physical system consisting of one error sensor and two control actuators. The transfer functions h_{11} and h_{12} are between each control actuator and the error sensor, while the transfer function h_{p1} is between the disturbance actuator and the error sensor.

For this system the expectation in equation (4-46) (ie. the expectation of the product of the matrix, containing backward prediction errors filtered by the cancellation path transfer functions, with its transform) becomes (note that the terms are numbered for further explanation):

$$E\begin{bmatrix} (e_{b0}(n)\otimes h_{11})^2 & (e_{b0}(n)\otimes h_{11})(e_{b1}(n)\otimes h_{11})\ ^{(1)} & (e_{b0}(n)\otimes h_{11})(e_{b0}(n)\otimes h_{12})\ ^{(2)} & (e_{b0}(n)\otimes h_{11})(e_{b1}(n)\otimes h_{12})\ ^{(3)} \\ (e_{b1}(n)\otimes h_{11})(e_{b0}(n)\otimes h_{11})\ ^{(1)} & (e_{b1}(n)\otimes h_{11})^2 & (e_{b1}(n)\otimes h_{11})(e_{b0}(n)\otimes h_{12})\ ^{(3)} & (e_{b1}(n)\otimes h_{11})(e_{b1}(n)\otimes h_{12})\ ^{(2)} \\ (e_{b0}(n)\otimes h_{12})(e_{b0}(n)\otimes h_{11})\ ^{(2)} & (e_{b0}(n)\otimes h_{12})(e_{b1}(n)\otimes h_{11})\ ^{(3)} & (e_{b0}(n)\otimes h_{12})^2 & (e_{b0}(n)\otimes h_{12})(e_{b1}(n)\otimes h_{12})\ ^{(1)} \\ (e_{b1}(n)\otimes h_{12})(e_{b0}(n)\otimes h_{11})\ ^{(3)} & (e_{b1}(n)\otimes h_{12})(e_{b1}(n)\otimes h_{11})\ ^{(2)} & (e_{b1}(n)\otimes h_{12})(e_{b0}(n)\otimes h_{12})\ ^{(1)} & (e_{b1}(n)\otimes h_{12})^2 \end{bmatrix} \quad [4\text{-}52]$$

As shown by equation (4-52) and (4-46), the independence of the control filter coefficients within each controller depends upon the terms in equation (4-52) numbered (1), while the independence of the control coefficients between control filters (linear combiners) depends on terms in equation (4-52) numbered (2) and (3). For complete independence of all the control coefficients, the terms in equation (4-51) numbered (1), (2) and (3) should equal zero. These terms will now be considered, with the assumption that each cancellation path transfer function has only two coefficients and is of FIR type.

Terms of type (1) can be written similar to

$$h_{11_0}h_{11_1}E[e_{b0}(n)e_{b1}(n-1) + e_{b0}(n-1)e_{b1}(n)] \quad [4\text{-}53]$$

This term represents the standard independence condition (ie. represented by equation (4-47)), which is modified for more than one error sensor, as shown by equation (4-49). Terms of this type will be zero provided the reference signal is a pure tone.

Terms (2) and (3) represent the inter-channel coupling terms. A typical type (2) term

can be written similar to

$$(h_{11_0}h_{12_0} + h_{11_1}h_{12_1})E[e_{b0}^2] + (h_{11_0}h_{12_1} + h_{11_1}h_{12_0})E[e_{b0}(n)e_{b0}(n-1)] \qquad [4\text{-}54]$$

Terms of this type will be zero if the cancellation path transfer functions, h_{11} and h_{12}, are orthogonal (ie. 90° phase difference between the transfer functions). This will enable partial decoupling of the channels, but they will not be completely decoupled unless terms of type (3) are also zero. Terms of type (3) can be written similar to

$$E[e_{b0}(n)e_{b1}(n-1)]h_{11_0}h_{12_1} + E[e_{b0}(n-1)e_{b1}(n)]h_{11_1}h_{12_0} \qquad [4\text{-}55]$$

For this type of term the cancellation path transfer functions are entwined with the standard independence condition. Hence it appears very difficult to ensure that this term is zero. Therefore it appears unlikely that the channels can ever be completely decoupled.

As discussed, there should be at least as many error sensors as control actuators to ensure no transducers are redundant. It will be shown by simulation, that if there are more control actuators than error sensors, the system will be over-determined possibly resulting in less attenuation.

4.8.2 Control Coefficient Adaptation Methods

For multi-channel systems, the Independent Quadratic Optimisation algorithm may be implemented using two alternative methods, described fully in Tables 4-1 and 4-2.

- Method 1 : All the control coefficients for a control filter can be adapted before continuing to the next control filter;

- Method 2 : A control coefficient for all the control channels may be updated before continuing to the next control coefficient.

As for a single channel system, it is only the control filters (linear combiners) that use the Independent Quadratic Optimisation algorithm. The lattice filter uses the recursive algorithm discussed in chapter 3. Simulations will now be considered using these two methods of adaptation for a multi-channel system. The number of control actuators relative to error sensors will be considered, as will their coupling effects. Simulations will be performed for a pure tone only, since as discussed, the Independent Quadratic Optimisation algorithm performs most efficiently for this type of signal.

4.8.3 Simulations

The simulations performed in this section are for a pure tone only, and will show the effect of the number and location of error sensors and control actuators, by comparison with a single channel case. The power and sampling ratio of the pure tone were arbitrarily chosen as 0.5 and 20 respectively. The control filter coefficient step size factor used was $\alpha = 0.05$ for both control filter coefficients of all control filters. The coefficients for each control filter were initialised to zero. The mean square error was estimated using 200 samples (ie. averaging performed over 10 periods), with a delay of 20 samples before averaging. The arbitrary transfer functions between the disturbance and control actuators, and the error sensors were used as per the single channel simulations discussed in section 4.4, and shown in Figure 4-5.

Table 4-1. **METHOD 1:** Adapt all the control coefficients for a control channel, before continuing to the next channel.

Initialise the control coefficients for each control filter (linear combiner).

For each ***control filter (linear combiner)*** *do the following:*

For each ***control coefficient:***

- ***(a)*** *Delay estimating the mean square error by a number of samples equivalent to a time greater than the largest time taken for the signals emitted from the control actuators to reach the error sensors;*
- ***(b)*** *Perform a sufficient average of the mean square error dependent upon the accuracy (i.e. minimum mean square error) required;*
- ***(c)*** *Change the value of the particular control coefficient, based upon the level of the mean square error and the accuracy (ie. minimum mean square error) required. Perform (a) to (b) twice more;*
- ***(d)*** *Determine the optimum value for the particular control coefficient by fitting the estimated points to a quadratic function.*

Advance to the next ***control coefficient.***

Advance to the next ***control filter (linear combiner).***

Table 4-2. **METHOD 2:** Adapt a control coefficient for all the channels before continuing to the next control coefficient.

Initialise the control coefficients for each control filter (linear combiner).

For each ***control coefficient*** *do the following:*

For each ***control filter (linear combiner)****:*

(a) *Delay estimating the mean square error by a number of samples equivalent to a time greater than the largest time taken for the signals emitted from the control actuators to reach the error sensors;*

(b) *Perform a sufficient average of the mean square error dependent upon the accuracy (i.e. minimum mean square error) required;*

(c) *Change the value of the particular control coefficient, based upon the level of the mean square error and the accuracy (ie. minimum mean square error) required. Perform (a) to (b) twice more;*

(d) *Determine the optimum value for the particular control coefficient by fitting the estimated points to a quadratic function.*

Advance to the next ***control filter (linear combiner).***

Advance to the next ***control coefficient.***

The final control filter coefficients, amount of attenuation and error signal are shown for the single channel case with arbitrary disturbance and cancellation path transfer functions (as used in section 4.4), in Figures 4-20(a) and (b). These results are similar to those shown in section 4.4.1.

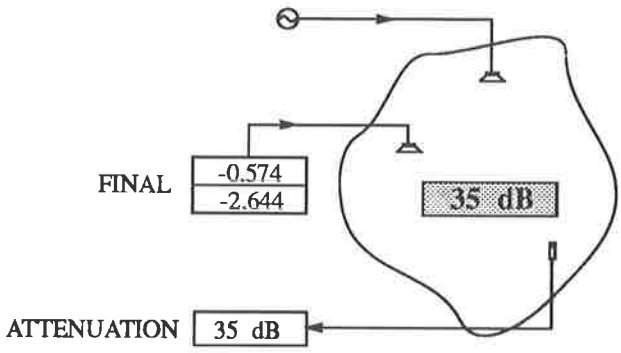

Figure 4-20(a). Attenuation and optimal control filter coefficients with arbitrary transfer functions, as for single channel case.

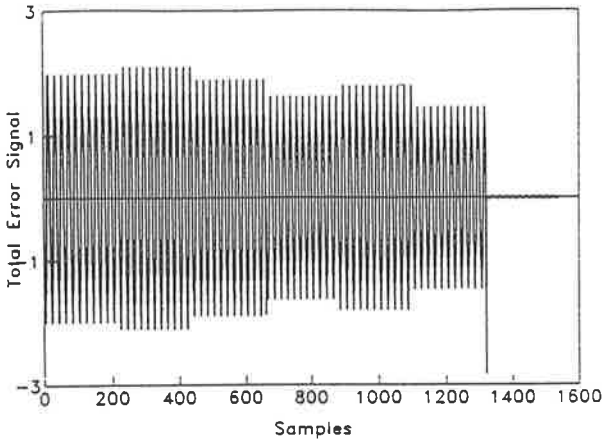

Figure 4-20(b). Error signal magnitude with arbitrary transfer functions, for single channel case.

Figures 4-21(a) and (b) show similar results for the system when the number of error sensors is increased. Increasing the number of error sensors reduces the attenuation at each error sensor, however it increases the amount of global attenuation. The amount of attenuation decreases as the number of error sensors increases, due to the controller reaching the limit of the achievable minimum mean square error set by the system configuration [Snyder, Clarke and Hansen, 1993]. The optimum control filter coefficients will be an average of those for controlling the signal at each error sensor

independently. That is they will be determined by equation (4-44) to achieve good reduction of the total mean square error for the given system configuration.

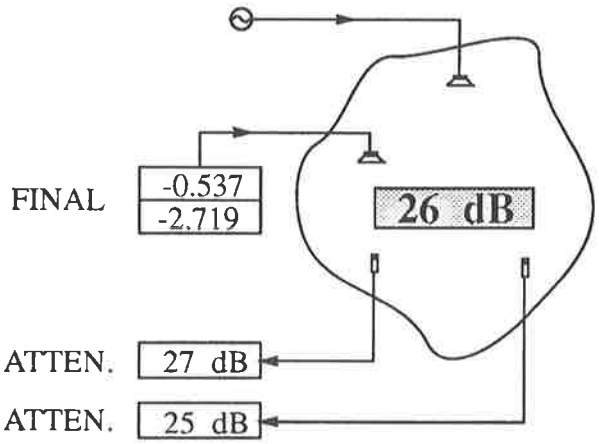

Figure 4-21(a). Attenuation and optimal control filter coefficients with arbitrary transfer functions, for two error sensors and one control actuator.

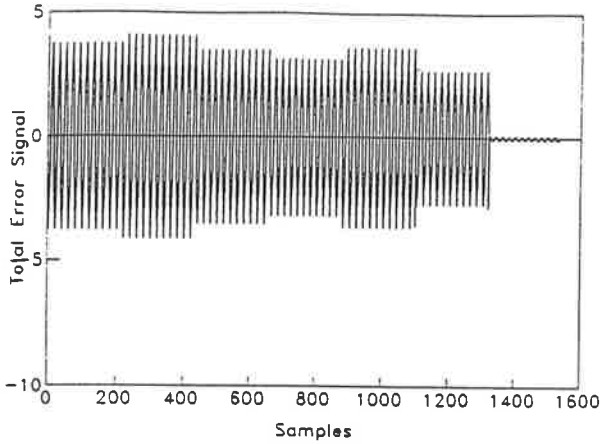

Figure 4-21(b). Total error signal magnitude with arbitrary transfer functions, for two error sensors and one control actuator.

In section 4.8.1 it was claimed that if the relative phase and amplitude of the transfer functions between the disturbance actuator and the error sensors were the same as the relative phase and amplitude of the transfer function between the control actuator and error sensors, then the minimum cost function will be equivalent to that of a single channel system. This is shown in Figures 4-22(a) and (b), with a relative phase of 90° and a relative amplitude of 1.0. Control of this system configuration yields the same attenuation as for the single channel case (shown in Figures 4-20(a) and (b)), but possibly greater global attenuation (dependent upon whether the error sensors sense the same mode or different modes; the same mode could be sensed by separating the sensors by a quarter of a wavelength).

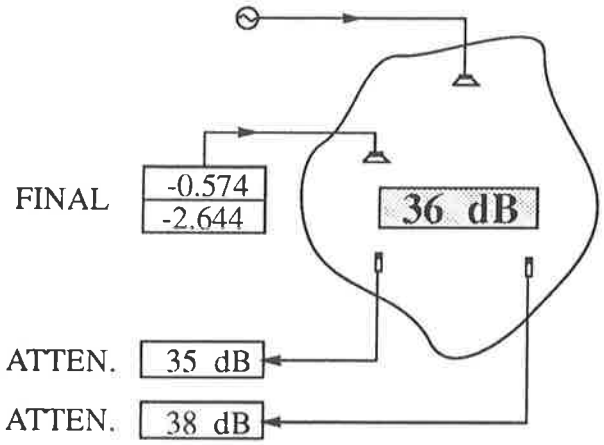

Figure 4-22(a). Attenuation and optimal control filter coefficients for orthogonal transfer functions between the disturbance actuator and each error sensor, and the control actuator and each error sensor.

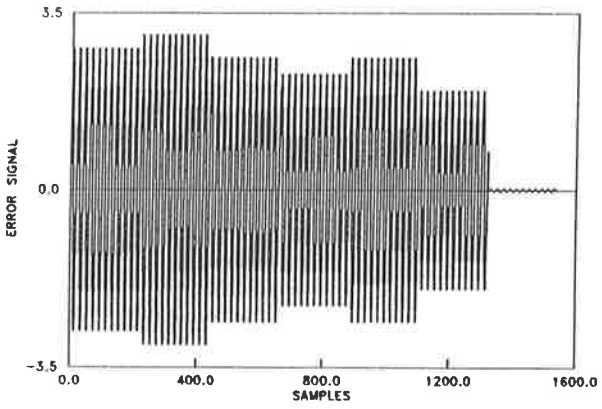

Figure 4-22(b). Total error signal for orthogonal transfer functions between the disturbance actuator and each error sensor, and the control actuator and each error sensor.

Simulations shown in Figures 4-23(a) and (b), using two control actuators with a single error sensor, highlight the difference between the two methods of control discussed in section 4.8.2. Note that in theory, only a single control actuator is required for a single error sensor for cancellation of a pure tone.

Consider Figures 4-23(a) and (b). For arbitrary transfer functions, **method 1** (ie. update all coefficients for a control filter before continuing to next control filter) uses only one control actuator and achieves attenuation equal to that of a single channel controller. When considering optimisation of the second channel using this method, the Independent Quadratic Optimisation algorithm realises that the second channel is not required (since optimal reduction of the mean square error has already been

achieved by only the single channel) and it therefore leaves the second channel essentially unchanged (ie. control filter coefficients have a value close to zero, and a control signal is not generated). However **method 2** (ie. update a coefficient for all control filters before continuing to next control filter) attempts to use both control actuators and achieves significantly less attenuation than for the single channel case. This is because only a single channel is required, and therefore attempting to use two control actuators to cancel the disturbance results in an over-determined system, as discussed previously. Snyder et al [1993] remark that using a similar "round-robbin" approach to control filter adaptation can result in excess effort by a controller using method 1 (possibly leading to overloading of the control actuator), while method 2 can distribute the control effort between the actuators.

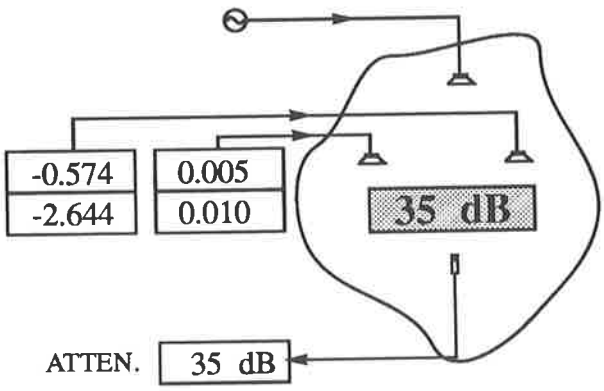

Figure 4-23(a). Attenuation and optimal control filter coefficients with arbitrary transfer functions, using **method 1** for control using two actuators and one error sensor.

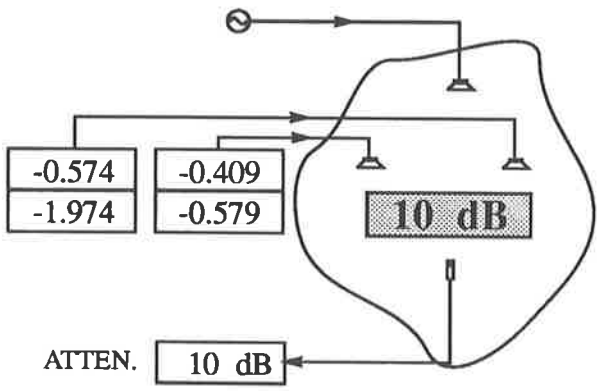

Figure 4-23(b). Attenuation and optimal control filter coefficients with arbitrary transfer functions, using **method 2** for control using two actuators and one error sensor.

4.9 Summary

In this chapter the Independent Quadratic Optimisation algorithm concept was introduced and formally derived. It fits a quadratic curve to three estimates of the cost function for each independent control filter coefficient. It was shown that the use of Newton's Method as outlined in recent papers is similar to the Independent Quadratic Optimisation algorithm presented here. This comparison has led to formalising the heuristic comments (regarding number of averages, control filter coefficient step size and degree of cost function curvature) made about the Independent Quadratic Optimisation algorithms performance, using Widrow and Stearns [1985] analysis of Newton's Method for a multi-coefficient single channel system.

Simulations were presented for a pure tone and white noise separately and in combination, illustrating the effects on control filter coefficient independence of a transfer function in the cancellation path, as presented theoretically in chapter 3. It was shown that loss of independence only a limitation in that it reduced the speed of convergence, but not stability, of the Independent Quadratic Optimisation algorithm for all but pure tone signals. The Independent Quadratic Optimisation algorithm has been extended to control periodic noise/vibration by Gibbs et al [1993] and Kewley et al [1995].

Simulations were also performed in this chapter, for a multi-channel system using the Independent Quadratic Optimisation algorithm with two alternative methods of

control filter coefficient adaptation. Theory was developed with regard to the conditions for independence of control filter coefficients within each channel and between channels. It was shown that for the case of a control actuator and two error sensors, control filter coefficient independence was assured provided the independence condition presented in chapter 2 was met, or the cancellation path transfer functions and the primary disturbance to error sensor transfer functions were orthogonal; However, if these transfer functions were not orthogonal, the system would be over-determined, with redundancy of an error sensor as found by Snyder, Clark and Hansen [1993] in an analysis of the standard filtered-X LMS algorithm. It was further shown that for the case of one error sensor and two control actuators, independence of the control filter coefficients between channels was impossible; This result suggests that it is more effective to use method 1 for adaptation of control filter coefficients as the coefficients are independent for each channel.

5.1 Introduction

This chapter describes the issues of concern when practically implementing the Independent Quadratic Optimisation algorithm. It describes the essence of the electronic hardware and software chosen to best suit the Independent Quadratic Optimisation algorithm. Additionally, the filtered-X LMS algorithm was implemented on two types of processor configurations (ie. serial integer and parallel floating types), and a comparison of the implementation issues found from these configurations is also made.

A comparison is made between the effectiveness of the Independent Quadratic Optimisation algorithm relative to the filtered-X LMS algorithm, in terms of:

- Achievable attenuation;
- Signal types (with particular regard to those with a high eigenvalue disparity);
- The ability to track changing system conditions;
- The ability to not only reduce vibro-acoustic levels but also vibro-acoustic intensity or power flow.
- The effect of uncorrelated noise on the achievable attenuation.

It will be shown that the Independent Quadratic Optimisation algorithm achieves good attenuation without any knowledge of the system transfer functions. The effect of the parameters of the Independent Quadratic Optimisation algorithm on the misadjustment and achievable minimum mean square error will be assessed to compare practical results with the theory developed in chapter 4.

The effect of Independent Quadratic Optimisation algorithm parameters, and a comparison of this algorithm with the filtered-X LMS algorithm is performed for:

- Verification of algorithm implementation;

  This scenario was performed first to confirm the theory presented in chapter 3, relating to the reduction in power of the backward prediction error signals with increasing stages of the lattice filter, and the orthogonality and statistics of the backward prediction error signals for pure tones, periodic and broadband disturbances. This assessment will show that the power of the backward prediction error signals give an indication of the disturbance statistics, thereby also giving an indication of the number of control filter coefficients required for control.

  The self-induced noise scenario effectively mimiced the case of simply a delay (ie. a certain number of sampling periods) in the cancellation path, with results shown for both algorithms. This test was performed prior to tests with apparatus using actuators and sensors that could be easily damaged.

- Vibro-acoustic apparatus;

  Results are presented for the Independent Quadratic Optimisation algorithm when used in single-channel form on experimental apparatus to reduce plane-wave radiation constrained to one-dimension in a duct with zero air-flow, and finally

when used in multi-channel form to reduce the vibration levels (and/or power flow) in a semi-infinite plate.

5.2 Hardware/Software Design

The Independent Quadratic Optimisation algorithm concept and filtered-X LMS algorithm both have parallel natures. That is, the Independent Quadratic Optimisation algorithm concept requires orthogonal signals to be generated (and maintained orthogonal), control signals to be generated from these orthogonal signals (for each control actuator) and the control filter coefficients to be adapted to generate the optimum control signals. The filtered-X LMS algorithm requires the cancellation path filter coefficients to be estimated, the control signals to be generated, and the control filter coefficients to be adapted to generate optimal control signals.

Due to the parallel natures of these algorithms, their implementation was performed using a network of parallel processors. The processors used were developed by Inmos and are known as Transputers. Transputers are very similar to standard DSP's (Digital Signal Processors) in that they have a CPU (Central Processing Unit) that performs arithmetic operations and data storage and retrieval from memory (RAM, ROM etc). However, they are quite different from other DSP's as the communication links between transputers can be considered as DMA (Direct Memory Access) controllers, capable of transferring data from the memory of one processor to another without interrupting the CPU. Transputers can perform arithmetic using floating point (real) or fixed-point

(integer) operations. Fixed point processors have the advantage of fast arithmetic operations at low cost, but have many disadvantages, namely:

- Scaling;
- Overflow;
- Precision or Round-Off Errors.

Floating point processors are slower at performing arithmetic operations and more costly, but they do not have any of the above disadvantages. The Transputer network used floating-point transputers for coefficient (control filter or lattice filter) adaptation and fixed-point transputers for control signal generation. Code for the Transputers was written with regard to the hardware architecture (ie. the transputer layout and communication links were initially defined in the software), using a high level language known as OCCAM (and an associated editor that used Hyertext). It is interesting to note that OCCAM was designed with communication protocol as a priority (in contrast to PASCAL and C), since communication is essential to the concurrent operation of parallel processors. Key features of OCCAM are PRI (a prioritised instruction), ALT (an alternation or multi-tasking instruction) and PAR (a parallel or concurrent processing instruction).

The transputer architecture is shown in Figure 5-1. This network is defined specifically for the Independent Quadratic Optimisation algorithm, although in this form it can also operate using the filtered-X LMS algorithm, as was done during this work but will not be discussed further. This network was used as a development system with T414's (fixed-point) interchangeable with T800's (floating-point). The converters (ADC's and DAC's) were memory mapped 16-bit devices (Motorola DSP56-ADC16 and DSP56-DAC16). The

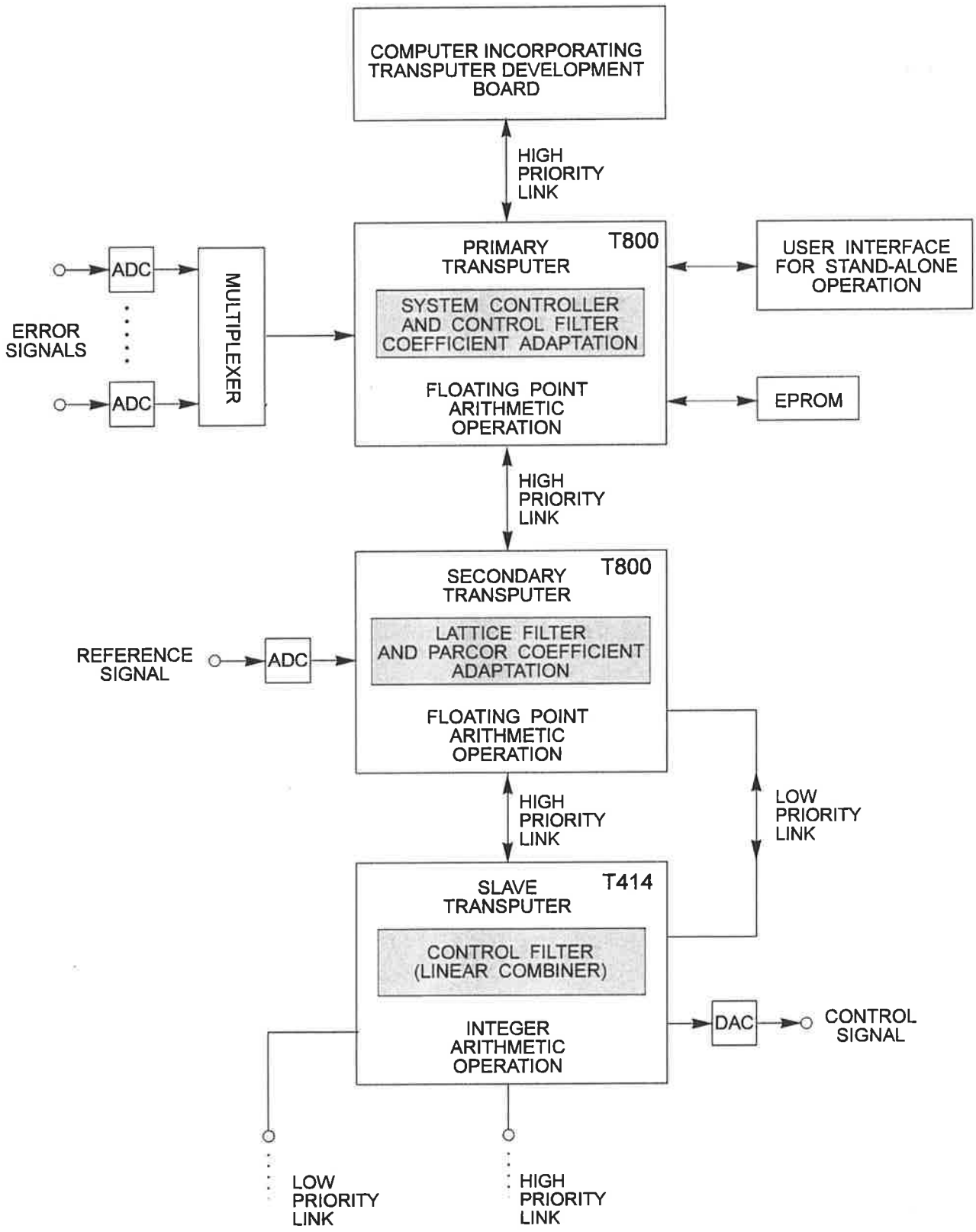

Figure 5-1. Transputer network architecture.

converters used analog anti-aliasing and reconstruction (anti-imaging) filters that were external to the system, and as such they required sample and holds. Programmable gain amplifiers were not used. The sampling rate used was 1250 Hz (divided down from the 20MHz processor clock), to ensure sufficient time for the generation of orthogonal signals by the lattice filter.

The network was connected to a development board from which the code was compiled and downloaded to each transputer accordingly. This board used a transputer to run programs for monitoring the algorithm performance and to store data in a file on the computer for later analysis. The development board also ran standard Inmos software to assess hardware architecture features. The network was connected to a terminal for stand-alone system operation.

The primary transputer (a T800) in the network was responsible for collecting the error signal samples, storage of information (ie. parameters), definition of the required operation (eg. type of algorithm; Independent Quadratic Optimisation algorithm or filtered-X algorithm) and adaptation of control filter coefficients. The secondary transputer (also a T800) was solely responsible for sampling the reference signal and generating orthogonal signals. Once generated the orthogonal signals were passed on a high priority communication link to the slave transputers (T414's). The slave transputers generated the control signals according to their current filter configuration. A low priority link was used to transfer new filter coefficients (and other information) between the transputers.

The T800 uses 64 bit floating point arithmetic at a rate of 1.5 MFLOPS (million floating point operations per second). There is only 4K of on-chip RAM (access rate of 80 Mbytes/second). It is capable of operating at a rate of 10 MIPS (million instructions per second). The T414 uses 32 bit integer arithmetic, and can perform arithmetic operations about 10 times faster than the floating point operation rate of the T800.

During the period this work was undertaken, the filtered-X LMS algorithm was not only implemented on the transputer network, it was also implemented in multi-channel form on a serial integer processor known as the Texas Instruments TMS320C25 (16 Bit Integer Arithmetic). This processor used multi-tasking (since it had only one CPU) to perform the algorithm operations that could be adapted concurrently on the transputer network.

The TMS320C25 was programmed using assembly language to initially develop efficient code that could later be used as a library of procedures or functions for a C-compiler. The library formed a "real-time Kernel", which enabled control signal generation at interrupts, and data to be passed from the interrupt work-space to the non-real-time adaptive workspace. The real-time kernel needed to be efficiently designed to ensure minimum time was spent processing interrupts. Therefore internal memory was used for variables and circular buffers were used to store delayed signal samples. Attention to data transfer between the interrupt and non-real-time adaptive workspace was required to minimise the possibility of an interrupt occurring during this transfer.

At times when the CPU was not attending to interrupts, it adapted filter coefficients (both control filter and cancellation path filter coefficients). The control filter and

cancellation path filter coefficient adaptive programs were written in C using the library for the real-time kernel. Storage of the relevant variables in the slower external memory enabled transfer of data to a computer for later analysis. The code was down-loaded to the TMS320C25 using a Motorola MC 68000 processor, that also ran a program known as SPaM (Signal Processing and Matrices) which enabled controller operation to be altered easily using user defined parameters. A summary of this system is shown in Figure 5-2.

When completed this system was as easy to program using C as the Transputer system was in OCCAM. Initially though, all the code for the TMS320C25 was written in assembly, which proved difficult to debug, and used only integer arithmetic. It was only after the real-time kernel was written that C was used to purely adapt coefficients using floating point arithmetic.

For both the Transputer Development System, and the TMS320C25 system, care with DC offsets was required for the filtered-X LMS algorithm. If DC offsets were not accounted for in the filtered-X LMS algorithm using leakage (see chapter 2), or through differencing (ie. a digital high pass filter) the two most recent input signals (whether reference or error), they caused overflow or saturation of the filter coefficients (whether control or cancellation path). The DC offsets did not affect the Independent Quadratic Optimisation algorithm, as the control filter coefficients are not adapted directly using instantaneous signals values (as is the filtered-X LMS algorithm). The PARCOR coefficients of the lattice filter (associated with the Independent Quadratic Optimisation algorithm concept) were not found to be affected by DC offsets.

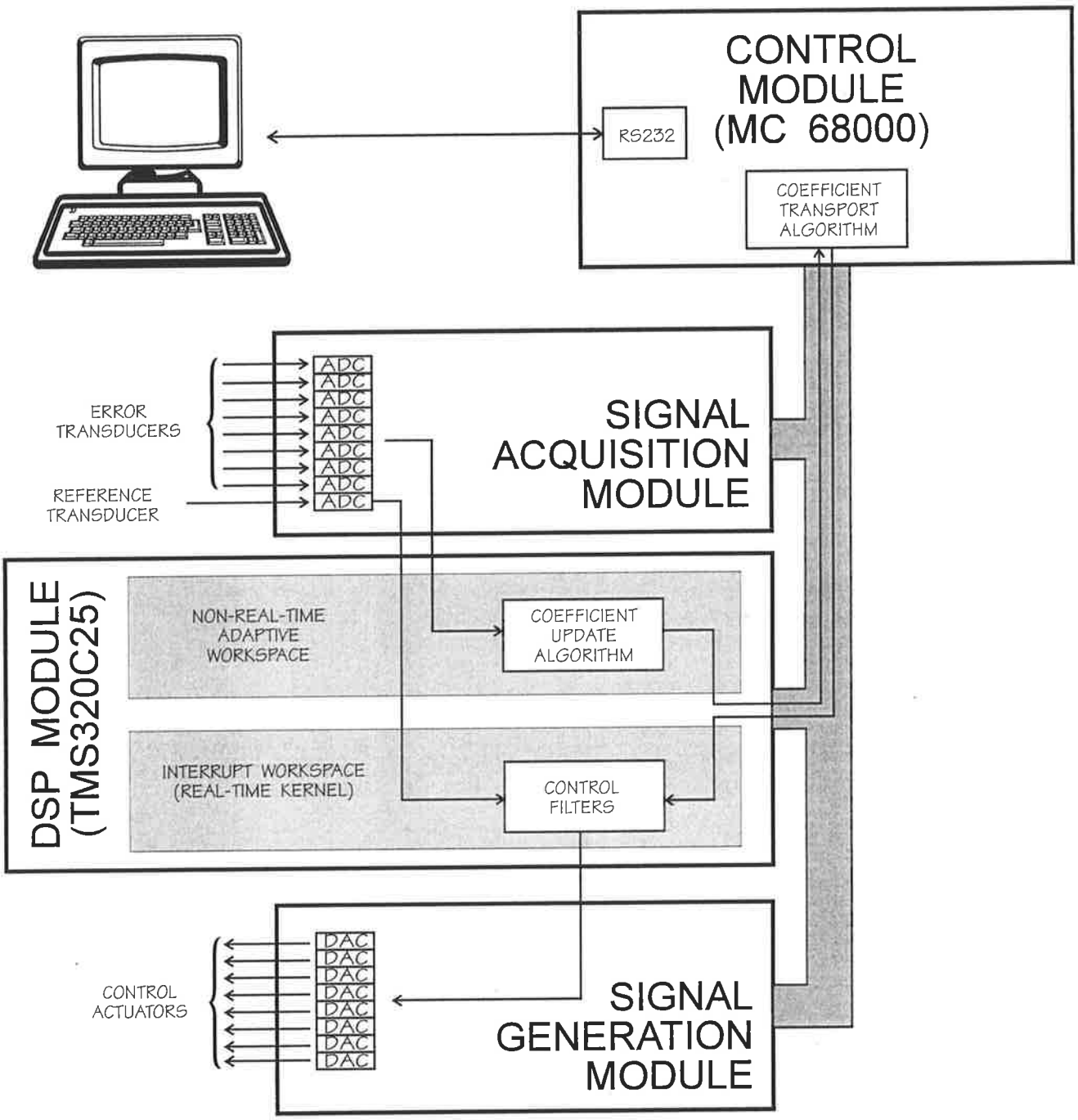

Figure 5-2. TMS320C25 Architecture.

5.3 Experimental Verification

Before conducting experiments using specific acoustic and vibration test apparatus, the following initial experiments were performed:

- Analysis of Lattice Filter Implementation.

  This was done to assess the influence of the number of control filter coefficients and the PARCOR convergence coefficient on the auto and cross correlations of the tapped backward prediction errors (orthogonal signals) for a pure tone of different frequencies, multiple tones (not necessarily harmonics), and variable band-passed white noise. This assessment will confirm the theory presented in chapter 3, relating to the reduction in power of the backward prediction error signals with increasing stages of the lattice filter, and the orthogonality and statistics of the backward prediction error signals for pure tones, periodic and broadband disturbances. This assessment will also show that the power of the backward prediction error signals give an indication of the disturbance statistics, thereby also giving an indication of the number of control filter coefficients required for control.

- Analysis of a Single Channel System with Self Induced Noise.

  To ensure the Independent Quadratic Optimisation algorithm was implemented correctly before testing on apparatus using actuators and sensors that could be

easily damaged, self induced noise was generated using suitably initialised control filter coefficients. The control signal was generated and fed back into the controller as an error signal. The unknown plant in this case consisted of only the control system transfer functions at input and output (ie. The converters and filters). The influence of various Independent Quadratic Optimisation algorithm parameters on the attenuation characteristics were assessed for pure tone, multi-tone and band-passed white noise inputs. Comparisons were made with the filtered-X LMS algorithm.

5.3.1 Lattice Filter Assessment

In this section the lattice filter parameters will be assessed to not only ensure its correct implementation, but also to illustrate how various types of input/reference signals are orthogonalised.

The lattice filter was implemented experimentally and adapted using the stochastic approximation (ie. LMS) algorithm as discussed in chapter 3. The structure of the lattice filter is shown in Figure 5-3, for ease of reference.

The lattice filter implementation was firstly tested with a pure tone reference signal of 125 Hz, and a PARCOR convergence coefficient of about 0.03. The reference signal had an amplitude of about 2V pp, which corresponds to a signal power of 2.0 V^2. The first test of the lattice filter implementation was to illustrate how the power of the backward

prediction errors changed with increasing stages, as the backward prediction errors are an essential part of the Independent Quadratic Optimisation algorithm. It should be noted that a pure tone requires only one stage of a lattice filter, as it can only have one orthogonal signal.

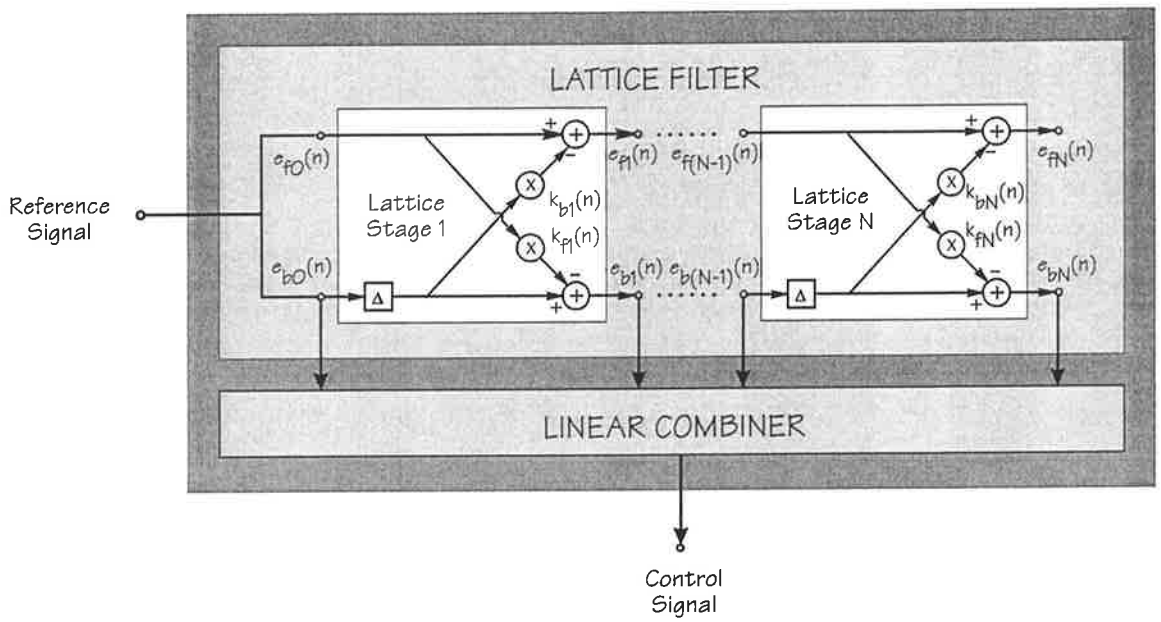

Figure 5-3. Structure of lattice filter coupled to a linear combiner. $e_{fi}(n)$ and $e_{bi}(n)$ represent forward and backward prediction errors respectively, $k_{fi}(n)$ and $k_{bi}(n)$ represent the forward and backward PARCOR coefficients, and Δ represents a single sample delay.

Table 5-1 gives the expectations of the backward prediction errors with themselves (autocorrelation) and with others (cross correlation), by averaging their products. The diagonal shaded terms represent the autocorrelations of the backward prediction errors. The off-diagonal terms represent the cross correlation of the backward prediction errors. Since Table 5-1 is diagonal, results are only shown for the diagonal and upper triangle.

All results have been estimated from 1000 samples of the backward prediction error signals after the PARCOR coefficients had converged.

	$e_{b0}(n)$	$e_{b1}(n)$	$e_{b2}(n)$	$e_{b3}(n)$
$e_{b0}(n)$	2.0	0.03	-0.06	-0.06
$e_{b1}(n)$		0.64	0.06	0.001
$e_{b2}(n)$			0.01	0.007
$e_{b3}(n)$				0.01

Table 5-1. Auto and cross correlations of backward prediction errors for a pure tone reference/input signal.

As anticipated, the only backward prediction errors with significant powers were the reference signal ($e_{b0}(n)$) and the first stage backward prediction error ($e_{b1}(n)$). It is also apparent from Table 5-1, that as the cross-correlation between pairs of backward prediction error signals is so small, it indicates orthogonality. This was observed also by comparing time traces and Lissajous figures of the signals; The Lissajous figures began as ellipses with arbitrary axes (ie. not principal), and were transformed in time through the adaptation of the PARCOR coefficients, to ellipses with principal axes.

It can be shown that the power of the first backward prediction error is given by $A^2/(2\sin^2\omega_0)$, with A representing the input/reference signal amplitude of 2.0, and $\omega_0 = 2\pi/X$, where X is the sampling ratio of 20. Using these values, the power of the

first backward prediction error signal is 0.69, in good agreement with that found experimentally.

It is worthwhile examining the first PARCOR coefficient as it is adapted with differing convergence coefficients. It is seen from Figure 5-4, that increasing the convergence coefficient of the stochastic gradient approximation (LMS) algorithm (used for the PARCOR coefficient adaptation), results in extremely fast convergence of the PARCOR coefficients with little variance upon convergence. This is very useful for the Independent Quadratic Optimisation algorithm, as it indicates that the orthogonal backward prediction error signals will be available almost immediately after adaptation of the PARCOR coefficients commences, using the stochastic gradient (ie. LMS) algorithm discussed in chapter 3.

Similar results were found for frequencies of 156.25 Hz and 208.3 Hz (ie. Sampling ratios of 8 and 6 respectively). It is interesting to note what effect additional tones in the input/reference signal, have on the auto and cross correlations of the backward prediction errors generated by the lattice filter. Tones of 125 Hz, 156.25 Hz and 208.3 Hz were combined with varying phases but equal amplitudes. The auto and cross correlations of the backward prediction errors were determined as for Table 5-1, and are shown in Table 5-2, with shaded numbers indicating auto-correlations. In Table 5-2, the powers have been normalised by that of the reference signal, and only the results for the diagonal and upper diagonal are shown as Table 5-2 is diagonal. The results have been estimated from 1000 samples of the backward prediction error signals, after the PARCOR coefficients had converged.

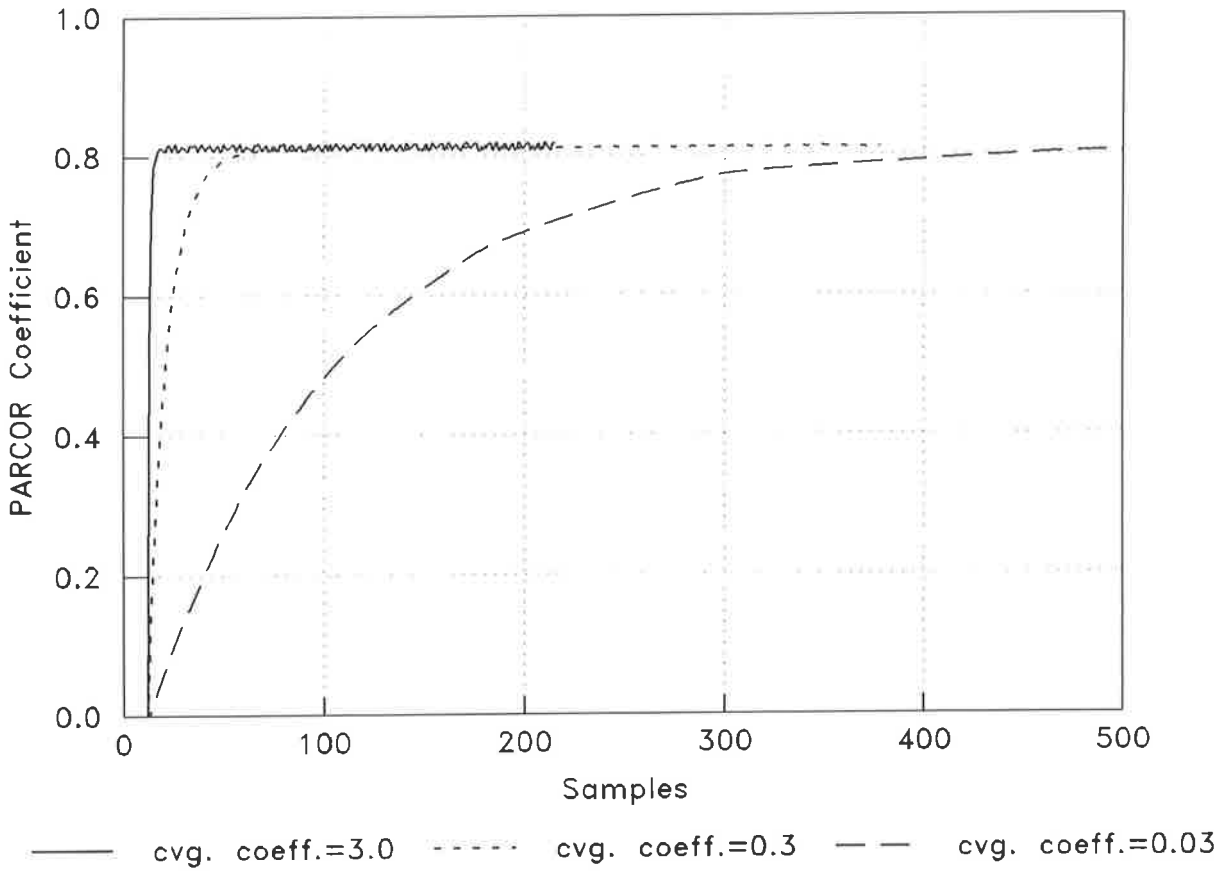

Figure 5-4. Adaptation of PARCOR coefficients with differing convergence coefficients.

From Table 5-2 it is apparent that the power of the backward prediction error signals decreases dramatically with increasing stages of the lattice filter. As discussed in section 3.4.2.2, the tonal components of the reference signal are not just shifted in phase by 90°; This was also confirmed in these experiments by measuring the phase difference between each tone in the input/reference signals, and each tone in the backward prediction error signals. This suggests the control filter coefficients may overflow due to the low backward prediction error signal magnitudes at higher stages of the lattice. The control filter coefficients, when adapted in this manner will be further examined for control of a multi-tone acoustic disturbance.

	$e_{b0}(n)$	$e_{b1}(n)$	$e_{b2}(n)$	$e_{b3}(n)$	$e_{b4}(n)$	$e_{b5}(n)$	$e_{b6}(n)$
$e_{b0}(n)$	1.0	0.02	0.01	0.003	0.003	0.001	0.004
$e_{b1}(n)$		0.55	0.005	0.003	0.0003	0.002	-0.002
$e_{b2}(n)$			0.07	0.002	0.0006	0.0001	0.0005
$e_{b3}(n)$				0.03	0.0001	0.00001	0.0001
$e_{b4}(n)$					0.01	0.00001	0.00001
$e_{b5}(n)$						0.001	0.00001
$e_{b6}(n)$							0.001

Table 5-2. Auto and cross correlations of backward prediction errors for a multi-tone reference/input signal.

Table 5-2 indicates that the estimated power of the backward prediction errors should be used inversely, as a factor in determining the control filter coefficient step size, as discussed in chapter 4 and shown by equation (4-10). It was discussed in chapter 4 that this factor was not to be used since it was affected by the cancellation path transfer function, however it will only be used as a guide to provide an order of magnitude for steps of the control filter coefficients. The Independent Quadratic Optimisation algorithm will still perform without knowledge of the cancellation path transfer function.

Finally, it is interesting to consider the powers of the backward prediction error signals for a reference/input signal consisting of white noise filtered through a band pass filter

with width 50 Hz and centre frequency 300 Hz, in comparison to white noise filtered through a band pass filter with width 200 Hz and centre frequency 300 Hz. Table 5-3 and 5-4 respectively give the normalised auto and cross correlations of the backward prediction errors for 50 Hz and 200 Hz band passed white noise reference/input signals. Again, only the results for the diagonal and upper diagonal are shown, as Table 5-3 is diagonal. The results have been estimated from 1000 samples of the backward prediction error signals, after the PARCOR coefficients had converged.

	$e_{b0}(n)$	$e_{b1}(n)$	$e_{b2}(n)$	$e_{b3}(n)$	$e_{b4}(n)$
$e_{b0}(n)$	1.0	0.04	0.04	0.07	0.06
$e_{b1}(n)$		1.2	0.003	0.01	0.003
$e_{b2}(n)$			0.3	0.05	0.03
$e_{b3}(n)$				0.3	0.06
$e_{b4}(n)$					0.2

Table 5-3. Auto and cross correlations of backward prediction errors for a white noise input/reference signal filtered through a band-pass filter with width 50 Hz and centre frequency 300 Hz.

It is interesting to note that a comparison of the diagonal terms (shaded) of Tables 5-3 and 5-4, shows less of a dramatic decline in the powers of the backward prediction errors as the width of the band passed white noise is increased. This is considered to result

from the increasing bandwidth of white noise causing the input/reference signal to be increasingly white. Since the samples of a purely white noise sequence are orthogonal, the PARCOR coefficients will not need to be adapted, and the lattice filter will act as a tapped-delay-line (or transversal filter). The lattice filter will also act as a tapped-delay-line, if the PARCOR coefficients are initialised to zero.

	$e_{b0}(n)$	$e_{b1}(n)$	$e_{b2}(n)$	$e_{b3}(n)$	$e_{b4}(n)$
$e_{b0}(n)$	1.0	0.05	0.02	0.002	0.01
$e_{b1}(n)$		0.88	0.01	0.02	0.02
$e_{b2}(n)$			0.65	0.02	0.04
$e_{b3}(n)$				0.63	0.01
$e_{b4}(n)$					0.63

Table 5-4. Auto and cross correlations of backward prediction errors for a white noise input/reference signal filtered through a band-pass filter with width 200 Hz and centre frequency 300 Hz.

Figure 5-5 shows the PARCOR coefficients during adaptation, with a white noise reference/input signal filtered through a 400 Hz band pass filter with a centre frequency of 300 Hz. As shown from Figure 5-5, the PARCOR coefficients vary randomly about zero for high order stages of the lattice filter, and converge close to a non-zero but small value for lower order stages of the lattice filter. This is likely to be a result of the noise

not being completely white across 400 Hz, with the higher order stages having zero PARCOR coefficients as expected.

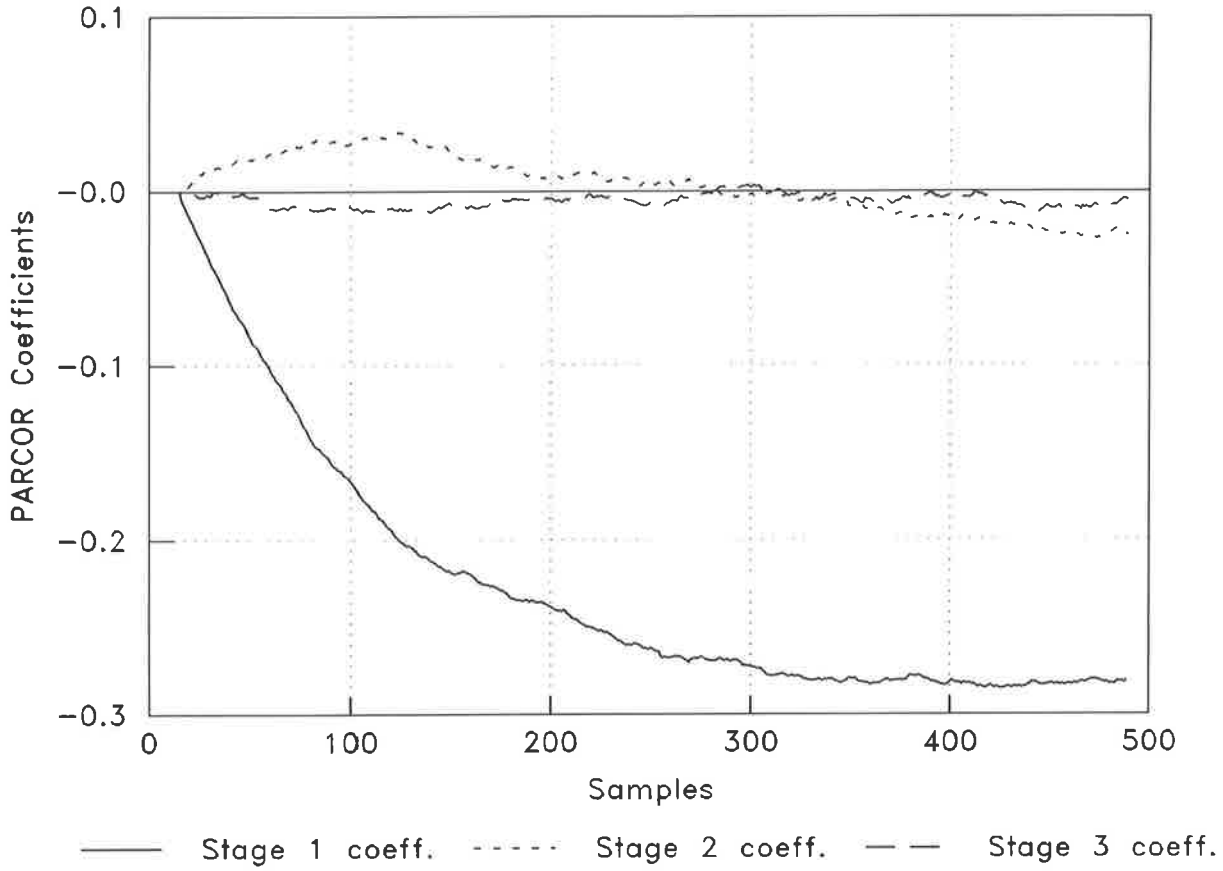

Figure 5-5. PARCOR coefficients for different stages of the lattice filter, fed with a 400Hz band passed (300Hz centre frequency) white noise input/reference signal.

5.3.2 Self Induced Noise

In this section the Independent Quadratic Optimisation algorithm implementation is assessed before conducting tests using actuators and sensors that could be damaged (eg. piezoceramic crystals). All the control filter coefficients were initialised to the maximum positive 16 bit integer (2's complement) of 32767. The control signal generated was fed

directly back into the controller through an error signal input. The cancellation path transfer function therefore comprised of the delays, phase and amplitude changes in the converters, and anti-aliasing and reconstruction filters. This system is shown in Figure 5-6(a).

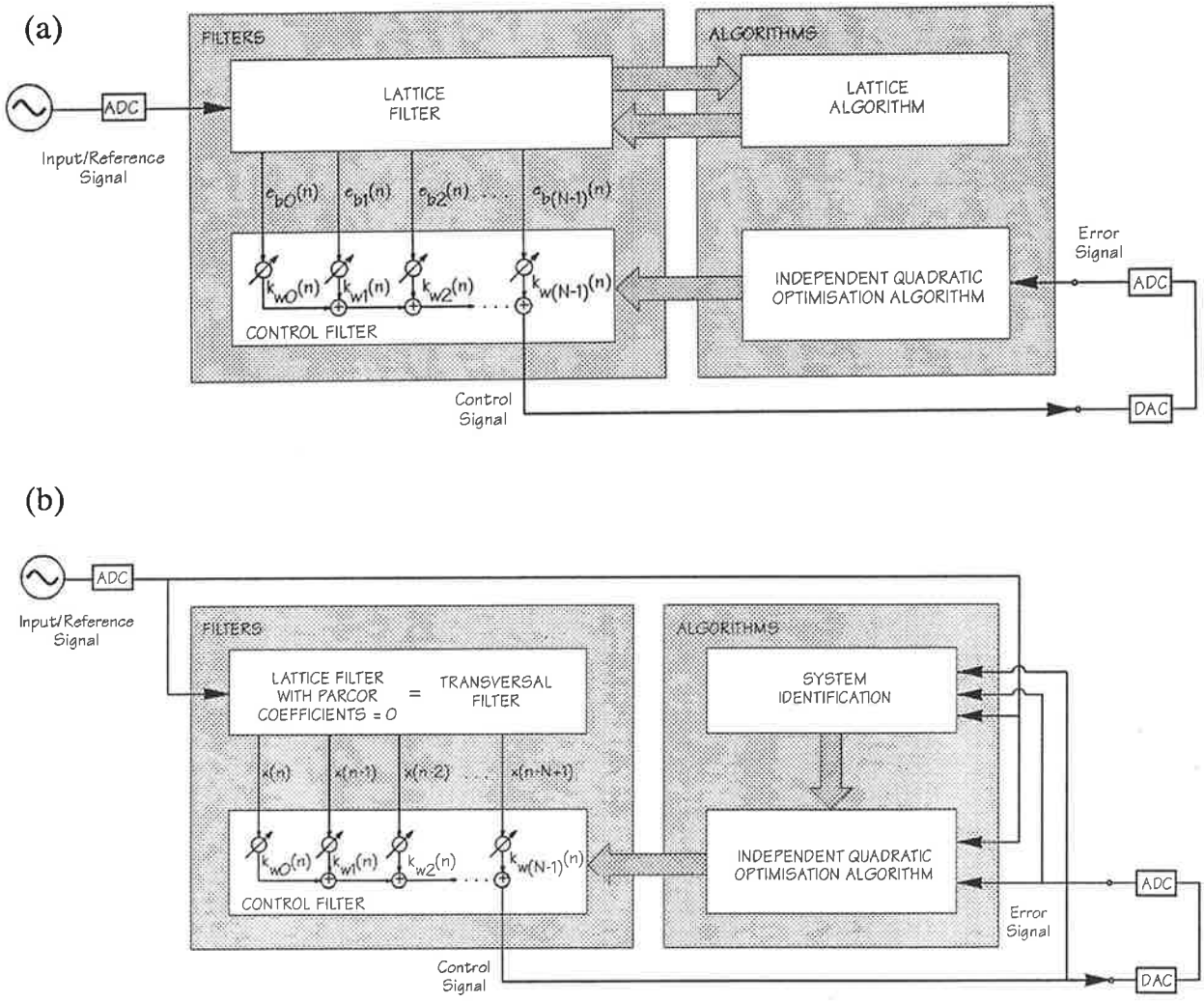

Figure 5-6(a) and (b). Structure for the control of self induced noise, with the control signal is fed directly back as the error signal. $e_{bi}(n)$ represent the backward prediction errors, $k_{wi}(n)$ represent the control filter coefficients, and $x(n)$ represent the reference signal. The Analogue to Digital Converter is shown as ADC, and the Digital to analogue converter is likewise DAC.

Throughout this work the Independent Quadratic Optimisation algorithm was considered to commence with the adaptation of the lattice filter PARCOR coefficients. As the lattice filter PARCOR coefficients were initialised to zero, it acted initially as a tapped-delay-line (transversal filter), and therefore the before control situation was identical to that for the filtered-X LMS algorithm, as shown in Figure 5-6(b). The attenuation achieved by the Independent Quadratic Optimisation algorithm, for each type of input/reference signal, will be directly compared with that achieved by the filtered-X LMS algorithm. The influence of the various Independent Quadratic Optimisation algorithm parameters on the attenuation of self induced noise will be assessed for a pure tone, multi-tones and band-passed white noise reference signals.

Consider firstly the attenuation of a pure tone reference signal with a frequency of 125 Hz. The control filter had two coefficients. Figures 5-7 (a) and (b) show the path of the control filter coefficients to the optimum of the cost function (shown by contours), when adapted by the Independent Quadratic Optimisation algorithm and filtered-X LMS algorithms respectively. The corresponding error signals are shown in Figures 5-8 (a) and (b). It is interesting to note the difference in the path of the control filter coefficients to the optimum and the comparative speed in reaching the optimum, between the Independent Quadratic Optimisation algorithm and the filtered-X LMS algorithm. Note that a system identification is performed by the filtered-X LMS algorithm between 0 and 2000 samples (also using only two filter coefficients to identify the cancellation path transfer function). The convergence coefficient for the filtered-X LMS algorithm was increased to its value corresponding to "critical convergence", and the Independent Quadratic Optimisation algorithm used only 10 averages to estimate the cost function (approximately one period of the error signal), though with a delay of 50 before averaging (this is considered to have been too long, but no shorter delays were tested).

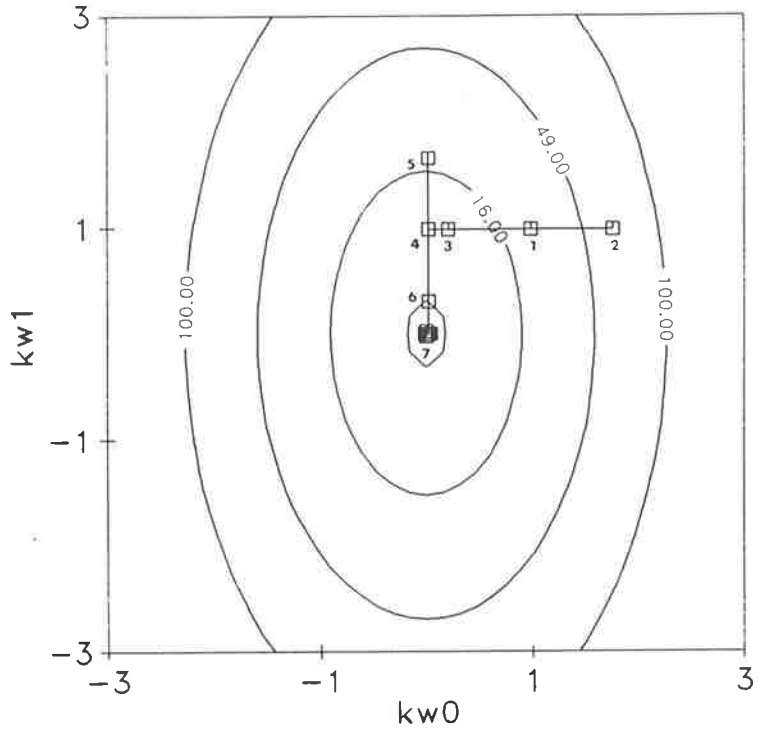

Figure 5-7(a). Path of the independent control filter coefficients ⊡—— (shown as *kw0* and *kw1*) used by the Independent Quadratic Optimisation algorithm, to reach the optimum of the cost function (represented by the contours ——) for a self-induced pure-tone (125 Hz) disturbance. The cost function estimates are represented by a □.

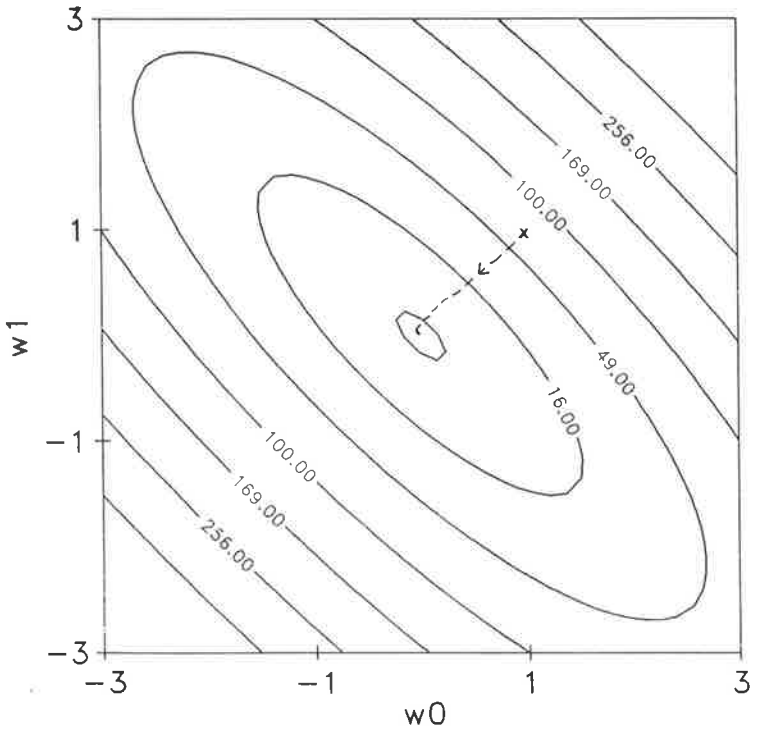

Figure 5-7(b). Path of the control filter coefficients ---- (shown as *w0* and *w1*) used by the filtered-X LMS algorithm to reach the optimum of the cost function (represented by contours ——) for a self-induced pure-tone (125 Hz) disturbance.

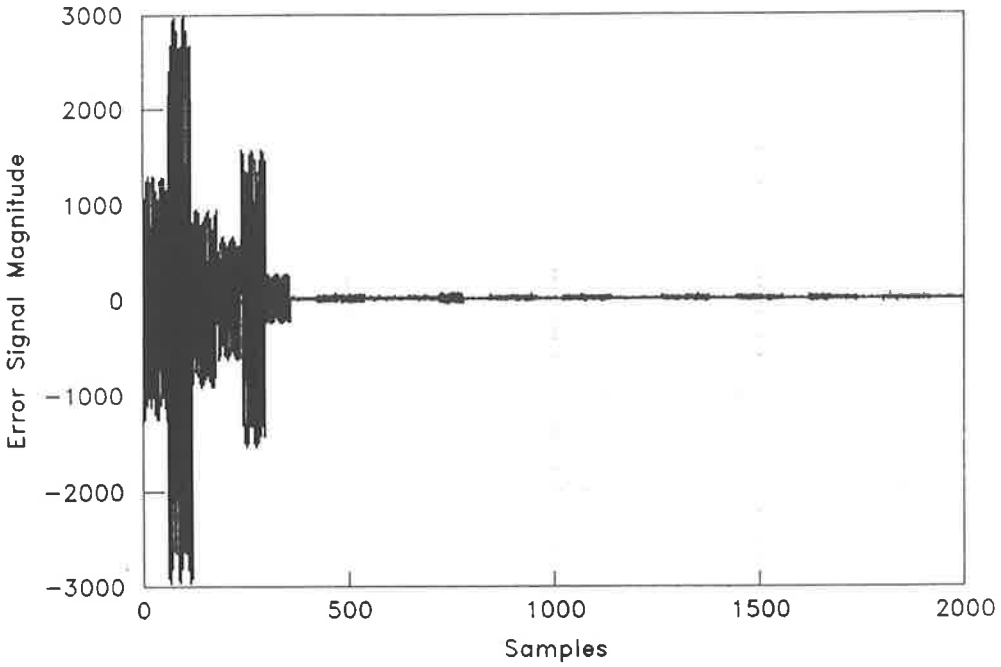

Figure 5-8(a). Error signal magnitude versus sample number, using the Independent Quadratic Optimisation algorithm to minimise the error, for a self-induced pure-tone (125 Hz) disturbance.

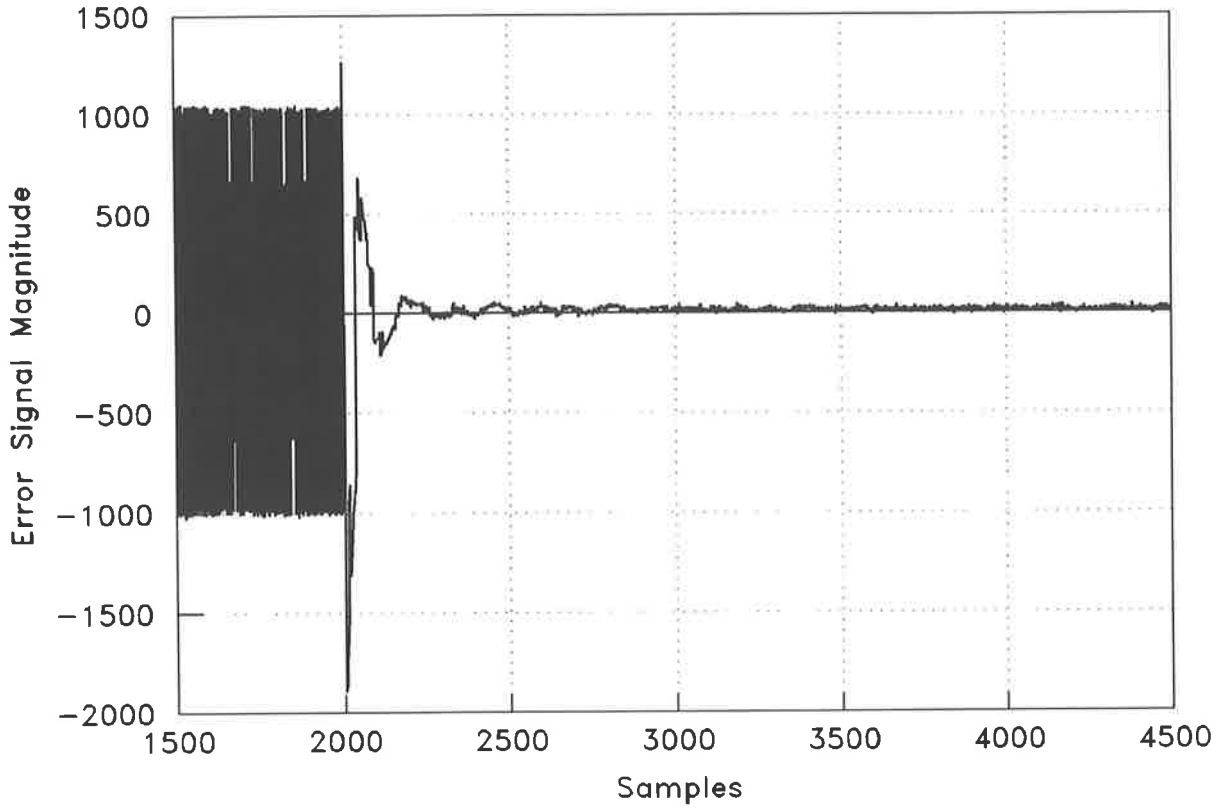

Figure 5-8(b). Error signal magnitude versus sample number, using the Independent Quadratic Optimisation algorithm to minimise the error, for a self-induced pure-tone (125 Hz) disturbance.

It is apparent from Figure 5-7 (a) and (b) that the control filter coefficients used by the Independent Quadratic Optimisation algorithm formed principal axes of the cost function (ie. they were independent), while the control filter coefficients used by the filtered-X LMS algorithm were not principal axes of the cost function (ie. they were dependent). Finally it is worth noting the minimum variance of the control filter coefficients upon reaching the optimum, resulting in reduced excess mean square error.

It is interesting to compare the attenuation achieved by each algorithm, shown in Figure 5-9 (the peak at 150 Hz is from a ground loop). As shown Figure 5-9, the filtered-X LMS algorithm achieves an additional 20 dB of attenuation over the Independent Quadratic Optimisation algorithm. This is considered to result from extraneous noise in the error signal that is uncorrelated with the error signal. That is, the filtered-X LMS algorithm uses the instant error signal to adapt the control filter coefficients, whereas the Independent Quadratic Optimisation algorithm uses the cost function estimates, thereby losing frequency content information. Figure 5-10 shows the effect of the number of averages on the level of attenuation (the peak at 150 Hz is from a ground loop). In Figure 5-10, case 1 corresponds to 500 samples, case 2 corresponds to 250 samples, and case 3 corresponds to only 10 samples (ie. one complete period) of the error signal used to estimate the cost function. It is apparent from Figures 5-9 and 5-10, that despite the low number of samples of the error signal used to estimate the cost function, the attenuation remained unchanged at the frequency corresponding to the pure tone (ie. 125 Hz). The attenuation at frequencies on either side of the tone was reduced for case 3 since the control filter coefficients were adapted at a faster rate than for the other cases, and with fixed variance (step size).

Figure 5-11 shows the convergence of the error signal with a control filter coefficient step size factor one tenth that used to obtain the error signal in Figure 5-8(a). It is apparent from comparing Figure 5-8(a) and Figure 5-11, that a lower control filter coefficient step size factor results in slower convergence as the quadratic fit is not as accurate. It is also apparent, from a comparison of the error signal after convergence, that the excess mean square error is however reduced with a lower control filter coefficient step size factor.

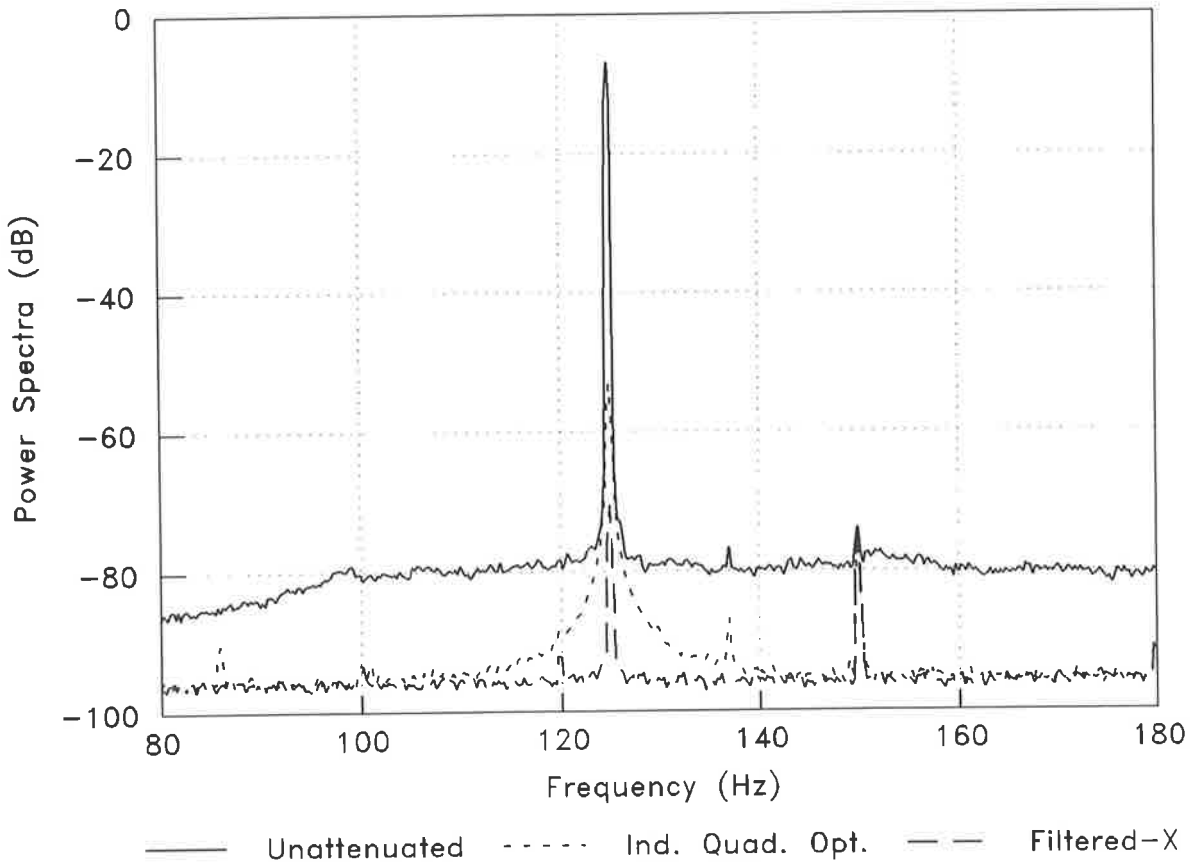

Figure 5-9. Comparison of the reduction of self induced pure tone (125 Hz) disturbance by the Independent Quadratic Optimisation algorithm and the filtered-X LMS algorithm. The power spectra of the error signal before and after control is shown versus frequency.

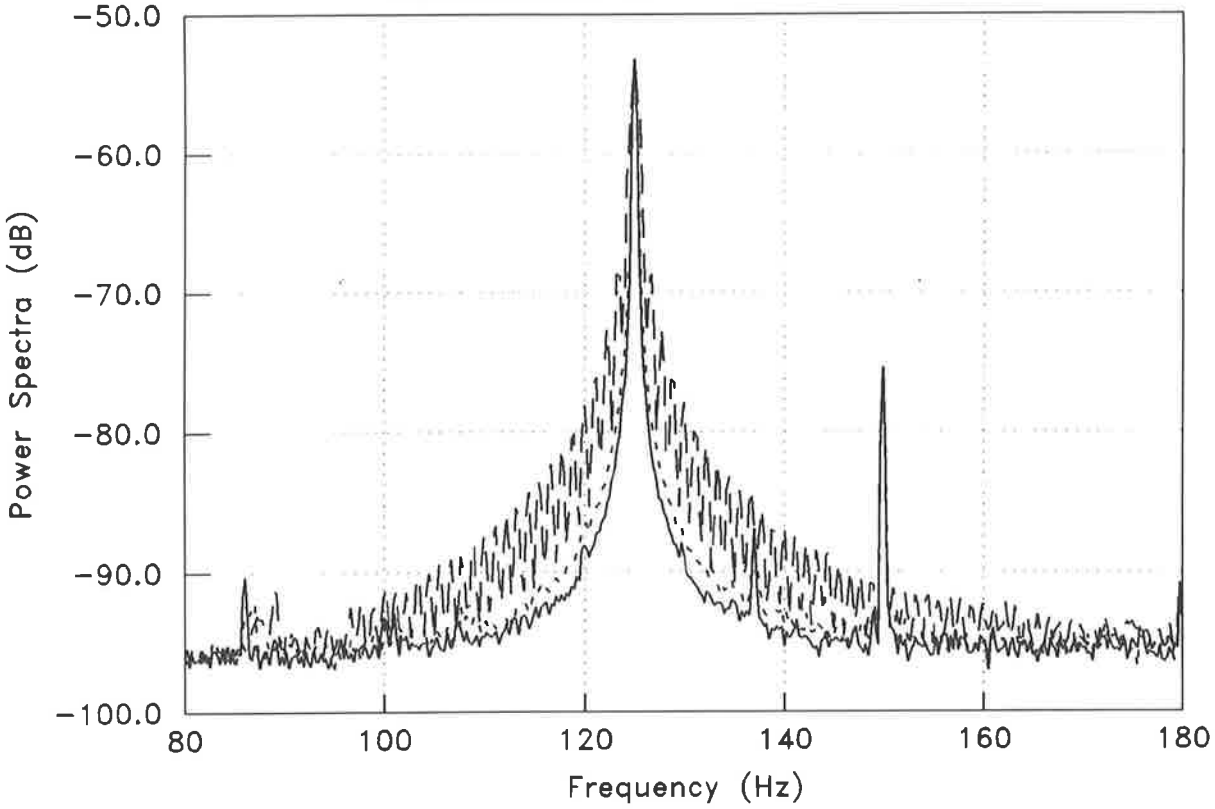

Figure 5-10. Comparison of the power of the error signal after control of self induced pure tone (125 Hz) disturbance by the Independent Quadratic Optimisation algorithm with differing numbers of samples of the error signal used to estimate the cost function. Case 1 (——) used 500 estimates, case 2 (- - - -) used 250 estimates and case 3 (— —) used 10 estimates.

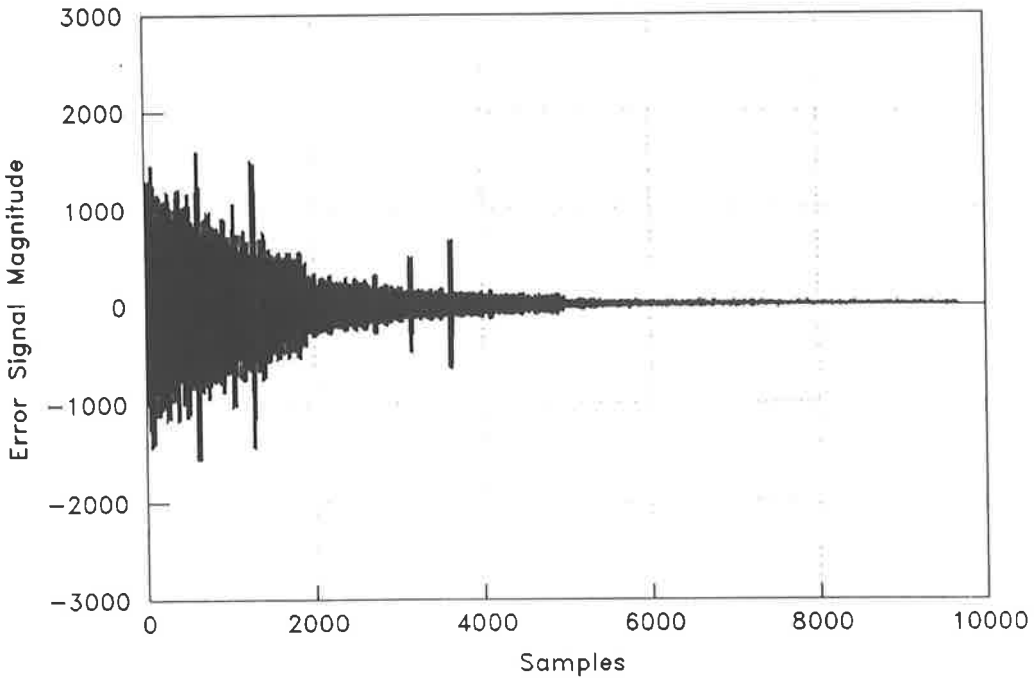

Figure 5-11. Error signal magnitude versus sample number, using the Independent Quadratic Optimisation algorithm to minimise the self induced pure tone (125 Hz) disturbance, with the control filter coefficient step size factor one tenth that used for the error signal shown in Figure 5-8(a).

The Independent Quadratic Optimisation algorithm was tested with a reference signal containing two tones, namely 125 Hz and 156.25 Hz. The attenuation obtained for the Independent Quadratic Optimisation algorithm in this case was greater than that for the filtered-X LMS algorithm, as shown in Figure 5-12. This was most likely a result of the eigenvalue disparity, as was evident from the error signal for the filtered-X LMS algorithm (although not shown here), which initially converged quickly and then converged very slowly to the optimum of the cost function. The control filter for both algorithms used four coefficients.

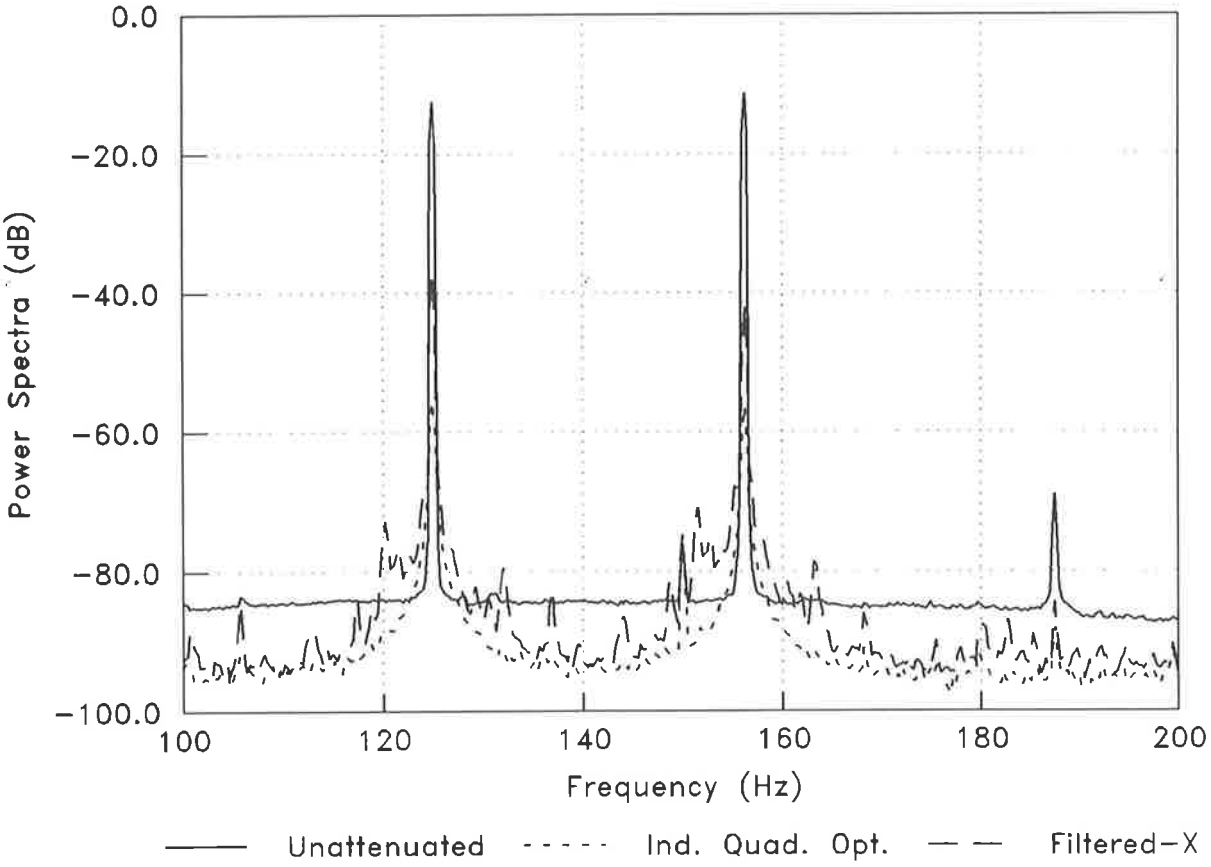

Figure 5-12. Comparison of the reduction of self induced noise (from 125 Hz and 156.25 Hz tones) by the Independent Quadratic Optimisation algorithm and the filtered-X LMS algorithm. The power spectra of the error signal before and after control is shown versus frequency.

Finally a reference signal comprised of white noise filtered through a band-pass filter with a centre frequency of 300 Hz (and with variable bandwidth) was considered. Figures 5-13 (a) to (d) show a comparison of the attenuation achieved between the Independent Quadratic Optimisation algorithm and the filtered-X LMS algorithm for band passed white noise centred at 300 Hz with bandwidths of 50 Hz, 100 Hz, 200 Hz and 400 Hz respectively. It is apparent from these Figures that the bandpass filter was not ideal, with not all frequencies passed. Both algorithms used 8 control filter coefficients. The Independent Quadratic Optimisation algorithm used 500 averages, with the control filter coefficient step size factor equivalent to that used for the analysis of pure tones.

It is apparent from Figures 5-13 (a) to (d) that generally the filtered-X LMS algorithm performs better, particularly at high frequencies (greater than 300 Hz), than the Independent Quadratic Optimisation algorithm. This is considered to result from the filtered-X LMS algorithm using the error signal directly to adapt the control filter coefficients rather than adapting them based on the cost function estimate, thereby losing frequency information within the signal. It is also considered that complete attenuation was not possible as the delay in the cancellation path exceeded the number of control filter coefficients (in later sections a FIFO will be used to reduce the required number of control filter coefficients as determined by the delay in the cancellation path transfer function).

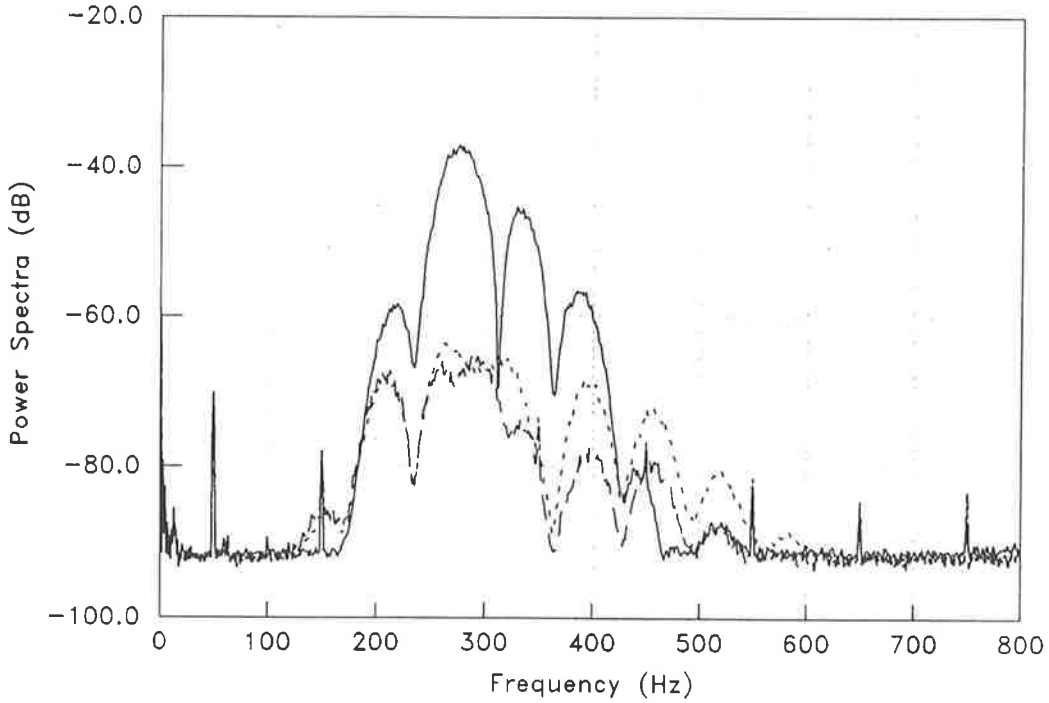

Figure 5-13(a). Comparison of the reduction of self induced noise (white noise filtered through a band pass filter with a width of 50 Hz and centre frequency of 300 Hz) by the Independent Quadratic Optimisation algorithm (- - - -) and the filtered-X LMS algorithm (— —). The power spectra of the error signal before (——) and after control is shown versus frequency.

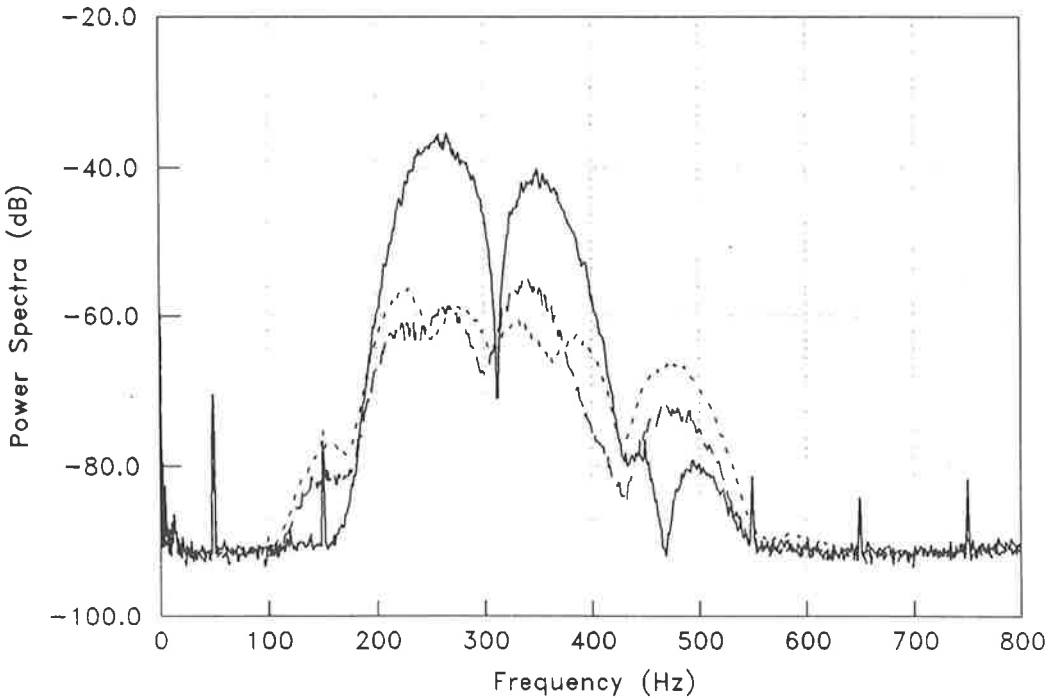

Figure 5-13(b). Comparison of the reduction of self induced noise (white noise filtered through a band pass filter with a width of 100 Hz and centre frequency of 300 Hz) by the Independent Quadratic Optimisation algorithm (- - - -) and the filtered-X LMS algorithm (— —). The power spectra of the error signal before (——) and after control is shown versus frequency.

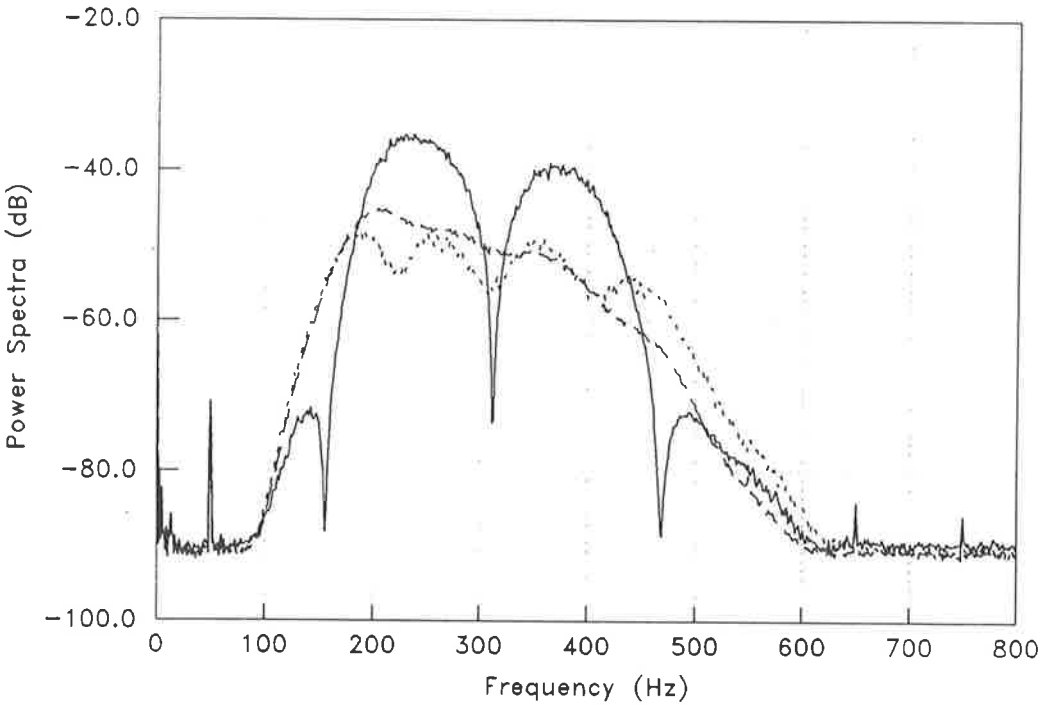

Figure 5-13(c). Comparison of the reduction of self induced noise (white noise filtered through a band pass filter with a width of 200 Hz and centre frequency of 300 Hz) by the Independent Quadratic Optimisation algorithm (- - - -) and the filtered-X LMS algorithm (— —). The power spectra of the error signal before (———) and after control is shown versus frequency.

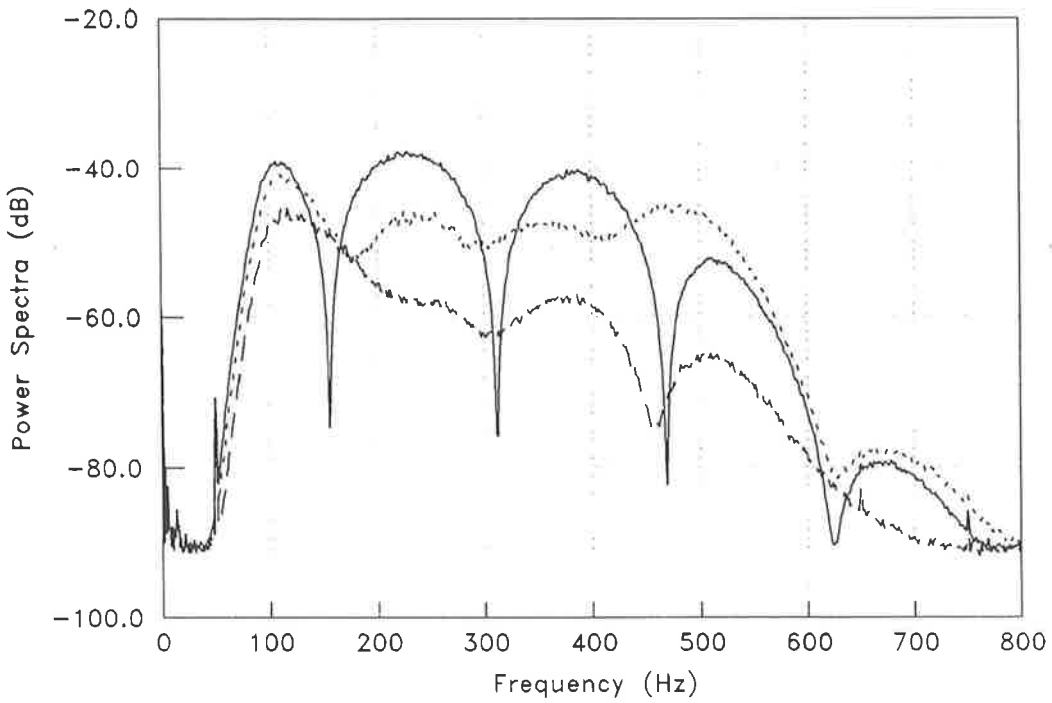

Figure 5-13(d). Comparison of the reduction of self induced noise (white noise filtered through a band pass filter with a width of 400 Hz and centre frequency of 300 Hz) by the Independent Quadratic Optimisation algorithm (- - - -) and the filtered-X LMS algorithm (— —). The power spectra of the error signal before (———) and after control is shown versus frequency.

5.4 Acoustic Control

In section 5.3 the Independent Quadratic Optimisation algorithm implementation and lattice filter implementation were briefly assessed, based on control of self-induced noise (where the cancellation path is effectively a certain number of samples delay), and shown to work effectively for control of pure tone, multi-tone and band passed white noise signals.

In this section results will be presented in more detail, for the performance of a single channel controller incorporating the Independent Quadratic Optimisation algorithm, when tested on an actual acoustic system with more general actuator and sensor transfer functions. More specifically, the performance of the Independent Quadratic Optimisation algorithm will be compared with the filtered-X LMS algorithm, for various types of disturbances (those used in chapter 3 and 4), in terms of convergence speed, achievable attenuation, bandwidth of attenuation, and the ability to track changing system conditions. The effects of the Independent Quadratic Optimisation algorithms parameters (specifically number of samples used to estimate the cost function, and the control filter coefficient step size, and the power of the backward prediction error signals and associated number of control filter coefficients) on control performance will also be assessed and compared with the theory developed in chapter 4, with regard to the same performance descriptive terms.

The system used was a replica of a small air-conditioning duct constructed from 0.8mm galvanised sheet metal, with dimensions 215mm x 215mm square. The duct was

terminated anechoically at one end, and a disturbance loudspeaker (with a cone diameter of about 100mm) was placed at the other end of the duct. A control loudspeaker (with a cone diameter of about 100mm) was placed mid-way along the duct, and an error sensing microphone was placed towards the end of the duct. The layout is shown in Figure 5-14.

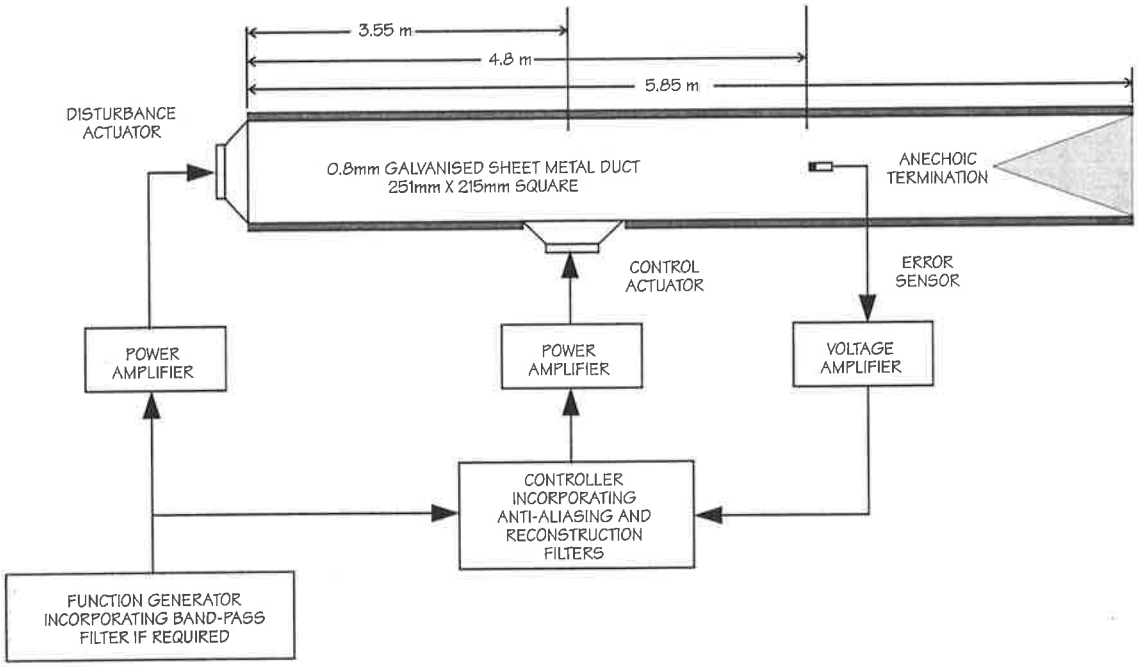

Figure 5-14. Layout of acoustic control structure; A detailed description of the controller layout is shown in Figure 5-1.

Control of a pure tone was firstly attempted. The attenuation achieved for this system using the Independent Quadratic Optimisation algorithm and the filtered-X LMS algorithm are shown in Figure 5-15. Figure 5-15 gives the power spectra of the error signal before control and after control. It is apparent that both algorithms achieve the same level of attenuation using only two control filter coefficients. It is also apparent

that the bandwidth of attenuation by the filtered-X LMS algorithm is greater than that for the Independent Quadratic Optimisation algorithm. It is considered that this results from the filtered-X algorithm using the error signal sample to adapt the control filter coefficients, whereas the Independent Quadratic Optimisation algorithm uses the estimate of the cost function to adapt the control filter coefficients, thereby losing information about the frequency content of the error signal; That is, the cost function estimate is affected by the power of the other frequencu components of the error signal. The fixed variance of the control filter coefficients at the optimum also reduces the bandwidth of attenuation about the tone.

Figure 5-16 gives a comparison of the power spectra of the error signal for differing parameters of the Independent Quadratic Optimisation algorithm. Case 1 can be considered the standard, with case 2 having twice the control filter coefficient step size factor as case 1, and case 3 having ten times as many samples used to estimate the cost function as case 1. It is apparent that increasing the number of averages narrows the bandwidth of the error signal spectra about the tone. This is considered to result from less variance in the error signal as the control filter coefficients are adapted less frequently, and improved accuracy of the cost function estimates as a result of an increased number used of samples used in the estimation (although it would be expected that the attenuation at the frequency of the tone would increase with improved accuracy of the estimates, which is not evident from Figure 5-16). Increasing the control filter coefficient step size factor had little effect on the power spectra of the error signal, however on viewing the error signals for cases 1 and 2 (not shown here) the excess mean square error was found to increase with the increased control filter coefficient step size factor (as found in section 5.3). Both changes from the standard (case 1) did not result in increased attenuation.

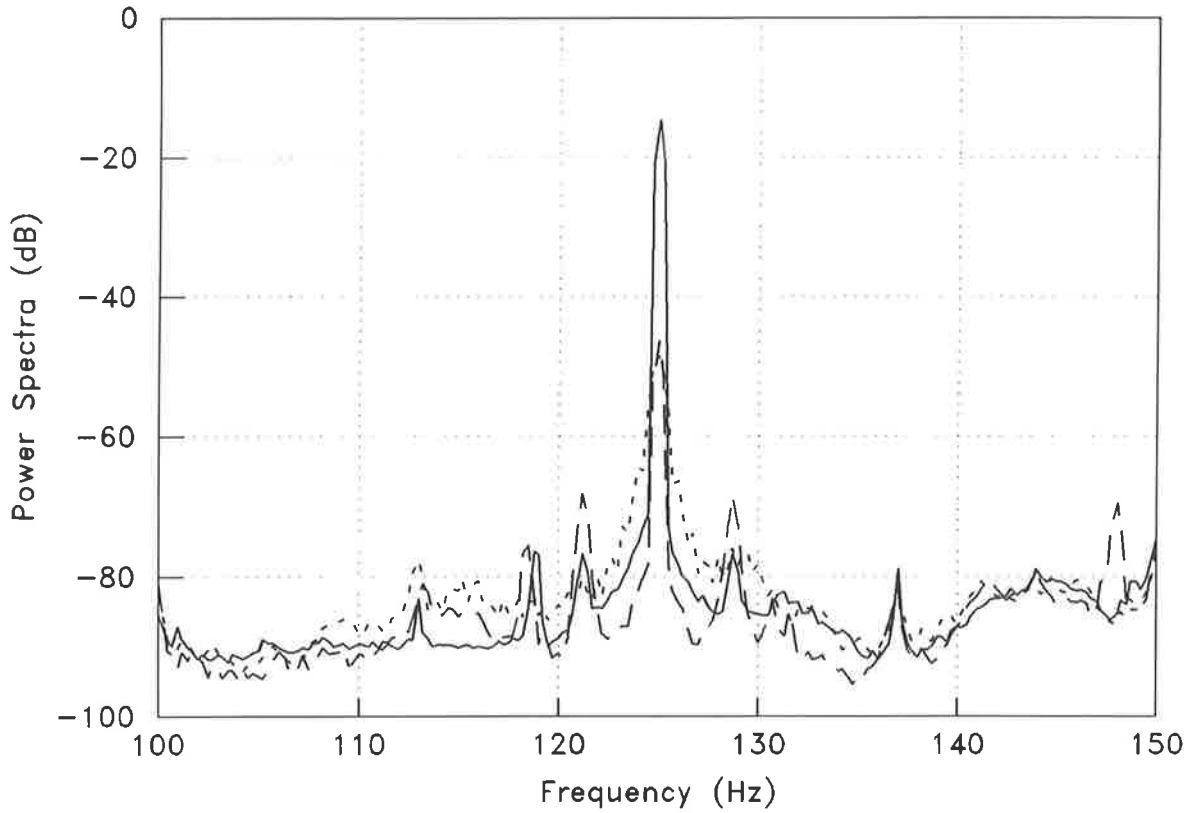

Figure 5-15. Comparison of the reduction of a pure tone in the acoustic test apparatus by the Independent Quadratic Optimisation algorithm (- - -) and the filtered-X LMS algorithm (— —). The power spectra of the error signal before (——) and after control is shown versus frequency.

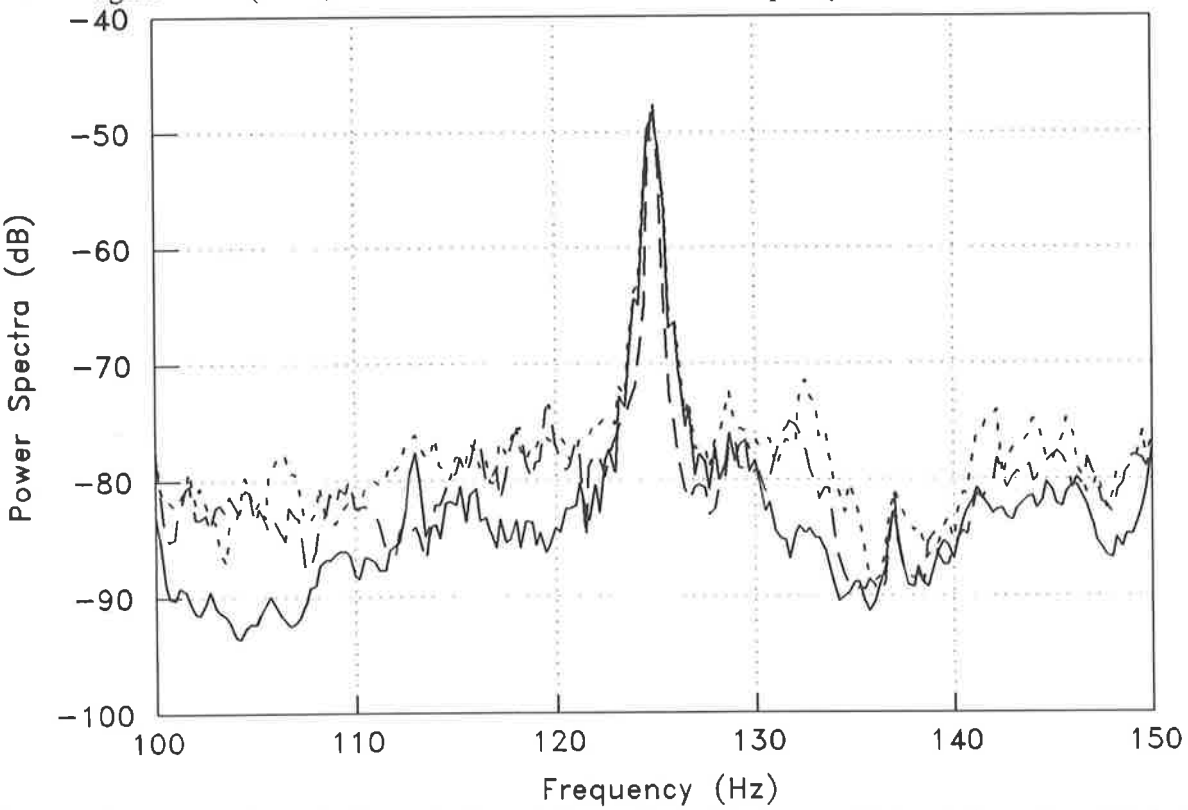

Figure 5-16. Comparison of the reduction of the acoustic disturbance by the Independent Quadratic Optimisation algorithm using case 1 (——) as the standard, with case 2 (- - - -) having twice the control filter coefficient step size factor as case 1, and case 3 (— —) having ten times as many samples used to estimate the cost function as case 1. The power spectra of the error signal after control is shown versus frequency.

The tracking ability of the Independent Quadratic Optimisation algorithm was examined. Control of a tone at 125 Hz was firstly achieved. The frequency of the tone was then changed to 156.25 Hz. This test was performed for both the Independent Quadratic Optimisation algorithm and the filtered-X LMS algorithm. A system identification was performed on-line by the filtered-X LMS algorithm. As with all other tests, the control filter coefficients were initialised to zero. Only two control filter coefficients were used by both algorithms.

Figures 5-17 and 5-18 show control of the disturbance by the Independent Quadratic Optimisation algorithm. Figure 5-17 shows the error signal initially converging for 125 Hz, and subsequently converging as the frequency is changed instantly to 156.25 Hz. Figure 5-18 shows the path of the control filter coefficients (with the cost function estimates numbered), mapped onto the contours of the cost functions for a tone of 125 Hz and a tone of 156.25 Hz. Figure 5-19 and 5-20 show similar results for the error signal and control filter coefficients, as control is performed by the filtered-X LMS algorithm.

A comparison of the error signals shown in Figures 5-17 and 5-19 shows that initially the filtered-X LMS algorithm needs to identify the system before control can commence (ie. system identification performed up to sample number 2000). Control by the filtered-X LMS algorithm appears to be slower than that by the Independent Quadratic Optimisation algorithm, probably resulting from the use of a control filter convergence coefficient that was too small. As the frequency was suddenly changed, the error signal corresponding to the Independent Quadratic Optimisation algorithm deviated to a larger extent than the filtered-X LMS algorithm. If the lattice filter implementation had used

the Recursive Least Squares algorithm to adapt the PARCOR coefficients, then the error ratio used by this adaptation method would have indicated a sudden change in the reference signal. This could be used by the Independent Quadratic Optimisation algorithm to alert it of an imminent change, and cause it to reset the control filter coefficients before adapting to the change. It should be noted that the Independent Quadratic Optimisation algorithm is not designed for fast tracking capabilities, but for more stable control of noise and vibration in slowly changing system conditions. It should however be noted that if the sudden system change had been too immediate to be tracked by the on-line system identification algorithm used by the filtered-X LMS algorithm, it could have caused instability in this algorithm, whereas the Independent Quadratic Optimisation algorithm would not have been affected as it requires no knowledge of the cancellation path.

Finally a comparison between the paths of the control filter coefficients shown by Figures 5-18 and 5-20 show the difference in the orthogonal nature of the coefficients used by the Independent Quadratic Optimisation algorithm, as opposed to the non-orthogonal nature of those used by the filtered-X LMS algorithm. It is apparent from Figure 5-18 that the variance in the control filter coefficients is reduced upon reduction of the cost function, resulting in reduced excess mean square error at the optimum. From Figure 5-18, it is apparent that more than one curve-fit is required to reach the optimum; This is because of the effect of extraneous (or uncorrelated) noise on the accuracy of the cost function estimates. The path of the control filter coefficients to the optimum, as adapted by the filtered-X LMS algorithm appears to be oscillating, and drifting away from the optimum, possibly a result of DC offsets.

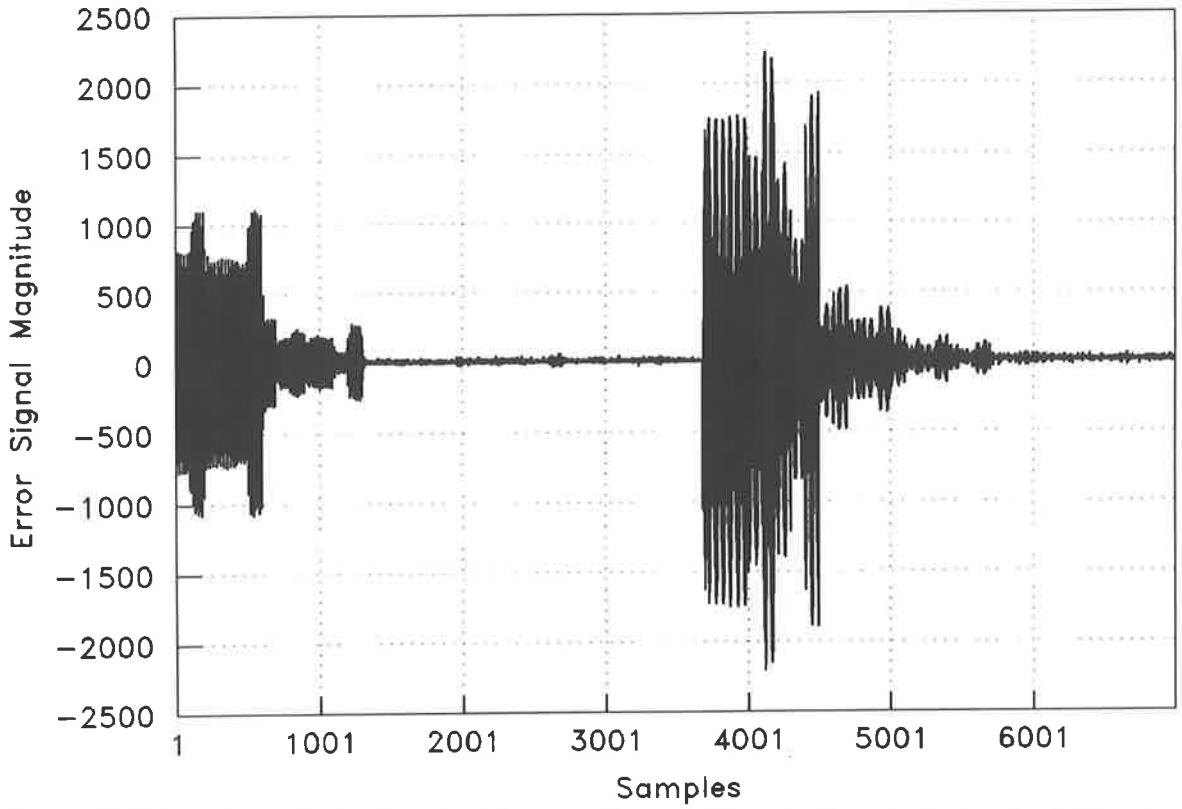

Figure 5-17. The error signal showing the ability of the Independent Quadratic Optimisation algorithm to track changing system conditions. The error signal magnitude is shown versus the number of samples.

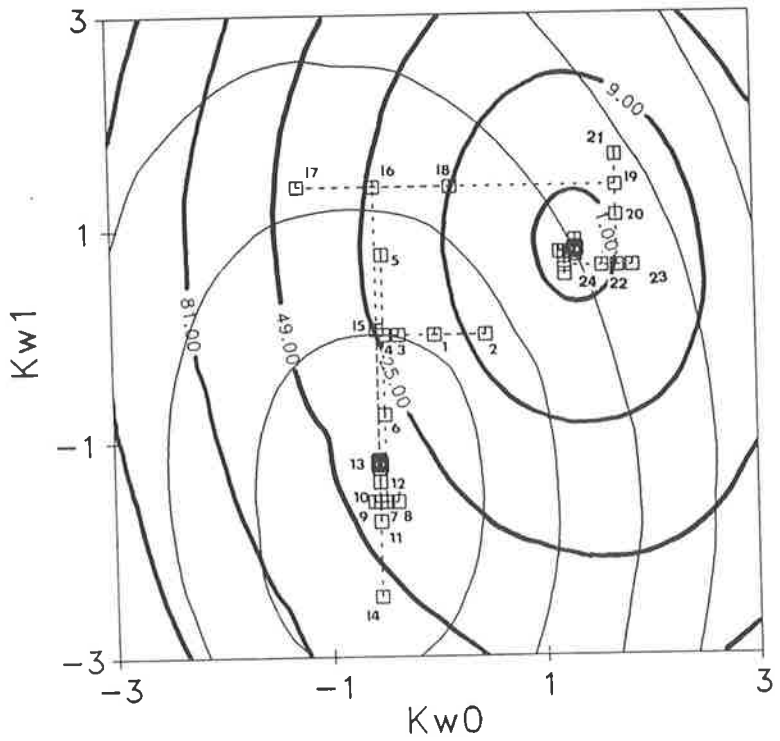

Figure 5-18. Path of the control filter coefficients ·····□ to the optimum of the cost functions for 125 Hz (represented by contours ———), and 156.25 Hz (represented by contours ———). The cost function estimates (numbered) are represented by □ . The control filter coefficients are adapted by the Independent Quadratic Optimisation algorithm.

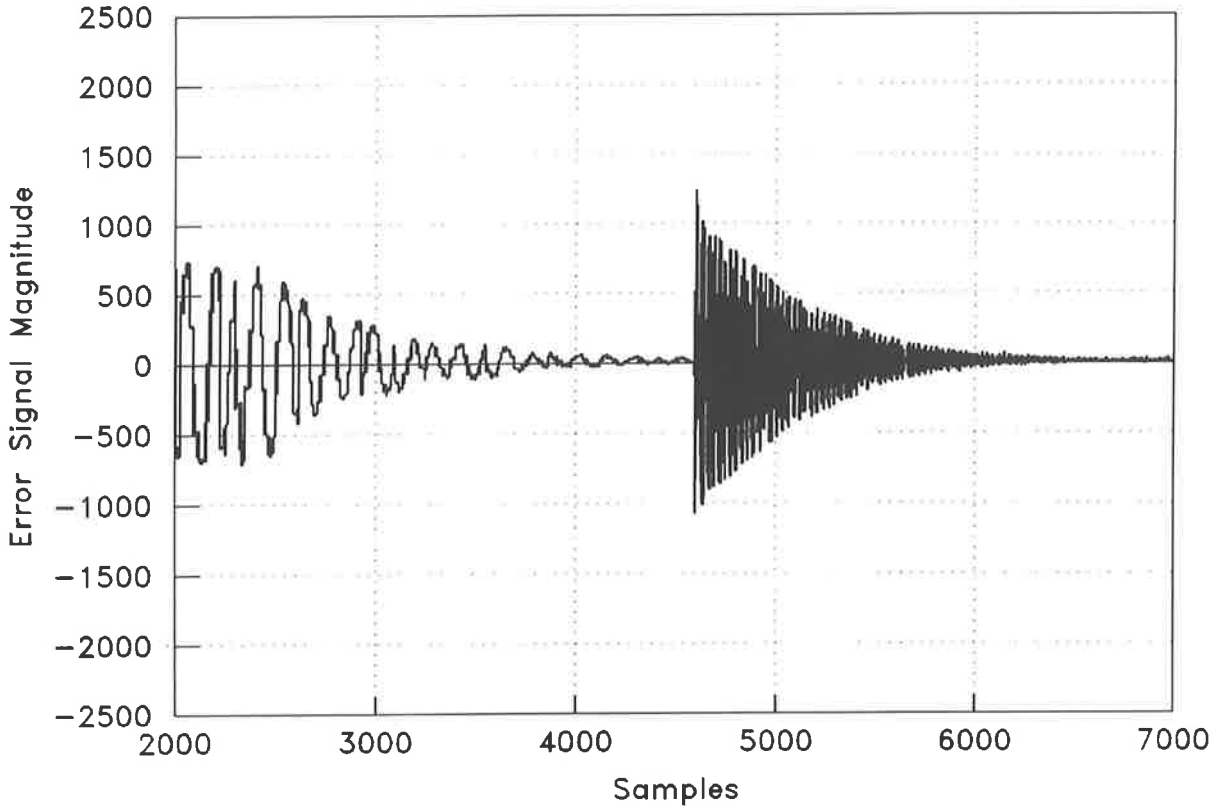

Figure 5-19. The error signal showing the ability of the filtered-X LMS algorithm to track changing system conditions. The error signal magnitude is shown versus the number of samples.

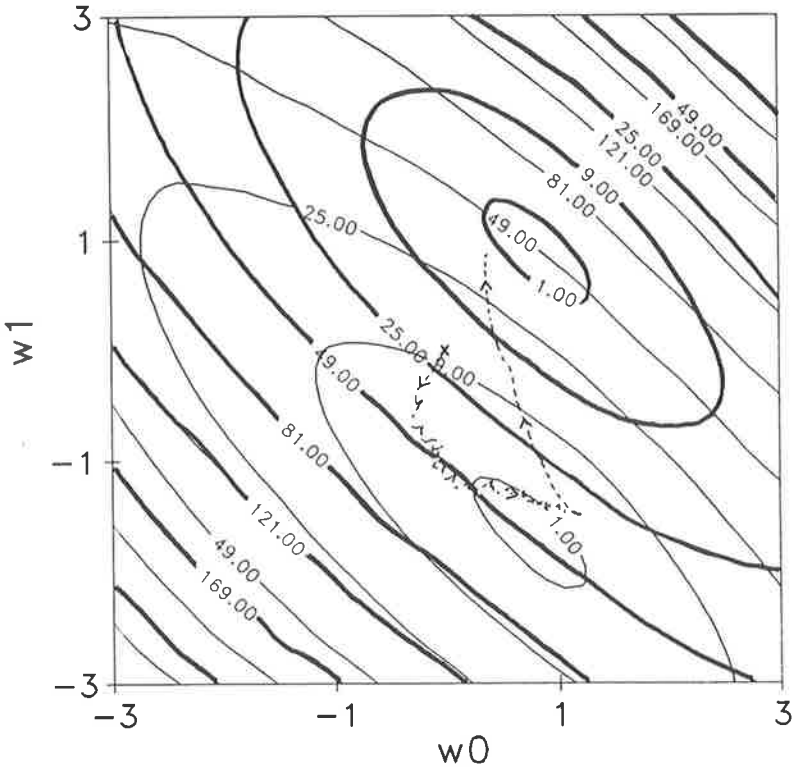

Figure 5-20. Path of the control filter coefficients ----- to the optimum of the cost functions for 125 Hz (represented by contours ———), and 156.25 Hz (represented by contours ———). The control filter coefficients are adapted by the filtered-X LMS algorithm.

The final test for control of a disturbance consisting of a pure tone, was to corrupt the pure tone using variable magnitude band passed white noise. The tone used had a frequency of 125 Hz. The band pass filter had a bandwidth of 50 Hz and a centre frequency of 125 Hz, but was without an ideal flat response. Results are shown for the tone 15 dB and 35 dB above the level of filtered white noise, in Figure 5-21 (a) and (b) respectively. Figures 5-21 (a) to (c) show the power spectra of the error signal before and after control by the Independent Quadratic Optimisation algorithm, and the filtered-X LMS algorithm. Only two control filter coefficients were used by both algorithms. It is apparent from Figures 5-21(a) to (c), that the filtered-X LMS algorithm achieves almost twice as much attenuation as the Independent Quadratic Optimisation algorithm. This is considered to result from the use of the error signal samples to directly adapt the control filter coefficients, as opposed to the Independent Quadratic Optimisation algorithm which uses the error signal to estimate the cost function estimates thereby losing information about the frequency content of the error signal. The Independent Quadratic Optimisation algorithm therefore attempts to cancel other disturbances, even if they aren't correlated to the reference signal. This effect has been noted previously. The number of control filter coefficients was insufficient to result in cancellation of the filtered white noise, as expected.

The path of the control filter coefficients to the optimum for a pure tone 35 dB above the level of filtered white noise, as adapted by the Independent Quadratic Optimisation algorithm, is shown in Figure 5-22. Figure 5-22 also indicates a reason for less attenuation by the Independent Quadratic Optimisation algorithm compared with the filtered-X LMS algorithm, since there appears a large variance of the control filter coefficients about the optimum. The variance of the control filter coefficients about the optimum, as adapted by the filtered-X LMS algorithm, are shown in Figure 5-23. It is apparent from Figure 5-23 that the variance after convergence is smaller (as a result of a lower minimum mean square error) than that caused by the Independent Quadratic Optimisation algorithm.

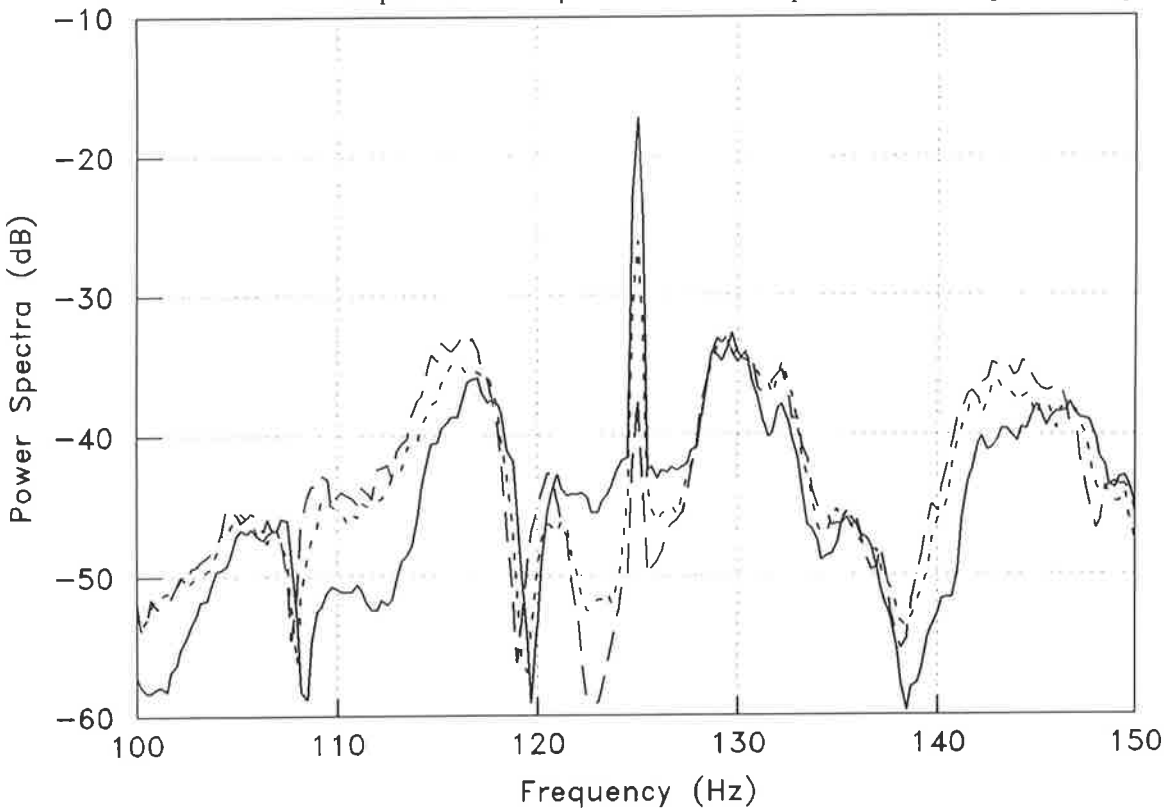

Figure 5-21(a). The power spectra of the error signal before (——) and after control by the Independent Quadratic Optimisation algorithm (- - - -) and the filtered-X LMS algorithm (— —). The disturbance comprised a tone at 125 Hz corrupted by band pass filtered white noise (bandwidth of 50 Hz and centre frequency of 125 Hz). The tone was 15 dB above the filtered white noise level.

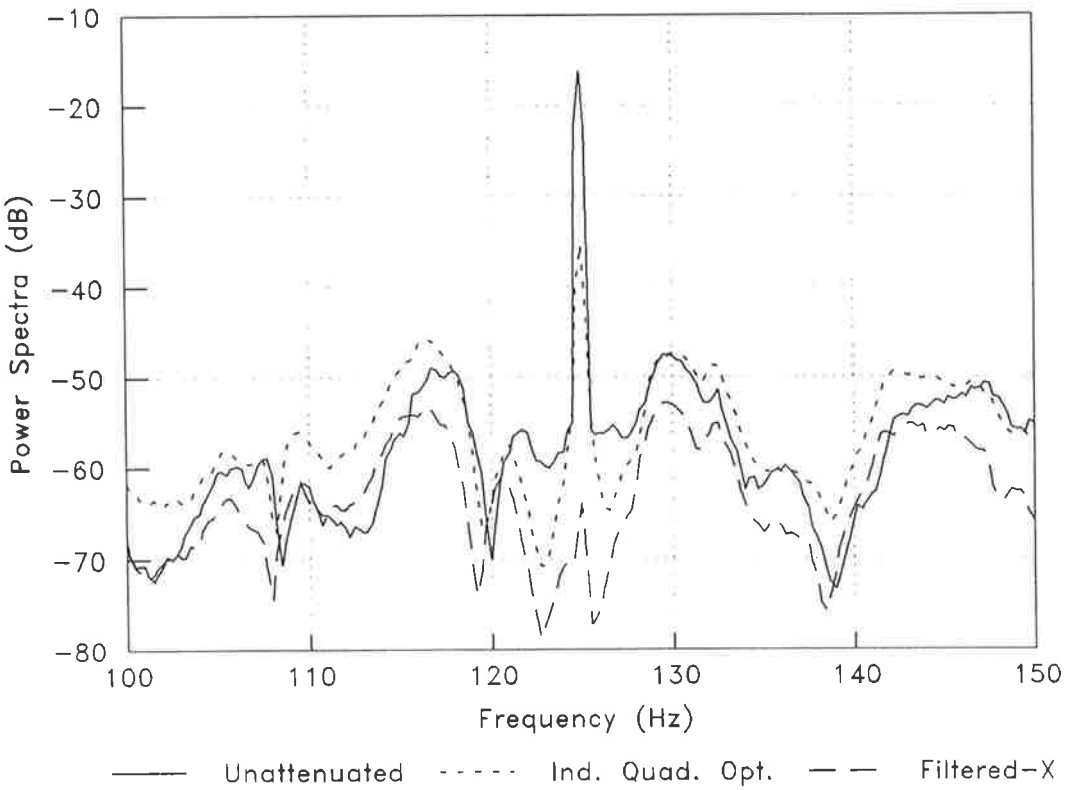

Figure 5-21(b). The power spectra of the error signal before and after control by the Independent Quadratic Optimisation algorithm and the filtered-X LMS algorithm. The disturbance comprised a tone at 125 Hz corrupted by band pass filtered white noise (bandwidth of 50 Hz and centre frequency of 125 Hz). The tone was 35 dB above the filtered white noise level.

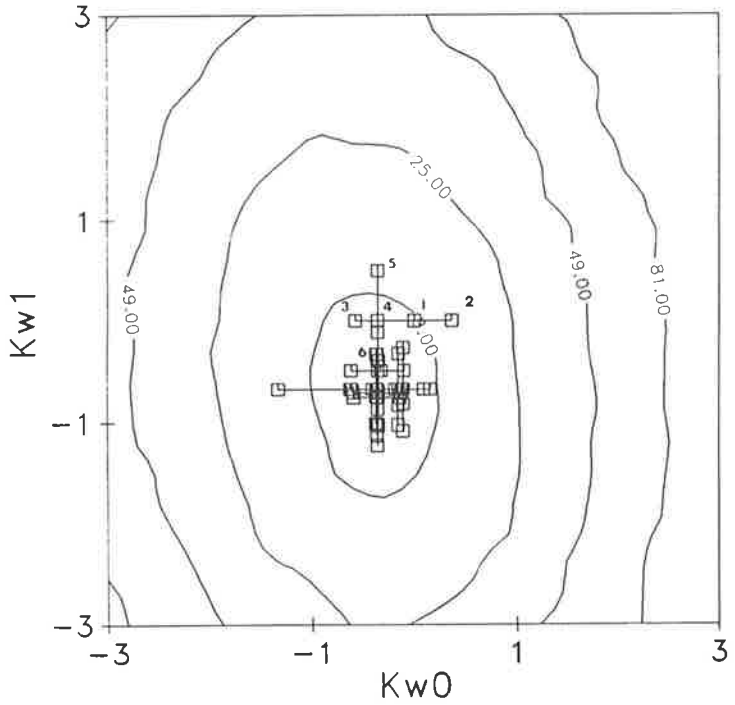

Figure 5-22. Path of the control filter coefficients ⊡—— to the optimum of the cost function (represented by contours ——). The cost function estimates are represented by □ . The control filter coefficients are adapted by the Independent Quadratic Optimisation algorithm. The disturbance comprised a tone at 125 Hz corrupted by band pass filtered white noise (bandwidth of 50 Hz and centre frequency of 125 Hz). The tone was 35 dB above the filtered white noise level.

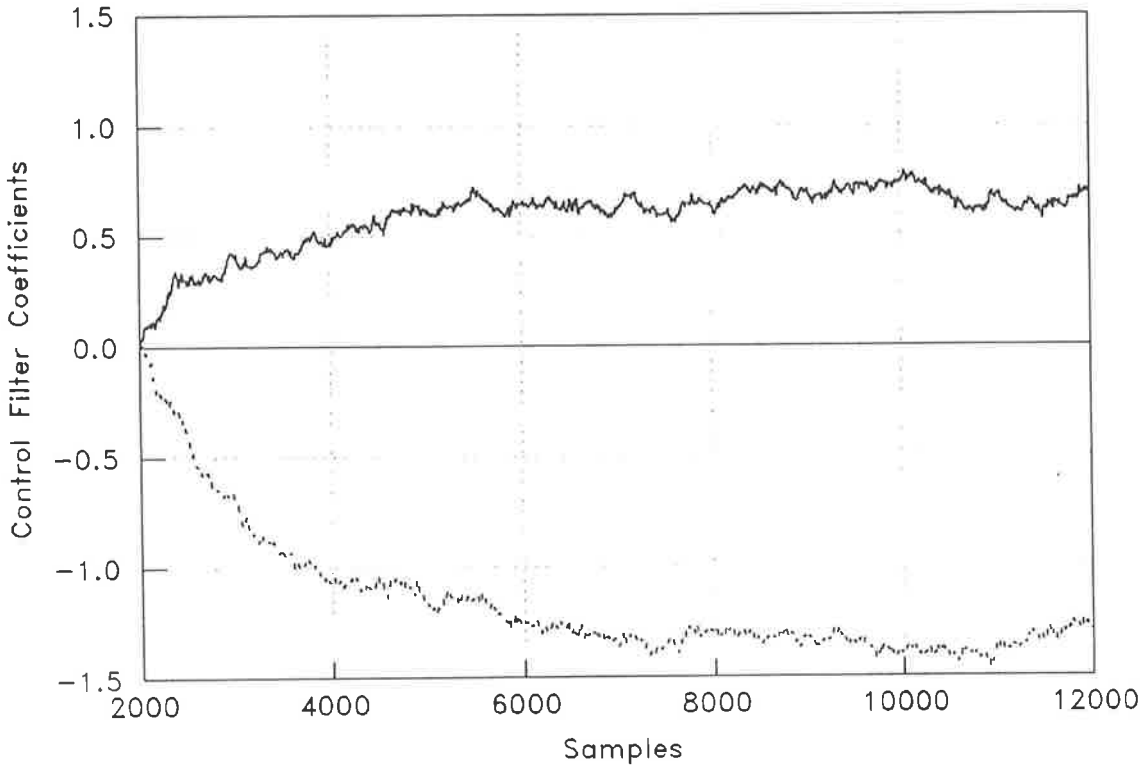

Figure 5-23. The control filter coefficients (Coeff. 0——, Coeff. 1 - - - -) during adaptation by the filtered-X LMS algorithm. The disturbance comprised a tone at 125 Hz corrupted by band pass filtered white noise (bandwidth of 50 Hz and centre frequency of 125 Hz). The tone was 35 dB above the filtered white noise level.

Control of dual-tones was attempted, with the Independent Quadratic Optimisation algorithm (with four control filter coefficients) achieving marginally more attenuation than the filtered-X LMS algorithm (with six control filter coefficients), as shown in Figure 5-24.

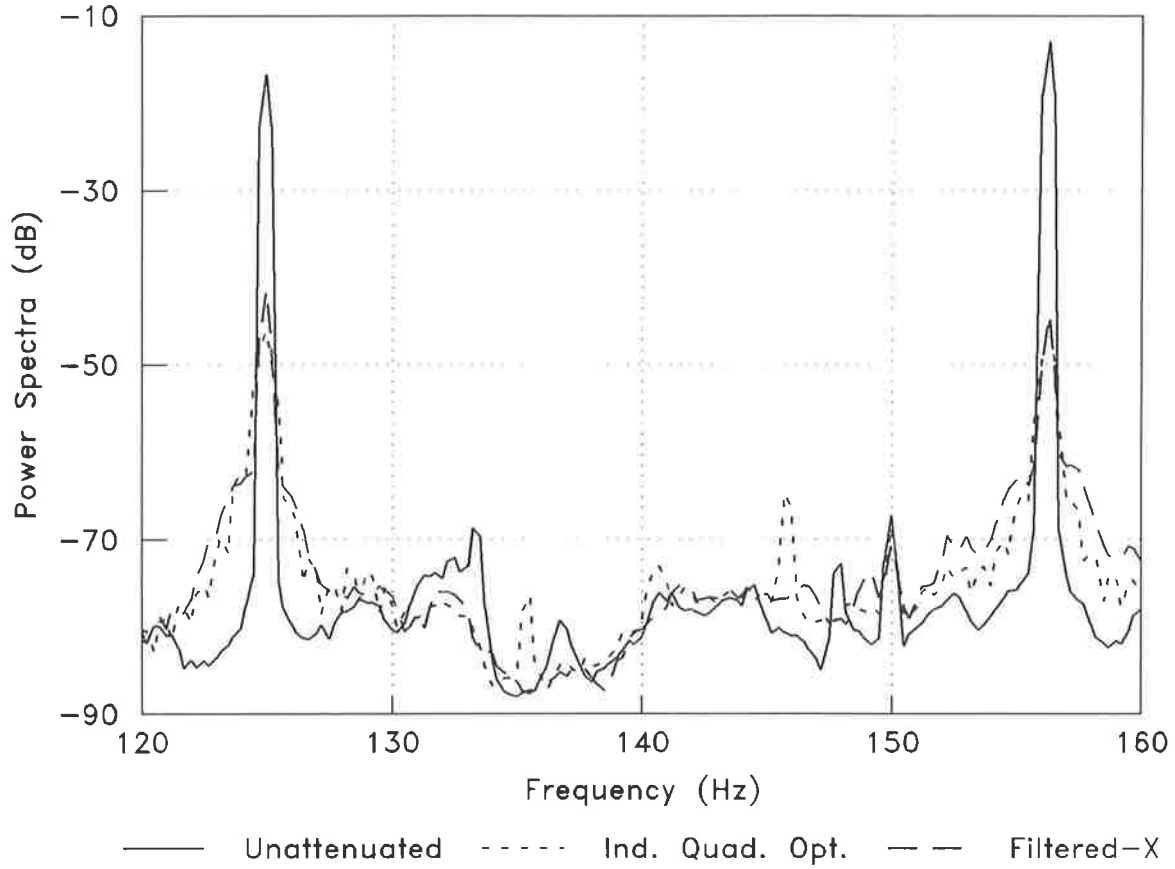

Figure 5-24. The power spectra of the error signal before and after control by the Independent Quadratic Optimisation algorithm and the filtered-X LMS algorithm. The disturbance comprised a tone at 125 Hz and another at 156.25 Hz.

Figure 5-25 shows the effect on the attenuation achieved by the Independent Quadratic Optimisation algorithm, through doubling the control filter coefficient step size factor (case 2) and increasing the number of samples used to estimate the cost function by a multiple of five (case 3), in comparison with case 1. Doubling the control filter coefficient step size factor had an insignificant effect on the power spectra of the error

signal after control, whereas increasing the number of samples used to estimate the cost function resulted in an additional 7 dB of attenuation. This relates well with the theory, specifically the level of misadjustment defined by equation (4-34), which predicts a change of 7dB.

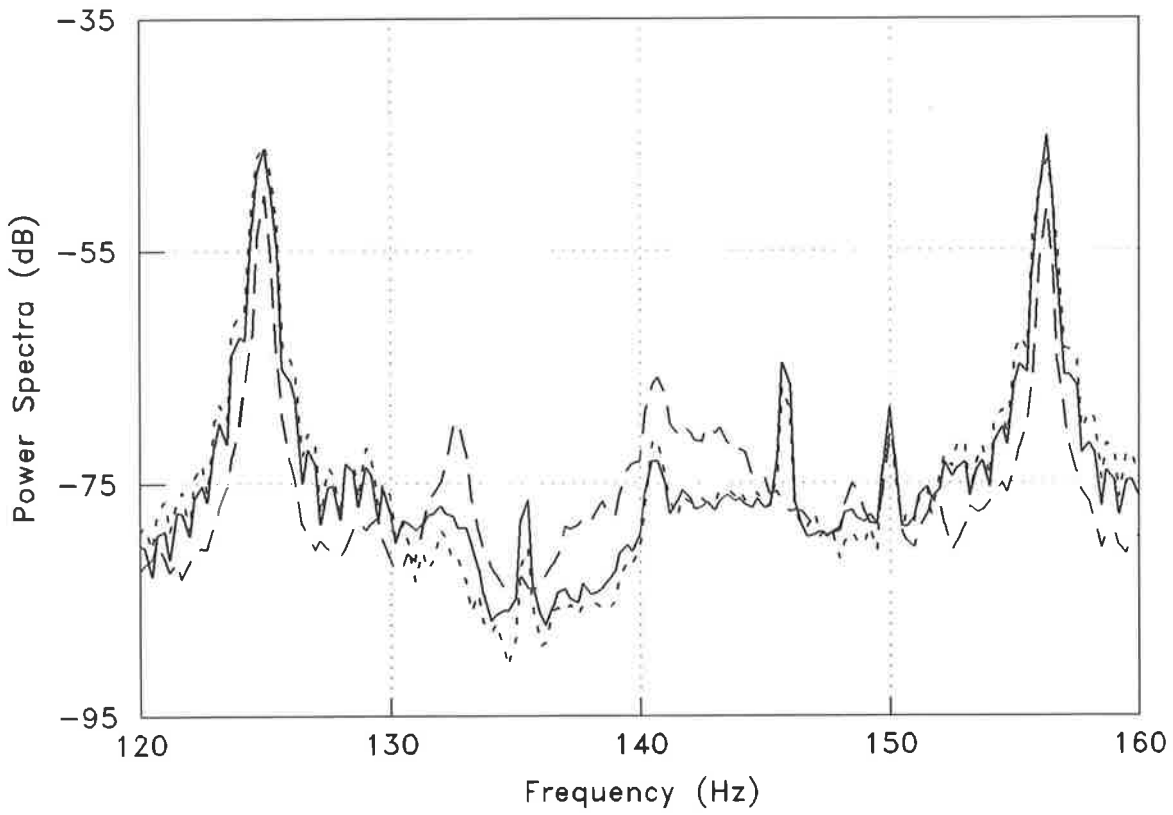

Figure 5-25. The power spectra of the error signal before and after control by the Independent Quadratic Optimisation algorithm. The disturbance comprised a tone at 125 Hz and another at 156.25 Hz. Case 2 (- - - -) has double the control filter coefficient step size factor as case 1 (——), and case 3 (— —) has five times the number of samples used to estimate the cost function as case 1.

The effect of low power (ie. small magnitude) backward prediction errors has been discussed in chapters 3 and 4, as well as previously in this chapter. It was found that the

power of the backward prediction errors reduce with increasing stages of the lattice, possibly leading to overflow of the control signal. Figure 5-26 shows the control filter coefficients normalised to the maximum possible 16 bit integer. The control filter coefficients corresponding to backward prediction errors of higher order stages (ie. greater than the first stage) of the lattice are shown to be significantly larger than those for lower order stages. The magnitude of the control filter coefficient step size is also shown to vary inversely in proportion to the estimated power of the backward prediction errors, as suggested in chapter 4. Figure 5-27 shows the convergence of the error signal, showing initial reduction after convergence of the first two control filter coefficients, and subsequent further reduction after convergence of the next two control filter coefficients (corresponding to backward prediction errors with low powers).

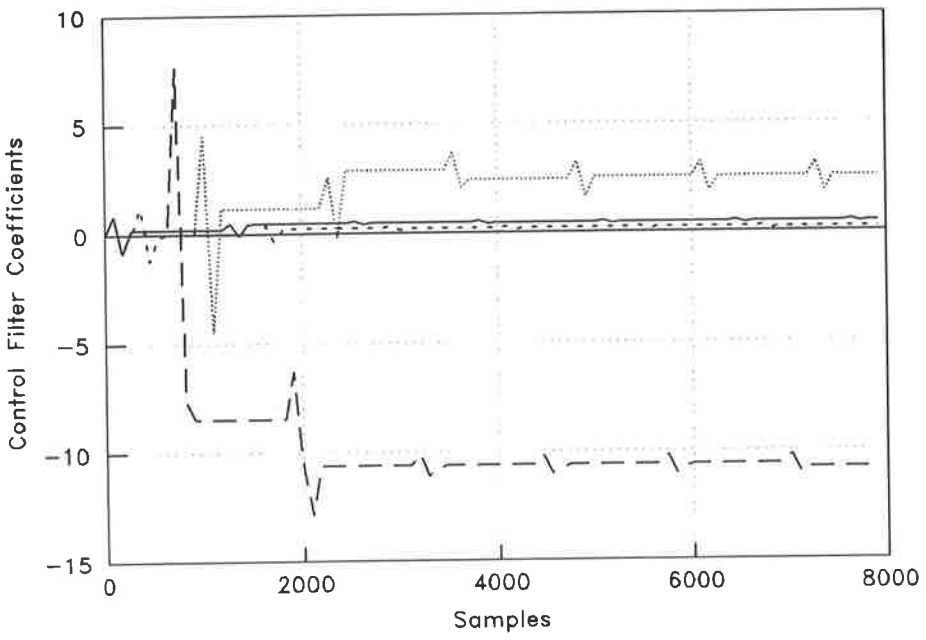

Figure 5-26. Convergence of the control filter coefficients for control of a dual-tone disturbance, with low order coefficients (0 —— and 1 - - - -) converging to much lower values than higher order coefficients (2— —and 3 ——).

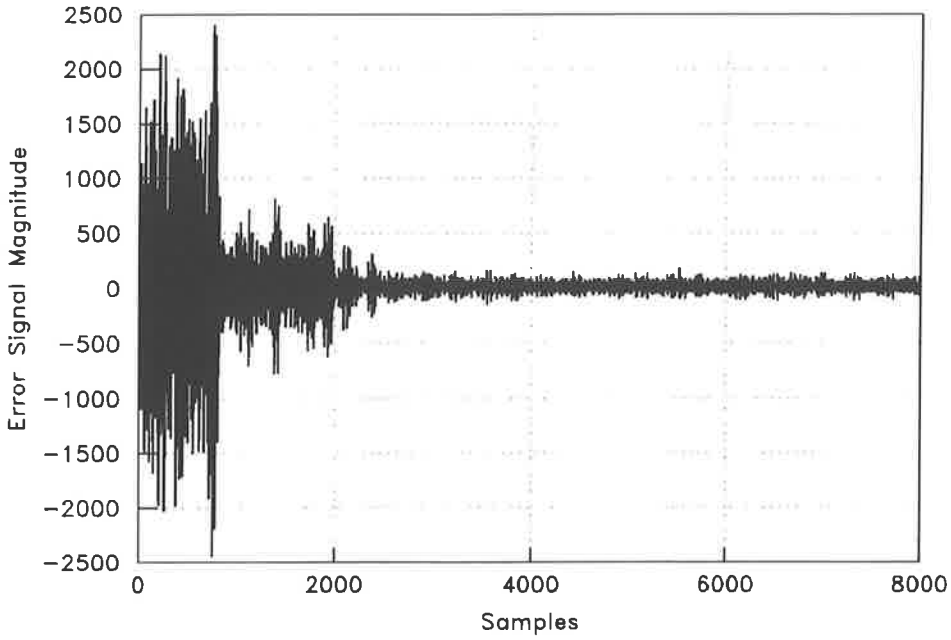

Figure 5-27. Convergence of the error signal for control of a dual-tone disturbance, with initial convergence for low order stages and subsequent convergence for higher order stages.

It is interesting to note the effect of the number of control filter coefficients used by the filtered-X LMS algorithm. To achieve the same attenuation as the Independent Quadratic Optimisation algorithm required six control filter coefficients. The power spectra of the error signal after control by the filtered-X LMS algorithm, using four and six control filter coefficients, is shown in Figure 5-28. It is apparent that an additional 10dB of attenuation is achieved by increasing the number of coefficients, but there also appears to be a reduction in attenuation about the tone (considered to result from the additional coefficients attempting to cancel uncorrelated components of the signal and in effect creating an overdetermined system). It should be noted that the persistent excitation condition discussed in chapter 2 and the appendix, requires sufficient noise in

the filtered reference signal to ensure that the autocorrelation matrix for this signal is invertible. Should there be insufficient noise in the filtered reference signal for the number of control filter coefficients, instability can result.

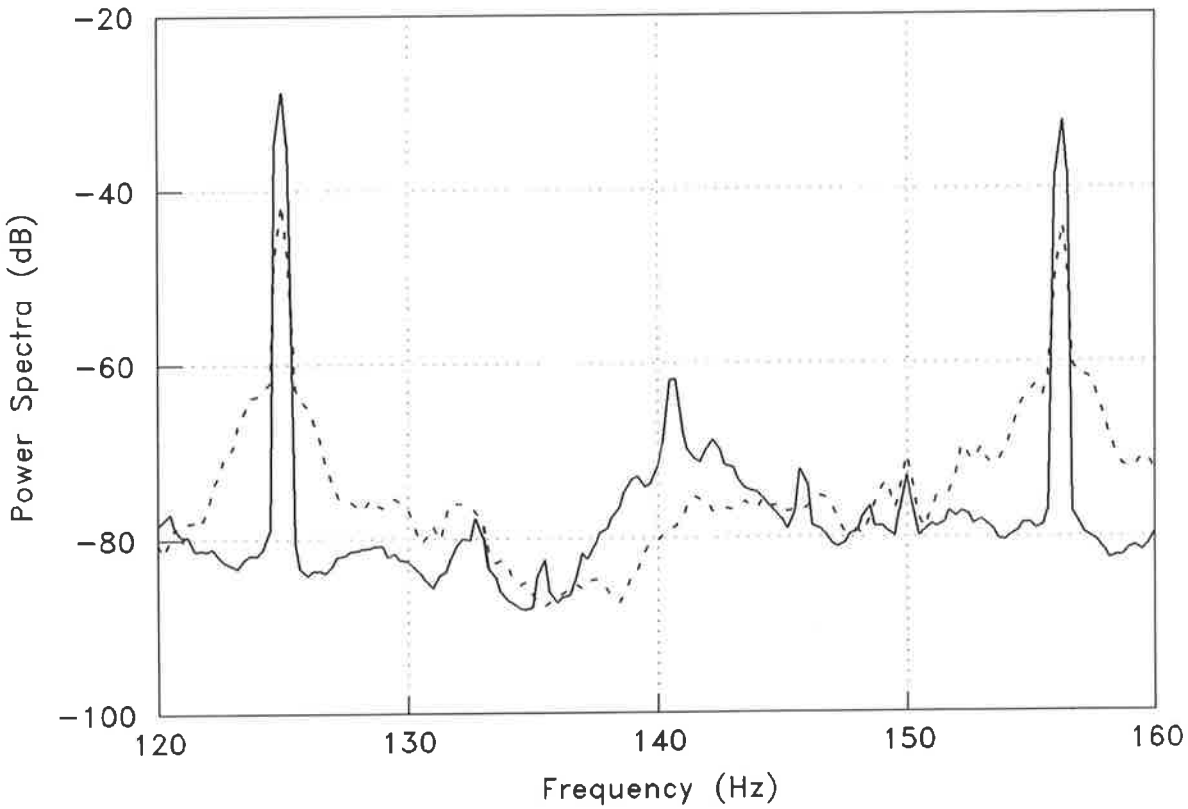

Figure 5-28. The power spectra of the error signal before and after control by the filtered-X LMS algorithm using four ——and six - - - - control filter coefficients.

Consider now the control of white noise filtered through a band-pass filter. A FIFO (First-In-First-Out) delay was included in the algorithms to reduce the number of control filter coefficients (ie. A delay of 10 samples in the cancellation path would require at least 10 control filter coefficients to achieve any attenuation, therefore with a 10 sample delay FIFO, a smaller number of control filter coefficients is required). Figure 5-29 shows the power spectra of the error signal before and after control of 50 Hz band

passed white noise (with centre frequency of 300 Hz) by the Independent Quadratic Optimisation algorithm and the filtered-X LMS algorithm. The control filters for both algorithms used 8 coefficients with a FIFO delay of 8 (as the time delay between the control source and the error sensor was about 10 samples at a sampling frequency of 1250 Hz). It is apparent from Figure 5-29, that with this number of control filter coefficients, about the same level of attenuation is achieved by both algorithms.

Figure 5-30 shows the power spectra of the error signal before and after control of 400 Hz band passed white noise (with centre frequency of 300 Hz) by the Independent Quadratic Optimisation algorithm and the filtered-X LMS algorithm. A FIFO delay of 8 was used only for the Independent Quadratic Optimisation algorithm. Figure 5-30 shows the level of attenuation achieved by the Independent Quadratic Optimisation algorithm with and without the FIFO delay, and by the filtered-X LMS algorithm without the FIFO delay. The control filter had 15 coefficients for both algorithms. It is apparent from Figure 5-30 that the attenuation achieved by the Independent Quadratic Optimisation algorithm was significantly greater with the inclusion of a FIFO delay.

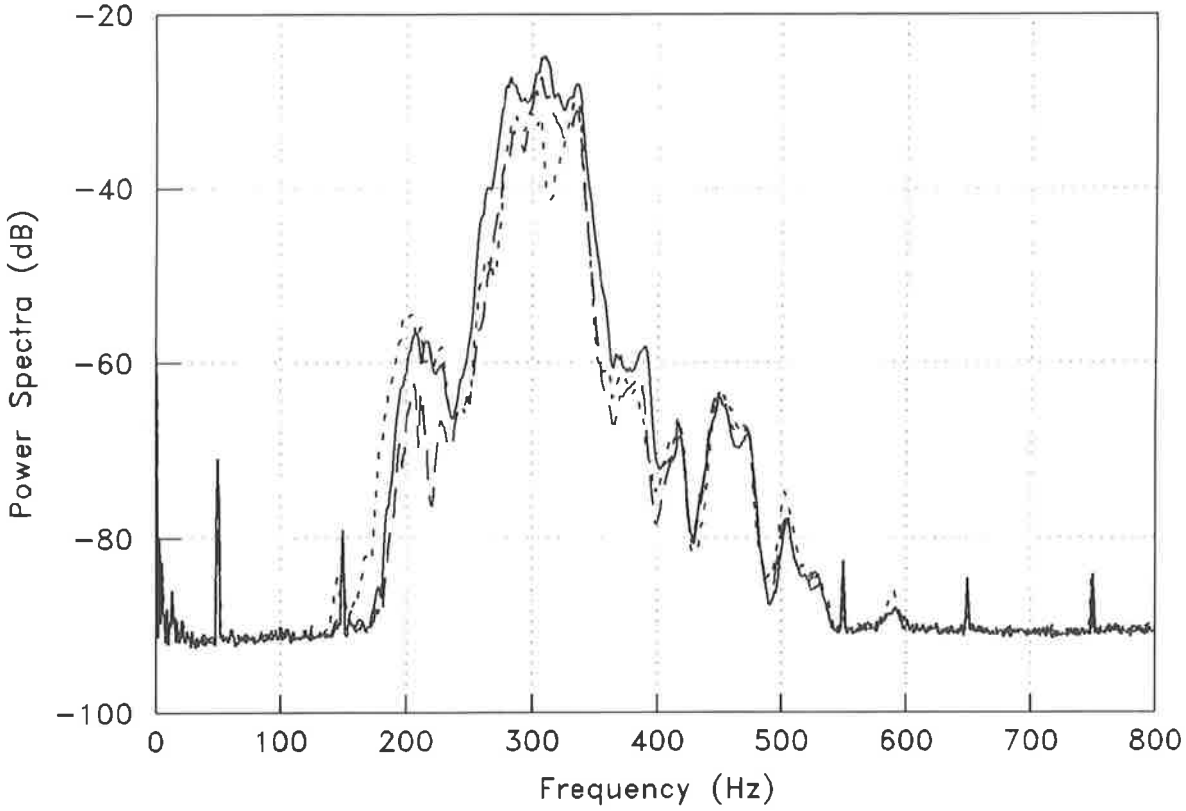

Figure 5-29. The power spectra of the error signal before (——) and after control by the Independent Quadratic Optimisation algorithm (- - -), and the filtered-X LMS algorithm (— —), both incorporating a FIFO delay. The disturbance was 50 Hz band passed white noise centred on 300 Hz.

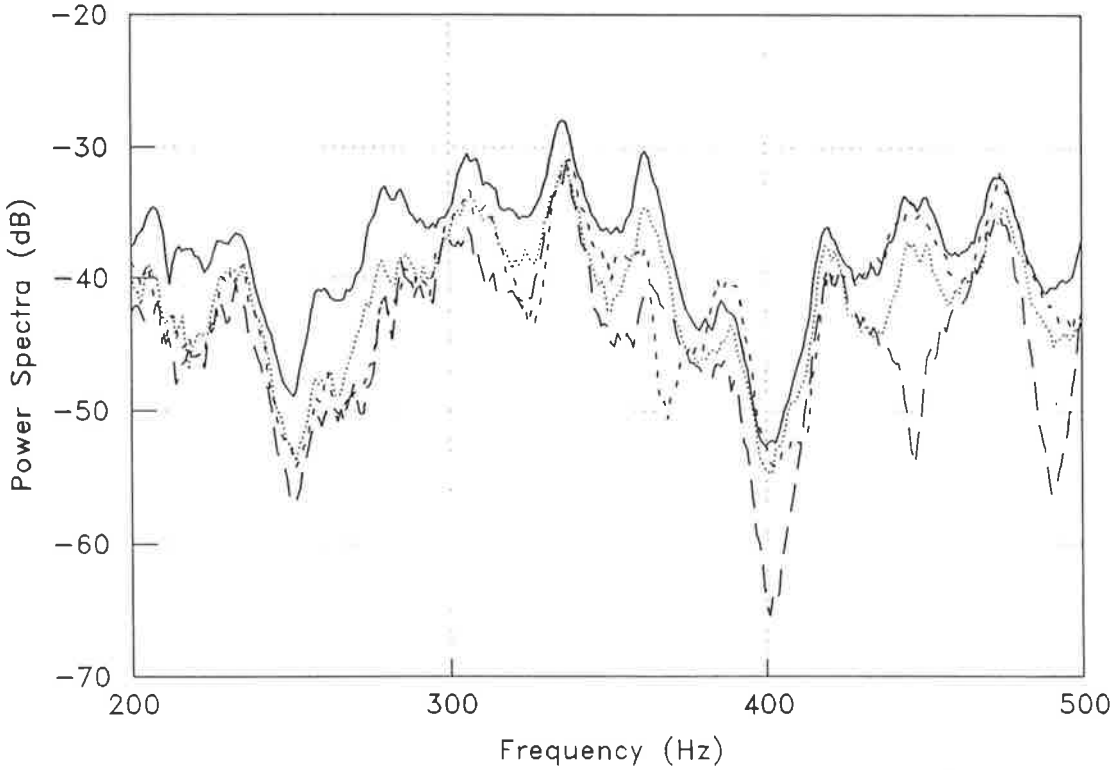

Figure 5-30. The power spectra of the error signal before (——) and after control by the Independent Quadratic Optimisation algorithm (with a FIFO delay (— —), and without a FIFO delay (- - -), and the filtered-X LMS algorithm (·····) (without a FIFO delay). The disturbance was 400 Hz band passed white noise centred on 300 Hz.

5.5 Vibration Control

In section 5.3, results were presented to verify the implementation of both the Independent Quadratic Optimisation algorithm and associated lattice filter, with tests performed using self-induced noise (ie. effectively a time delay in the cancellation path). In section 5.4, the analysis of the Independent Quadratic Optimisation algorithm was extended to the more general cancellation path, with an assessment of single channel control of an acoustic disturbance in a semi-infinite duct. The results of section 5.4 relate to the effect on performance of the Independent Quadratic Optimisation algorithm's parameters, and a comparison was made with the performance obtained using the filtered-X LMS algorithm. The results of section 5.3 and 5.4 related to all types of disturbances considered in chapters 3 and 4, and the theory presented in these chapters was confirmed.

In this section, results for the multi-channel control of vibration levels (and power flow or structural intensity) in a semi-infinite plate will be presented for the case of a pure tone disturbance only. This section will highlight the effects of the different methods of control coefficient adaptation discussed in chapter 4, and relate the effects of changes in the control filter coefficient step size and number of averages to the theory presented in chapter 4. This section will also show how the Independent Quadratic Optimisation algorithm has the advantage over other types of algorithms in that it can work with any type of cost function; For example, the Independent Quadratic Optimisation algorithm can minimise structural power flow, whereas the standard filtered-X LMS algorithm cannot. This section will therefore consider the effectiveness of far field attenuation for

the following types of cost function (where the error signals are denoted by $e_i(n)$, with brackets [..] indicating paired error sensors):

- Error signal amplitude ie. $e_1^2(n) + e_2^2(n) + \ldots$;
- Structural power flow ie. $[e_1(n).e_2(n)] + [e_3(n).e_4(n)] + \ldots$; and
- Acoustic intensity ie. $[e_1^2(n) - e_2^2(n)] + [e_3^2(n) - e_4^2(n)] + \ldots$.

The experimental arrangement consisted of a 3mm steel plate, with a free length of 1.4m and width 0.5m. One end of the plate was embedded in a triangular box filled with sand, while the other end was not supported. The sides of the plate were mounted on thin steel shims (modelling simply supported boundary conditions).

Bending waves were excited in the plate using a pair of piezoceramic crystals bonded to both sides of the plate, and driven out of phase but with the same amplitude. Three pairs of this type of actuator were linked together and used to generate a disturbance, and another three pairs of this type of actuator were driven individually to control the vibration levels (or power flow) in the plate. Four pairs of accelerometers were used as error sensors. They were located in pairs so that not only could they act as eight individual error sensors, but they could also act as four structural intensity sensors. A rov accelerometer was used to measure the vibration levels on the plate before and after control. Figure 5-31 shows the experimental setup.

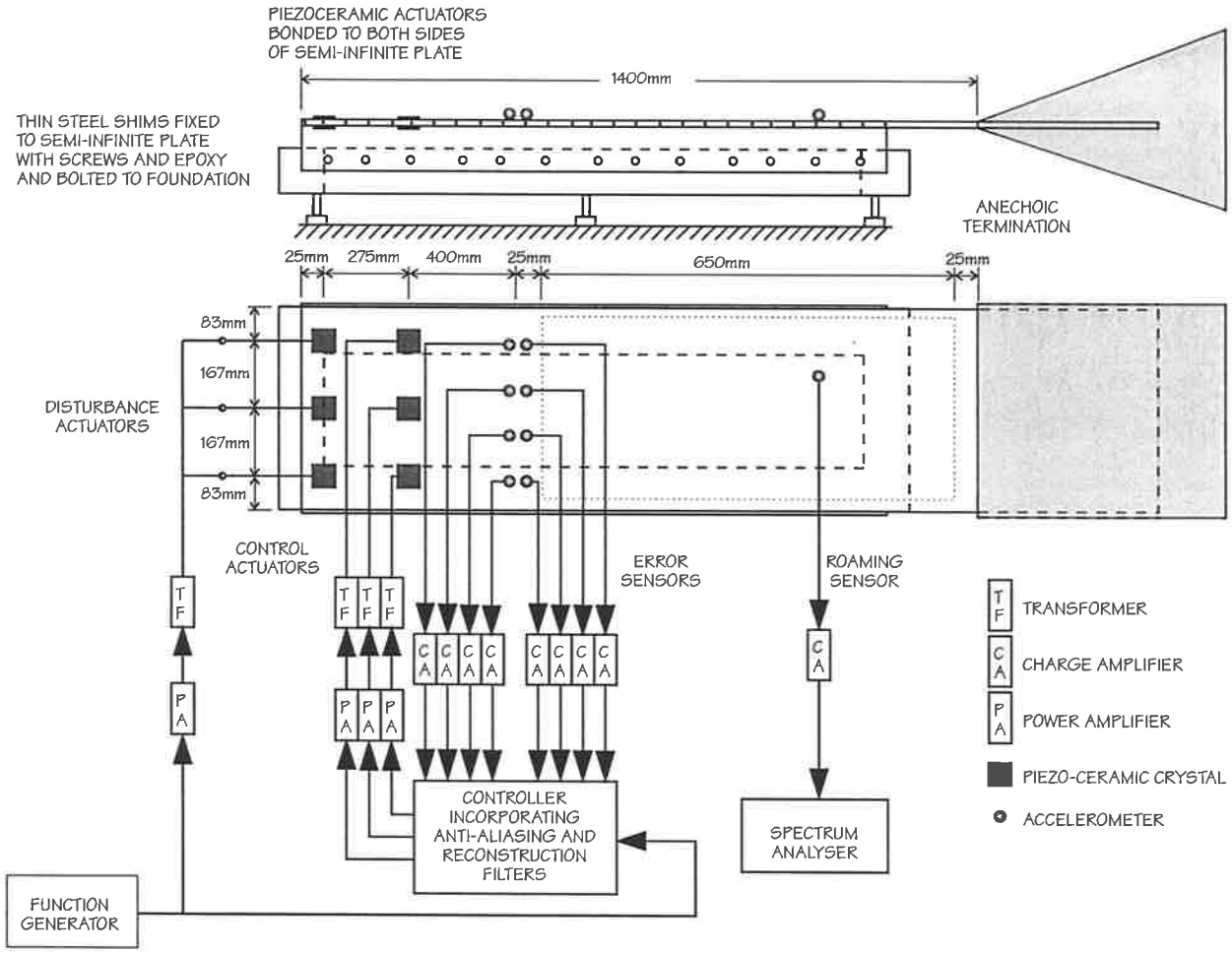

Figure 5-31. Experimental arrangement of actuators, sensors and associated equipment for the control of vibration levels in a semi-infinite plate. A detailed description of the controller is shown in Figure 5-1.

As discussed, control of intensity illustrates another advantage of the Independent Quadratic Optimisation algorithm, since for example, the instantaneous acoustic intensity is given by the sample product of pressure and particle velocity for a particular frequency. This product corresponds to an "adaptive" error signal having twice the frequency and a constant term dependent upon the phase difference between the pressure and particle velocity; Since the "adaptive" error signal has twice the frequency, it means that adaptation of the control filter coefficients using this type of error signal (as per adaptation using stochastic gradient methods) cannot take place. However the Independent Quadratic Optimisation algorithm uses the estimate of the time averaged product of pressure and particle velocity to achieve reduction of intensity as it would for any type of cost function. That is, the cost function used is the intensity (or mean square intensity).

It has been shown that the structural power flow is proportional to the product of the signals from two closely spaced accelerometers [Pavic, 1976]. It has also been shown that this is only a measure of the power flow if the accelerometers are in the near field of the control actuators [Pan and Hansen, 1993]. If the accelerometers are in the far field of the control actuators then they act as amplitude sensors.

The semi-infinite plate was excited at the 3rd modal resonance frequency (259 Hz). Structural power flow in the plate was initially controlled using all of the control actuators linked together and driven using a single control filter, with all eight error sensors used in pairs to reduce the power flow in the plate. The attenuation achieved from this type of control is shown in Figure 5-32, and ranged from -10 dB to 25 dB. The

control filter coefficients were adapted using method 1 of the Independent Quadratic Optimisation algorithm (ie. all coefficients of a channel were adapted before continuing to the next channel). It is apparent from Figure 5-32, that the peak attenuation was in small isolated regions near the edge of the plate and near the control actuators.

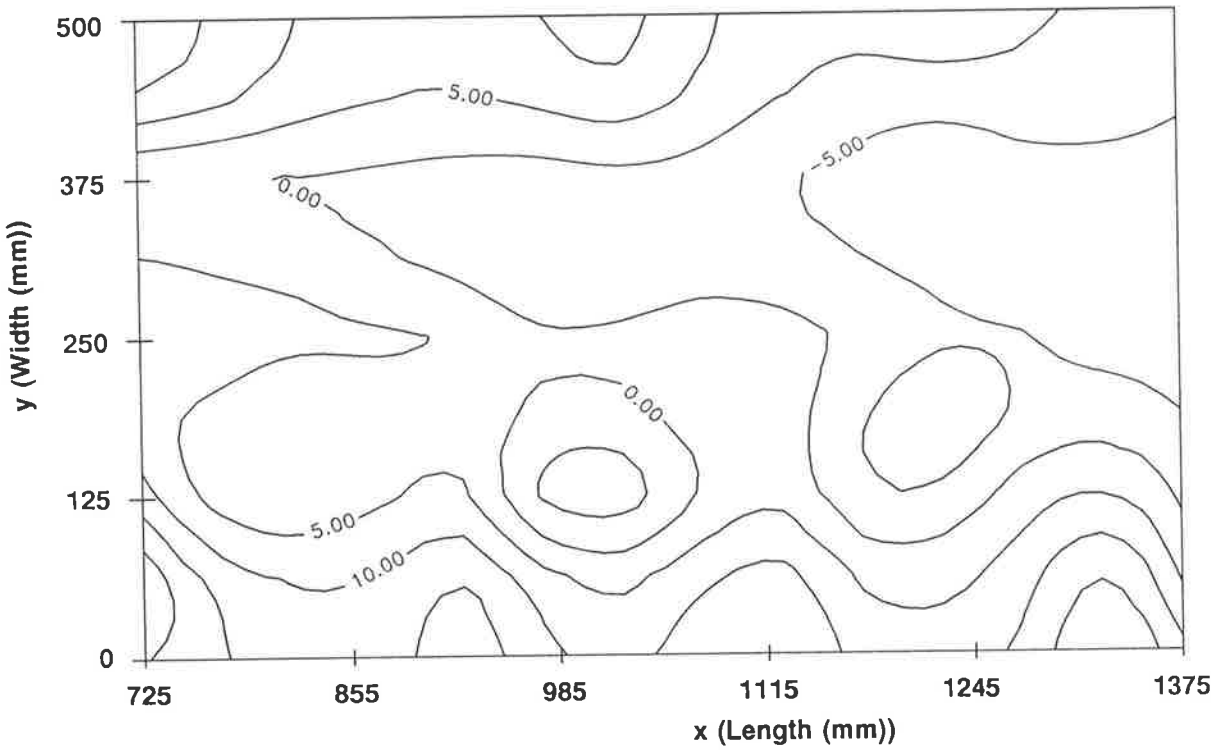

Figure 5-32. Attenuation achieved in the semi-infinite plate between the error sensors and the anechoic termination, as determined from control of power flow using all of the control actuators linked together as a single channel. The length of the plate runs from the error sensor location to the anechoic termination. Refer to Figure 5-31 for locations of primary sources, control sources and error sensors.

Results from minimisation of the cost function estimate (ie. total structural power flow) by the Independent Quadratic Optimisation algorithm with different parameters is shown in Figure 5-33. In Figure 5-33, the estimates of the cost function are those made by the Independent Quadratic Optimisation algorithm to determine the optimal control filter coefficients corresponding to the minimum of the cost function. In Figure 5-33, case 1

corresponds to the standard, case 2 has the control filter coefficient step size factor reduced to one fifth that of case 1, and case 3 has the number of samples used to estimate the cost function doubled in comparison to case 1. As expected the steps in the cost function are the same for case 1 and 3, but for case 2 they have been reduced.

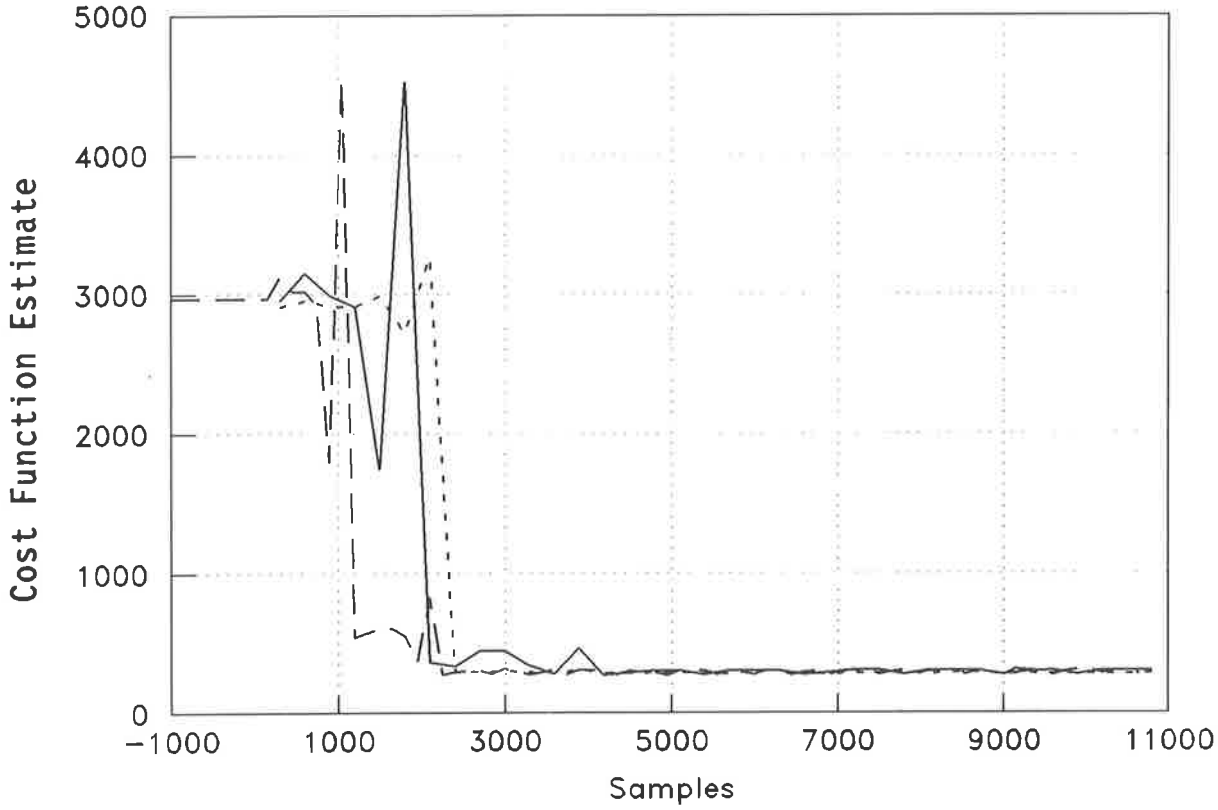

Figure 5-33. The reduction of the cost function (total structural power flow) estimate by adaptation of the control filter coefficients using the Independent Quadratic Optimisation algorithm. Control was achieved using all of the control actuators linked together as a single channel. Case 1 (——) corresponds to the standard, case 2 (- - - -) has the control filter coefficient step size factor reduced to one fifth that of case 1, and case 3 (— —) has the number of samples used to estimate the cost function doubled in comparison to case 1.

The cost function at convergence (ie. for samples greater than 5000) is shown in Figure 5-34, for the same sets of parameters. The theory presented in chapter 4 suggested that if the control filter coefficient step size factor was reduced by a fifth, then the excess cost

function estimate would be reduced by about 7 dB. This is shown clearly in Figure 5-34 for case 2. However doubling of the number of samples used to estimate the cost function should have resulted in a 3dB decrease in the excess cost function estimate, which is not apparent from Figure 5-34.

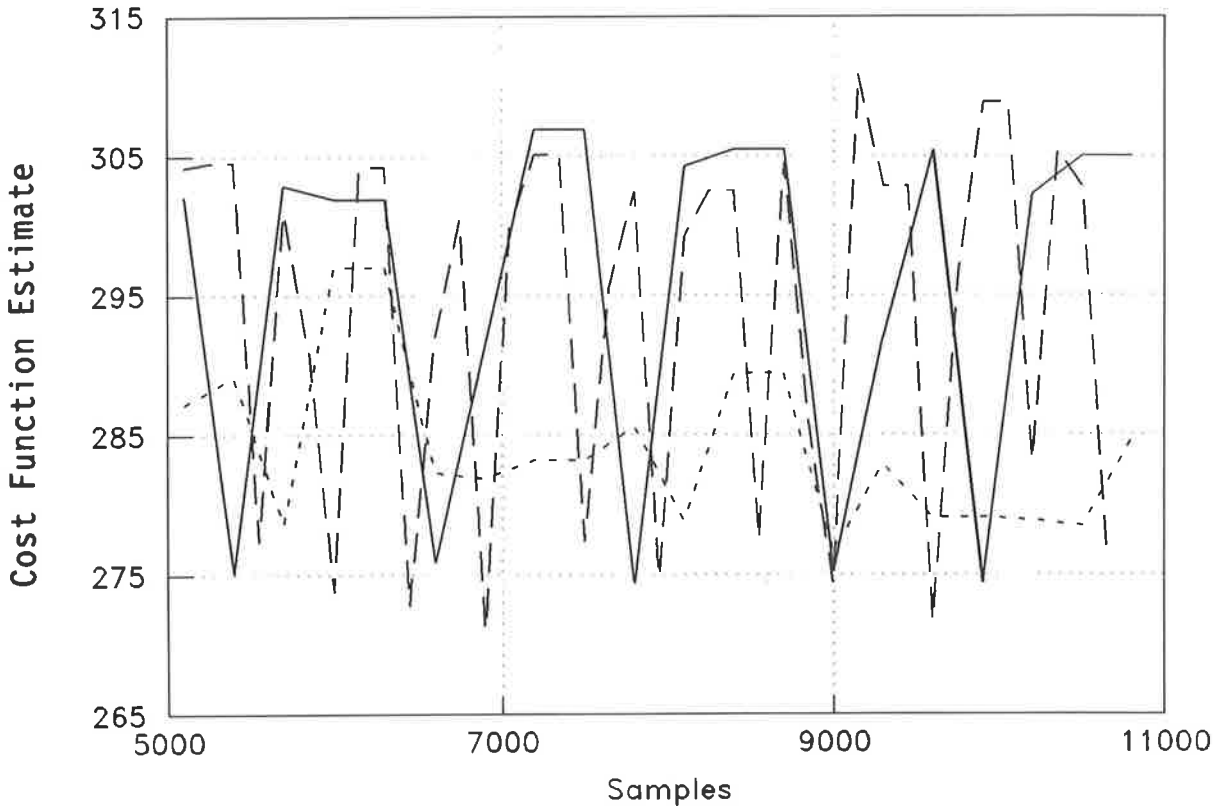

Figure 5-34. The reduction of the cost function (total structural power flow) estimate by adaptation of the control filter coefficients using the Independent Quadratic Optimisation algorithm. Control was achieved using all of the control actuators linked together as a single channel. Case 1 (——) corresponds to the standard, case 2 (- - - -) has the control filter coefficient step size factor reduced to one fifth that of case 1, and case 3 (— —) has the number of samples used to estimate the cost function doubled in comparison to case 1.

The control actuators were next driven independently, with the control filter coefficients again adapted using method 1 of the Independent Quadratic Optimisation algorithm. The power flow was again minimised using pairs of error sensors. The level of

attenuation achieved is shown in Figure 5-35, and ranged from 0 to 30 dB. It is apparent from Figure 5-35, that levels of attenuation greater than 10 dB were achieved over large regions of the plate. To compare the effectiveness of control approaches on far field attenaution, instead of minimising power flow in the plate, the total sum of the squares of each error signal was minimised. The attenuation achieved for this form of cost function is shown in Figure 5-36, and also ranged from 0 to 30 dB. The attenuation levels and distribution over the plate is similar to that for power flow reduction shown in Figure 5-35, therefore an indication that the error sensors were in the far field; that is, $e_i(n).e_j(n) \approx e_i^2(n) \approx e_j^2(n)$.

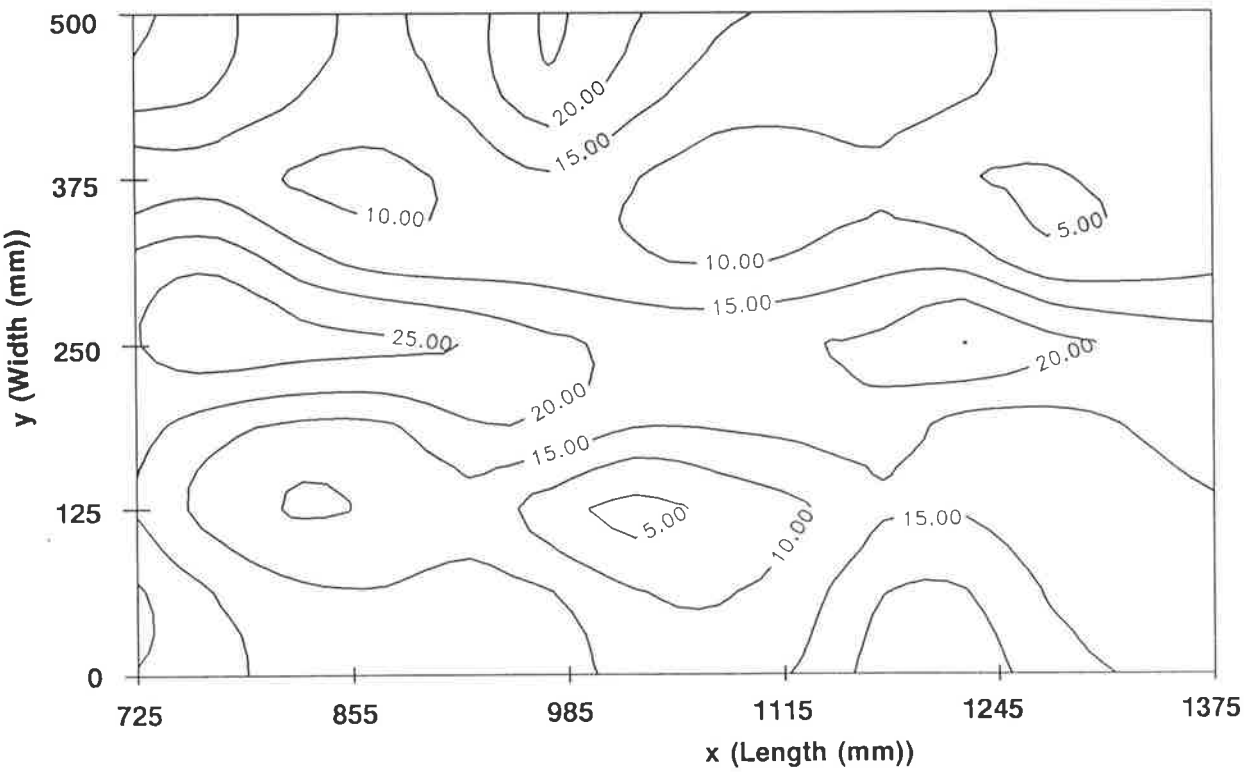

Figure 5-35. Attenuation achieved in the semi-infinite plate between the error sensors and the anechoic termination, as determined from control of power flow using all of the control actuators driven individually. The length of the plate runs from the error sensor location to the anechoic termination.

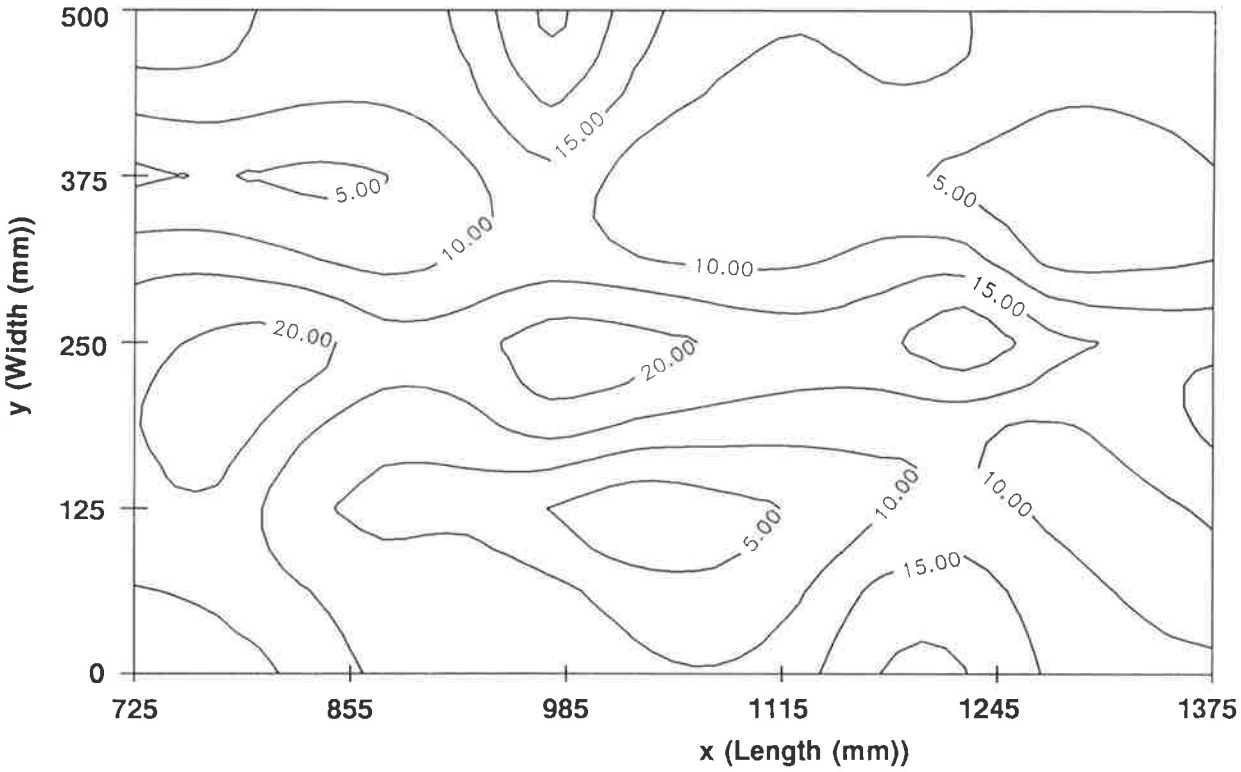

Figure 5-36. Attenuation achieved in the semi-infinite plate between the error sensors and the anechoic termination, as determined from control of sum of the square of each error signal using all of the control actuators driven individually. The length of the plate runs from the error sensor location to the anechoic termination.

An assessment will now be made of the effectiveness (based on far field attenuation) of the control approach using a cost function criterion equivalent to that of "acoustic intensity" (ie. The difference between the square of each error sensor pair was used, or equivalently, the product of the sum of the signals from the error sensor pair by their difference). Again the control filter coefficients were adapted using Method 1 of the Independent Quadratic Optimisation algorithm, with the level of attenuation achieved shown in Figure 5-37. In Figure 5-37, a 10 dB increase in attenuation levels can be observed, with the attenuation ranging from 10 dB to 40 dB. Although a detailed investigation of the physical control mechanisms, underlying active noise or vibration

control in any context, is outside the scope of this work, it is broached that the attenuation increased with this type of cost function as it is a more appropriate cost function for measuring power flow in the far field.

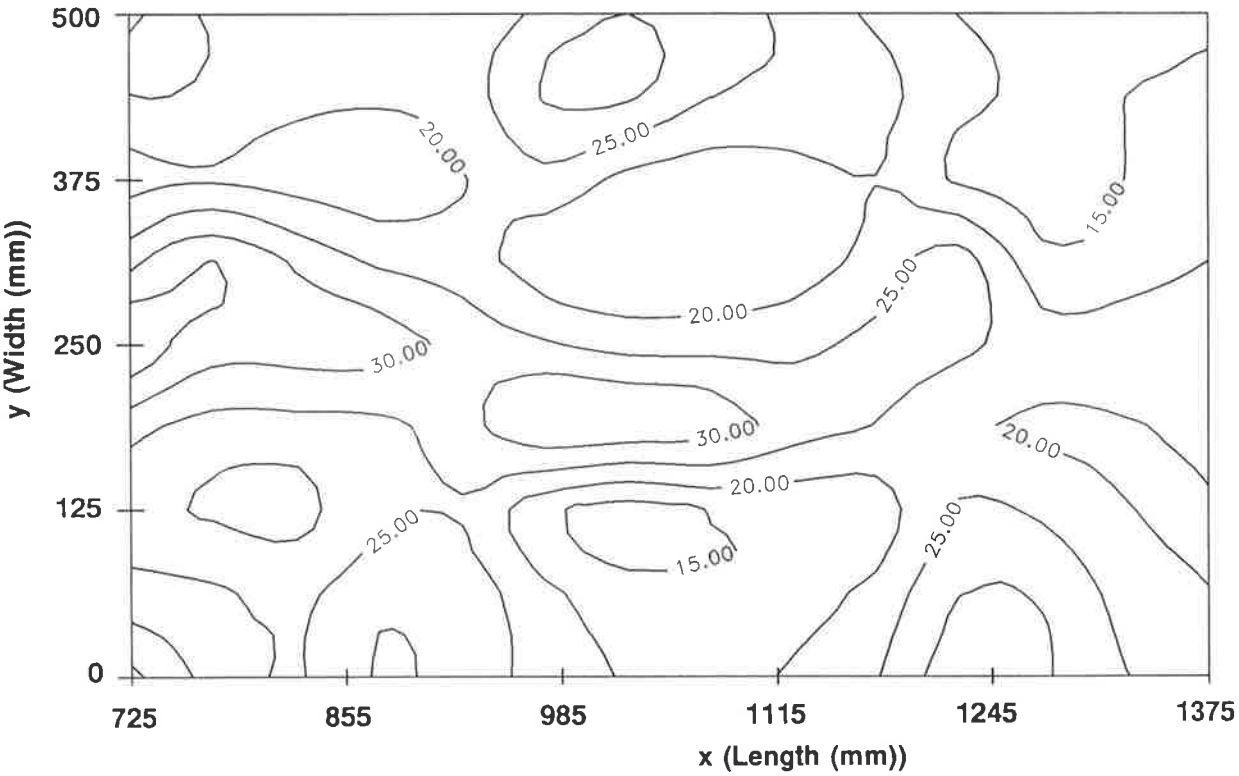

Figure 5-37. Attenuation achieved in the semi-infinite plate between the error sensors and the anechoic termination, as determined from control of "acoustic intensity" using all of the control actuators driven individually. The length of the plate runs from the error sensor location to the anechoic termination.

The two methods of adapting the control filter coefficients using the Independent Quadratic Optimisation algorithm (ie. method 1 - optimising all the coefficients of a channel before continuing to the next channel, or method 2 - optimising a coefficient of all the channels before continuing to the next coefficient) were compared by minimising the amplitudes at four accelerometer positions, using three pairs of control actuators driven individually. Figure 5-38 shows the reduction of the total mean square error estimates using each method. It is apparent from Figure 5-38, that the Independent

Quadratic Optimisation algorithm takes longer to converge using method 2 than using method 1. This is considered to result from the control filter coefficients being independent within each channel, but not between channels. The final level of attenuation was about 16 dB at the error sensor locations for both methods.

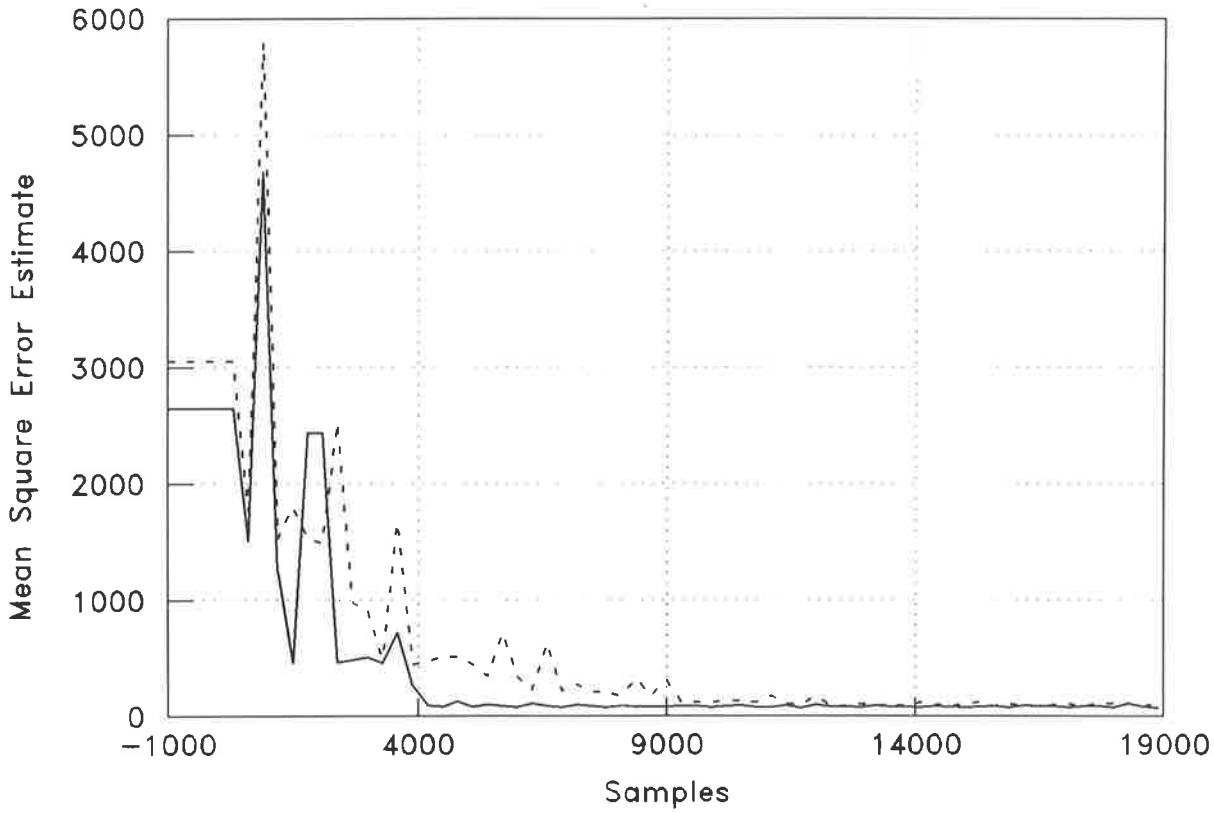

Figure 5-38. The reduction of the cost function (amplitude based) estimate by adaptation of the control filter coefficients using the two alternative methods (method 1 ——, method 2 - - - -) associated with the Independent Quadratic Optimisation algorithm. Control was achieved using all of the control actuators linked together as a single channel.

An example of the convergence of the error signal from a particular error sensor is shown for each method in Figures 5-39 (a) and (b). It is also apparent from Figures 5-39 (a) and (b), that the convergence of the Independent Quadratic Optimisation algorithm is slower for method 2. Finally the control filter coefficients were assessed for each method of control filter coefficient adaptation. Figures 5-40 (a) to (c) show the convergence of

the coefficients for each control filter. Figure 5-40(a) shows that the coefficients of the first channel (control filter) are very similar for both methods 1 and 2, while Figure 5-40(b) and (c) show that the coefficients of the channels (control filters) are quite different for each method of adaptation using the Independent Quadratic Optimisation algorithm.

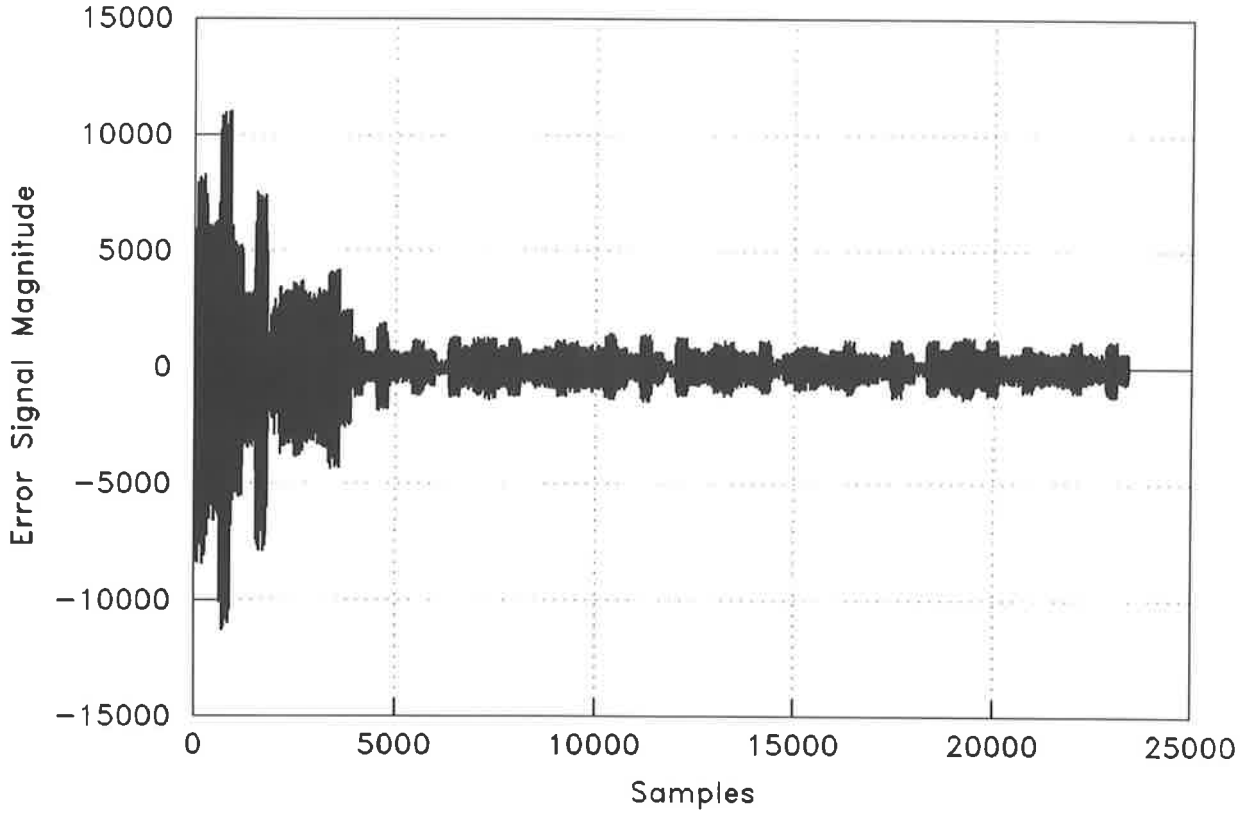

Figure 5-39(a). Error signal for control coefficient adaptation using method 1 of the Independent Quadratic Optimisation algorithm.

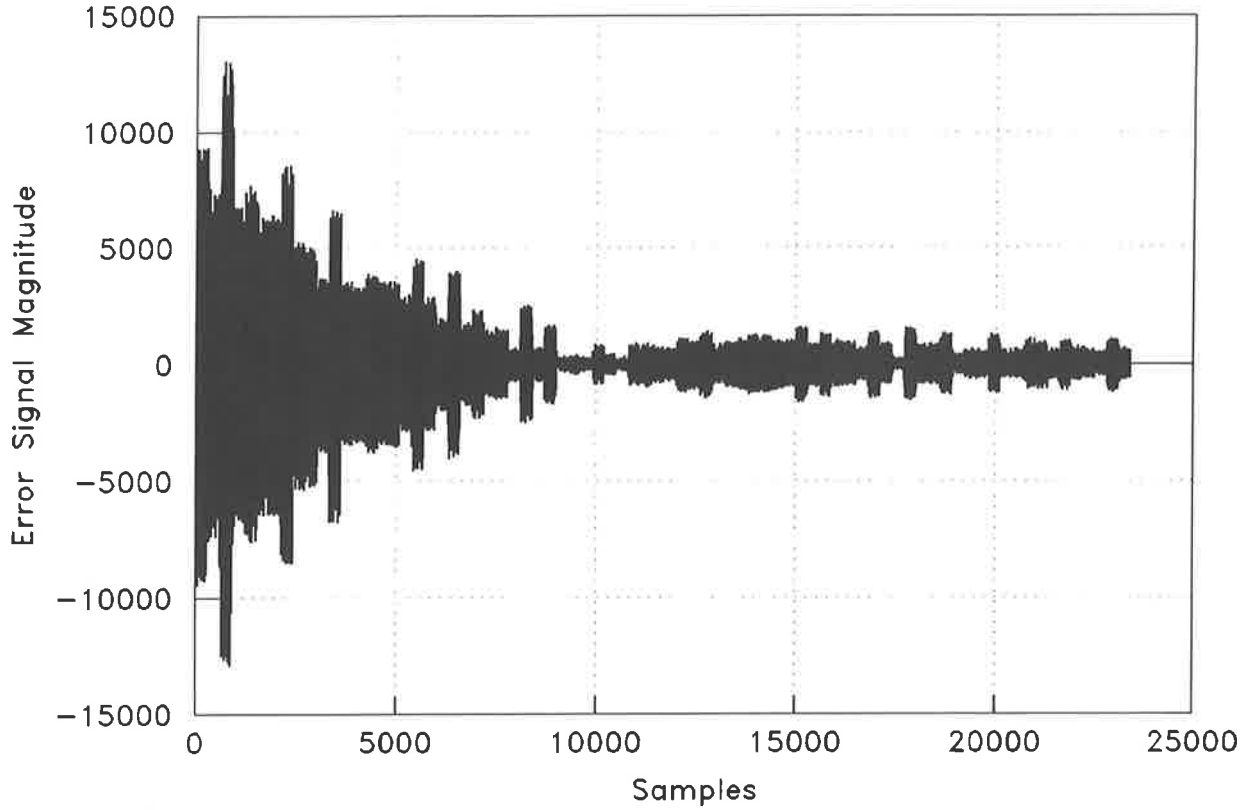

Figure 5-39(b). Error signal for control coefficient adaptation using method 2 of the Independent Quadratic Optimisation algorithm.

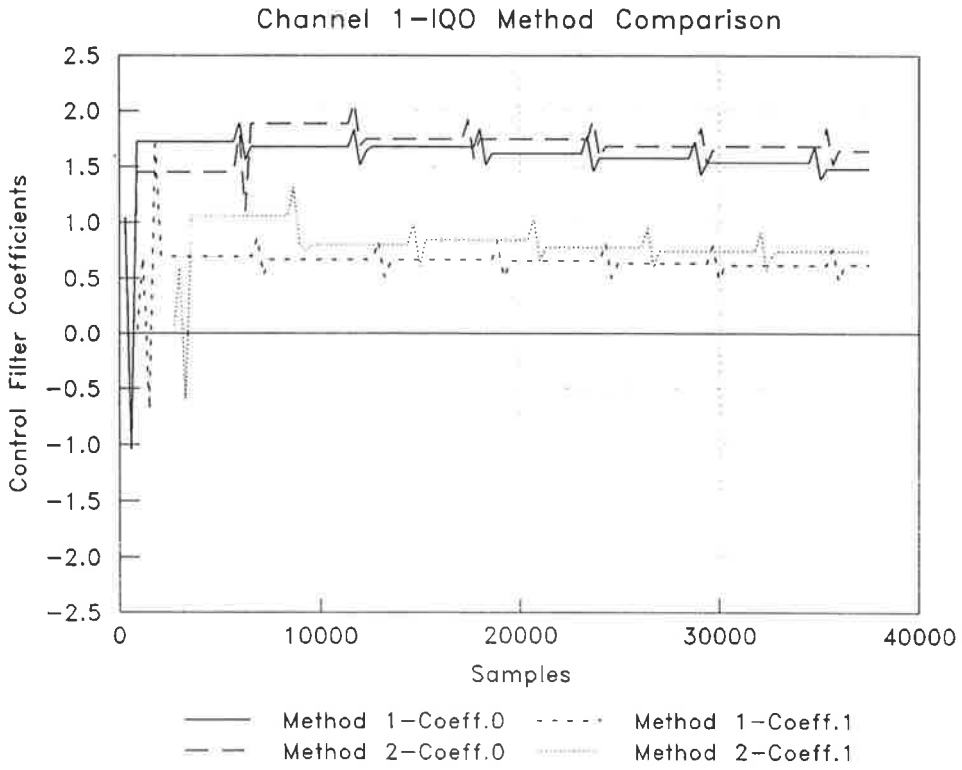

Figure 5-40(a). Control filter coefficients versus sample number for both methods of control filter coefficient adaptation by the Independent Quadratic Optimisation algorithm.

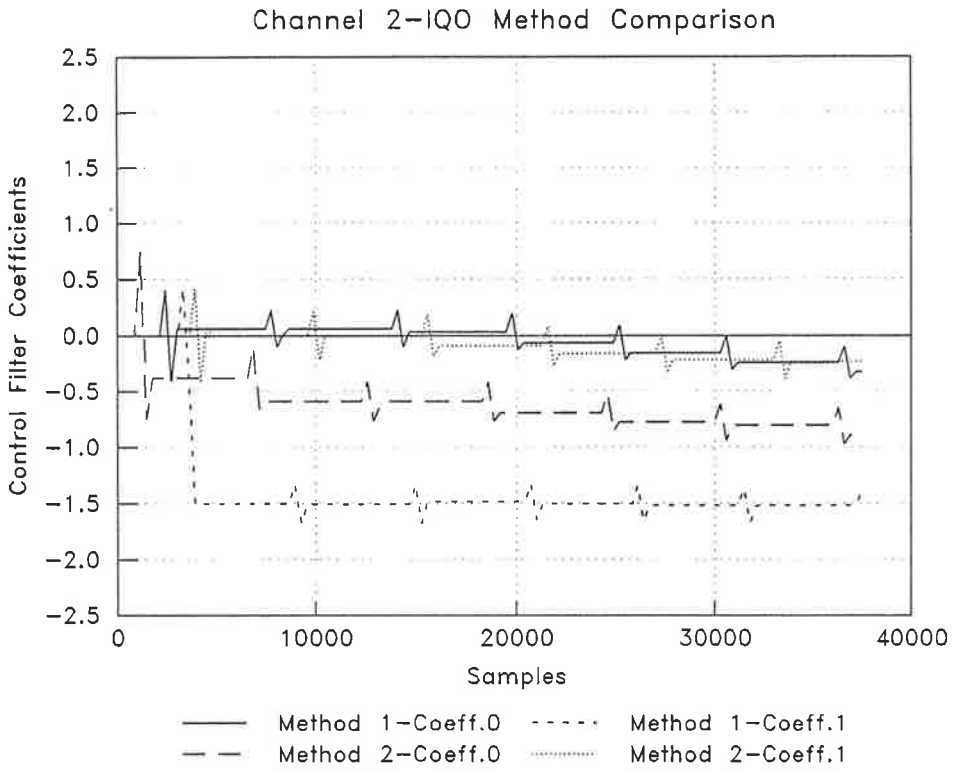

Figure 5-40(b). Control filter coefficients versus sample number for both methods of control filter coefficient adaptation by the Independent Quadratic Optimisation algorithm.

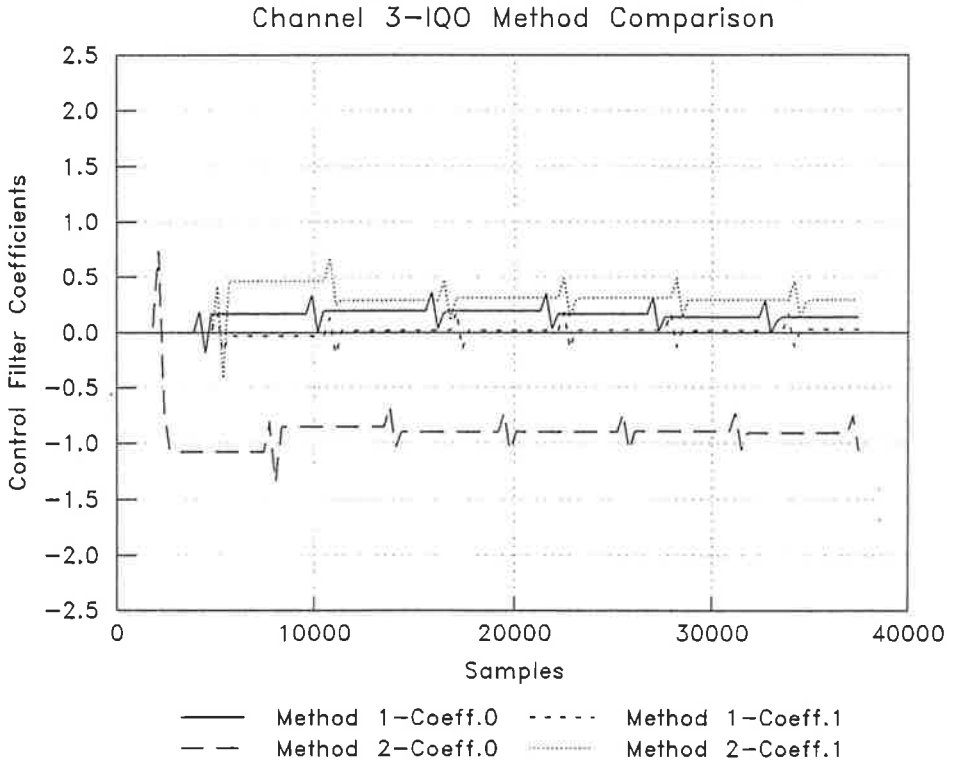

Figure 5-40(c). Control filter coefficients versus sample number for both methods of control filter coefficient adaptation by the Independent Quadratic Optimisation algorithm.

5.6 Summary

In this chapter the Independent Quadratic Optimisation algorithm, and associated lattice filter, implemented in both single and multi-channel form, have been tested experimentally for the control of both an acoustic disturbance and a vibration disturbance.

In verifying the lattice filter implementation, it was observed that the power of the backward prediction errors gave an indication of the statistics of the reference signal, and therefore an indication of the number of control filter coefficients required. This is not obvious when using a transversal filter and the filtered-X LMS algorithm. Too many control filter coefficients used for the filtered-X LMS algorithm can not only result in instability (since the persistent excitation condition may not be satisfied) as discussed in chapter 2 and the appendix, but also in reduced attenuation bandwidth as was shown later in this chapter. The estimated power of the backward prediction error signals was also used to provide a means of adjusting the control filter coefficient step size in the Independent Quadratic Optimisation algorithm, as suggested in chapter 4.

The Independent Quadratic Optimisation algorithm was found to perform as effectively in most cases as the filtered-X LMS algorithm. The Independent Quadratic Optimisation algorithm was able to achieve good attenuation for disturbances ranging from pure tones to broadband noise (for which a FIFO was used to reduce the required number of control filter coefficients) without the need for system identification of the physical system. It was also shown to be capable of tracking sudden changes in system conditions. The

Independent Quadratic Optimisation algorithm was found to have an advantage over the filtered-X LMS algorithm for control of disturbances with high eigenvalue disparity (ie. tones with high powers well separated in frequency), and for control of structural or acoustic intensity. The effect of uncorrelated noise on the level of attenuation, alongwith the possibility of the control filter coefficient overflowing, were the key disadvantages of the Independent Quadratic Optimisation algorithm. These key disadvantages can be overcome as follows:

- The use of individual harmonics [Clark et al, 1992;Gibbs et al, 1993;Kewley et al, 1995] or tones (through band pass filtering the reference signal) eliminates the possibility of overflow of the control filter coefficients; That is, the coefficients overflow as a result of low powers of their corresponding backward prediction error signals, and this overflow can be avoided with the use of individual harmonics (that may be synthesised) of constant power. Alternatively a variable gain factor can be used with the control filter coefficients with, however, a loss in resolution.

- The level of uncorrelated noise could be reduced by band pass filtering key frequencies in the error signal.

The effect of parameters (ie. control filter coefficient step size and number of averages) of the Independent Quadratic Optimisation algorithm on performance (ie. attenuation level, bandwidth of attenuation and convergence speed) were assessed and found to compare favourably with the theory presented in chapter 4.

The use of different types of cost function (ie. Based on amplitude, and structural or acoustic intensity) was shown to give differing results for attenuation achieved in the far field of a semi-infinite plate, with results dependent on whether the error sensors were in the near or far field.

Besides the experimental verification of the Independent Quadratic Optimisation algorithm in this work, its performance has also been demonstrated recently. Botteldooren [1993] used the Independent Quadratic Optimisation algorithm to reduce pure tones in the drivers cabin of a large agricultural machine. The tones originated from rotating machinery components. The overall noise level was reduced by 15 dB in about 10 seconds.

6.1 Conclusions

The objective of this work was the development of an adaptive algorithm and control architecture, for implementation in active noise and vibration control systems, that avoids the instabilities associated with phase inaccuracies in the cancellation path (or otherwise known as the error path, secondary path, or auxiliary path) transfer function estimation. Current methods of control require knowledge of the cancellation path to reach the optimum of the performance surface in a stable manner.

Chapter 2 provided a basis from which to branch into the novel work presented in this thesis. In this chapter modern control theory was applied to active noise and vibration control to unify the most commonly used algorithms. This theory involved the use of a model of the system, an algorithm to estimate the parameters of the system model, and a control scheme to achieve the desired process output. The common algorithms were heuristically developed, and the approach presented in chapter 2 highlighted the following improvements that could be made to these algorithms (note that these improvements were not tested in simulations or experiments).

- Use of the "augmented-error" approach that avoids the interplay between system identification and control schemes.

- Use of a single adaptive scheme to estimate the parameters of the system model on-line (ie. It is not necessary to identify the cancellation path transfer

function parameters and control filter coefficients in parallel; This can result in instability, with the convergence conditions for the control algorithm affected by the accuracy of the cancellation path transfer function estimates).

- Use of the simplified forms (stochastic gradient) of the more accurate recursive prediction error methods for both output-error and equation-error models.

- Use of a Generalised Minimum Variance (GMV) criterion, instead of a minimum variance criterion, to reduce the effect of minimum-phase plants.

- In many of the models considered in this chapter, numerator polynomials have been assumed to be close to unity so that algorithms for output-error and equation-error forms (eg. ARMAX) can be simplified. This can result in a reduction of broadband attenuation, with the prediction of the zeroes of the disturbance model ignored (avoiding effects of non-minimum-phase zeroes).

- Use of the Linear Quadratic Gaussian control scheme with spectral factorisation to control systems with non-minimum-phase transfer functions.

Alternative methods were considered to avoid the need to identify the parameters of the system model. This led to the concept of the Independent Quadratic Optimisation algorithm.

Chapter 3 introduced the lattice filter as a means of providing orthogonal signals for

use by the Independent Quadratic Optimisation algorithm. The lattice filter was shown to be particularly suited to the extremely fast recursive least squares algorithm, enabling the orthogonal backward prediction errors to be quickly available. The lattice filter was found to have many desirable properties that were specifically suited to the Independent Quadratic Optimisation algorithm, namely:

- The lattice filter is a form of linear prediction with the prediction accuracy determined by the magnitude of the backward prediction error signals. That is, the more complex the input/reference signal (in terms of signal statistics), the more stages will be required for prediction. Hence the lattice filter, through the generated backward prediction error signals, gives an indication of the number of control filter coefficients required for control.

- PARCOR coefficients of each stage of the lattice are adapted independently to later stages, therefore the lattice can be extended to the required number of stages to achieve optimum control, without affecting previously converged PARCOR coefficients.

- The lattice filter is defined such that, provided the absolute magnitude of the PARCOR coefficients is less than unity, stability is assured; This links well with the established stability concept of the Independent Quadratic Optimisation algorithm.

Although the backward prediction error signal generated by the lattice are orthogonal,

it should be emphasised that they represent **prediction errors**, and as such will decrease in power with increasing stages of the lattice (ie. with increasing numbers of samples used in prediction) eventually becoming white noise sequences with low signal powers. As the power of the backward prediction error signals decrease, this means that the control filter coefficients magnitude must increase to generate the control signal, possibly leading to an overflow. This represents the only disadvantage of the lattice filter when used to generate orthogonal signals.

When the backward prediction errors used with the individual coefficients of the control filter (linear combiner), the control filter coefficients were found to be independent provided no transfer function existed in the cancellation path. It was shown that a delay in the cancellation path did not affect the independence of the control filter coefficients; However, any other type of transfer function in the cancellation path reduced the independence of the control filter coefficients for all signals other than pure tones. Orthogonalising each harmonic individually has been shown to provide a means of overcoming this limitation. It was noted that loss of independence of the control filter coefficients only reduced the speed of convergence and not the stability of the Independent Quadratic Optimisation algorithm.

In chapter 4, the Independent Quadratic Optimisation algorithm concept was introduced and formally derived. It fits a quadratic curve to three estimates of the cost function for each independent control filter coefficient. It was shown that the use of Newton's Method as outlined in recent papers is similar to the Independent Quadratic Optimisation algorithm presented here. This comparison led to formalising

the heuristic comments (regarding number of averages, control filter coefficient step size and degree of cost function curvature) made about the Independent Quadratic Optimisation algorithms performance, using Widrow and Stearns [1985] analysis of Newton's Method for a multi-coefficient single channel system.

Simulations were presented for a pure tone and white noise separately and in combination, illustrating the effects on control filter coefficient independence of a transfer function in the cancellation path, as presented theoretically in chapter 3. It was shown that loss of independence only a limitation in that it reduced the speed of convergence, but not stability, of the Independent Quadratic Optimisation algorithm for all but pure tone signals. The Independent Quadratic Optimisation algorithm has been extended to control periodic noise/vibration by Gibbs et al [1993] and Kewley et al [1995].

Simulations were also performed in this chapter 4, for a multi-channel system using the Independent Quadratic Optimisation algorithm with two alternative methods of control filter coefficient adaptation. Theory was developed with regard to the conditions for independence of control filter coefficients within each channel and between channels. It was shown that for the case of a control actuator and two error sensors, control filter coefficient independence was assured provided the independence condition presented in chapter 2 was met, or the cancellation path transfer functions and the primary disturbance to error sensor transfer functions were orthogonal; However, if these transfer functions were not orthogonal, the system would be over-determined, with redundancy of an error sensor as found by Snyder, Clark and

Hansen [1993] in an analysis of the standard filtered-X LMS algorithm. It was further shown that for the case of one error sensor and two control actuators, independence of the control filter coefficients between channels was impossible; This result suggests that it is more effective to use method 1 for adaptation of control filter coefficients as the coefficients are independent for each channel.

In chapter 5, the Independent Quadratic Optimisation algorithm, and associated lattice filter, implemented in both single and multi-channel form, were tested experimentally for the control of both an acoustic disturbance and a vibration disturbance.

In verifying the lattice filter implementation, it was observed that the power of the backward prediction errors gave an indication of the statistics of the reference signal, and therefore an indication of the number of control filter coefficients required. This is not obvious when using a transversal filter and the filtered-X LMS algorithm. Too many control filter coefficients used for the filtered-X LMS algorithm can not only result in instability (since the persistent excitation condition may not be satisfied) as discussed in chapter 2 and the appendix, but also in reduced attenuation bandwidth as was also shown in chapter 5. The estimated powers of the backward prediction error signals were also used to provide a means of adjusting the control filter coefficient step size in the Independent Quadratic Optimisation algorithm, as suggested in chapter 4.

The Independent Quadratic Optimisation algorithm was found to perform as

effectively in most cases as the filtered-X LMS algorithm. The Independent Quadratic Optimisation algorithm was able to achieve good attenuation for disturbances ranging from pure tones to broadband noise (for which a FIFO was used to reduce the required number of control filter coefficients) without the need for system identification of the physical system. It was also shown to be capable of tracking sudden changes in system conditions. The Independent Quadratic Optimisation algorithm was found to have not only an inherent stability advantage over the filtered-X LMS algorithm, but it was also found to perform better for control of disturbances with high eigenvalue disparity (ie. tones with high powers well separated in frequency), and for control of structural or acoustic intensity. The effect of uncorrelated noise on the level of attenuation, alongwith the possibility of the control filter coefficient overflowing, were the key disadvantages of the Independent Quadratic Optimisation algorithm. These key disadvantages can be overcome as follows:

- The use of individual harmonics [Clark et al, 1992; Gibbs et al, 1993; Kewley et al, 1995] or tones (through band pass filtering the reference signal) eliminates the possibility of overflow of the control filter coefficients; That is, the coefficients overflow as a result of low powers of their corresponding backward prediction error signals, and this overflow can be avoided with the use of individual harmonics (that may be synthesised) of constant power. Alternatively a variable gain factor can be used with the control filter coefficients with, however, a loss in resolution.

- The level of uncorrelated noise could be reduced by band pass filtering key frequencies in the error signal.

The effect of parameters (ie. control filter coefficient step size and number of averages) of the Independent Quadratic Optimisation algorithm, on performance (ie. attenuation level, bandwidth of attenuation and convergence speed) were assessed and found to compare favourably with the theory presented in chapter 4.

The use of different types of cost function (ie. Based on amplitude, and structural or acoustic intensity) was shown to give differing results for attenuation achieved in the far field of a semi-infinite plate, with results dependent on whether the error sensors were in the near or far field.

6.2 Recommendations

As discussed throughout this work, and summarised above, the Independent Quadratic Optimisation algorithm performs optimally for periodic or deterministic disturbances, where the tonal components of the disturbance can be individually orthogonalised (as has already been presented by Clark and Gibbs [1992, 1993] and Kewley et al [1995]).

Narrow band filtering of the offending tones from the error signal, for use in the cost function estimate can reduce the effect of uncorrelated noise. Alternatively, instead of narrowband filtering using fixed filters, an adaptive notch or comb filter could be

used to extract from the error signal, only those frequencies of interest. This approach should then provide as much attenuation as the filtered-X LMS algorithm in the experimental studies of chapter 5.

A further development of the Independent Quadratic Optimisation algorithm would be to incorporate poles into the lattice filter structure. The poles can be generated using the feedback form of the lattice filter shown in chapter 3. The stability of the transfer function defined by the lattice structure can be ensured by maintaining the PARCOR coefficients less than unity. The use of an IIR filter in this form would also reduce the number of coefficients used in the linear combiner. A IIR filter would be in the form of an output-error IIR filter, which would not necessarily have a quadratic cost function [Widrow and Stearns, 1985]. A form of equation-error IIR filter that would have a quadratic cost function could be formed by passing not only the reference signal through a lattice, but also the error signal, thus forming a feedforward/feedback controller. This could increase the bandwidth about minimised tonal components.

The Independent Quadratic Optimisation algorithm has been shown to be ideal only for periodic disturbances, and since periodic disturbances are easiest to obtain using a reference signal that is not affected by the control actuator, acoustic feedback was not considered in this work. The effect of acoustic feedback on the Independent Quadratic Optimisation algorithm should however be examined.

The inclusion of an effort weighting term in the cost function could ensure control

actuators are not overdriven. This is particularly important for the Independent Quadratic Optimisation algorithm, in view of the fact that simulations in chapter 4 suggested that it was best to optimise the coefficients of each control filter in turn. This type of criterion is identical to that used for the Generalised minimum variance control scheme.

Coupling between the control actuators was shown to reduce the effectiveness of the Independent Quadratic Optimisation algorithm. Recent results [Elliott et al, 1991] suggest that a set of single channel feedforward controllers could be used in place of a multi-channel controller, provided certain conditions are met, thus eliminating strong coupling between control actuators and error sensors.

The convergence speed of the Independent Quadratic Optimisation algorithm could be dramatically improved by optimising all the coefficients of the control filter at once, instead of optimising each individually. This would mean only three cost function estimates would be required. The optimal control filter coefficients should not be too difficult to calculate from these three estimates.

The Independent Quadratic Optimisation algorithm can be used with any cost function of quadratic nature. It is recommended that its use with non-linear filters such as those based on a Volterra approach [Klippel, 1995] be considered.

The Independent Quadratic Optimisation algorithm could be applied to a frequency domain approach, since harmonic bandpass filter outputs would be independent. This

could extend the bandwidth of application of the Independent Quadratic Optimisation algorithm, from not only tonal noise but to broad band noise.

The Independent Quadratic Optimisation control strategy could be particularly useful in large ducts, for control of the blade passage frequency (and associated harmonics) of large centrifugal fans. Multiple single-channel controllers could be used to minimise the tone particularly if the tones propagate as higher-order modes. The Independent Quadratic Optimisation algorithm is also particularly suited to using a measure of intensity as a performance criterion. This could further assist with the reduction of tones propagating as higher-order modes.

As the Independent Quadratic Optimisation algorithm is suited to tonal control, it could prove successful at reducing vibration levels, or minimising structure-borne sound using modal actuators and sensors [Nitzsche, 1993].

The lattice form of IIR filter has observable stability characteristics [Honig and Messerschmitt, 1984]. This would make it extremely suitable to other alternative optimisation approaches that do not require the cost function to be quadratic, such as a "stochastic learning automaton" which could result in broadband attenuation using the parameters of an output-error form of IIR lattice.

The lattice filter form is such that minimum modelling approaches, as described in Chalam [1987], should be considered. That is, the order of the lattice can be increased without affecting previously optimised coefficients (unlike a transversal

filter).

Finally, the lattice filter structure relative to the statistics of the input signal suggest that it could be used in conjunction with the Linear Quadratic Gaussian control scheme and robustness conditions defined by H_∞ control theory, since the statistics of the input signal play a major part in defining the degree of "cautiousness" a controller should apply. From the literature review of chapter 2, LQG control has a great potential in active noise and vibration control systems, and together with H_∞ control, controllers with good performance, stability and robustness conditions will be achievable in the not too distant future.

Besides research efforts into control algorithms, other work could be directed towards improving the minimum-phase characteristics of transducers, developing uni-directional compact transducers, improving modal sensing and actuating transducers, and finally designing "feedback transducers" that have minimal time delay between the sensor and the actuator.

Astrom, K.J. and Wittenmark, B. (1973), "On Self-Tuning Regulators", *Automatica*, **9**, 185-199.

Astrom, K.J. and Wittenmark, B. (1980), "Self-tuning controllers based on pole-zero placement", *Proc. IEE*, **127**, Pt. D:120-130.

Astrom, K.J. and Wittenmark, B. (1989), *Adaptive Control*, Addison-Wesley, USA.

Bai, M. and Shieh, C. (1995), "Active Noise Cancellation by using the Linear Quadratic Gaussian Independent Modal Space Control", *Journal of the Acoustical Society of America*, **97(5)**, 2664-2674.

Bao, C., Sas, P. and Van Brussel, H. (1993), "Comparison of two on-line identification algorithms for active noise control", *Proc. Recent Advances in Active Control of Sound and Vibration*, 38-51.

Bellanger, M.G. (1984), *Adaptive Digital Filters and Signal Analysis*, Marcel Dekker.

Beltran, C.I. (1995), "Acoustic transducer non-linearities and how they effect the performance of active noise control systems", *Proc. Active-95*, 837-848.

Bendat J.S. and Piersol, A.G. (1986), *Random Data*, 2nd edn, John Wiley and Sons.

Bennett, W.H. (1991), "Digital Signal Processing Methods for Control of Vibrations in Structures", *Proc. Recent Advances in Active Control of Sound and Vibration*, 783-795.

Berengier, M. and Roure, A. (1980), "Broad-band active sound absorption in a duct carrying uniformly flowing fluid", *Journal of Sound and Vibration*, **68**, 437-449.

Bitmead, R.R., Gevers, M., and Wertz, V. (1990), *Adaptive Optimal Control : The Thinking Man's GPC*, Prentice-Hall, New Jersey.

Botteldooren, D. (1993), "Feasibility Study of Active Control of Noise Perceived by Operators of Large Agricultural Machines", *Noise Control Engineering Journal*, **40(3)**, 221-229.

Boucher, C.C., Elliott, S.J. and Nelson, P.A. (1991), "The effect of errors in the plant model on the performance of algorithms for adaptive feedforward control", *Special Issue of the Proc. IEE : Pt. F on Adaptive Filters*, **138**, 313-319.

Bozich, D.J. and MacKay, H.B. (1991), "Neurocontrollers Applied to Real-Time Vibration Cancellation at Multiple locations, *Proc. of recent advances in Active Control of Sound and Vibration*, Virginia Polytechnic and State of University, USA, 326-337.

Brown, D.E. and Cabell, R. (1993), "An application of Filtered-X Techniques and Neural Networks to the Active Control of Non-Linear Systems", *Proc. of recent advances in Active Control of Sound and Vibration*, Virginia Polytechnic and State of University, USA, 3-14.

Burgess, J.C. (1981), "Active adaptive sound control in a duct : a computer simulation", *Journal of the Acoustical Society of America,* **70**, 715-726.

Canevet, G. (1978), "Active sound absorption in an air conditioning duct", *Journal of Sound and Vibration*, **58**, 333-345.

Carme, C. (1987), "Absorption acoustique active dans les cavities", *These presentee pour obtenir le titre de Docteur de l'Universite D'Aix-Marseille II*, Faculte des Sciences de Luminy.

Chalam, V.V. (1987), *Adaptive Control Systems : Techniques and Applications*, Marcel Dekker.

Chaplin, G.B.B. and Smith, R.A. (1978), "The Sound of Silence", *Engineering (London)*, **218**, 672-673.

Chaplin, G.B.B. (1980), "The Cancellation of Repetitive Noise and Vibration", *Proc. Inter-Noise 80*, 699-702.

Chaplin, G.B.B., (1983), "Anti-sound - the Essex breakthrough", *Chartered Mechanical Engineer*, **30**, 41-47.

Char, K. and Kuo, S.M. (1994), "Performance Evaluation of Various Active Noise Control Algorithms", *Proc. Noise-Con 94*, 331-336.

Clark, R.L. and Gibbs, G.P. (1992), "A Novel Approach to Feedforward Higher-Harmonic Control", *Journal of the Acoustical Society of America*, **96**, 926-936.

Clarke, D.W., and Gawthrop, P.J. (1975), "Self-Tuning Controller", *Proc. IEE*, **122**, 929-934.

Clarke, D.W., and Gawthrop, P.J. (1979), "Self-Tuning Control", *Proc. IEE*, **126**, 633-640.

Clarke, D.W., (1985), "Chapter 2 : Introduction to Self-Tuning Control", *Self-Tuning and Adaptive Control : Theory and Applications*, 2nd Edn. Edited by Billings, C.J. and Harris, S.A., IEE Control Engineering Series, Peter Peregrinus, London, 36-71.

Conover, W.B. (1956), "Fighting noise with noise", *Noise Control*, **2**, 78-82.

Cowan, C.F.N. and Grant, P.M. (1985), *Adaptive Filters,* Prentice Hall, Englewood Cliffs, New Jersey.

Curtis, A.R.D. (1991), "An Application of Genetic Algorithms to Active Vibration Control", *Proc. Recent advances in active noise control and vibration*, 338-347.

Darlington, P. (1991), "Passband disturbance in active sound control systems", *Proc. Recent Advances in Active Control of Sound and Vibration*, 731-741.

Dines, P.J. (1984), "Active control of flame noise", *Ph.D. Thesis*, University of Cambridge. England.

Dohner, J.L., and Shoureshi, R. (1989), "Modal Control of Acoustic Plants", *Trans. ASME*, **111**, 326-330.

Doelman, N.J. (1991), "A Unified Control Strategy for the Active Reduction of Sound", *Proc. Recent Advances in Active Control of Sound and Vibration*, Virginia Polytechnic and State University, USA, 271-289.

Doelman, N.J. (1993), "On the Optimal Design of a Controller for the Active Reduction of Random Noise", *Proc. Recent Advances in Active Control of Sound and Vibration*, 26-37.

Doyle, J.C., Francis, B.A., and Tannenbaum, A.R. (1994), *Feedback Control Theory*, Maxwell Macmillan.

Eghtesadi, Kh. and Leventhall, H.G. (1981), "Active Attenuation of Noise : The Chelsea Dipole", *Journal of Sound and Vibration*, **75**, 127-134.

Eghtesadi, Kh., Hong, W.K.W. and Leventhall. H.G. (1983), "The tight-coupled monopole active attenuator in a duct", *Noise Control Engineering Journal,* **20**, 16-20.

Elliott, S.J. and Darlington, P. (1985), "Adaptive cancellation of periodic, synchronously sampled interference", *IEEE Trans. Acoustics Speech and Signal Processing*, **ASSP 33**, 715-717.

Elliott, S.J., Stothers, I.M. and Nelson, P.A. (1987), "A multiple error LMS algorithm and its application to the active control of sound and vibration", *IEEE Trans. on Acoustics, Speech and Signal Processing,* **ASSP-35**, 1423-1434.

Elliott, S.J., Boucher, C.C. and Nelson, P.A. (1991), "The effect of acoustic coupling on the stability and convergence of independent controllers", *Proc. Inter-Noise 91*, 157-160.

Elliott, S.J., Boucher, C.C. and Nelson, P.A. (1992), "The behaviour of a multiple channel active control system", *IEEE Trans. on Signal Processing*, **40(5)**, 1041-1052.

Elliott, S.J. (1993), "Tyndall Medal Lecture : Active Control of Structure-Borne Sound", *Proc. Institute of Acoustics*, **15**, 93-120.

Elliott, S.J. and Nelson, P.A. (1994), "Active Noise Control", *Noise News International*, **2(2)**, 75-98.

Elliott, S.J., Sutton, T.J., Rafaely, B. and Johnson, M. (1995), "Design of Feedback Controllers using a Feedforward Approach", *Proc. of Active-95*, Newport Beach California, 863-874.

Eriksson, L.J. (1985), "Active Sound Attenuation Using Adaptive Digital Signal Processing Techniques", *Ph.D. thesis*, University of Wisconsin-Madison.

Eriksson, L.J., Allie, M.C. and Greiner, R.A. (1987), "The Selection and Application of an IIR Adaptive Filter for Use in Active Sound Attenuation", *IEEE Trans ASSP*, **ASSP-35(4)**, 433-437.

Eriksson, L.J. and Allie, M.C. (1989), "Use of random noise for on-line transducer modelling in an adaptive active attenuation system", *Journal of the Acoustical Society of America*, **85(2)**, 797-802.

Eriksson, L.J. (1990), "Development of the Filtered-U algorithm for active noise control", *Journal of the Acoustical Society of America*, **89(1)**, 257-265.

Eriksson, L.J. (1991), "Recursive Algorithms for Active Noise Control", *Proc. of the International Symposium on Active Control of Sound and Vibration*, April 9-11, Tokyo, Japan.

Eriksson, L.J. (1992), "Chapter 15" in *Active Noise Control, Noise and Vibration Control Engineering : Principles and Applications*, Ed. Beranek, L.L. and Ver, I.L., John Wiley and Sons Inc., 565-583.

Etter, D.M. and Masukawa, M.M. (1981), "A comparison of algorithms for adaptive estimation of the time delay between sampled signals", *Proc. ICASSP-81*, 1253-1256.

Feintuch, P.L. (1976), "An adaptive recursive LMS filter", *Proc. IEEE,* **64**, 1622-1624.

Feintuch, P.L., Bershad, N.J. and Allen, K.O. (1993), "A frequency domain model for "Filtered" LMS Algorithms - Stability analysis, Design and elimination of the training mode", *IEEE Trans on Signal Processing*, **41(4)**, 1518-1531.

Flockton, S.J. (1991), "Fast Adaptation Algorithms in Active Noise Control", *Proc. Recent Advances in Active Control of Sound and Vibration*, 802-810.

Franklin, G.F., Powell, J.D. and Workman, M.L. (1990), *Digital Control of Dynamic Systems*, Addison-Wesley.

Gawthrop, P.J. (1977), "Some Interpretations of the self-tuning controller", *Proc. IEE*, **124**, 889-894.

Gibbs, G.P. and Clark, R.L. (1993), "Feedforward Higher-Harmonic Control using the H-TAG algorithm", *Proc. NOISE-CON 93*, 541-546.

Gitlin, R.D., Meadors, H.C. and Weinstein, S.B. (1982), "The tap-leakage algorithm : An algorithm for the stable operation of a digitally implemented , fractionally spaced adaptive equaliser", *Bell Syst. Tech. J.*, **61**, 1817-1839.

Glover, J.R. (1977), "Adaptive noise cancellation applied to sinusoidal noise interferences", *Proc. IEEE Trans.*, **ASSP-25**, 484-491.

Goodwin, G.C. and Sin, K.S. (1985), *Adaptive Filtering : Prediction and Control*, Prentice Hall, Englewood Cliffs, New Jersey.

Grimble, M.J. (1984), "Implicit and Explicit LQG Self-Tuning Controllers", *Automatica*, **20**, 661-669.

Grimble, M.J. and Johnson, M.A. (1988), *Volume 2 - Optimal Control and Stochastic Estimation : Theory and Applications*, John Wiley and Sons.

Honig, M.L. and Messerschmitt, D.G. (1984), *Adaptive Filters : Structures, Algorithms and Applications,* Kluwer Academic Publishers, Boston.

Hsia, T.C. (1981), "A Simplified Adaptive Recursive Filter Design", *Proc. IEEE*, **69(9)**, 1153-1155.

Hull, A.J., Radcliffe, C.J. and MacCluer, C.R. (1991), "State Estimation of the Nonself-Adjoint Acoustic Duct System", *Trans ASME*, **113**, 122-126.

Imai, H. and Hamada, H. (1995), "Active Noise Control System Based on the Hybrid Design of Feedback and Feedforward Control", *Proc. Active-95*, 875-880.

Ionescu, T., and Monopoli, R.V. (1977), "Discrete-model reference adaptive control with an augmented error signal", *Automatica*, **13**, 507-518.

Isermann, R. (1991), *Digital Control Systems : Volume II. Stochastic Control, Multivariable Control, Adaptive Control, Applications*, Springer-Verlag, New York.

Jessel, M.J.M. (1968), "Sur les absorbeurs actifs", *Proc. 6th International Congress on Acoustics,* Tokyo, Paper F-5-6, 82.

Jessel, M.J.M. and Mangiante, G.A. (1972), "Active sound absorbers in an air duct", *Journal of Sound and Vibration,* **23(3)**, 383-390.

Johnson, C.R., Jr. and Larimore, M.G. (1977), "Comments on and Additions to 'An Adaptive Recursive LMS Filter'", *Proceedings IEEE*, **65(9)**, 1399-1401.

Johnson, C.R., Jr., Treichler, J.R., and Larimore, M.G. (1979a), "Remarks on the use of SHARF as an Output-Error Identifier", *Proceedings 17th IEEE Conference on Decision and Control*, San Diego, California, 1094-1095.

Johnson, C.R., Jr. (1979b), "A convergence proof for a Hyperstable Adaptive Recursive Filter", *IEEE Trans.*, **IT-25(6)**, 745-749.

Johnson, C.R., Jr., Larimore, M.G., Treichler, J.R., and Anderson, B.D.O. (1981), "SHARF Convergence Properties", *IEEE Trans.*, **ASSP-29(3)**, 659-670.

Johnson, M. (1990), "A new adaptive algorithm for active duct noise control", *Proc. ISSPA*, 283-286.

Johnson, M. (1992), "Active control applied to duct-borne noise", *Ph.D. Thesis*, University of Auckland, New Zealand.

Jones, J.D. (1987), "A study of active control techniques for noise reduction in an aircraft fuselage model", *PhD Dissertation*, Virginia Polytechnic and State University.

Kabal, P. (1983), "The stability of adaptive minimum mean square error equalisers using delayed adjustment", *IEEE Trans. on Communications,* **COM-31**, 430-132.

Kewley, D.L., Clark, R.L. and Southward, S.C. (1995), "Feedforward control using the higher-harmonic, time-averaged gradient descent algorithm", *Journal of the Acoustical Society of America*, **97(5)**, 2892-2905.

Kido, K. (1975), "Reduction of noise by use of additional sound sources", *Proceedings of Inter-Noise 75*, Sendai, 647-650.

Kim, I.S., NA, H.S., Kim, K.J., and Park, Y. (1994), "Constraint filtered-x and filtered-u least-mean-square algorithms for the active control of noise in ducts", *Journal of the Acoustical Society of America*, **95(6)**, 3379-3389.

Klippel, W. (1995), "Active attenuation of non-linear sound", *Proc. Active-95*, 413-422.

Kucera, V. (1980), "Stochastic multivariable control : A Polynomial Equation Approach", *IEEE Trans. Automatic Control*, **AC-25(5)**, 913-919.

Kuo, B.C. (1980), *Digital Control Systems*, Holt Reinhart and Winston.

Kuo, S.M., Wang, M. and Chen, K. (1991), "Active Noise Control System with Parallel On-Line Error Path Modelling Algorithm", *Noise Control Engineering Journal*, **39(3)**, 119-127.

Kuo, S.M. and Luan, J. (1993), "Multiple-channel Error Path Modelling with the Inter-channel Decoupling Algorithm", *Proc. Recent Advances in Active Control of Sound and Vibration*, 767-777.

La Fontaine, R.F. and Shepherd, I.C. (1983), "An experimental study of a broadband active attenuator for cancellation of random noise in ducts", *Journal of Sound and Vibration*, **90**, 351-362.

La Fontaine, R.F., Shepherd, I.C., and Cabelli, A. (1985), "A Bidirectional Microphone for the Measurement of Duct Noise", *Journal of Sound and Vibration*, **101(4)**, 565-573.

Landau, I.D. (1976), "Unbiased recursive identification using model reference techniques", *IEEE Trans. Automatic Control*, **AC-21**, 194-202.

Landau, I.D. (1979), *Adaptive Control; The Model Reference Approach*, Marcel Dekker, New York.

Larimore, M.G., Treichler, J.R. and Johnson, C.R. Jr. (1980), "SHARF: An Algorithm for Adaptive IIR Digital Filters", *IEEE Trans. Acoustics, Speech, Signal Processing*, **ASSP-28(4)**, 428-440.

Lebow, L.G., Blankenship, G.L. and Bennett, W.H. Jr. (1991), "Disturbance Rejection in Distributed Systems using Rule-Based Adaptive Controllers", *Proc. Recent advances in active noise control and vibration*, 313-325.

Leug, P. (1933), *German Patent No.655.508*, Filed : Jan 27, 1933, Patented : Dec 30, 1937.

Leung, R.C.N. (1993), "Enhanced LMS Control Algorithm", *Proc. Recent Advances in Active Control of Sound and Vibration*, 543-549.

Leventhall H.G. (1976), "Developments in active attenuators", *Proceeding of 1976 noise control conference*, Warsaw, 33-42.

Ljung, L. and Soderstrom, T. (1983), *Theory and Practice of Recursive Identification*, MIT Press, London.

Ljung, L. (1987), *System Identification; Theory for the User,* Prentice-Hall, New Jersey.

Mackenzie, N.C. and Hansen, C.H. (1991a), "The Implementation of a lattice filter structure and suitable algorithms for an adaptive active noise control system", *Proc. Recent advances in active noise control and vibration*, 372-388.

Mackenzie, N.C. and Hansen, C.H. (1991b), "The use of an Alternative Adaptive Algorithm coupled with a Lattice Structured Filter for a Multi-Channel Active Noise or Vibration Control System", *Proc. INTER-NOISE 91*, 177-180.

Malyuzhinets, G.D. (1969), "An inverse problem in the theory of diffraction", *Soviet Physics Doklady,* **14**, 118-119.

Meirovitch, M. (1990), *Dynamics and Control of Structures*, Wiley-Interscience.

Morari, M. and Zafiriou, E. (1989), *Robust Process Control*, Prentice-Hall.

Morgan, D.R. (1980), "An analysis of multiple correlation cancellation loops with a filter in the auxiliary path", *IEEE Trans. Acoustics, Speech and Signal Processing*, **ASSP-28**, 454-467.

Morgan, D.R. and Thi, J. (1993), "A Multitone Pseudocascade Filtered-X LMS Adaptive Notch Filter", *IEEE Trans. on Signal Processing*, **41(2)**, 946-956.

Nelson, P.A. and Elliott, S.J. (1992), *Active Control of Sound*, Academic Press Ltd.

Newton, G.C., Gould, L.A. and Kaiser, J.F. (1956), *Analytical Design of Feedback Controls*, John Wiley.

Nitzsche, F. (1993), "Smart Modal Sensors and Actuators for Aeroservoelastic Applications", *Proc. Recent advances in active noise control and vibration*, 3681-692.

Olson H.F. and May E.G. (1953), "Electronic Sound Absorbers", *Journal of the Acoustical Society of America*, **25(6)**, 1130-1136.

Olson, H.F. (1956), "Electronic control of noise vibration and reverberation", *Journal of the Acoustical Society of America*, **28**, 966-972.

Oppenheim, A.V. and Schafer, R.W. (1975), *Digital Signal Processing*, Prentice Hall, Englewood Cliffs, New Jersey.

Oz, H. and Meirovitch, M. (1983), "Stochastic Independent Modal Space Control of Distributed Parameter Systems", *J. Optimisation Theory Appl.*, **40**, 121-154.

Park, Y.C. and Sommerfeldt, S.D. (1994), "An enhanced noise control algorithm based on the lattice structure", *Proc. Inter-Noise 94*, 1217-1220.

Peterka, P. (1984), "Predictor-based Self-Tuning Control", *Automatica*, **20**, 39-50.

Powell, J.D. (1964), "An efficient method for finding the minimum of a function of several variables without calculating derivatives", *Comput. J.*, **7**, 155-162.

Procyk, T.J. and Mamdani, E.H. (1979), "A linguistic self-organising process controller", *Automatica*, **15**, 15-30.

Reichard, K.M. and Swanson, D.C. (1993), "Frequency domain implementation of the filtered-x algorithm with on-line system identification", *Proc. Recent Advances in Active Control of Sound and Vibration*, 562-573.

Ren, W. and Kumar, P.R. (1989), "Adaptive Active Noise Control : Structures, Algorithms and Convergence Analysis", *Proc. Inter-Noise 89*, Newport Beach, California, 435-440.

Ross, C.F. (1982), "An Adaptive Digital Filter for Broadband Active Sound Control", *Journal of Sound and Vibration*, **80**, 381-388.

Roure, A. (1985), "Self-Adaptive Broadband Active Sound Control System", *Journal of Sound and Vibration*, **101**, 429-441.

Saunders, W.R., Robertshaw, H.H. and Burdisso, R.A. (1993), "An Evaluation of Feedback, Adaptive Feedforward and Hybrid Controller Designs for Active Structural Control of a Lightly-Damped Structure", *Proc. Recent Advances in Active Control of Sound and Vibration*, 339-354.

Schroeder, M.G. (1984), *Number Theory in Science and Communications,* Springer, Berlin.

Shen, Q. and Spanias, A.S. (1992), "Time and Frequency Domain X Block LMS algorithms for Single Channel Active Noise Control", *Proc. 2nd International Congress on Recent Developments in Air- and Structure- Borne Sound and Vibration*, 353-360.

Shepherd, I.C., La Fontaine, R.F. and Cabelli, A. (1985), "A bi-directional microphone for the measurement of duct noise", *Journal of Sound and Vibration*, **101**, 563-573.

Silcox, R.J., Lester, H.C. and Abler, S.B. (1987), "An evaluation of noise control in a cylindrical shell", *NASA TM89090.*

Simshauser E.D. and Hawley M.E. (1955), "The noise cancelling headsets", *Journal of the Acoustical Society of America*, **27(1)**, 207.

Smith, R.A. and Chaplin, G.B.B. (1983), "A comparison of some Essex algorithms for major industrial applications", *Proceedings of Inter-Noise 83,* Edinburgh, 407-410.

Snyder, S.D. and Hansen, C.H. (1989), "Active Noise Control in Ducts : Some Physical Insights", *Journal of the Acoustical Society of America*, **86**, 184-194.

Snyder, S.D. and Hansen, C.H. (1990), "The Influence of Transducer Transfer Functions and Acoustic Time Delays on the Implementation of the LMS algorithm in Active Noise Control Systems", *Journal of Sound and Vibration*, **141(3)**, 409-424.

Snyder, S.D. (1991a), "Chapter 11 : The Active Control of Periodic Sound Transmission into Enclosed Spaces" in *Course notes on Active Control of Sound and Vibration*, University of Adelaide, Australia.

Snyder, S.D., Mackenzie, N.C. and Hansen, C.H. (1991b), "A Comparison of Orthogonal and Non-orthogonal filter structures and Algorithms Implemented in Active Noise and Vibration Control Systems", *Proc. INTER-NOISE 91*, 161-164.

Snyder, S.D., and Hansen, C.H. (1992a), "Design Considerations for active noise control systems implementing the multiple input, multiple output LMS algorithm", *Journal of Sound and Vibration*, **159**, 157-174.

Snyder, S.D., Clark, R.L. and Hansen, C.H. (1992b), "Convergence Characteristics of the multiple input, multiple output LMS algorithm", *J. Intell. Mat. Sys. Struct.*, **3**, 115-133.

Sommerfeldt, S.D. and Tichy, J. (1990), "Adaptive control of a two-stage vibration isolation mount", *Journal of the Acoustical Society of America*, **88(2)**, 938-944.

Sommerfeldt, S.D. (1991), "Multi-channel Adaptive Control of Structural Vibration", *Noise Control Engineering Journal*, **37(2)**, 77-89.

Subramaniam, R., Reinhorn, A., and Nagarajaiah, S. (1993), "Hybrid Control Using Fuzzy Set Theory", *Proc. of recent advances in Active Control of Sound and Vibration*, Virginia Polytechnic and State of University, USA, 303-314.

Swanson, D.C. (1986), "Active attenuation of acoustic noise using adaptive ARMAX controller", *PhD. Thesis*, The Pennsylvania State University.

Swanson, D.C. (1991a), "A stability robustness comparison of adaptive feedforward and feedback control algorithms", *Proc. of recent advances in Active Control of Sound and Vibration*, Virginia Polytechnic and State of University, Blacksburg, Virginia, USA, 754-767.

Swanson, D.C. (1991b), "Lattice Filter Embedding Techniques for Active Noise Control", *Proc. Inter-Noise 91*, 165-168.

Swanson, D.C. (1993), "The Generalised multi-channel Filtered-X LMS Algorithm", *Proc. Recent Advances in Active Control of Sound and Vibration*, 550-561.

Swinbanks, M.A (1973), "Active control of sound propagation in long ducts", *Journal of Sound and Vibration*, **27(3)**, 411-436.

Tang, C.K.K., and Mars, P. (1991), "Stochastic learning automata and adaptive IIR filters", *IEE Proc.-F*, **138(4)**, 331-340.

Thi, J. and Morgan, D.R. (1993), "Delayless subband active noise control", *Proc. IEEE International Conference on Acoustics, Speech and Signal Processing*, Minneapolis, Minnesota.

Thomas, D.R. and Nelson, P.A. (1995), "The Application of an Implicit Self-Tuning LQG Algorithm to the Active Control of Sound Transmission", *Proc. Active-95*, 299-310.

Tohyama, M. (1991), "Reverberant Phase in a Room and Zeroes in the Complex Frequency Domain", *Journal of the Acoustical Society of America*, **89**, 1701-1707.

Trinder, M.C.J. and Nelson, P.A. (1983), "Active noise control in finite length ducts", *Journal of Sound and Vibration,* **89**, 95-105.

Wangler, C.T., and Heiland, T. (1992), Personal communication.

Wangler, C.T. and Hansen, C.H. (1994), "Genetic algorithm adaptation of nonlinear filter structures for active sound and vibration control", *Proc. of the IEEE Int. Conf. on Acoustics, Speech and Signal Processing*, **3**, Adelaide, South Australia, 505-508.

Wangler, C.T. and Hansen, C.H. (1995), "Genetic Algorithm adaptation of IIR Filters by direct adjustment of poles and zeroes for active control of sound and vibration", *Proc. Active-95*, Newport Beach, USA.

Warnaka G.E. (1982), "Active Attenuation of Noise - The State of the Art", *Journal of Noise Control Engineering*, **18(3)**, 100-110.

Warnaka, G.E., Poole, L.A. and Tichy, J. (1984), "Active Acoustic Attenuator", *US Patent No. 4,473,906.*

Wellstead, P.E., Prager, D.L. and Zanker, P.M. (1979), "Pole-assignment self-tuning regulator", *Proc. IEE*, **126**, 781-787.

Wheeler, P.D. (1986), "Voice communications in the cockpit noise environment - the role of active noise reduction", *PhD. Thesis*, University of Southampton, England.

White, S. (1975), "An adaptive recursive digital filter", *Proc. 9th Annual Asilomar Conf. on Circuits, Systems and Computers*, 21-25.

Widrow, B., Glover, J.R., McCool, J.M., Kaunitz, J., Williams, C.S., Hern, R.H., Zeidler, J.R., Dong, E. and Goodlin, R.C. (1975), "Adaptive noise cancelling: Principles and applications", *Proc. IEEE*, **63**, 1692-1716.

Widrow, B., McCool, J.M. and Ball, M. (1975), "The Complex LMS algorithm", *Proc. of the IEEE*, **63**, 719-720.

Widrow, B. and McCool, J.M. (1976), "A comparison of adaptive algorithms based on the method of steepest-descent and random search", *IEEE Trans.*, **AP-24(5)**, 615-637.

Widrow, B. and Stearns, S.D. (1985), *Adaptive Signal Processing*, Englewood Cliffs, New Jersey, Prentice-Hall.

Wu, Z., Varadan, V.K., Varadan, V. and Lee, K.Y. (1995), "Active absorption of acoustic waves using state-space model and optimal control theory", *Journal of the Acoustical Society of America*, **97(2)**, 1078-1087.

Youla, D.C., Bongiorno, J.J. and Jabr, H.A. (1976), "Modern Weiner-Hopf Design of optimal controllers - parts 1 and 2", *IEEE Trans. Automatic Control*, **AC-21**, 3-13 and 319-338.

Zadeh, L.A. (1973), "Outline of a new approach to the analysis of complex systems and decision processes", *IEEE Trans. Systems, Man and Cybernetics*, **SMC-3**, 28-44.

A.1 Adaptive Filters

This section will consider systems defined in discrete-time using adaptive filters [Widrow and Stearns, 1985; Bellanger, 1984; Cowan and Grant, 1985; Honig and Messerschmitt, 1984]. A digital filter is adaptive if its coefficients defining its response can be altered with time. The response of a digital filter in the time domain is known as the "impulse response", denoted $h(n)$ (with n representing the number of samples), and in the frequency domain it is known as the "frequency response", denoted $H(e^{j\omega})$ (the Fourier transform of the impulse response, with ω representing the frequency, and the response normalised by the sampling frequency and limited to half the sampling frequency.

A filter with a finite impulse response is non-recursive, and is known as a "tapped-delay-line", a "transversal" or a "moving average (MA)" filter. The output of the filter is defined as the weighted sum of current and previous inputs:

$$u(n) = \sum_{i=0}^{I-1} a_i x(n-i) \qquad [A\text{-}1]$$

where $u(n)$ is the filter output, $h(i) = a_i$ defines the filter coefficients (of which there are I) and the impulse response, and $x(n)$ is the input to the filter. Taking z-transforms yields the characteristic equation of the filter, with the roots of this equation defining the zeroes (or dips in the spectrum with a white Gaussian noise input) of the filter.

$$H(z) = \frac{U(z)}{X(z)} = a_0 + a_1 z^{-1} + \ldots + a_{I-1} z^{-I+1} \qquad [A\text{-}2]$$

A filter with an infinite impulse response is recursive, and is also known as an "autoregressive-moving average (ARMA)" filter. The output of this filter may be defined as the sum of the current input and previous inputs and outputs:

$$u(n) = \sum_{i=0}^{I-1} a_i x(n-i) - \sum_{k=1}^{K} b_k u(n-k) = \sum_{i=0}^{\infty} c_i x(n-i) \qquad [A\text{-}3]$$

where $u(n)$ is the filter output, $h(i) = c_i$ defines the impulse response, a_i and b_k represent the filter coefficients, and $x(n)$ is the input to the filter. An "autoregressive" filter can be formed from the sum of only the previous **outputs.** Taking z-transforms of equation (A-3) yields

$$H(z) = \frac{U(z)}{X(z)} = \frac{a_0 + a_1 z^{-1} + \ldots + a_{I-1} z^{-I+1}}{1 + b_1 z^{-1} + \ldots + b_K z^{-K}} \qquad [A\text{-}4]$$

The roots of the numerator polynomial (in z^{-1}) define the zeroes (or dips in the spectrum with a white Gaussian noise input) of the filter, while the roots of the denominator polynomial (in z^{-1}) define the poles (or peaks in the spectrum with a white Gaussian noise input). The denominator polynomial is termed **monic** if its first coefficient is unitary.

The "direct" forms (there are other "canonical" forms) of these filters can be defined from the above equations and are shown in figures A-1 (a) and (b). An alternative "canonical" form is infact the lattice filter, the introduction of which is left to chapter 3.

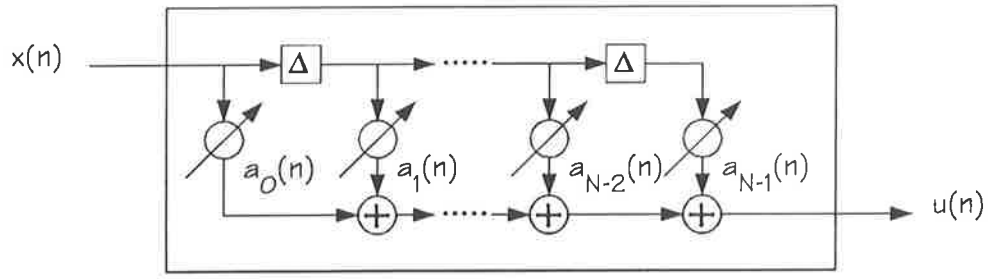

Figure A-1(a). Finite impulse response filter in direct form implementation. The coefficients of this filter are a_i, with input $x(n)$, and output $u(n)$.

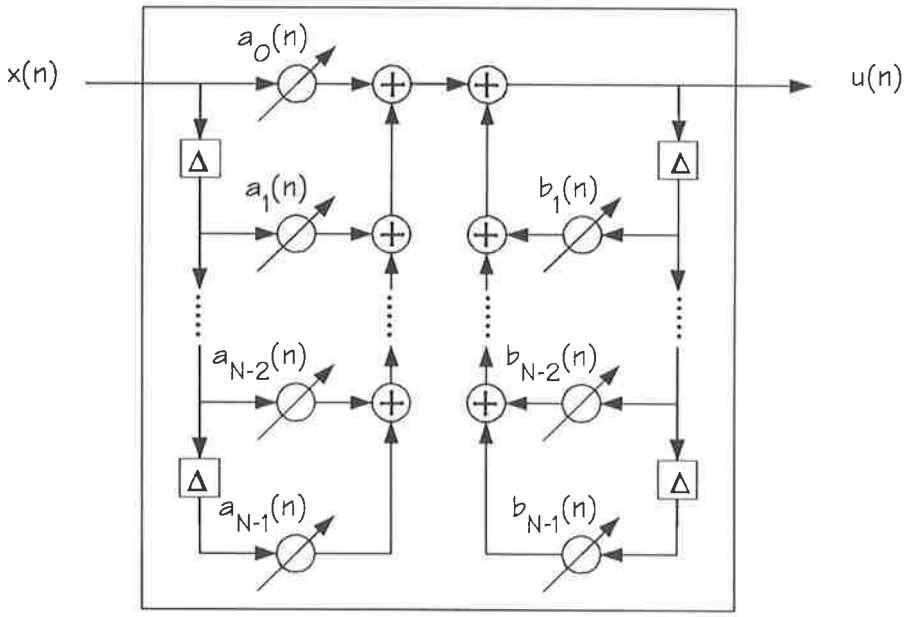

Figure A-1(b). Infinite impulse response filter in direct form implementation. The coefficients of this filter are a_i and b_i, with input $x(n)$, and output $u(n)$.

It should be noted that a discrete-time transfer function is only realisable if the **causality principle** is satisfied (that is, the filter cannot respond before excitation). Thus a realisable filter has a zero response until the instant an impulse is applied at

the input. Causality is observed easily in a time-domain analysis, but is concealed in a frequency domain analysis.

A filter is **stable** if its response is appropriate for a given excitation. External stability relates to the external inputs and outputs of the filter. It can be shown that bounded input-bounded output (BIBO) stability requires

$$\sum_{k=0}^{\infty} |h(k)| < \infty \qquad [A\text{-}5]$$

This condition also ensures the convergence of the transfer function $H(z)$ for $|z| \geq 1$, implying that $H(z)$ is analytic on and outside the unit circle and therefore only has poles in $|z| < 1$ [Ljung, 1987]. Thus it can be said that a transfer function $H(z)$ is stable provided its poles lie within the unit circle. A transfer function can be divided into partial fractions, with at most second order denominators. The poles of second order denominators define the transient behaviour of the system, with the proximity of poles to the unit circle defining their degree of damping. If the zeroes of a system lie within the unit circle in the z-domain, then the system is termed "**minimum-phase**", and its inverse is stable. This concept is critical to the discussions on control schemes throughout chapter 2.

Rather than using z-transforms to define transfer functions for system modelling, it is also common to use the "forward shift operator", q, and the backward shift operator, q^{-1}, and work in the time-domain. Thus a convolution in the z-domain as given by equation (A-1) would become

$$u(n) = \sum_{i=0}^{I-1} a_i q^{-i} x(n) = H(q)x(n) \qquad [A\text{-}6]$$

where $H(q)$ is a polynomial in the delay operator, q^{-1}.

A.2 System Identification

System identification is necessary to determine how a process responds to certain inputs, so that the most appropriate control signal can be generated to regulate the output. System identification involves defining a model of the system, and then identifying the parameters of this model. Figure A-2 shows the typical layout of the flow diagram showing the input and output to and from the process to be identified (usually the cancellation path transfer function) and the input and output to and from the model of the process. The aim is to ensure that the parameters defining the model are as close as possible to those of the process, with the prediction error ($\varepsilon(n) = y(n) - \hat{y}(n)$) giving a measure of the parameter estimation errors. The location of the identification scheme within the controller is shown in figure 2-3 of chapter 2. In this section, the models and algorithms used to identify the model parameters will be briefly reviewed.

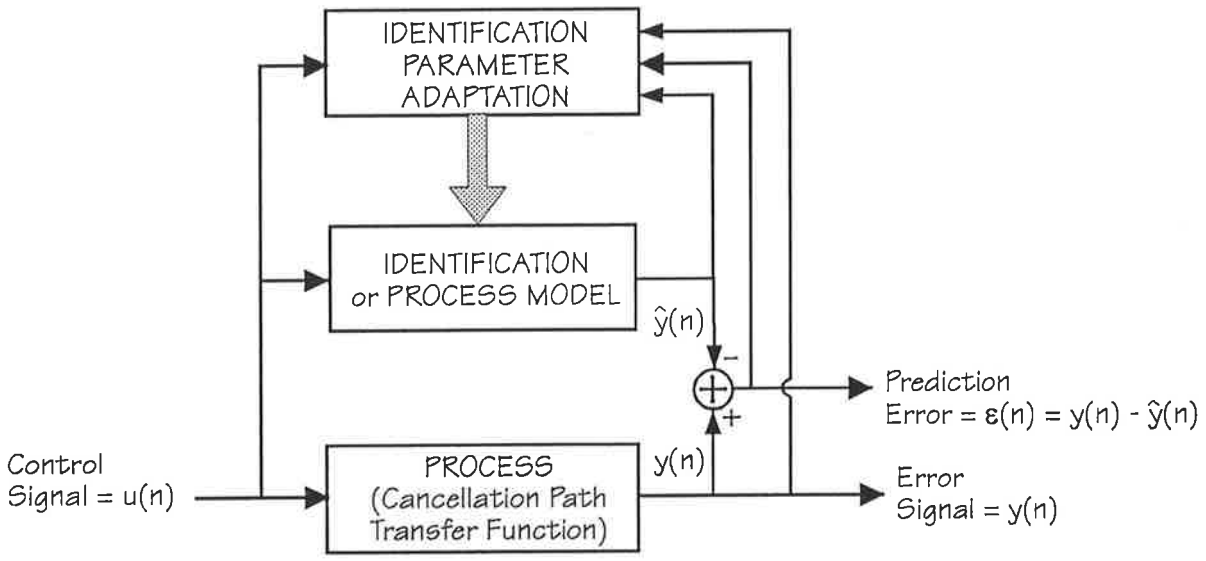

Figure A-2. Classical system identification problem.

A.2.1 Models

A model of a process requires a model of the transfer function linking the input to the output, as well as a model of the disturbance from white Gaussian noise passed through a transfer function to the output. There are two basic forms of model, known as "output-error" (or equivalently "Model Reference Adaptive Control") and "equation-error" (or "ARX" meaning Auto-Regressive noise model with eXogeneous input). A very common extension to the equation-error form is known as the "ARMAX" (meaning Auto-Regressive Moving-Average noise model with eXogeneous input) structure. The output-error form does not model the disturbance, while the equation-error form models the disturbance in different ways (ie. there are many types of equation-error form). The properties of these three common models will be briefly discussed as they will be referred to in section 2.4 of chapter 2.

A.2.1.1 Output-Error

The model used to identify the process is shown in figure A-3(a). When linked with the input and outputs from the unknown system, its relation to "Model Reference Adaptive Control" [Landau,1979] is evident by comparison of figure A-3(b) with figure 2-2. The disturbance, $v(n)$, is not modelled, and is shown here as white Gaussian noise, $e(n)$. In figures A-3(a) and (b) the system is shown as $B(q)/F(q)$.

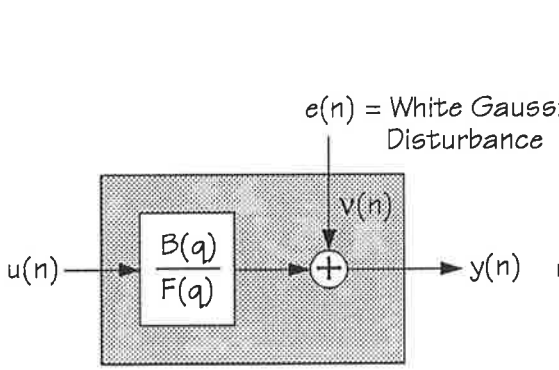

Figure A-3(a). Output-Error Model of a system with $u(n)$ the input, $y(n)$ the output, and $v(n)$ the unknown disturbance equal to white Gaussian noise, $e(n)$.

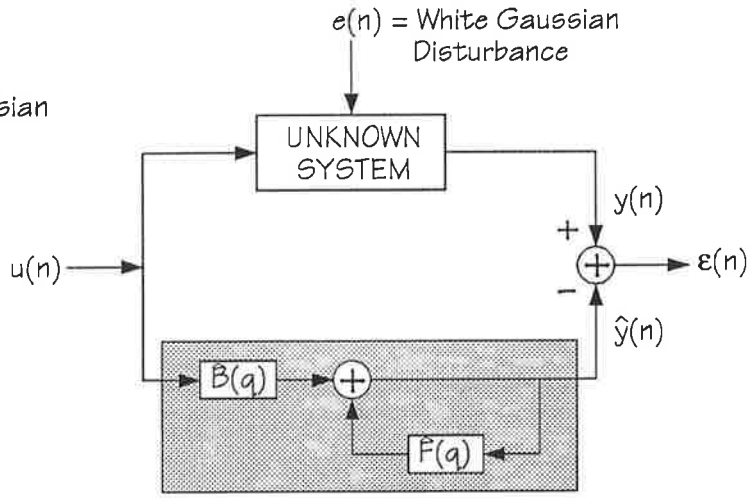

Figure A-3(b). Output-Error Model applied to unknown system, with $\hat{y}(n)$ the predictor used to estimate the system output $y(n)$, with prediction error $\varepsilon(n)$.

The predictor (ie. the predicted system output) at time n is dependent on the parameter vector (ie. the vector of parameters defining the model), θ, at that time. Hence the parameter vector, θ, is included in the predictor at time n, with descriptor, $\hat{y}(n|\theta)$, to highlight this dependency. The predictor can be written as (with $\hat{F}(q)$ monic as defined in A.1)

$$\hat{y}(n|\theta) = \frac{\hat{B}(q)}{\hat{F}(q)}u(n) = \hat{\theta}^{T}\phi(n,\theta) \qquad [A\text{-}7]$$

where the parameter vector is written as

$$\hat{\theta} = [\hat{b}_1,\ldots,\hat{b}_{n_b},\hat{f}_1,\ldots,\hat{f}_{n_f}]^{T} \qquad [A\text{-}8]$$

and the regressor (being a vector of samples of the input and output signals to and

from the process and estimation models) is written as

$$\phi(n,\theta) = [u(n-1),\ldots,u(n-n_b), -\hat{y}(n-1|\theta),\ldots, -\hat{y}(n-n_f|\theta)]^T \qquad [A\text{-}9]$$

The parameter vector is included in both the predictor and regressor to highlight its effect on both. If the system model (again note that the disturbance is not modelled) is accurate, the prediction error will equal the disturbance (ie. white noise), with the parameters (within the parameter vector) being adapted until the prediction error is whitened. This form of parameter estimation is known as a pseudo-linear regression since the effect of including the predictor in the regressor is non-linear.

A linear regression results if $F(q)=1$, leaving $B(q)$ which is then a FIR filter. However the general form is a recursive filter, and as such requires approximations (due to the non-linearity) to be implemented efficiently. Since this method does not estimate a model for the disturbance, it will be shown later, that it is not susceptible to biassed parameter estimates. A family of output-error related models can be represented by the "Box-Jenkins" model structure [Ljung, 1987].

A.2.1.2 Equation-Error (ARX)

The model used to identify the process in an equation-error (or ARX) approach is shown in figure A-4(a). Figure A-4(b) shows this system linked with the unknown system inputs and outputs. The disturbance is now modelled as white Gaussian noise passed through an autoregressive (AR) process. Hence the name ARX, with X corresponding to the exogenous input, $u(n)$.

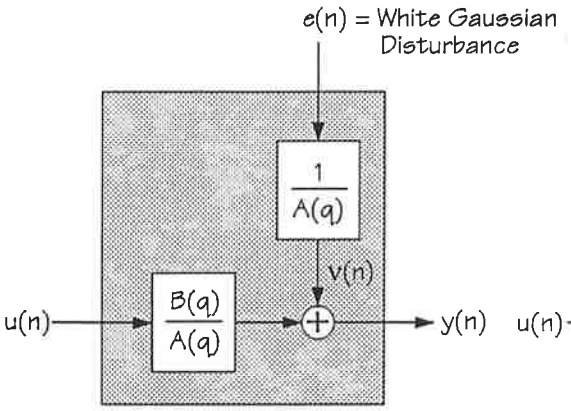

Figure A-4(a). Equation-Error Model of a system with $u(n)$ the input, $y(n)$ the output and $e(n)$ the white Gaussian noise input to generate the disturbance $v(n)$.

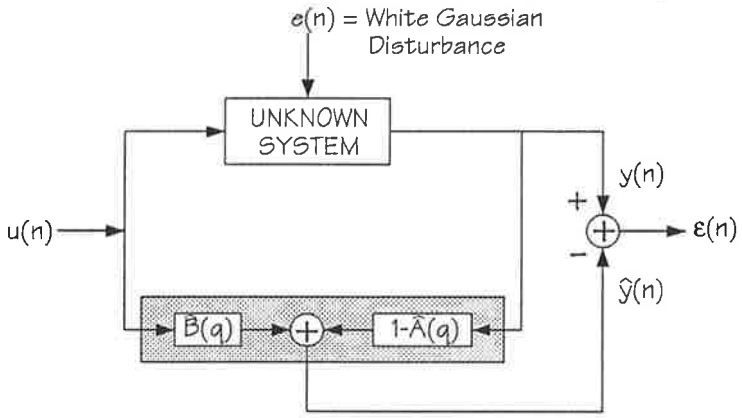

Figure A-4(b). Equation-Error Model applied to unknown system, with $\hat{y}(n)$ the predictor used to estimate the system output $y(n)$, with prediction error $\varepsilon(n)$.

In this form, the predictor can be written as (with $\hat{A}(q)$ monic, as defined in section A.1)

$$\hat{y}(n|\theta) = \hat{B}(q)u(n) + (1-\hat{A}(q))y(n) = \hat{\theta}^{T}\phi(n) \qquad [A\text{-}10]$$

where the parameter vector is written as

$$\hat{\theta} = [\hat{a}_1,\ldots,\hat{a}_{n_a},\hat{b}_1,\ldots,\hat{b}_{n_b}]^{T} \qquad [A\text{-}11]$$

and the regressor can be written as

$$\phi(n) = [-y(n-1),\ldots,-y(n-n_a),u(n-1),\ldots,u(n-n_b)]^{T} \qquad [A\text{-}12]$$

If the system model and the disturbance model are accurate, then the prediction error

will be whitened. This model is important as the predictor defines a linear regression, and is non-recursive (linear) since it feeds back the actual process output, $y(n)$, rather than the estimated process output, $\hat{y}(n)$ (note $\phi(n)$ in equation (A-10) and (A-12) as opposed to $\phi(n,\theta)$ in equation (A-7) and (A-9)). It is however susceptible to biassed parameters (as will be shown later) since if the disturbance model is not accurate, the process output used in the regressor will be correlated with the unmodelled disturbance.

A.2.1.3 ARMAX

Finally consider the most common model of a process that models the disturbance as an ARMA sequence (hence the name ARMAX, with X corresponding to the "exogenous" input, $u(n)$), distinct from the AR disturbance model shown above. The process model is shown in figure A-5, with the association with the unknown system as it is a simple modification to that shown in figure A-4(b).

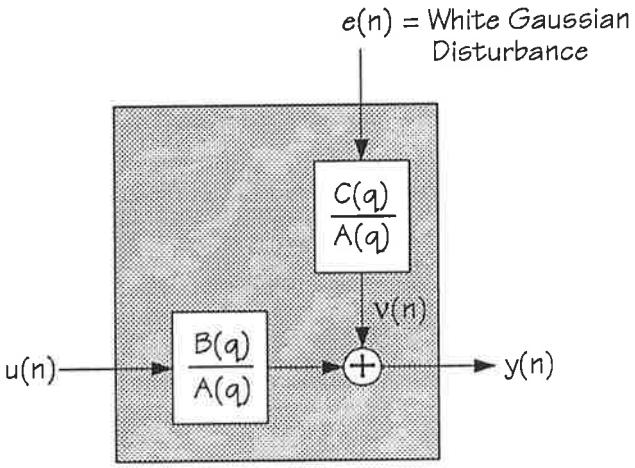

Figure A-5. ARMAX model of a process.

In this form, the predictor (termed a pseudo-linear regression) can be written as

$$\hat{y}(n|\theta) = \frac{\hat{B}(q)}{\hat{C}(q)}u(n) + (1-\frac{\hat{A}(q)}{\hat{C}(q)})y(n) = \hat{\theta}^{T}\phi(n,\theta) \qquad [A\text{-}13]$$

The prediction error (or innovation) can be written as (for all models)

$$\varepsilon(n,\theta) = y(n) - \hat{y}(n|\theta) \qquad [A\text{-}14]$$

and therefore it can be shown that the regressor can be written as

$$\phi(n,\theta) = [-y(n-1),\ldots,-y(n-n_a),u(n-1),\ldots,u(n-n_b), \varepsilon(n-1,\theta),\ldots,\varepsilon(n-n_c,\theta)]^{T} \qquad [A\text{-}15]$$

and the parameter vector can written as

$$\hat{\theta} = [\hat{a}_1,\ldots,\hat{a}_{n_a},\hat{b}_1,\ldots,\hat{b}_{n_b},\hat{c}_1,\ldots,\hat{c}_{n_c}]^{T} \qquad [A\text{-}16]$$

As for the equation-error model, biassed parameters result for inaccurate disturbance models. As the ARMAX model is recursive and can be written as a pseudo-linear regression, it can be treated in a similar manner to the output-error model. The ARMAX model is a form of equation-error model.

A model that incorporates both equation error and output-error model types in their most general form has been described by Ljung [1987] and Ljung and Soderstrom [1983].

A.2.2 Cost Functions and Parameter Estimation

The model parameters forming the parameter vectors, are adapted to minimise (or whiten) the magnitude of the prediction error (or innovation). The cost function to be minimised can be based on the expectation of the squared prediction error

(forming the "Mean Square Error" or "Stochastic" approach [Ljung and Soderstrom, 1983]), or the expectation can be approximated by sample means (forming the "Least-Squares" approach [Ljung and Soderstrom, 1983]). The cost functions can thus be written as:

$$J(\theta) = E[\varepsilon^2(n)] \approx \frac{1}{n}\sum_{k=1}^{n} \varepsilon^2(k) = J(\theta,Z^n) \qquad [A\text{-}17]$$

where $\varepsilon(n)$ is the prediction error, $J(\theta)$ is the stochastic cost function, and $J(\theta,Z^n)$ is the estimate of the cost function using the average of samples of the prediction error to time n. The cost function can also be viewed as a performance surface [Cowan and Grant, 1985; Widrow and Stearns, 1985]. The prediction error can be prefiltered to provide a means of frequency weighting [Ljung, 1987]. A "windowing" term can be added to the least squares estimate, to allow for quasi-stationary processes, in which stationarity is definite for only a certain number of samples [Ljung, 1987]. The estimated cost function with a windowing term (or forgetting factor) can be written as:

$$J(\theta,Z^n) = \gamma(n)\sum_{k=1}^{n} \beta^{n-k}\varepsilon^2(k) \qquad [A\text{-}18]$$

where β is the forgetting factor and takes a value close to but less than unity (usually between 0.98 and 0.995), giving an effective memory (or number of samples which can be considered to be generated from a stationary process) of $1/(1-\beta)$. The term $\gamma(n)$ is a normalising term (which can be approximated by $(1-\beta)$), and is included so that $J(\theta,Z^n)$ approaches $J(\theta)$ as n approaches infinity.

The stochastic approach will now be used together with an equation-error model (chosen because it is non-recursive) to define by example the critical concepts of biassed parameter estimates, persistent excitation, the difference between minimum

and excess mean square (as defined by the misadjustment), and finally the definition of the principal axes of the cost function, all of which are relevant to the Independent Quadratic Optimisation (IQO) algorithm.

Using the linear regression model (equation-error), the optimum parameter estimates can be found from derivatives of the stochastic cost function (defined by equation (A-17)) in expanded form, such that

$$\theta_{opt} = R_{\phi\phi}^{-1} C_{y\phi} \qquad [A\text{-}19]$$

where

$$R_{\phi\phi} = E[\phi(n)\phi^{T}(n)] \qquad [A\text{-}20]$$

represents the autocorrelation matrix of the regressor and

$$C_{y\phi} = E[y(n)\phi(n)] \qquad [A\text{-}21]$$

represents the cross-correlation vector of the regressor and the process output. Suppose now that the observed data was actually generated by

$$y(n) = \theta_0^{T}\phi(n) + \nu_0(n) \qquad [A\text{-}22]$$

If this were true, it means that the disturbance model is not accurate, resulting in a coloured unmodelled disturbance $\nu_0(n)$ instead of white Gaussian noise. The optimum parameter estimates can be found by substituting equation (A-22) into (A-19), such that

$$\theta_{opt} = \theta_0 + R_{\phi\phi}^{-1} E[\nu_0(n)\phi(n)] \qquad [A\text{-}23]$$

The parameter estimates are termed "consistent" if $\theta_{opt} = \theta_0$, which will occur provided the following conditions are met:

- The autocorrelation matrix, $R_{\phi\phi}$, is non-singular. This will require the input to the process to be **persistently exciting.** The persistently exciting condition implies that the number of parameters in a linear model that can be uniquely determined is limited by the power spectrum of the input irrespective of the complexity of the unknown process [Honig and Messerschmitt, 1984]. If this condition is not met the parameter estimates will not converge to their true values.

- The disturbance, $v_0(n)$, is independent of the regressor, $\phi(n)$, components. This requires that the disturbance, $v_0(n)$, be a sequence of independent random variables with zero mean. That is, the model of the disturbance must be exact to ensure unbiased parameter estimates. If this condition is not met, the parameters will be **biassed** by the correlation of the unmodelled disturbance with the regressor components (these components specifically being the process output and the prediction error).

Biassing can be eliminated by using the method of instrumental variables [Ljung and Soderstrom, 1983], using a more accurate model of the disturbance, or injecting an uncorrelated signal into the system. The method of instrumental variables is equivalent to using an output-error (or model reference) approach, since no attempt is made to model the disturbance. That is, since the regressor of the output-error model uses the process output estimate rather than the actual process output, there can be no correlation between the unmodelled disturbance and any component of the regressor. This is the key difference between the output-error and the equation-error

methods of system identification.

The distinction between equation-error and output-error forms has been well explained by Bitmead et al [1990], who note the advantages of each scheme as:

- The equation-error method predicts a model of both the system and the disturbance.

- The output-error method predicts a model only for the system therefore avoiding biassed parameter estimates.

Bitmead et al [1990] note that the use of the equation-error method will provide a good disturbance model that is essential to achieve adequate disturbance rejection (as will be seen when considering minimum variance control), while use of the output-error method will provide a close (unbiased) system model that is required for stability and robustness.

It can further be shown [Tang and Mars, 1991] that the equation-error method has a unique global minimum, with no local minima (however the resulting parameter estimates that form the recursive system model need to be checked to ensure the model is not unstable as a result of biassed parameter estimates). This can be contrasted to the output-error method which has multiple local minima and requires stability monitoring since it uses a recursive filter. This has particular relevance to alternative methods of optimisation to be discussed in section 2.5 of chapter 2.

Returning now to the stochastic cost function, it can be shown that the stochastic cost function optimum (or minimum mean square error) is given by

$$J_{opt} = r_{yy} - C_{y\phi}^{T}\theta_{opt} \qquad [A\text{-}24]$$

where r_{yy} is the autocorrelation or power of the process output. This equation shows that the stochastic cost function optimum (minimum mean square error) is dependent upon the correlation of the regressor components with the process output. It can further be shown that the cost function is composed of the minimum mean square error and the excess mean square error:

$$J(\theta) = J_{opt} + (\theta - \theta_{opt})^{T} R_{\phi\phi} (\theta - \theta_{opt}) \qquad [A\text{-}25]$$

The excess mean square error is dependent upon the variance of the parameter estimates about their optima. Another term that gives a useful indication of the performance of an algorithm is the misadjustment, which is the ratio of the excess mean square error to the minimum mean square error. These items are discussed in chapters 4 and 5 with regard to the Independent Quadratic Optimisation algorithm.

Finally, the autocorrelation matrix can be written in normal form using its eigenvalue matrix, Λ (in which the off diagonal terms are zero and the diagonal terms correspond to the eigenvalues of the autocorrelation matrix), and the corresponding modal matrix of eigenvectors, Q, such that

$$J(\theta) = J_{opt} + V^{*T} \Lambda V^{*} \qquad [A\text{-}26]$$

where the components of $V^{*} = Q^{T}(\theta - \theta_{opt})$ define the principal axes of the cost function, and the eigenvalues of the autocorrelation matrix correspond to the second derivative of the cost function relative to the principal axes. That is, the eigenvalues relate to the degree of curvature of the cost function in the direction of the principal

axes. The principal axes can also be formed using orthogonal components of the regressor. This is a critical concept for the Independent Quadratic Optimisation algorithm, for which the regressor consists of orthogonal signals generated by a lattice filter, as will be shown in chapter 3.

The concepts of minimum and excess mean square error, principal axes and degree of curvature of the cost function in the direction of the principal axes, are important to the Independent Quadratic Optimisation algorithm to be developed in subsequent chapters. The concepts of biassed parameters and persistent excitation are critical to system identification, and therefore to many of the common control algorithms.

A.2.3 Optimisation Methods

The parameters defining a model can be updated using a steepest-descent approach, or the modified steepest-descent approach known as Newton's Method. These approaches can be written generally as [Ljung and Soderstrom, 1983]:

$$\hat{\theta}(n+1) = \hat{\theta}(n) - \gamma(n)J'(\theta,Z^n)J''(\theta,Z^n) \qquad [A\text{-}27]$$

where $J''(\theta,Z^n)$, represents the double derivative of the stochastic cost function and is known as the "Hessian" matrix, and $J'(\theta,Z^n)$, represents the derivative of the stochastic cost function and is known as the "gradient vector", and $\gamma(n)$ corresponds to the step factor. The gradient vector defines the direction of steepest descent, while the Hessian matrix modifies this direction to account for differences in the gradient with respect to each parameter (ie. The inclusion of the Hessian matrix avoids

eigenvalue disparity effects that plague algorithms based solely on the method of steepest descent or approximations thereof).

The models discussed in section A.2.1 can be divided into a linear regression type and a pseudo-linear regression type. The linear-regression can be treated as a special type of pseudo-linear regression, and therefore will not be treated specifically. Recursive parameter estimates for pseudo-linear regression can be classified as "Recursive Prediction Error Methods" or "Recursive Pseudo Linear Regressions".

- **Recursive Prediction Error Methods (RPEM)**

  The recursive update equation uses the gradient of the cost function to update the parameter vector. It can be shown [Ljung, 1987] that the gradient vector and the Hessian matrix of the cost function are given by

$$J'(\theta,Z^n) = -\varepsilon(n,\theta)\psi(n,\theta)$$
$$J''(\theta,Z^n) = R_{\psi\psi}^{-1}(n) \qquad \text{[A-28a,b]}$$

  where

$$\psi(n,\theta) = \frac{\partial \hat{y}(n,\theta)}{\partial \theta} \qquad \text{[A-29]}$$

  has become known as the gradient vector, $R_{\psi\psi}$ is the autocorrelation matrix for this form of gradient vector, and $\varepsilon(n,\theta)$ is the prediction error. It can be shown that the gradient vector for the output-error model is given by $\hat{F}(q)\psi(n,\theta) = \phi(n,\theta)$, while the gradient vector for the ARMAX model is $\hat{C}(q)\psi(n,\theta) = \phi(n,\theta)$, and finally the gradient vector for the **linear regressive** equation-error (or ARX) model is equal to the regressor, $\psi(n) = \phi(n)$.

Calculating $\varepsilon(n,\theta)$ and $\psi(n,\theta)$ is computationally inefficient as they are recursive, hence their dependence on θ is ignored [Ljung, 1987], and the recursive prediction error algorithm becomes:

$$\begin{aligned} \varepsilon(n) &= y(n) - \hat{y}(n) = y(n) - \phi^{T}(n)\hat{\theta}(n-1) \\ \hat{\theta}(n) &= \hat{\theta}(n-1) + \gamma(n)R_{\psi\psi}^{-1}(n)\psi(n)\varepsilon(n) \\ R_{\psi\psi}(n) &= R_{\psi\psi}(n-1) + \gamma(n)[\psi(n)\psi(n) - R_{\psi\psi}(n-1)] \end{aligned} \qquad \text{[A-30a,b,c]}$$

- **Recursive Pseudo-Linear Regression (RPLR) Method**

The recursive prediction error method ultimately required the approximation that $\hat{y}(n,\theta)$ was non-recursive in θ. If this approximation is taken from the beginning, then the gradient vector becomes

$$\psi(n,\theta) = \frac{\partial\hat{y}(n,\theta)}{\partial\theta} \simeq \phi(n,\theta) \qquad \text{[A-31]}$$

The use of this approximation gives the recursive pseudo-linear regression algorithm, such that

$$\begin{aligned} \varepsilon(n) &= y(n) - \hat{y}(n) = y(n) - \phi^{T}(n)\hat{\theta}(n-1) \\ \hat{\theta}(n) &= \hat{\theta}(n-1) + \gamma(n)R_{\phi\phi}^{-1}(n)\phi(n)\varepsilon(n) \\ R_{\phi\phi}(n) &= R_{\phi\phi}(n-1) + \gamma(n)[\phi(n)\phi(n) - R_{\phi\phi}(n-1)] \end{aligned} \qquad \text{[A-32a,b,c]}$$

The recursive prediction error method is a more accurate method as it uses less approximations, but in so doing requires more computations than the recursive

pseudo-linear regression algorithm. The discerning difference between these algorithms lies in the use of ϕ (as per RPEM) instead of ψ (as per RPLR). The effect of this approximation will be discussed shortly. As discussed above, the gradient vector for the equation-error (ARX) model is $\psi(n) = \phi(n)$, hence for the equation-error model the recursive prediction error method is equivalent to the recursive pseudo-linear regression method, and the resulting algorithm is commonly known as the "Recursive Least Squares (RLS)" algorithm, with the inverse autocorrelation matrix defined by recursive adaptation as will now be discussed.

In both these methods, the autocorrelation matrix (of either the regressor or the gradient vector) $R^{-1}(n)$ can be adapted recursively using the matrix inversion lemma [Ljung, 1987], with $P(n) = R^{-1}(n)$. The recursive update of $P(n)$ can be defined using this lemma as (with ß a constant defined to avoid division by zero at initialisation of the algorithm):

$$R^{-1}(n) = \frac{P(n-1)}{ß + \phi^{T}(n)P(n-1)\phi(n)}$$

$$P(n) = \frac{1}{ß}\left[P(n-1) - \frac{P(n-1)\phi(n)\phi^{T}(n)P(n-1)}{ß + \phi^{T}(n)P(n-1)\phi(n)}\right] \qquad \text{[A-33a,b]}$$

Alternatively the matrix $R^{-1}(n)$ can be approximated using the stochastic cost function, and the "Robbins-Munro" scheme [Ljung and Soderstrom, 1983]. The method so defined is known as the "Stochastic Gradient Method", with $R(n) = I$. The gain $\gamma(n)$ can be a constant or normalised by some means. This algorithm has been extensively used in adaptive signal processing by Widrow and Stearns [1985], with regard to a linear regression, and is commonly known as the "Least Mean Squares" algorithm.

The stochastic gradient method or least mean squares algorithm is affected by the eigenvalue disparity of the autocorrelation matrix. This disparity (given by the maximum difference in the powers of the spectral components of the reference signal) affects the speed of convergence of the parameter estimates. Eigenvalue disparity will not affect the speed of convergence if a recursive algorithm is used (like the recursive least squares (RLS)). The recursive least-squares approach is based on Newton's Method of searching a cost function, with instead of the parameters adapted in the direction of steepest descent, they are adapted in a modified direction towards the optimum of the cost function. The stochastic gradient method or least mean squares algorithm also has a greater misadjustment than the algorithms that incorporate a more accurate estimate of the inverse autocorrelation matrix, because the approximation of the gradient estimate is so "noisy" it results in increased variance of the parameter estimates about their optima.

The recursive identification schemes have been developed and named for different types of systems and models. These are summarised in table A-1, only for the models considered in section A.2.1 [Ljung, 1987]. In table A-1, RML stands for the "Recursive Maximum Likelihood" algorithm developed from a Bayesian approach, and ELS stands for the "Extended Least Squares" algorithm. A good summary of these methods, which can be derived from the models given in section A.2.1, is presented in Isermann [1991] and Ljung [1987].

Model Structure	Algorithm Type	
	Recursive Prediction Error Method (RPEM)	Recursive Pseudo-Linear Regression Method (RPLR)
ARX (Equation-Error)	RLS	RLS
Output-Error (Model Reference)	White [1975], Hsia [1981]	Landau [1976], Feintuch [1976]
ARMAX (Equation-Error type)	RML	ELS

Table A-1. Summary of algorithms defined from the use of recursive pseudo-linear regression and prediction error methods for different process/disturbance models.

As discussed, the difference between the RPLR approach and the RPEM approach lies in the use of ϕ instead of ψ. The effect of this approximation will now be considered for the equation-error model type (ie. ELS algorithm). It can be shown [Ljung, 1987; Ljung and Soderstrom, 1983] for the ARMAX model that a sufficient condition for convergence of the parameter vector to the true parameters is dependent upon

$$Re\left\{\frac{1}{C_0(e^{j\omega})}\right\} \geq \frac{1}{2} \quad \forall\omega \qquad [A\text{-}34]$$

where $C_0(q)$ is the true moving average polynomial defining the moving average component of the disturbance (see section A.2.1 for the model definition). This is known as the "strictly positive real (SPR)" condition, and can alternatively be written as

$$|C_0(e^{j\omega}) - 1| < 1 \quad \forall\omega \qquad [A\text{-}35]$$

It is apparent from this equation that convergence to the true parameters depends

upon the roots of $C(z) = 0$ lying within the unit circle in the z-domain (ie. minimum phase condition). This theory was developed by Popov and Lyapunov, with a good discussion given in Cowan and Grant [1985], who relate it to the Nyquist stability criterion. Ljung and Soderstrom [1983], using an ordinary differential equation (ODE) approach to convergence analysis, further show that

$$Re\{C_0(e^{j\omega})\} > 0 \quad \forall\omega \qquad \text{[A-36]}$$

Astrom and Wittenmark [1989] note that a system with a frequency response that satisfies this "positive real" condition is termed passive. Thus passivity and minimum-phase conditions are closely related.

The stability criteria for the RPLR method can be related to those just defined for the RPEM. As the recursive prediction error method uses an estimate of the function, $\hat{C}(e^{j\omega})$, then it is considered the stability conditions defined for the RPLR method will hold for the difference between the estimate of $C(e^{j\omega})$ and the actual function. Thus the above conditions may be extended to the recursive prediction error method, with the difference in phase and magnitude between the estimate of $C(e^{j\omega})$ and the actual value to be no more than 90° for convergence of the parameter estimates, as indicated by equation (A-36). The conditions discussed relate to the equation-error model type (ie. ARMAX) and associated algorithms; similar conditions can be shown for the output-error model type.

Feintuch [1976] used a stochastic gradient form of the recursive pseudo-linear regression approach and applied it to an output-error model (Landau [1976] first proposed the exact form of the RPLR method using the model reference approach).

This algorithm was shown to converge to false minima [Johnson and Larimore, 1977]. The convergence coefficients must be kept very small for convergence to a non-unique minimum of the cost function, dependent upon the initial values of the coefficients [Cowan and Grant, 1985; Tang and Mars, 1991]. Johnson [1979b] then proposed an algorithm known as the "Hyperstable Adaptive Recursive Filter (HARF)", in which the prediction error was pre-filtered by a fixed filter. Johnson [1979a, 1981] also proposed a stochastic gradient form known as the "Simple HARF (SHARF)". Ljung and Soderstrom [1983] note that these algorithms are identical to the recursive prediction error method provided the prefilter is time-variant and equivalent to $1/\hat{F}(q)$. Hsia [1981] developed the stochastic gradient form of the recursive prediction error method for the output-error model type, with the exact algorithm originally defined by White [1975].

Of final note in the identification of systems is the work by Isermann [1991]. In his summary an attempt is made to define the impact of biassing on closed-loop (ie. feedback control system) parameter estimation. It was stated earlier that biassed parameter estimates can be avoided using an instrumental variables approach (of which the output-error or model-reference is a special case) or by injecting an uncorrelated signal into the system (ie. an external perturbation signal). Isermann [1991] notes that if an instrumental variables approach is used in closed-loop (ie. feedback control system) it could result in biassed parameter estimates. In closed-loop, the RLS, ELS and RML algorithms provide unbiased estimates provided the disturbance is correctly modelled. An external perturbation signal yields unbiased estimates provided it is sufficiently persistently exciting.

A.3 Minimum Variance Control

The previous section addressed methods for identifying the parameters of a process. These methods will now be coupled with a control law defined from a minimum-variance approach, which is shown in section 2.4 of chapter 2, to be particularly suitable to active noise and vibration control. The common algorithms used in active noise and vibration control will be shown to follow directly from this control theory approach.

Consider the control of an ARMAX process, shown in figure A-6. The disturbance is generated by passing white Gaussian noise through an ARMA filter, and the system has a time delay (or dead-time) of k samples (typical of the propagation delay between a control actuator and an error sensor) also with an infinite impulse response. It is to be noted that the same denominator polynomial is used, as it relates to the modes of the physical system, as described in section A.1.

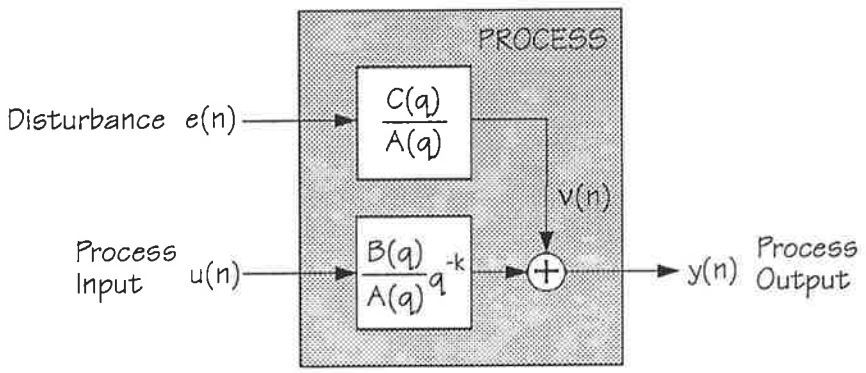

Figure A-6. ARMAX process, with $e(n)$ represents a white Gaussian noise sequence, $u(n)$ is the control input, $y(n)$ is the process output, and $v(n)$ is an ARMA disturbance.

The minimum variance control scheme (originally proposed by Astrom and Wittenmark [1973]) obtains its name as it attempts to minimise the variance of the process output. The cost function to be minimised by the controller (using only data upto time n) is given by

$$J = E[y^2(n+k) \mid n] \qquad [A\text{-}37]$$

with

$$y(n+k) = \frac{B(q)}{A(q)}u(n) + \frac{C(q)}{A(q)}e(n+k) \qquad [A\text{-}38]$$

Equation (A-38) can alternatively be written as

$$e(n+k) = \frac{A(q)y(n+k) - B(q)u(n)}{C(q)} \qquad [A\text{-}39]$$

It is important to note that the only data available to generate the control signal is that up to time n (ie. $u(i)$, $y(i)$, and $e(i)$ for $i \leq n$). It can be seen however that to predict $y(n+k)$ using data up to time n is not possible since $e(n+k)$ is required (as per equation (A-38)), and yet $e(n+k)$ depends on the process output $y(n+k)$ (as per equation (A-39)), which is unavailable. That is, there is a causality constraint which restricts the amount by which the variance can be minimised. Optimal control would reduce the variance to a white sequence, therefore the minimum variance controller is known as a sub-optimal controller.

With regard to predicting $y(n+k)$, as per equation (A-38), the polynomial $C(q)$ must be separated into that part of $e(n)$ that is available (ie. samples up to time n), and that part which is unavailable (ie. samples in the range $n+1 \leq n \leq n+k$). The equation that redefines $C(q)$ in this manner is termed a "Diophantine equation", and

can be written as

$$\frac{C(q)}{A(q)} = F(q) + \frac{G(q)}{A(q)} q^{-k} \qquad [A\text{-}40]$$

where the polynomial $F(q)$ has order $(k\text{-}1)$, and $G(q)$ has order $(n_a - 1)$. Thus it can be shown that the minimum achievable prediction error (or equivalently, that part of the disturbance that cannot be predicted using the data available upto time n) is given by

$$\varepsilon(n+k|n) = y(n+k) - \hat{y}(n+k|n) = F(q)e(n+k) \qquad [A\text{-}41]$$

It is apparent that the prediction error is not a white sequence for $k>1$. In this equation the minimum variance predictor is given by

$$\hat{y}(n+k|n) = \frac{B(q)F(q)}{C(q)} u(n) + \frac{G(q)}{C(q)} y(n) \qquad [A\text{-}42]$$

Therefore the control law that provides optimal regulation to a zero set point is given by

$$u(n) = -\frac{G(q)}{B(q)F(q)} y(n) \qquad [A\text{-}43]$$

Thus the minimum-variance control scheme obtained its name since it is based on the form of the predictor that minimises the variance of the process output. The certainty-equivalence control law can be written with $E(q)=B(q)F(q)$, such that

$$u(n) = -\frac{1}{\hat{e}_0}[\, \hat{g}_0 y(n) + \ldots + \hat{g}_{n_G} y(n-n_G) + \hat{e}_1 u(n-1) + \ldots \hat{e}_{n_E} u(n-n_E)\,] \qquad [A\text{-}44]$$

where estimates of the parameters required to form the control law have now been introduced. The polynomials $\hat{G}(q)$ and $\hat{E}(q)$ must be predicted using the ELS or RML algorithms since the predictor given by equation (A-42) is of equivalent form to the ARMAX predictor presented in section A.2.1.3 (note in passing that the prediction error component of the regressors, see equation (A-15), can be made more

accurate by using the updated parameter estimate, with the prediction error then known as the *a posteriori* prediction error, or residual as will be shown in section 2.4 by example). Since the polynomials $B(q)$ and $C(q)$ are inverted, they must be minimum-phase to ensure stability of the controller. The SPR condition for convergence of the parameter estimates has been addressed in the previous section.

The direct (or implicit) estimation of $\hat{G}(q)$ and $\hat{E}(q)$ represents a more efficient means of obtaining the controller parameters, since $A(q)$, $B(q)$ and $C(q)$ do not need to be identified explicitly before solving the Diophantine equation for $F(q)$ and $G(q)$. This type of controller is termed "certainty equivalence" as the estimates of the parameters are assumed to be exact.

Clarke [1985] notes that the polynomial $C(q)$ can be neglected without affecting the controller since $\hat{G}(q)$ and $\hat{E}(q)$ are only required, and therefore the RLS algorithm can be used to estimate $\hat{G}(q)$ and $\hat{E}(q)$ (since the model would then become linear). Clarke [1985] also notes that the polynomials $\hat{G}(q)$ and $\hat{E}(q)$ are not unique, and can be governed in some way by fixing the parameter $\hat{e}_0$.

For unique determination of the parameters, Isermann [1991] notes that two identifiability conditions must be met:

- The orders of the process model must be exactly known;

- The order of the control numerator, $G(q)$, must be greater than or equal to

(n_b-k), and the order of the control denominator, $E(q) = B(q)F(q)$, must be greater than or equal to n_a.

The minimum variance controller has been extended to more general cost functions that include an effort weighting:

$$J = E[\{P(q)y(n+k) + Q(q)u(n)\}^2 | n] \qquad [A\text{-}45]$$

This type of control is known as Generalised Minimum Variance (GMV) control, and was proposed by Clarke and Gawthrop [1975, 1979] and Gawthrop [1977]. Isermann [1991] notes that the use of $Q(q)=r$ allows $B(q)$ to be non-minimum-phase. The use of this criterion with regard to active noise and vibration control, will be discussed in section 2.4.